Fetal Germ Cell Development in the Rat Testis and the Impact of Di (n-Butyl) Phthalate Exposure

Matthew S Jobling
MSc Medical Genetics, University of Newcastle-upon-Tyne
BSc (Hons) Human Genetics, University of Newcastle-upon-Tyne

Medical Research Council
Human Reproductive Sciences Unit
Queen's Medical Research Institute
47 Little France Crescent
Edinburgh EH16 4TJ

Thesis submitted to the University of Edinburgh for the degree of Doctor of Philosophy

November 2009

Declaration

The studies described in this thesis is the sole work of the author, except where acknowledgement has been made. These studies have not been submitted in support of another degree or qualification at the University of Edinburgh or any other educational institute.

Matthew Jobling

November 2009

Acknowledgements

Phewth! What a way to spend three years! And I guess I must now thank all the people who helped me get through it. First and foremost Richard Sharpe, the best supervisor a student could hope for and without whom I would never have produced this mighty tome. Next, the charming and talented post-docs who guided me through testicular troubles; Gary Hutchison my first year "Yoda", Hayley Scott the finest singing partner a testis dissector could ask for and Sander van den Driesche for injecting some testosterone into the Sharpe group. And special thanks to Mandy Drake for helping guide me through methylation madness.

For all their technical support, I would like to thank the rest of the Sharpe group members past and present, especially Marion Walker and Chris McKinnell, and the Histology team, for enduring my endless pestering questions and dealing with my tiny, tiny testes. I must especially thank Mark Fisken for his expert help and patience with animal studies and treatment. I should also take this opportunity to thank Hayley Scott and Sarah Auharek for performing the Sertoli cell counts used in this thesis.

During my PhD study, I have been most fortunate to have been joined by a great group of fellow students: Rod Mitchell, another examiner of male germ cell development and "fake" PhD student, who I should thank for daily "scientific" discussions over coffee. Carol Fitz a feisty office companion to be sure. The wonderful Wallace's for her winning ways. Naomi and Margaret for their constant good humour. Rowan and George, our very own Goose and Maverick, for pub quizzes, quiet pints, regrettable Friday nights and everything in-between. Laura, Doug, Sharon, Afshan, you guys rock too!

Oh, and anyone else who thinks I should thank them, this is for you!

Special thanks should be given to Nigella Lawson for designing cakes that are like science experiments, but always work and are deliciously edible.

Abstract

During gonad development and fetal life, the germ cells (GC) undergo a range of different developmental processes necessary for correct postnatal gametogenesis and the production of the next generation. If these fetal events are disrupted by genetic or environmental factors, there could be severe consequences that may not present until adulthood. This is of particular importance in relation to human testicular GC tumours (TGCT), the most common cancer of young men, as TGCT is thought to arise from fetal GCs that have failed to differentiate normally during development and thus persist into adulthood, eventually becoming tumourigenic. TGCT is one of several related disorders of male reproductive health thought to comprise a Testicular Dysgenesis Syndrome (TDS), in which faulty testis development in fetal life may predispose to the development of cryptorchidism, hypospadias, reduced sperm count and TGCT.

Currently there is no accepted animal model for TGCT, but some insight into human TDS has been gained through the use of a rat model using *in utero* Di (n-Butyl) Phthalate (DBP) exposure to induce cryptorchidism, hypospadias, low sperm count and reduced fertility (but not TGCT). However, a previous study suggested that DBP exposure can disrupt GC differentiation, resulting in significantly reduced GC number prior to birth and postnatal consequences. This thesis has been directed at investigating the normal process of GC development in the fetal rat and how this is altered by DBP exposure; such understanding may give insights into the origins of human TGCT by showing how and when disruption of normal fetal GC differentiation can occur.

The first objective was to characterise GC development in both the rat testis and ovary to understand the normal events that occur between embryonic day (e)13.5 and e21.5, as most data in the literature is based on the mouse. Analysis by immunohistochemical, stereological and mRNA expression indentified that during this time period, a GC will undergo a dynamic sequence of changes involving migration, proliferation followed by differentiation (manifested by loss of specific

protein markers), whilst undergoing germ-line specific remethylation. Whilst whole gonad development is vastly different between testes and ovaries, GC development was broadly the same with only minor differences up to the point where GCs in the ovary enter meiosis.

Having established the normal process of GC development in the fetal rat testis, the effects of *in utero* DBP exposure was then investigated. DBP exposure reduced GC number at all ages investigated even after only 24 hours of exposure and simultaneously prolonged GC proliferation. As apoptosis was unaltered by DBP exposure, the consistent reduction in GC number was suggested to be due to an initial reduction in GC number that does not recover to control levels. GC differentiation was assessed by the expression and localization of specific protein markers (OCT4, DMRT1 and DAZL). The pattern of expression of OCT4 and DMRT1 was altered by DBP exposure. GCs in DBP exposed animals also showed a delay in disaggregation from within the centre of seminiferous cords. These results suggested that a delay in GC differentiation was occurring with DBP exposure. This delay in GC development persisted into early postnatal life, following cessation of DBP exposure. Thus at postnatal day (D)6, GC specific re-expression of DMRT1, GC migration to the basal lamina and resumption of GC proliferation all showed a delay. DBP also induced an increase in the presence of multinucleated gonocytes.

DNA methylation in the fetal rat testis was also investigated as a mechanism that could be disrupted by DBP exposure. DNA methylation of GCs increased during the last week of fetal life by global methylation of the GC genome and the increased expression of DNA methyl transferases. No effect of DBP exposure was detected. Inhibition of methylation by 5-aza-2'deoxycytidine was then investigated as a way to block GC differentiation in fetal rat testes and this resulted in a similar transient delay in GC differentiation but was perinatally lethal to the fetus. Bisulphite sequencing of the OCT4 promoter was also performed but proved inconclusive. Methylation patterns may be being altered by DBP exposure, but such changes could not be identified in this thesis.

To complement the *in vivo* DBP exposure studies, an *in vitro* testis explant system using e14.5 testes was investigated. These *in vitro* testis explants showed some GC effects with MBP, the active metabolite of DBP, and also suggested a novel role for Hedgehog signalling in GC survival in the fetal rat testis.

The studies in this thesis have characterised several aspects of fetal GC development in the rat and identified which of these are affected by DBP exposure, resulting in a delay in GC development. As DBP exposure delays but does not block GC differentiation, this may explain why TGCT is not induced in the DBP exposure rat model for TDS.

Presentations relating to this thesis

Poster presentation at 4th Workshop on Endocrine Disruptors 2007, Copenhagen, Denmark: *Germ Cell Proliferation and Differentiation in the Fetal Rat Testis and the Impact of Di (n-Butyl) Phthalate Exposure or Experimentally-induced Fetal Growth Restriction*

Poster presentation at British Andrology Society Meeting 2007, Ware, UK: *Use of rat fetal testis explants for study of mechanisms of chemical-induced disruption of testis development and function: studies using Monobutyl Phthalate and Cyclopamine*

Oral presentation at European Testis Workshop 2008, Naantali, Finland: *Inhibition of fetal Leydig cell development by monobutyl phthalate (MBP) in vitro and by its parent compound in vivo*

Poster presentation at Workshop on Germ cell-soma interactions in Gonadal Development 2008, Baeza, Spain: *Fetal Germ Cell Development in the Rat Testis and the Impact of Di (n-Butyl) Phthalate Exposure and Methylation Inhibitor 5-Aza-2'-Deoxycytidine*

Poster presentation at 5th Workshop on Endocrine Disruptors 2009, Copenhagen, Denmark: *Fetal Germ Cell Development in the Rat Testis and the Impact of Di (n-Butyl) Phthalate (DBP) Exposure*

Abbreviations

AIS	Androgen Insensitivity Syndrome
AMH	Anti Müllerian Hormone
AZC	5-aza-2'deoxycytidine
B	Bound cell fraction
BORIS	Brother Of Regulator of Imprinted Sites
BrdU	5-Bromo-2'deoxyuridine-5'monophosphate
BSA	Bovine Serum Albumin
cKIT	c-KIT receptor of KIT/Stem cell factor
CIS	Carcinoma in Situ
CpG	Cytidine-Guanosine dinucleotide
Cyc	Cyclopamine
CYP26B1	Cytochrome P450 member 26B1
D	Postnatal Day
DAB	3,3 DiAminoBenzidine
DAPI	4',6-diamidino-2-phenylindole
DAZL	Deleted in Azoospermia Like
DBP	Di (n-Butyl) Phthalate
DEHP	Di (2-EthylHexyl) Phthalate
DHH	Desert Hedgehog
DMRT1	Doublesex- and Mab-3 Related Transcription factor
DMSO	Dimethyl sulfoxide
DNA	Deoxyribose Nucleic Acid
DNase	Deoxyribonuclease
DNMT	DNA Methyl Transferase
DNMT1	DNA Methyl Transferase 1
DNMT3A	DNA Methyl Transferase 3A
DNMT3L	DNA Methyl Transferase 3L
e_m	Embryonic day (mouse)
e_r or e	Embryonic day (rat)
ES	Embryonic Stem cell
EtOH	Ethanol
EW	Early window of DBP treatment (e13.5-e15.5)
Ext	Extended window of DBP treatment (e11.5-e20.5)
FS-PBS	Filter Sterilised Phosphate Buffered Saline
GC	Germ Cell
IHC	Immunohistochemical
INSL3	Insulin-like 3
iPS	induced Pluripotent State
MACS	Magnetic-Activated Cell Sorting

MBP	Monobutyl Phthalate
MEHP	Mono EthylHexyl Phthalate
MNG	Multinucleated Gonocyte
mRNA	messenger Ribonucleic Acid
MW	Middle window of DBP treatment (e15.5-e17.5)
OCT4	Octamer-binding transcription factor 3/4
PBS	Phosphate Buffered Saline
PGC	Primordial Germ Cell
PTCH1	Patched 1
PTMC	Peritubular Myoid Cell
Q RT-PCR	Quantitative Real-Time Polymerase Chain Reaction
RA	Retinoic Acid
RNA	Ribonucleic Acid
rpm	revolutions per minute
RT-PCR	Real-Time Polymerase Chain Reaction
SC	Sertoli Cell
SEM	Standard Error of the Mean
SSEA1	Stage-Specific Embryonic Antigen 1
Std or DBP500	Standard window of DBP exposure (e13.5-e20.5)
SMA	Smooth Muscle Actin
SMO	Smoothened
SOX9	SRY-related HMG box gene 9
SRY	Sex-determining region of the Y-chromosome
TBS	Tris Buffered Saline
TDS	Testicular Dysgenesis Syndrome
TGCT	Testicular Germ Cell Tumour
TUNEL	Terminal deoxynucleotidyl transferase dUTP Nick End Labelling
UB	Unbound cell fraction
US	Unsorted cell fraction
VASA	Vasa/Mouse Vasa Homologue/DDX11
3β HSD	3β-Hydroxysteroid Dehydrogenase
5MeC	5-Methyl Cytidine
H_2O	Water

N.B. Throughout this thesis, the abbreviation GC stands for germ cell, regardless of sex or age, unless otherwise stated. All embryonic ages stated are for the rat, unless otherwise stated. For gene nomenclature the following convention is used, when referring to the protein capitals are used, i.e. PROTEIN, and italics for genes, i.e. *Gene.*

Contents

List of figures

1. Literature Review

2. General Materials and Methods

3. Germ cell development during the last week of fetal life in the rat

4. The effect of exposure in utero to Di (n-Butyl) Phthalate on fetal germ cell development

5. Investigation of methylation as a potential mechanism for effects of Di (n-Butyl) Phthalate on germ cells

6. Studies on in vitro manipulation of fetal testis explants

List of tables

1. Literature Review

2. General Materials and Methods

3. Germ cell development during the last week of fetal life in the rat

4. The effect of exposure in utero to Di (n-Butyl) Phthalate on fetal germ cell development

5. Investigation of methylation as a potential mechanism for effects of Di (n-Butyl) Phthalate on germ cells

6. Studies on in vitro manipulation of fetal testis explants

1 Literature Review

During gonad development and fetal life, the germ cells (GC) undergo a range of different developmental processes necessary for correct postnatal gametogenesis and the production of the next generation. If these fetal events are disrupted by genetic or environmental factors, there can be severe consequences that may not present until adulthood. This is of particular importance in relation to human testicular GC tumours (TGCT), the most common cancer of young men, as TGCT is thought to arise from fetal GCs that have failed to differentiate normally during development and thus persist into adulthood, eventually becoming tumourigenic (Rajpert-De Meyts, 2006; Skakkebaek, 1978). TGCT is one of several related disorders of male reproductive health thought to comprise a Testicular Dysgenesis Syndrome (TDS), in which faulty testis development in fetal life may predispose to the development of cryptorchidism, hypospadias, reduced sperm count and TGCT (Sharpe, 2003; Skakkebaek et al., 2001).

Currently there is no accepted animal model for TGCT, but some insight into human TDS has been gained through the use of a rat model using *in utero* Di (n-Butyl) Phthalate (DBP) exposure to induce cryptorchidism, hypospadias, low sperm count and reduced fertility (but not TGCT) (Fisher et al., 2003). However, a previous study suggested that DBP exposure can disrupt GC differentiation, resulting in significantly reduced GC number prior to birth and postnatal consequences (Ferrara et al., 2006). This thesis has been directed at investigating the normal process of GC development in the fetal rat and how this is altered by DBP exposure; such understanding may give insights into the origins of human TGCT by showing how and when disruption of normal fetal GC differentiation can occur.

1.1 Sex determination

The first event of sex determination in mammals occurs at fertilisation when genetic sex is established by the presence or absence of the Y chromosome (from the sperm). However phenotypic sex of the organism is dependent on the establishment of either an ovary or a testis later in development. Both the testis and ovary arise from

bipotential undifferentiated gonad pairs. When the undifferentiated gonad is removed *in utero* in rabbits (Jost, 1947), the resulting embryo has female anatomical development, illustrating the need of the testis for the subsequent sexually dimorphic duct structures and external genitalia, leading to the hypothesis of an active "male sex determining pathway" with female morphogenesis as the default developmental pathway. In the mouse, the bipotential gonads originate as paired thickenings of the ventral-medial surface of the mesonephros by mouse embryonic day (e_m)11.0 (Capel, 2000) and comprises layers of undifferentiated somatic cells that are eventually joined by migrating Primordial Germ Cells (PGC, which are discussed in Section 1.3.1). By around e_m12.5 seminiferous cords can be seen, indicating the earliest sign of testis differentiation (Brennan and Capel, 2004; Capel, 2000). During this 36 hour period of time a careful balance of signals is required for commitment to this testis fate.

1.1.1 Sry

The dependence on the Y-chromosome for testis determination eventually led to identification of the gene required for initiation as *Sry* (Sex-determining region of the Y-chromosome) (Hacker et al., 1995; Koopman et al., 1990; Sinclair et al., 1990). The importance of *Sry* was further established by mouse transgenic studies in which it was shown that genetic XY mice lacking *Sry* developed ovaries, whilst XX expressing *Sry* mice resulted in formation of testes (Koopman et al., 1991; Lovell-Badge and Robertson, 1990). *Sry* is expressed in a wave from the centre to anterior and posterior poles of the gonad and is restricted to pre-Sertoli cells, driving these to differentiate into Sertoli cells (Koopman et al., 1990; Palmer and Burgoyne, 1991).

Sry expression is first evident at e_m10.5 but its expression in the mouse is transient and is not required for Sertoli cell maintenance as expression is lost by e_m12.5 (Hacker et al., 1995). It is primarily thought to act as a transcription factor that regulates expression of downstream target genes such as *Sox9*, *Fgf9* and *Dax1* (Colvin et al., 2001; Kent et al., 1996; Meeks et al., 2003), which are themselves necessary for testis determination. A further role of *Sry* is to down regulate pro-ovarian genes such as *Wnt4* and *Rspo1* (Jeays-Ward et al., 2003; Tomizuka et al.,

2008). The current theory is that if pre-Sertoli cells are exposed to *Sry*, they will upregulate *Sox9*, which then promotes *Fgf9,* which in turn then reinforces *Sox9* expression whilst inhibiting and lowering expression of *Wnt4* and *Rspo1*. As a result, the "balance" of *Sox9*/*Fgf9* against *Wnt4*/*Rspo1* decides between a Sertoli or granulosa cell fate and thus ultimately whether a testis or an ovary forms (Cool and Capel, 2009).

Sry driven Sertoli cell differentiation is what ultimately decides the fate of the gonad and involves the recruitment of non-*Sry* expressing cells, as illustrated by chimaeric studies in the mouse in which XX somatic cells (without autonomous *Sry*) are recruited to a Sertoli cell fate (Palmer and Burgoyne, 1991) by paracrine signals (Wilhelm et al., 2009). These same studies have also established that a certain threshold of Sertoli cells is required to permanently differentiate the gonad into a testis, as gonads with less than 30% of XY cells fail to become Sertoli cells and instead express ovarian markers (Palmer and Burgoyne, 1991).

Sry also drives both cell proliferation in the fetal gonad (Schmahl et al., 2000) and triggers the migration of cells from the mesonephros that is necessary for the formation of the seminiferous cords by e_m12.5 (Capel et al., 1999). Once cord formation has occurred, the gonad is committed to testis formation and the subsequent phenotypic sex of the embryo decided. The initiation of *Sry* expression and the downstream events of testis formation have been studied extensively in the mouse, but have also been examined in several other species in which similar events occur. Table 1.1 summarizes the timings of these events in the human, mouse and rat.

Table 1.1 Timings of early testis development in the human, mouse and rat. Taken from (Cupp and Skinner, 2005) in "Sertoli Cell Biology".

Species	Genital ridge	Bipotential gonad	Sry expression	Testis cord formation
Human gestation week	5	6	7	7-8
Mouse embryonic day (e_m)	9-10	10-11.5	10.5	11.5-12.5
Rat embryonic day (e_r)	10-11	11.5-12.5	12	13.5-14

1.2 Gonad formation and development

Once the eventual fate of the gonad has been decided by the presence or absence of sufficient Sertoli cells, distinct morphological changes begin to occur that permanently distinguish a testis from an ovary. These changes include an increase in size due to *Sry* driven cellular proliferation and migration from the mesonephros combined with the organisation of Sertoli and PGCs into the seminiferous cords by $e_m12.5$ and, in the rat, on embryonic day $e_r14.5$ (Buehr et al., 1993a; Jost et al., 1981), whilst ovarian development begins later with the organization of granulosa and GCs into follicles from $e_m18.5$ (Brennan and Capel, 2004).

The organization of the testis is needed to fulfil the two requirements of the fetal testis, normally to create the correct environment for the development of the germ-line and for the hormone production needed to masculinise the embryo. Migration of cells from the mesonephros is required for both of these functions, as cords fail to form when such migration is blocked by separating the gonad from the mesonephros (Buehr et al., 1993a) or by mechanically blocking migration (Tilmann and Capel, 1999), and endothelial cells that migrate into the gonad are also required within the interstitium. This migration is male-specific as exemplified by *in vitro* studies of gonads that form ovotestes, as these cultures show no cellular migration into ovarian-like regions of the gonad, but in areas where testis cords arise migration does occur (Albrecht et al., 2000).

1.2.1 Seminiferous cord formation

Following the same pattern of *Sry* expression in the gonad, is the organization of the Sertoli cells (at around $e_m10.5$) and Peritubular Myoid cells (PTMC) around the aggregates of PGCs to form the seminiferous cords that become visible by $e_m12.5$ and $e_r14.5$ (Buehr et al., 1993a; Jost et al., 1981). For the correct establishment of the cords, both differentiated Sertoli cells and PTMCs are required but not the GCs themselves (McLaren, 1991; Merchant, 1975). PTMCs were originally believed to be a subset of cells that migrated in from the mesonephros, but recently they have been suggested to be induced from pre-existing cells in the gonad (Cool et al., 2008).

Sertoli cells and PTMCs also cooperate to lay down the basement membrane that surrounds the seminiferous cords and which effectively separates the cords from the interstitium (Skinner and Fritz, 1985; Tung and Fritz, 1986; Tung and Fritz, 1987).

1.2.2 Sertoli cells

The origin of the pre-Sertoli cells, prior to sex determination by *Sry*, is from epithelial cells that have migrated from the coelomic epithelium of the genital ridge (Karl and Capel, 1998). The fate of these migrating epithelial cells is temporally regulated, as labelling studies in the mouse showed that migrating epithelial cells prior to the 18 somite stage become both Sertoli and interstitial cells, while after the 18 somite stage these cells will contribute only to the interstitium (Karl and Capel, 1998). This migration from the coelomic epithelium eventually ceases by $e_m12.5$ with the creation of the tunica albuginea from the basement membrane layer below the coelomic epithelium. This tunica acts as a capsule that surrounds the testis and may physically block further migration into the gonad (Karl and Capel, 1998) and also corresponds with the first appearance of seminiferous cords.

Postnatally, mature Sertoli cells are required to support the germ-line and facilitate spermatogenesis by maintaining the spermatagonial stem cell niche (Hess et al., 2006; Orth et al., 1988). This supporting role involves complex signalling between Sertoli cells to PTMCs (Skinner and Fritz, 1985; Tung and Fritz, 1987) and to GCs (Griswold, 1995; Loveland et al., 2005).

Once seminiferous cord formation has occurred, the Sertoli cells have another important role in fetal life by producing Anti Müllerian Hormone (AMH or Müllerian Inhibiting Substance MIS) necessary for the correct regression of the Müllerian ducts and development of the Wolffian ducts.

1.2.2.1 AMH

AMH is a member of the transforming growth factor-β (TGF-β) family, and this glycoprotein is produced by Sertoli cells in fetal life (Fitzpatrick et al., 1998) from e_m11.5 onward (Arango et al., 1999; Munsterberg and Lovell-Badge, 1991) to induce regression of the Müllerian ducts. In the absence of AMH, the Müllerian ducts persist and differentiate into the upper vagina, uterus and oviducts. To induce this sexual dimorphism AMH binds and acts through its receptor AMHR2, which is present on the surface of the Müllerian duct mesenchymal cells, to cause apoptosis of the Müllerian epithelial cells, probably through production of matrix metalloproteinase 2 (Roberts et al., 2002). In the rat, the timing of Müllerian duct regression occurs between e_r14-17 (Behringer, 1994; Mishina et al., 1996). AMH is also expressed within the postnatal ovary where it is produced from granulosa cells with a role in ovarian folliculogenesis (Weenen et al., 2004), but this postnatal ovarian role is of little relevance in this thesis. AMH is used as a marker for Sertoli cells from e_r14.5 onwards.

1.2.2.2 DMRT1

Another important gene associated with fetal Sertoli cells is doublesex- and mab-3 related transcription factor 1 (*Dmrt1*), a gene that regulates postnatal testis differentiation (Raymond et al., 2000). *Dmrt1* is expressed from the genital ridge stage and persists in the testis throughout adult life in a variety of vertebrates (Kettlewell et al., 2000; Marchand et al., 2000; Raymond et al., 1999a). *Dmrt1* encodes a transcription factor containing a DNA binding motif called a DM domain. These DM domains were first identified as being crucial in sexual regulation in model organisms *Drosophila* (Doublesex gene) and *C. elegans* (MAB-3 gene) and DM domain containing genes have subsequently been identified as important in sexual differentiation for species beyond vertebrates (Zarkower, 2001). In the human, deletions of the chromosome region containing the *Dmrt1* gene is associated with dysgenetic areas being present in the adult testis (Raymond et al., 1999b), while amplification of this same region is associated with a type of testicular germ cell cancer (spermatocytic seminoma, (Looijenga et al., 2006)).

In the fetal mouse, *Dmrt1* is expressed in the undifferentiated gonad from e_m10.5 before being localized to the seminiferous cords in the testis after e_m12.5, whilst in the ovary *Dmrt1* expression (by whole mount in situ hybridisation data) is absent by e_m15.5 and is undetectable in the adult ovary (Raymond et al., 1999a). Within the seminiferous cords, DMRT1 protein is expressed in both Sertoli and germ cells and in adulthood expression is restricted to Sertoli and pre-meiotic germ cells, suggesting that DMRT1 has a role in co-ordinating the entry of GCs into meiosis (Raymond et al., 2000). In mice, in which the *Dmrt1* gene has been knocked-out, fetal testis development occurs as normal, but by postnatal day (D)10 GCs are severely reduced in number and do not enter meiosis. GCs are absent by D14 leaving Sertoli cell-only cords and abnormally smaller testes (Raymond et al., 2000). *Dmrt1* deleted female mice were apparently normal and fertile.

The use of two further *Dmrt1* mutant mouse lines has been used to elucidate the role of DMRT1 protein in each of two testis cell types. A Sertoli cell specific knockout of *Dmrt1* has established that DMRT1 protein is needed in Sertoli cells for their maturation (Kim et al., 2007a) and is also needed for GC meiotic progression and survival, whilst in the GC-specific *Dmrt1* knockout there were only effects on GC processes (Kim et al., 2007a). Loss of DMRT1 protein in the GCs affects postnatal migration to the periphery of the cords, mitotic and meiotic progression and GC survival (Kim et al., 2007a). The role of *Dmrt1* gene within rat fetal testis development will be further investigated within this thesis.

1.2.3 Leydig cells

Leydig cells outside of the seminiferous cords provide the steroidogenic machinery required for correct masculinisation of the developing embryo, otherwise female phenotypic development occurs even with the presence of testes (Jost, 1972). This requirement for androgens is most drastically illustrated in humans with complete Androgen Insensitivity Syndrome (AIS) where defects in the androgen receptor produce karyotypically 46, XY humans with undescended testes and external female genitalia (Chang et al., 1995).

In the rat, androgen synthesis must occur in a temporally regulated manner to correctly masculinise the embryo (Welsh et al., 2008), and both androgen receptor antagonism in males and exogenous testosterone exposure in females have suggested a "masculinisation programming window" for androgen action. In brief, androgens are required during e_r15.5-18.5 to program later masculinisation effects; including Wolffian duct development, prostate formation and eventual size, seminal vesicle size, penis formation and final length and anogenital distance (Welsh et al., 2008). Fetal androgen action is also required for brain masculinisation in both rat and primates but this occurs at a later age than masculinisation of the reproductive tract (Knickmeyer and Baron-Cohen, 2006; Perakis and Stylianopoulou, 1986).

From rodent studies, the steroidogenic Leydig cells are divided into two sub types due to different morphology and gene expression profiles; fetal Leydig cells and adult Leydig cells (Baker et al., 1999; O'Shaughnessy et al., 2003; Roosen-Runge and Anderson, 1959). These two populations are thought to arise from two distinct lineages, with fetal Leydig cells appearing shortly after testis differentiation and remaining until birth, where upon their numbers decline until fully replaced by the adult Leydig cells at puberty (Habert et al., 2001; Kerr and Knell, 1988). In humans, there is another population known as infantile Leydig cells that drive the primate-specific testosterone surge of "minipuberty" in early postnatal life; these infantile Leydig cells are also replaced by adulthood (Andersson et al., 1998; Griswold and Behringer, 2009; McKinnell et al., 2001). As this thesis is focussed on prenatal events, fetal Leydig cells alone will be discussed further in this review.

1.2.3.1 Fetal Leydig cells

The origin of fetal Leydig cell progenitors remains unknown but several different sources for migrating cells been suggested, such as neural crest cells, cells from the mesonephros or from the coelomic epithelium (reviewed in Griswold and Behringer, 2009). Regardless of their origin, fetal Leydig cell number increases throughout fetal life in the rat and peaks prior to birth; this increase is through differentiation of the

precursor population rather than through proliferation of the fully differentiated Leydig cells, which do not divide (Habert et al., 2001; Kerr and Knell, 1988). These differentiated cells have greater testosterone production per cell than adult Leydig cells (Huhtaniemi and Pelliniemi, 1992), so that testosterone production starts by $e_r15.5$ and increases until the end of fetal life (Haider, 2004). In this way, fetal Leydig cells produce the majority of androgens required for virilisation of the embryo.

In addition to androgens, fetal Leydig cells also produce insulin like factor three (INSL3) that plays a role in testicular descent. INSL3 is a hormone that binds to the relaxin/insulin-like family peptide receptor 2 in the gubernacular ligament (Adham and Agoulnik, 2004; Scott et al., 2005), such that INSL3 induces the contraction and thickening of the gubernaculum that is responsible for the first stage of testis descent, the transabdominal movement (Adham and Agoulnik, 2004; Hughes and Acerini, 2008; Nef and Parada, 1999; Scott et al., 2005). When the *Insl3* gene is knocked out, the testes do not descend and remain within the body cavity, are smaller and have defects in spermatogenesis and infertility in adulthood as a result (Nef and Parada, 1999). The later stage of testis descent, inguinoscrotal movement, is driven by androgen action (Hutson et al., 1997) and is usually complete by birth in humans but postnatally in rodents around postnatal D21-23. The failure of one or both testes to descend is known as unilateral or bilateral cryptorchidism, and may be associated with the Testicular Dysgenesis Syndrome which is discussed in Section 1.5.2.

1.2.3.2 Androgen synthesis

Androgen synthesis within the Leydig cells requires the correct series of enzymatic reactions and intermediate products to convert cholesterol into testosterone or, by the further action of 5α-reductase, dihydrotesterone (DHT). This process is summarized in Fig 1.1.

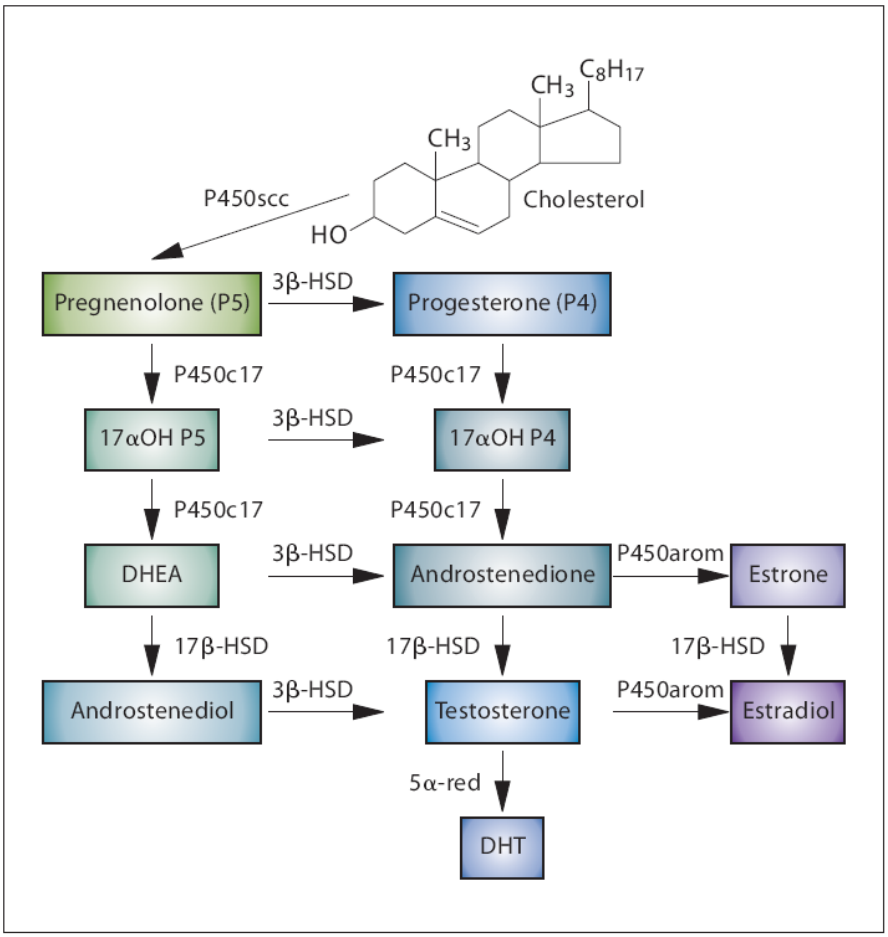

Figure 1.1 Summary of the steroid biosynthetic pathway. Taken from (Griswold and Behringer, 2009)

Fetal Leydig cells in the rat begin to express 3β-Hydroxysteroid Dehydrogenase (3β HSD) at e_r13.5 and become fully steroidogenic by e_r15.5 (Haider, 2004). In adult Leydig cells androgen synthesis is regulated by luteinising hormone (LH) through the hypothalamic-pituitary-gonadal axis. Fetal Leydig cells are, at least initially, gonadotrophin independent and can function in the absence of LH or LH receptor based on mice knock out studies (O'Shaughnessy et al., 1998; Zhang et al., 2004). The switch from gonadotrophin independent to dependent control seems to occur prior to birth around e_r19.5 (Migrenne et al., 2001; O'Shaughnessy et al., 1998). There have been several suggestions as to what drives the gonadotrophin independent Leydig cell stimulation including; vasoactive intestinal peptide (El-Gehani et al., 1998), pituitary adenylate cyclase-activating polypeptide (El-Gehani et al., 1998) and adrenocorticotropic hormone (Johnston et al., 2007). In this thesis, the

steroidogenic enzyme 3β HSD is used as a marker for Leydig cells within the testicular interstitium.

Testosterone or DHT must bind to the Androgen receptor (AR) to effect its action, with DHT having a higher receptor affinity, and seemingly more important role physiologically for virilisation (Imperato-McGinley, 2002). In addition, androgen synthesis is a process that is affected by Di (n-Butyl) Phthalate (DBP) exposure and will be discussed in Section 1.5.3.1.

1.2.3.3 Desert Hedgehog signalling

One of the cell signalling molecules important in both fetal and adult Leydig cell differentiation is Desert Hedgehog (DHH), a member of the Hedgehog signalling pathway (Clark et al., 2000; Yao et al., 2002). In the testis DHH is produced by the Sertoli cell and acts through the Patched 1 (PTCH1) receptor on the Leydig cell surface and other interstitial cells (Bitgood and Rozum, 1996). In mice with a *Dhh* gene knock-out, fetal Leydig cells fail to differentiate while their initial migration and survival are unaffected, (Yao et al., 2002). Postnatally, *Dhh* knock-out male mice were often feminised (92.5% of males) and lacked adult Leydig cells and had very limited spermatogenesis (Clark et al., 2000). In addition, DHH signalling must occur in a stage specific manner, as *in vitro* gonad organ culture using the DHH signalling inhibitor cyclopamine (which inactivates Smoothened, the first downstream target of activated PTCH1) showed that blocking DHH signalling on e_m11.5 prevented Leydig cell differentiation but, in 24 hour older (e_m12.5) testis cultures, cyclopamine did not prevent differentiation (Yao et al., 2002). *Dhh* null mice also have irregular cords by e_m16.5, and some GCs are found outside the cords, although these do not persist after birth (Clark et al., 2000), suggesting a patterning role for DHH signalling in cord formation.

1.2.4 Testicular vasculature

The final aspect of testis development to be discussed is formation of the testis specific vasculature that is needed for the export of androgens out of the testis so that virilisation of the whole embryo can occur. Briefly, a subset of the epithelial cells that migrate into the gonad become organized into a new vascular network starting at $e_m11.5$ and results in the prominent coelomic blood vessel on the surface of the testis (Brennan et al., 2002). These vascular structures are restricted to the interstitium and do not enter the seminiferous cords themselves, and have been suggested to have an associated role in seminiferous cord formation by partitioning the gonad (Brennan and Capel, 2004; Brennan et al., 2003).

1.2.5 Ovarian development

Whilst the events of testis formation are well studied and summarised above, mention should be made of the "default" gonad pathway that produces an ovary. In the absence of *Sry*-driven Sertoli cell differentiation ovary formation will occur. In stark contrast to the testis this process involves few morphological changes from the undifferentiated gonad. The main change occurs towards the end of gestation ($e_m18.5$) with the rounding off of the gonad and the internal formation of follicles within the ovarian cortex (Brennan and Capel, 2004). These ovarian follicles contain meiotically arrested GCs supported by granulosa cells and in contrast to seminiferous cords, it is the GCs that are necessary for follicular formation, as loss of GCs results in follicular degeneration (Merchant-Larios and Centeno, 1981; Merchant, 1975). The development of GCs within the ovary is discussed in Section 1.3.6.

1.3 Germ cells

The correct development of an ovary or testis and the establishment of secondary sexual tissues provide the necessary environment and machinery for sexual reproduction, but it is the germ cells that are responsible for the correct inheritance of the genome from one generation to the next. While the development of the somatic cells of the gonad occur within the gonad later in gestation, the GCs are specified earlier and then later migrate into the gonad at around the time of sex determination. Once in the gonad, the development of GCs into gonocytes or oocytes is dependent on the somatic environment and the GCs must develop and mature to ensure correct postnatal gametogenesis.

As with sex determination and gonad formation, the majority of studies have been done in mice and thus enables use of transgenic possibilities. From these mouse studies, it has been generally assumed that similar mechanisms occur in both the rat and human with different timings.

1.3.1 Primordial germ cells

The specification of primordial germ cells (PGC) occurs earlier in embryogenesis than sex determination, when after the implantation of the blastocyst signals from the extraembryonic ectoderm and visceral endoderm induces a small number of embryonic epiblast cells to become PGCs. The extraembryonic mesoderm and visceral endoderm give rise to the extraembryonic tissues needed to support the embryo that develops from the epiblast. Only one region of the epiblast will give rise to PGCs, the proximal epiblast which is adjacent to the extraembryonic ectoderm (Ginsburg et al., 1990; Lawson and Hage, 1994). This region, rather than a pre-existing cell type, is necessary for PGC specification, as transplantation of cells from the proximal to the distal end does not lead to their becoming PGCs, whilst transplantation of distal cells to the proximal epiblast does result in PGCs (Tam and Zhou, 1996).

The specification of the PGC fate from previously undifferentiated somatic cells of the proximal epiblast requires correct temporal and spatial signalling from both the extraembryonic ectoderm and visceral endoderm to the epiblast cells (de Sousa Lopes et al., 2007; Hayashi et al., 2007). Mouse knockout studies have identified several members of the Bone Morphogenic Protein family (BMP) as essential for this induction; including BMP2, 4 and 8b (Lawson et al., 1999; Ying et al., 2000; Ying et al., 2001; Ying and Zhao, 2001). BMP signalling is important in several embryogenic processes in which BMP dimers act on their receptors that signal through SMADs and induce their effect (reviewed in Gazzerro and Canalis, 2006). When either *Bmp4* or *Bmp8b* genes are knocked out, GCs fail to form suggesting these two proteins may work together to induce GCs (Lawson et al., 1999; Ying et al., 2001). BMP4 appears to be the earlier signal, as *Bmp4* knock-out epiblast cells from e_m5.5-6.0 can be induced to become PGCs by exogenous BMP4, but after e_m6.0 exogenous BMP4 cannot induce this (Pesce et al., 2002; Ying et al., 2001). BMP8b can act on later epiblast cells, and BMP2 seems to a have an additive effect to BMP4 (Ying et al., 2001; Ying and Zhao, 2001).

Several SMADs have been identified as being involved in PGC specification downstream of BMP signalling, including SMAD1 (Tremblay et al., 2001), SMAD5 (Chang and Matzuk, 2001) and SMAD4 (Saitou et al., 2003). These SMADs induce the expression of FRAGILIS, an interferon-inducible transmembrane protein within the proximal epiblast (Saitou et al., 2002), although not all cells that express FRAGILIS become PGCs. At e_m6.25, around 6 cells begin to express BLIMP1 from within the FRAGILIS positive population and this is the first germ cell lineage specific marker (Ohinata et al., 2005). BLIMP1 is a PR-domain containing zinc-finger transcriptional repressor that has a key role in PGC specification by repressing genes involved in the somatic fate (*Hoxa1* and *Hoxb1*) and upregulates PGC-specific and pluripotency associated genes (*Stella*, *Nanos3*, *Nanog* and *Sox2*) (Kurimoto et al., 2008; Ohinata et al., 2005). The BLIMP1 expressing cell population increases by either increased proliferation or, more likely, by increased induction of other FRAGILIS positive cells in the proximal epiblast (McLaren and Lawson, 2005), until by e_m7.25, there is a tight cluster of ~45 committed PGCs identified by expression of

Alkaline phosphatase (Ginsburg et al., 1990; McLaren and Lawson, 2005). One of the first genes expressed by the lineage committed PGCs is *Stella*, but it is not required for PGC specification as *Stella* knockout mice have normal fertility (Bortvin et al., 2004). This process of PGC induction is summarized in Fig 1.2.

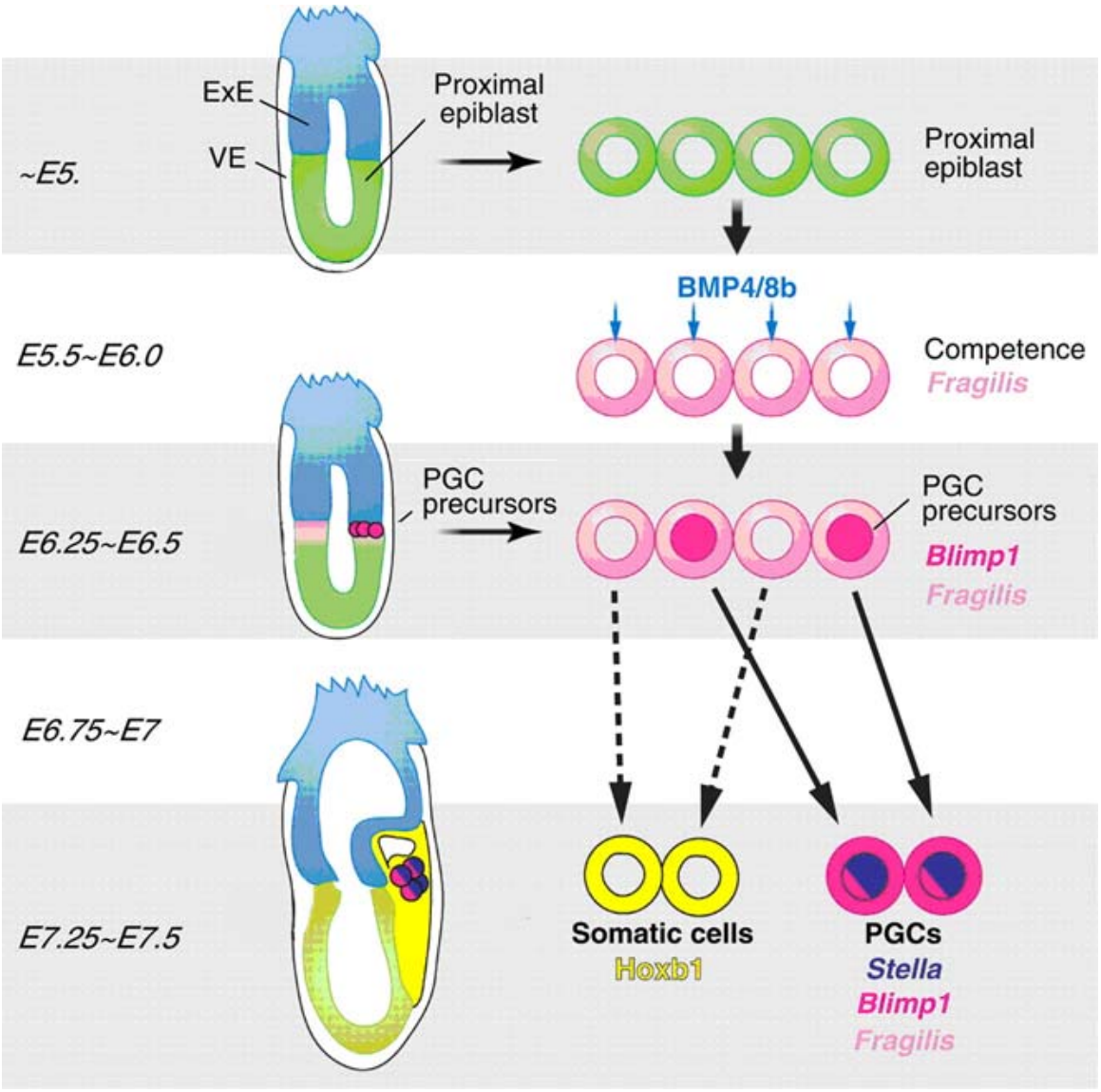

Figure 1.2 Specification of primordial germ cells in early mouse embryos from e_m5.0-7.5. Proximal epiblast cells receive signals from the extraembryonic cells (ExE), inducing *Fragilis*. A subset of *Fragilis* expressing cells then express *Blimp1* and eventually *Stella*. In this figure: E refers to mouse embryonic day (e_m), PGC to primordial germ cell and VE to visceral endoderm. Adapted from (Hayashi et al., 2007).

1.3.2 Migration into the developing gonad

Once the PGC population has been specified, these cells begin to migrate by e_m8.5 before arriving at the genital ridge at around the time of sex determination, between e_m10.5-e_m11.5 (Clark and Eddy, 1975; Molyneaux et al., 2001). The route of these migrating PGCs has been elucidated using transgenic mice expressing green fluorescent protein from a truncated *Oct4* promoter (Anderson et al., 2000; Molyneaux et al., 2001). The initial migration involves moving into the embryonic endoderm until by e_m7.5-8.5 the PGCs have become embedded in the developing hind-gut epithelium (Anderson et al., 2000; Molyneaux et al., 2001). Not all of the PGCs correctly migrate into the hind-gut epithelium and instead move into the extraembryonic mesoderm and do not contribute to embryonic tissue or the germ-line (Anderson et al., 2000). This initial migration into the endoderm may be due to active migration, as PGCs start to develop motility by e_m8, as seen in cultured cells from this age (Godin et al., 1991), or due to passive movement as the morphogenic remodelling of the embryo occurs. By e_m8.5, PGCs have altered morphology with small pseudopodial projections becoming visible that may be involved in GC motility (Clark and Eddy, 1975). Between e_m9-9.5, PGCs undergo active movement through the hind-gut and dorsal mesentery until they arrive at the developing gonad at e_m10.5-11.5 (Clark and Eddy, 1975; Molyneaux et al., 2001). Not all of these PGCs successfully arrive at the gonad, and some PGCs become situated ectopically and most may eventually enter meiosis until they are lost through apoptosis (Bendel-Stenzel et al., 1998; McLaren, 1983).

During the course of this migration, PGCs must be correctly targeted to the gonad, escape apoptosis and undergo several rounds of proliferation so that around 4000 PGCs arrive at the gonad (Tam and Snow, 1981). Mice knockout studies have identified several genes involved in PGC migration, such as *Nanos3*, *Dnd1* and most interestingly *cKit*.

NANOS3 is an RNA-binding protein that is expressed from e_m7.5 in the presumptive PGCs and is maintained during migration (Suzuki et al., 2008). In *Nanos3* knockout

mice, the PGCs are induced as normal but do not survive the migration (Tsuda et al., 2003). From this, NANOS3 is thought to repress both Bax-dependent and Bax-independent apoptosis (Suzuki et al., 2008). Another PGC gene associated with apoptotic suppression is Dead end (*Dnd1*), which encodes an RNA-binding protein. This gene was first identified from the Ter mutation in *Dnd1* that results in a recessive condition that involves progressive loss of PGCs between e_m8.5-e_m12.5 (Noguchi and Noguchi, 1985; Sakurai et al., 1994; Youngren et al., 2005). Mutation of *Dnd1* is also linked with development of testicular germ cell tumours postnatally in the mouse (Youngren et al., 2005).

cKit has a major role in the PGC migration process and has been suggested to be involved in survival, proliferation and directing the migration. *cKit* is expressed in PGCs from e_m7.5 and encodes a cell surface receptor with tyrosine kinase activity (Matsui et al., 1990). cKIT is activated by KIT ligand, a pleiotropic growth factor that is expressed by somatic cells along the migratory route and by the developing genital ridge itself (De Felici et al., 1996; Keshet et al., 1991; Matsui et al., 1990). In mice with mutations in either the ligand or receptor gene loci, there is a reduction in PGC number (Buehr et al., 1993b; McCoshen and McCallion, 1975) and hypomorphic KIT ligand mutants form PGC clumps that do not migrate (Besmer et al., 1993; Mahakali Zama et al., 2005). *In vitro* cultures of PGCs have identified that KIT signalling can prevent apoptosis and increase proliferation (Dolci et al., 1993; Runyan et al., 2006) and is also involved in the necessary adhesion of PGCs to somatic cells (Pesce et al., 1997). Recently KIT ligand has been suggested to be the crucial single chemoattractant for PGC migration and is responsible for reorganizing the actin skeleton to facilitate movement (Farini et al., 2007). Several other molecules exhibit evidence of a chemoattractant effect on PGCs, such as SDF1/CXCR4, TGFβ and BMP signalling and highlight the importance of somatic cell-PGC communication (Dudley et al., 2007; Godin and Wylie, 1991; Molyneaux et al., 2003). In addition, mutations in the *cKit* gene/chromosome region are often associated with Testicular Germ Cell Tumour in humans (Biermann et al., 2007; Rapley et al., 2009), discussed in Section 1.5.1.

1.3.3 Germ cell pluripotency

After specification, PGCs must undergo two further processes for correct function in the germ-line; epigenetic reprogramming (which is discussed further in Section 1.4) and acquiring GC-specific pluripotency in differentiated cells. Recently the *Prdm14* gene has been identified as critical for both of these roles (Yamaji et al., 2008). PRDM14 is a PR-domain containing transcriptional regulator like BLIMP1, and is expressed from around e_m7.0 until around e_m14.0 specifically in PGCs and starts earlier than *Stella* expression (Yamaji et al., 2008). In *Prdm14* knockout mice, PGCs undergo the normal repression of somatic fate but do not upregulate pluripotency genes such as *Sox2* and *Stella* and do not undergo epigenetic reprogramming, while leaving other crucial genes for PGC development unaffected (*Oct4*, *Dnd1*, *cKit* and *Nanos3*). Further highlighting the importance of *Prdm14*, is its induction by BMP4 independently of BLIMP1, although to maintain/upregulate this expression BLIMP1 is required (Yamaji et al., 2008).

The first of the pluripotency genes induced is *Sox2*, which encodes a transcription factor member of the *Sox* (SRY-related HMG box) gene family that is involved in early mouse development, with loss of *Sox2* gene having peri-implantation lethality (Avilion et al., 2003). In embryogenesis, SOX2 protein is restricted to the anterior neuroectoderm of the epiblast (by e_m7.5) and to the PGCs from e_m6.75 (Western et al., 2005; Yabuta et al., 2006). SOX2 can work as a heterodimer with OCT4 to regulate the expression of itself and other pluripotency genes (Avilion et al., 2003; Tomioka et al., 2002). In the human fetal gonad SOX2 is not induced and it has been suggested that the related factor SOX17 may fulfil this role in the human (de Jong et al., 2008; Perrett et al., 2008).

Octamer-binding transcription factor 3/4 (OCT4) is a POU domain containing protein that is expressed in the epiblast where it is required for establishing and maintaining pluripotency in early embryogenesis (Nichols et al., 1998). *Oct4* expression is lost during development, until by e_m7.5 it is restricted to PGCs, where

it is necessary for PGC survival (Kehler et al., 2004; Pesce and Scholer, 2000). *Oct4* expression is discussed in reference to promoter methylation in Section 1.4.5.1.

NANOG is a homeobox-containing transcription factor that is also essential for pluripotency maintenance and becomes upregulated in PGCs by e_m7.75 (Yamaguchi et al., 2005). This upregulation could be driven by OCT4/SOX2 heterodimers (Rodda et al., 2005). Chimaeric mouse studies that allow *Nanog*-null PGCs to escape early embryonic lethality have suggested a maintenance role for *Nanog*, where *Nanog*-null PGCs are still recruited to the genital ridge but are lost by e_m11.5 (Chambers et al., 2007).

These pluripotency genes can be used to induce pluripotency in terminally differentiated somatic cells in both mouse and human (Takahashi et al., 2007; Takahashi and Yamanaka, 2006) and *Oct4* in particular is also associated with human testicular germ cell tumour which will be discussed in Section 1.5.1.

1.3.4 Gonocyte or oocyte determination

Once the PGCs arrive in the gonad, they change their morphology and lose their motility and proliferate until by e_m12.5 around 26,000 GCs are present. Then they develop into meiotic oocytes or quiescent gonocytes (Donovan et al., 1986; Kocer et al., 2009; Tam and Snow, 1981). Until their arrival in the genital ridge, the PGCs are bipotential and require somatic signals to induce sex-specific behaviour (McLaren, 1995). Studies using chimaeric gonads have illustrated that the chromosomal sex of PGCs is unimportant in this decision as, regardless of genetic sex, PGCs will enter meiosis in an ovary but will not in a testis (Palmer and Burgoyne, 1991). However, postnatal gametogenesis does require the correct chromosomal content in the GCs (Burgoyne, 1987). At around e_m12.5-13.5, GCs in both testis and ovary have a post-mitotic/pre-meiotic morphological appearance and begin expressing some meiotic genes (McLaren, 2003). The expression of these meiotic genes are gradually lost as PGCs commit to spermatogenesis in the testis after e_m12.5, whilst it is maintained in

ovarian PGCs that commit to oogenesis a day later on e_m13.5 as evidenced by co-culturing experiments (Adams and McLaren, 2002; McLaren, 2003).

The factors that regulate whether a GC will enter meiosis or not are currently not fully understood, and it remains unclear whether there is a testis expressed meiotic preventing substance, or an ovarian expressed meiotic inducing substance, or a combination of the two (Kocer et al., 2009). However, as PGCs begin to express meiotic genes, such as SCP3 (Di Carlo et al., 2000), regardless of the gonad, and that both *in vivo* ectopic PGCs (in the adrenal gland) and cultured PGCs without testicular signalling enter meiosis around the same time as ovarian PGCs (McLaren and Southee, 1997; Zamboni and Upadhyay, 1983), suggests that the meiotic pathway is the default pathway of fetal GC development, with a local diffusible signal responsible for preventing meiosis in the testis. Recently, retinoic acid (RA), the small diffusible active metabolite of vitamin A, has been suggested to have a role in meiotic control (Bowles et al., 2006). RA signalling is involved in many aspects of embryogenesis and organogenesis and acts through activation of RA response elements in RA-responsive genes (Chambon, 1996; Mark et al., 2006).

One such RA-responsive gene is *Stra8*, which is expressed in female PGCs in an anterior-posterior wave around e_m12.5, and is followed by a similar wave of early meiotic genes (Bullejos and Koopman, 2004; Menke et al., 2003). *Stra8* is also expressed in premeiotic GCs of pubertal and adult mice testes (Oulad-Abdelghani et al., 1996). *Stra8* knock out mice fail to enter meiosis, so it is an essential gene for meiotic progression (Baltus et al., 2006). This suggests that it may be sexually dimorphic differences in levels of RA between fetal testes and ovaries that cause the initiation of *Stra8* expression and meiosis in the ovary only. This was supported by reports of expression of CYP26B1 enzyme, which metabolizes RA, in developing testes from e_m12.5 (Bowles et al., 2006). This has led to the hypothesis that RA, synthesized within the mesonephros, diffuses into the adjacent gonad where the local action of CYP26B1 in the testis creates a difference in RA levels in male and female gonads, such that *Stra8* expression and then meiosis is restricted to the female

(Bowles et al., 2006; Bowles and Koopman, 2007; MacLean et al., 2007). This role of RA is summarized in Fig 1.3.

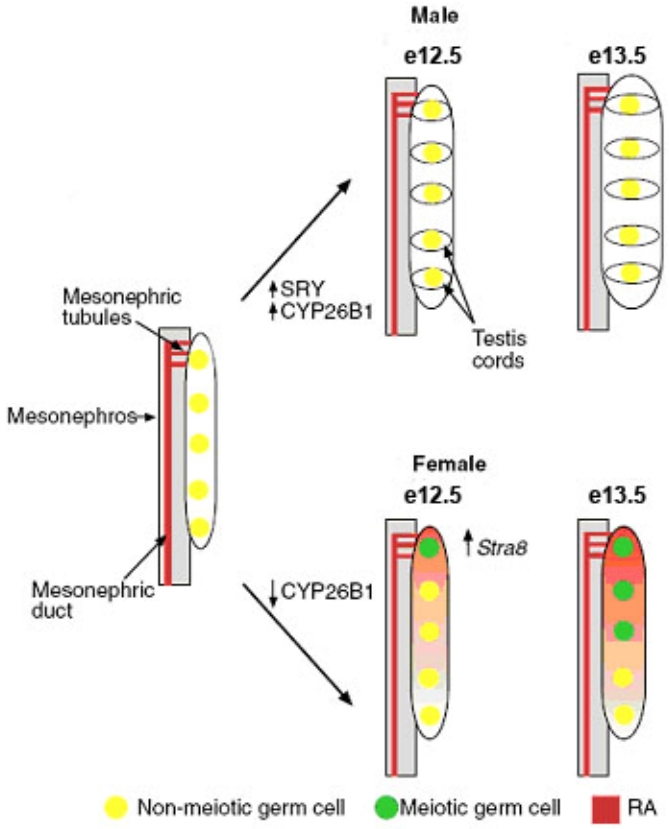

Figure 1.3 Diagram of regulation of germ cell entry into meiosis by retinoic acid levels. Retinoic acid, produced by the mesonephros, is degraded in the testis by upregulated CYP26B1 expression after sex determination. Retinoic levels are maintained in the ovary and upregulate *Stra8*, and thus promote meiosis. Adapted from Bowles and Koopman (2007).

The role of RA in meiotic induction is explained for adrenal ectopic and cultured GCs by the high levels of RA throughout the embryo and within culture media (Bowles and Koopman, 2007). However, it is unlikely that RA signalling is solely responsible for meiotic initiation, as some migratory PGCs in the human that become ectopic do not enter meiosis and can become GC tumours (Oosterhuis et al., 2007). In fact, several factors have been identified (Kocer et al., 2009), including the importance of secretion (most probably from Sertoli cells) of unknown molecules for correct mitotic arrest of GCs in the testis (Best et al., 2008).

One important downstream target in GC sex determination is *Nanos2*, which is expressed solely in male PGCs from e_m13.5. In *Nanos2* knockout mice, in which Bax-dependent apoptosis cannot occur, PGCs in a male environment abnormally express *Stra8* and enter meiosis by e_m17.0 (Suzuki and Saga, 2008). When the *Nanos2* gene is expressed within an ovary, *Stra8* expression is downregulated and meiosis avoided, highlighting the importance of *Nanos2* to effect sex-specific expression in PGCs (Suzuki and Saga, 2008).

1.3.5 Germ cells in the developing testis

In the developing testis, PGCs become organised into seminiferous cords and committed to the spermatogenic fate at around the same time at around e_m12.5-13.5 (McLaren, 2003). After this point, sex specific differences begin to occur and PGCs become identified as gonocytes. By this time the PGCs have lost their motility and become morphologically fixed as round cells with a large nucleus and scant cytoplasm. These PGCs start to express genes associated with GC differentiation, such as *Vasa*, *Dazl* and *Dmrt1* and lose the expression of pluripotency genes like *Oct4* and *Nanog*.

Mouse Vasa Homologue (*Mvh* or *Vasa*) encodes an ATP-dependent RNA helicase that is expressed in PGC cytoplasm once they reach the gonad and then has germ-line specific expression throughout mouse life (Toyooka et al., 2000). In *Vasa* -/- mice, GC proliferation is reduced and OCT4 expression is reduced and postnatal meiosis fails at the zygotene stage so that no sperm are produced, supporting the importance of VASA in GC development (Tanaka et al., 2000).

Deleted in Azoospermia like (*Dazl*) encodes an RNA-binding protein that is also first expressed in the cytoplasm of PGCs upon their arrival in the gonad (Seligman and Page, 1998). In *Dazl* -/- mice, adult testis size is reduced because of a loss of GCs, which is observable by e_m19.0 until only sparse spermatogonia and spermatocytes are observable in adulthood (Ruggiu et al., 1997; Schrans-Stassen et al., 2001).

The *Dmrt1* gene, which was previously described in Section 1.2.2.2, is expressed in GCs as well as in Sertoli cells where it is driven by different promoters (Lei et al., 2009). *Dmrt1* expression in GCs is initiated by e_m13.5 and lost by e_m15.5 whilst expression remains in the Sertoli cells (Lei et al., 2007). By birth, *Dmrt1* is re-expressed in the GCs of the testis, where it is required for meiotic progression and survival (Kim et al., 2007; Lei et al., 2007).

GCs also proliferate until e_m13.5, at which time they enter mitotic arrest (Monk and McLaren, 1981) and by the end of gestation the GCs migrate from the centre of the seminiferous cords to the basement membrane, becoming prespermatogonia. Shortly after birth, prespermatogonia resume mitosis and further differentiate into spermatogonia. These occupy the spermatogonial stem cell niche, maintained and supported by the Sertoli cells. Through the process of spermatogenesis, these spermatogonial stem cells produce the GCs that differentiate into other GC types and ultimately into spermatozoa, ensuring transmission of genetic information to the next generation for the length of the life of the mouse (reviewed in de Rooij (2001) and Culty (2009).

1.3.5.1 Germ cells in the developing human testis

In stark contrast to the mouse and rat, in which GC development in the testis is largely synchronised, human GCs are a heterogeneous population within a seminiferous cord (Fukuda et al., 1975; Gaskell et al., 2004). These heterogeneous GCs can be sub-divided into 3 groups based on morphology and marker expression; gonocytes, prespermatogonia and an intermediate cell type. Gonocytes are mitotic, with expression of OCT4 and cKIT but low levels of the protein MAGE-A4. Prespermatogonia are no longer mitotic, have lost/losing OCT4 and cKIT expression and have high levels of MAGE-A4. And the intermediate cell type is still mitotic but losing/lost OCT4 and cKIT, but still do not express MAGE-A4 (Gaskell et al., 2004). The relative proportion of these sub-types changes during human gestation, with gonocytes predominant in the 1st trimester, all three populations present during the 2nd and 3rd trimesters with the proportion of prespermatogonia increasing whilst the proportion of gonocytes decreasing progressively through to term (Gaskell et al.,

2004; Honecker et al., 2004). During the course of these thesis studies, understanding of human GC development has evolved and is further discussed in Section 3.4.

1.3.6 Germ cells in the developing ovary

In the developing ovary, the PGCs undergo the same loss of motility and have the same morphology as gonocytes, but become organised into nests of syncytial germ cells surrounded by stromal granulosa cells, where they become known as oogonia (McNatty et al., 2000). Oogonia continue to proliferate before entering meiosis between e_m13.5-15.5 and become classed as oocytes (McLaren and Southee, 1997). Oocytes undergo several stages of meiosis including leptotene, zygotene, pachytene and start meiotic arrest in diplotene at e_m17.5 with most oocytes reaching diplotene by postnatal D5 (Borum, 1961; Speed, 1982). As the oocytes enter meiotic arrest, they become surrounded by the granulosa cells to form ovarian follicles within the ovarian cortex (Brennan and Capel, 2004; Hirshfield, 1992). Meiosis is not completed until after puberty, just prior to ovulation, completing the role of the female germ-line.

Whilst meiotic entry is the major difference between gonocytes and oocytes, there are several similarities in the differentiation which will be briefly summarized here. Pluripotency genes such as *Oct4* and *Nanog* are also lost during differentiation of oocytes. *Vasa* is expressed in oogonia/oocytes but is not required in the female germ-line (Tanaka et al., 2000). *Dazl* is expressed in oogonia/oocytes and has been suggested to enable RA to initiate meiosis, because *Dazl* -/- female mice are infertile with few oocytes by e_m19.0 and no follicles/ova are present in adulthood (Lin et al., 2008; Ruggiu et al., 1997). *Dmrt1* is expressed solely in oocytes/oogonia from e_m13.5-15.5 in the fetal ovary (Lei et al., 2009). *Dmrt1* is not re-expressed postnatally and may not have an essential role in the female germ-line as *Dmrt1* -/- female mice are fertile and apparently normal (Raymond et al., 2000).

1.4 Epigenetics

In addition to passing on the correct genetic material, the DNA, to the next generation the GCs must also ensure that the correct "epigenetic" instructions are passed on. The term "epigenetic" means "above" genetics and refers to the mechanisms of inheritable changes in gene expression that do not alter the DNA sequence itself (Waddington, 1952). The most basic principle of epigenetics is that it is how a totipotent cell (fertilised egg) divides and the resulting cells differentiate, losing their totipotency and becoming the various terminally differentiated cell lineages that make up the whole organism. This occurs by the selective expression or inhibition of specific genes such that every cell retains the same DNA genome but a cell-specific complement of "active" genes. These epigenetic mechanisms include, but are not exclusively; DNA methylation, histone modification and silencing by RNA interference by small non-coding RNA, as summarized in Fig 1.4 (Egger et al., 2004). The field of "epigenetics" is expansive, so for clarity this section will focus on DNA methylation with regard to the germ-line, with some minor consideration of associated mechanisms.

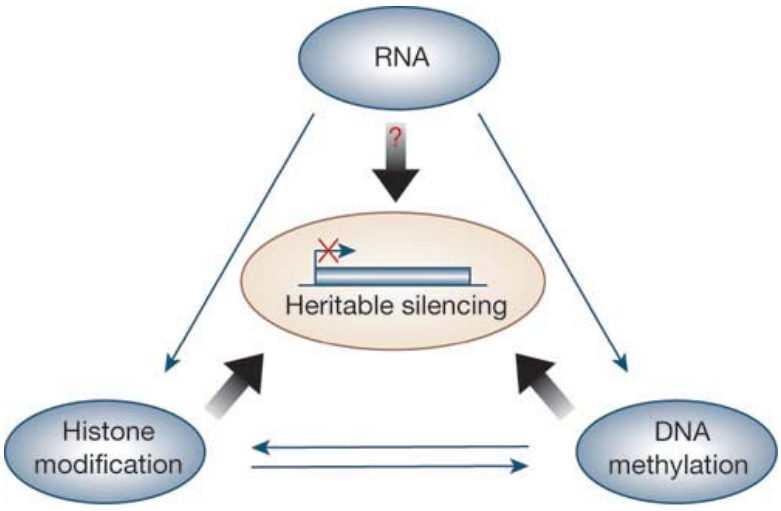

Figure 1.4 Summary of interconnection of processes of "epigenetics" on heritable gene silencing. RNA refers to small non-coding RNAs that could be involved in silencing of heterochromatic chromosome regions or to trigger histone modifications. Taken from (Egger et al., 2004).

1.4.1 DNA methylation

In mammals, DNA methylation occurs at the 5' position of the Cytidine residue within Cytidine-Guanosine dinucleotides (CpG) and occurs at 60-80% of the CpGs (20-30 million sites) in the genome (Trasler, 2009). DNA becomes methylated after DNA replication through the action of DNA methyl transferases (DNMTs) so that methylation patterns are retained in daughter DNA strands/cells or can be removed without altering the DNA. The acquisition of new DNA methylation patterns is termed "de novo methylation", which must then be maintained in subsequent DNA divisions (maintenance methylation), or else lost actively by demethylation or by prevention of DNMT action post replication (Klose and Bird, 2006; Trasler, 2009). DNA methylation of CpGs in gene promoter regions is associated with silencing of that gene through preventing the binding of transcription factors and/or the combined action of methyl-CpG binding proteins and DNMTs with histone modifications (histone deacetylases and methyltransferases) to cause chromatin remodelling that prevents nuclease action and gene transcription. In this way, DNA methylation is only one layer of epigenetic control that is readily examined in comparison to complex histone modifications that can occur (acetylation, methylation, phosphorylation, ubiquitination and sumoylation) (reviewed in Wang et al., 2004).

DNA methylation in gene silencing and regulation has been linked with a variety of roles in development and differentiation, genomic imprinting and X-chromosome inactivation, whilst altered DNA methylation patterns are associated with cancer and developmental abnormalities.

1.4.2 DNA methylation in the germ-line

Epigenetics in the germ-line has two major roles, which both involve the reprogramming of PGCs; the expression of pluripotent and GC-specific genes and the establishment of sex-specific genomic imprinting. This epigenetic reprogramming begins shortly after PGC specification (around $e_m8.5$) and continues during migration to the gonad. This initial reprogramming involves the loss of both DNA methylation and histone dimethylation (H3K9me2) and the upregulation of

histone trimethylation (H3K27me3) (Seki et al., 2005). This change in histone methylation results in transcriptional silencing of GCs until arrival in the genital ridge and is thought to be driven by PGC-specific repression of GLP, a histone methyltransferase (Seki et al., 2007). This transcriptional silencing is thought to prevent unwanted gene expression brought on by demethylation whilst reprogramming occurs (Seki et al., 2007). During this silenced period, regulation of mRNA has been suggested to control the protein expression required in the PGCs (Nakamura and Seydoux, 2008). This initial reprogramming requires the expression of PGC-specific *Prdm14* in order to repress GLP. In addition, *Prdm14* and this initial epigenetic reprogramming may be required for functional pluripotency (Yamaji et al., 2008).

By the time the PGCs arrive at the genital ridge, most DNA sequence methylation has been erased resulting in the loss of genomic imprinting and X chromosome reactivation in females (Hajkova et al., 2002; Maatouk et al., 2006). This DNA demethylation is thought to be a rapid process that leads to the PGCs having a "blank epigenetic slate" for the male or female specific methylation patterns to be established (Hajkova et al., 2002). This sex-specific difference in DNA methylation is known as genomic imprinting and is important in the mono-allelic expression of certain genes depending on the parental origin of the allele. The classic example is the *H19/Igf2* locus, in which *H19* is only expressed from the maternal allele and *Igf2* only from the paternal allele, even though both genes are within the same region. If an offspring erroneously inherits two copies of the maternally imprinted allele, there will be twice as much H19 expressed and no IGF2 (reviewed in Sasaki et al., 2000). For such "imprinted" genes, which only make up around 1% of autosomal genes, these imprints are retained in somatic cells but must be removed in the germ-line and re-established with a new imprint depending on the sex of the developing embryo.

Establishment of male-specific DNA methylation begins in the gonocytes and is not complete until after the pachytene stage of meiosis postnatally (Lees-Murdock et al., 2003; Oakes et al., 2007b), in contrast to the female-specific DNA methylation that does not start until after the pachytene stage of meiosis postnatally (Lucifero et al.,

2004; Obata and Kono, 2002). Post-meiotically, this established sex-specific gametic DNA methylation is retained until post-fertilisation of the next generation, when another period of rapid global demethylation occurs in the pre-implantation blastocyst. Note that not all DNA is demethylated at this stage, for example imprinted genes retain the parental methylation pattern. In this way, epigenetic programming through DNA methylation is continued every reproductive cycle to ensure the correct erasure and reacquisition of DNA methylation (Trasler, 2009). These changes in the level of DNA methylation are summarized in Fig 1.5

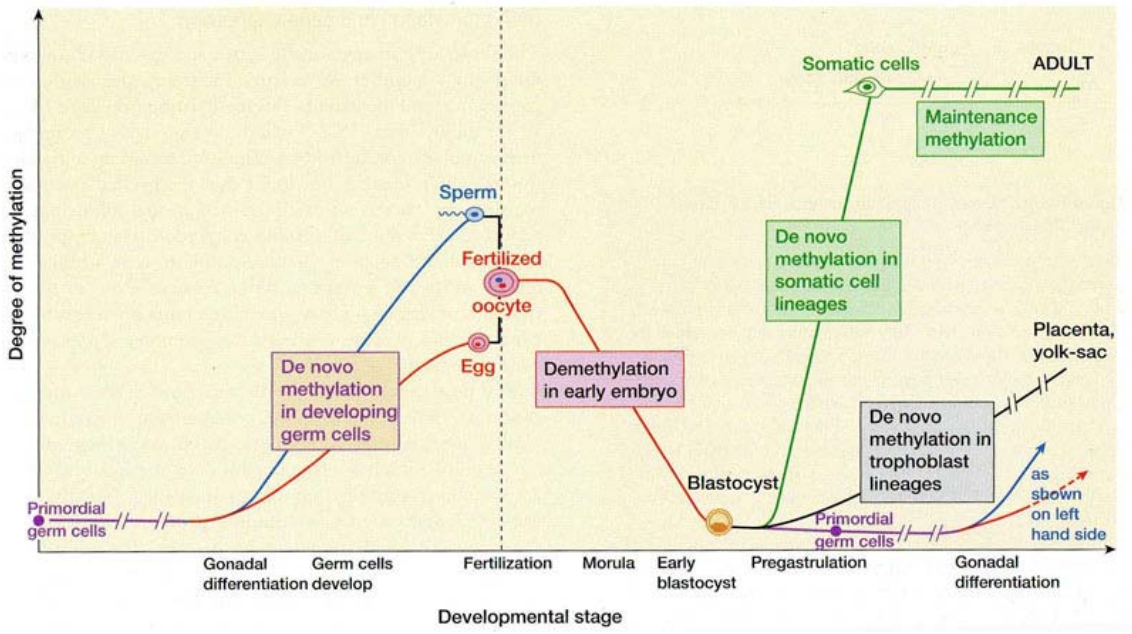

Figure 1.5 Diagrammatic representation of changing levels of DNA methylation from primordial germ cells to fertilization and gonadal differentiation. Taken from (Strachan, 2004).

1.4.3 Transgenerational inheritance

The role of DNA methylation in GC development allows for situations, in which the methylation patterns that are established *in utero* during gonadal development of the F1 generation do not have physiological consequences for that generation. Instead the methylation patterns of the GCs of the F1 only have consequences in the F2 generation, providing a non-Mendelian form of inheritance. In this way, novel or altered methylation patterns established *in utero* can be transgenerationally inherited and affect only the F2 generation, or possibly becoming permanently fixed in the

epigenome by escaping germ-line epigenetic reprogramming into the F3 generation and beyond (reviewed in Jirtle and Skinner, 2007). The possibility of such DNA methylation alterations having such long-term effects has become of increasing interest as it provides a mechanism via which environmental exposures during embryogenesis might influence disease risk down the generations long after that exposure is over. Physiologically, this probably represents a mechanism that allows relatively rapid adaptation to a changing environment without having to wait for (longer-term) genomic selective adaptation.

The ability of environmental exposures in embryogenesis to alter adult disease state is of particular interest in this review, discussed with regard to phthalates and Testicular Dysgenesis Syndrome in Section 1.5.3, but at this point there should be some brief discussion of vinclozolin and transgenerational inheritance. Vinclozolin is an anti-androgenic endocrine disruptor that has been reported to produce adult onset disorders in the rat up to 4 generations after embryonic exposure (e_r8-15) (Anway et al., 2005; Anway et al., 2006b). These disorders include reduced spermatogenic capacity, increased male infertility and cancers of the breast, prostate and kidney of variable incidence (Anway et al., 2006a). The transgenerational effect was passed only through the male germ-line and the time of exposure to vinclozodin was coincident with PGC demethylation and arrival at the genital ridge suggesting a precedent of endocrine disruption and altered DNA methylation that is important in Chapter 5 (Anway et al., 2006a; Anway et al., 2006b). However no mechanism for how vinclozolin alters PGC DNA methylation has been identified and whilst the anti-androgenic results of embryonic vinclozolin exposure are well documented (Colbert et al., 2005; Hellwig et al., 2000; Yamasaki et al., 2005), the transgenerational data (beyond F2) has proven to be controversial and unable to be repeated by other research groups (Inawaka et al., 2009; Schneider et al., 2008).

1.4.4 DNA methyl transferases in the germ-line

The enzymes responsible for DNA methylation are the DNA methyl transferases (DNMTs), which have been studied within the prenatal and postnatal germ-line in

the mouse. These studies have highlighted the roles of DNMT1 in maintaining DNA in the developing GCs and gonad and the DNMT3 group of DMNT3A, 3B and 3L, which are seemingly responsible for de novo methylation within the GCs (Jue et al., 1995; La Salle et al., 2004; La Salle and Trasler, 2006).

In mammals, DNMT1 is the most abundant DNMT and predominantly methylates hemi-methylated CpG dinucleotides, hence maintaining methylation patterns on newly synthesised DNA strands in both germ-line and somatic cells (Li et al., 1992; Yoder et al., 1997). In the fetal testis, it is expressed in the gonocytes from e_m14.5-18.5, with decreasing gonocyte expression after e_m15.5 until it is absent by e_m18.5 (La Salle et al., 2004). This expression pattern suggests that DNMT1 expression occurs after the initiation of re-methylation (Howell et al., 2001; Sakai et al., 2001). A similar expression pattern is reported in fetal oocytes, with DNMT1 being downregulated during meiotic prophase (La Salle et al., 2004). Postnatally, DNMT1 is re-expressed from D3 in GCs until the pachytene stage of spermatogenesis, where it is associated with upregulation upon mitotic resumption and down regulated to prevent aberrant meiotic methylation (Jue et al., 1995; La Salle et al., 2004). This loss of DNMT1 expression at the pachytene stage is also observed in the female mouse (La Salle et al., 2004). In addition there is an oocyte specific variant of DNMT1 that is necessary only within the pre-implantation embryo to maintain imprinted genes (Cirio et al., 2008; Ratnam et al., 2002).

DNMT3 is a family of 3 methyltransferases (DNMT3A, 3B and 3L) that can methylate hemi-methylated and unmethylated DNA and are predominantly involved in de novo methylation (Okano et al., 1999; Okano et al., 1998). Only DNMT3A and 3B have been shown to methylate DNA *in vivo* and the loss of either results in neonatal or mid gestation mortality. DNMT3L is restricted to GCs and loss of DNMT3L results in infertility and aberrant genomic imprinting (Bourc'his et al., 2001). DNMT3L has not been shown to have methyltransferase activity itself but has been suggested to interact with DNMT3A and 3B (or other factors) to regulate genomic imprinting (Bourc'his et al., 2001; Suetake et al., 2004). *In vitro* co-expression of DNMT3L with DNMT3A and 3B showed a stimulatory effect on de

novo methylation with DNMT3A but not 3B (Chedin et al., 2002). Expression analysis of the DNMT3s in the testis and ovary has identified 3A and 3L as highly expressed in the fetal testis, and 3L alone increased in the postnatal ovary (La Salle et al., 2004). These differences in expression match the differences in de novo methylation, supporting that 3A and 3L are crucial for testis de novo gene methylation. Additionally, male germ cell loss of DMNT3A results in infertility and aberrant imprinting (similar to DNMT3L loss), whilst loss of DNMT3B is not required for functional spermatozoa and only one imprinted locus is affected (Kaneda et al., 2004; Kato et al., 2007).

1.4.5 DNA methylation and pluripotency

DNA methylation as a mechanism of gene regulation of pluripotency in embryonic stem cells has been extensively studied (reviewed in Spivakov and Fisher, 2007), and will only be discussed briefly in relation to GC development.

As discussed previously, upon PGC specification there is an upregulation of pluripotency genes *Sox2* and *Nanog* and continued *Oct4* expression during GC migration to the genital ridge. In both human and mouse, these genes are crucial in embryonic stem cells (ES) for maintaining an ES state, where they promote survival and proliferation while repressing differentiation genes (Boyer et al., 2006; Loh et al., 2006). These "master regulators" are lost as lineage commitment occurs. However, ectopic expression of *Oct4* and *Sox2* (with *Klf4* and *c-Myc*) can "induce" differentiated cells from both human and mouse to return to the pluripotent state as iPS cells (Takahashi et al., 2007; Takahashi and Yamanaka, 2006)). DNA methylation and chromatin remodelling have been suggested as one way via which these transcription factors confer pluripotency as in mouse ES cells, as global methylation analyses have shown that pluripotency and housekeeping genes are relatively unmethylated compared with highly methylated differentiation genes (Fouse et al., 2008; Spivakov and Fisher, 2007).

1.4.5.1 DNA methylation of the OCT4 promoter

A particular interest of this thesis is whether promoter DNA methylation is involved in the expression of OCT4. In mouse ES cells, DNA methylation of the *Oct4* promoter regulates its expression, and it becomes methylated during cell differentiation (Ben-Shushan et al., 1993; Pesce and Scholer, 2000; Yeo et al., 2007). In fact *Oct4* promoter DNA methylation is often used to assess OCT4 protein expression itself, in particular as a register of induced pluripotency in iPS cells (Takahashi et al., 2007; Takahashi and Yamanaka, 2006; Wernig et al., 2007). This method of *Oct4* control appears to be retained in humans, as promoter methylation corresponds with gene expression (Cha et al., 2008; Takahashi et al., 2007). In *in vitro* ES cell studies, retinoic acid treatment cause ES cells to lose their OCT4 expression and it has been suggested that DNMT3A and 3B are involved in de novo methylation of *Oct4* in these differentiating mouse ES cells (Li et al., 2007; Pikarsky et al., 1994).

1.4.6 DNA methylation in cancer

It should also be noted that DNA methylation is a system that is aberrant in a variety of cancers. DNA methylation becomes globally dysregulated with an overall loss of DNA methylation coupled with hypermethylation of specific promoters, particularly of tumour suppressor genes (reviewed in Esteller, 2007). Naturally this is a huge field of research, so will only be briefly discussed with particular regard to human testicular germ cell cancer in Section 1.5.1.1.

1.4.7 Inhibition of DNA methylation

DNA methylation patterns in development can be altered through maternal dietary supplementation, as exemplified by work on the “viable yellow” mutation of the agouti gene in mice, in which coat colour is related to the methylation status of the agouti gene in development (Cooney et al., 2002). Briefly, maternal dietary supplement with methyl donors shifts the coat colour of offspring to the brown colour through methylation of the promoter, whilst hypomethylation of the promoter region leads to yellow coat colour (Cooney et al., 2002).

DNA methylation can also be inhibited through drug treatment, with the most common being cytidine analogues 5-azacytidine and 5-aza-2'deoxycytidine (Egger et al., 2004). These analogues become incorporated into the DNA during DNA replication as a cytidine residue but have a nitrogen at the C5 position and so cannot become methylated; they can also bind to DNMTs and inhibit methyl transferase action (Christman, 2002).

The effects of these cytidine analogues on postnatal spermatogenesis has been investigated in both the rat and mouse; DNA methylation is reduced and causes a reduction in sperm counts and testis weight and subsequent fertilisation and implantation are disrupted (Doerksen et al., 2000; Doerksen and Trasler, 1996; Kelly et al., 2003). This suggests a link between DNA methylation and infertility (Trasler, 2009). More detailed examination of the effects of 5-aza-2'deoxycytidine treatment on mouse spermatogenesis has suggested that it is de novo methylation that is inhibited rather than maintenance methylation (Oakes et al., 2007a). This has clinical implications as 5-aza-2'deoxycytidine is used as a chemotherapeutic agent in human cancer, particularly in leukaemia, and this treatment could cause persistent faulty DNA methylation in the sperm should it be used in adults (Kantarjian et al., 2003).

1.5 Testicular Germ Cell Tumours and Testicular Dysgenesis Syndrome

1.5.1 Testicular Germ Cell Tumours

In humans, abnormal development of GCs in men is linked with testicular germ cell cancers, that can arise in childhood (as teratomas and yolk sac tumours), young adulthood (seminomas and nonseminomas) or in older men (>50 years old, spermatocytic seminoma). The testicular germ cells tumours of young adulthood (TGCT) are the most common solid tumour in young men, aged 20-40 (McKiernan et al., 1999) and are further subdivided into uniform seminomas and the more variable and aggressive non-seminomas. Studies into the origin of TGCT, other than spermatocytic seminoma, have identified a non-malignant precursor cell type called carcinoma in situ (CIS). CIS cells are often detected in "high-risk" populations, and in normal tissue surrounding a tumour (Giwercman et al., 1987; Jacobsen et al., 1981; Skakkebaek, 1972). These observations were supported by evidence that within 5 years of detection of CIS cells in testis biopsies of infertile men, over half of patients were diagnosed with TGCT, while subjects without CIS at biopsy did not develop TGCT (Skakkebaek, 1978).

CIS cells possess a distinct morphology and express cell markers that other germ cells of the adult testis do not. In fact CIS cells more closely resemble fetal GCs (Looijenga et al., 2003; Rajpert-De Meyts et al., 2003). Recently, isolation by laser microdissection of CIS cells has shown that the gene expression profiles of CIS cells and fetal GCs/gonocytes are very similar (Sonne et al., 2009). This has led to the current hypothesis that CIS cells are fetal GCs that have failed to undergo correct differentiation but remain in the testis until malignant transformation in adulthood, probably driven by the same post pubertal signals that drive GC proliferation as part of spermatogenesis (Skakkebaek, 1972; Skakkebaek et al., 1982). This hypothesis is illustrated in Fig 1.6. The retention of fetal GC markers, such as placental alkaline phosphatase, OCT4 and NANOG (Giwercman et al., 1991; Hart et al., 2005; Looijenga et al., 2003) are used as diagnostic markers to identify CIS cells in the

human testis. This retention of pluripotency may contribute to the variability of tumour tissues that can arise in non-seminomas, which are the only known totipotent solid cancer (Honecker et al., 2006; van de Geijn et al., 2009).

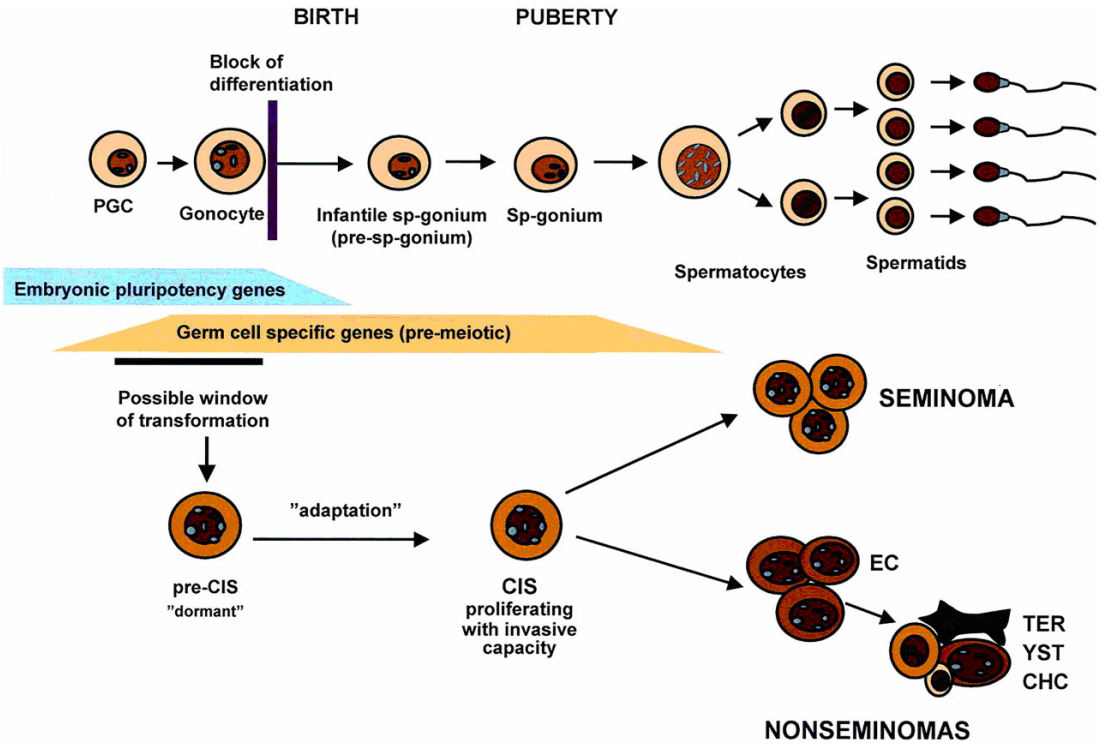

Figure 1.6 Diagrammatic illustration of the proposed fetal GC origin of CIS. This highlights the block of GC differentiation that prevents the normal pattern of postnatal GC development, causing fetal GC-like cells to persist in the testis as CIS. In this Figure: PGC=primordial germ cell, CIS=carcinoma in situ, EC=embryonic carcinoma, TER=teratoma, YST=yolk sac tumour and CHC=choriocarcinoma. Adapted from (Rajpert-De Meyts, 2006).

After puberty, CIS cells begin to replicate and can result in CIS/Sertoli cell only tubules. This increase in CIS replication is believed to be the pre-invasive step that causes expansion out of the tubule (Dieckmann and Skakkebaek, 1999; van de Geijn et al., 2009). Invasive growth migration may be related to a characteristic gain of chromosome 12p material (Ottesen et al., 2003; Rosenberg et al., 2000). Studying the origins of CIS/TGCT is obviously limited in the human and there is currently no animal model available, possibly due to the careful interplay between Sertoli, Leydig and GCs that are probably involved in its aetiology.

1.5.1.1 Methylation in TGCT

As mentioned in Section 1.4.6, incorrect DNA methylation is associated with cancer development, and there have been a number of studies into the epigenetics of human TGCT (reviewed in Lind et al., 2007). Global methylation patterns are different in seminomas and nonseminomas, with seminomas being relatively unmethylated and nonseminomas methylated. This difference is hypothesised to be related to whether the originating GC has undergone de novo methylation prior to becoming the precursor CIS cell (Netto et al., 2008; Smiraglia et al., 2002). Additionally, genomic imprinting appears to be lost in both TGCTs and CIS cells, with possible diagnostic implications (Kawakami et al., 2006; Kraggerud et al., 2003; Looijenga et al., 1998). At a gene specific level, it has been shown that the promoter region of OCT4 in TGCTs is predominantly hypomethylated, both in derived tumour cell lines as well as in the tumours themselves (De Jong et al., 2007). These DNA methylation patterns support the fetal origin of CIS cells and the importance of DNA methylation in testicular tumourigenesis.

1.5.2 Testicular Dysgenesis Syndrome

TGCT is one of a related group of disorders of male reproductive health that are thought to have a common fetal origin, in which abnormal fetal development of the testis impacts the function of the testis cell types and increases the risk of the disorders later in life. This group of related disorders includes; cryptorchidism (failure of testis descent), hypospadias (malformation of the penis), low sperm counts and TGCT. As these disorders are risk factors for each other in epidemiological studies, it has led to the hypothesis of a Testicular Dysgenesis Syndrome (TDS) (Sharpe, 2003; Skakkebaek et al., 2001). This proposes that if testicular development is perturbed by either genetic and/or environmental factors, one or more somatic cell types may function subnormally, leading to one or more of the related disorders, as summarised in Fig 1.7.

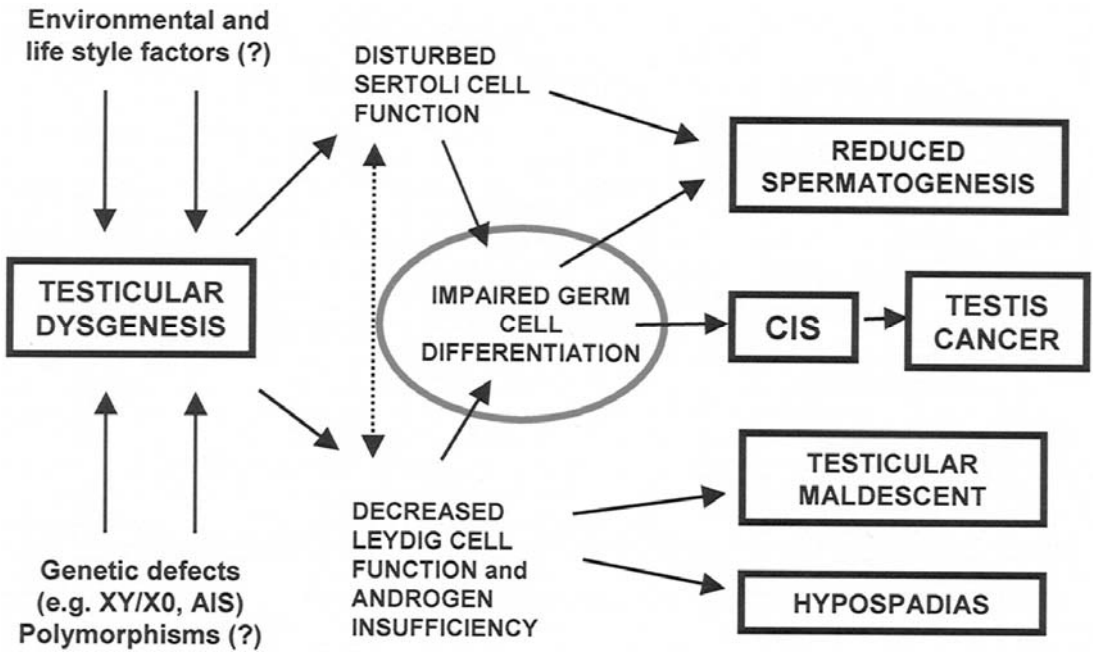

Figure 1.7 Diagrammatic representation of the potential links between disrupted fetal testis formation and the TDS disorders. In this Figure: AIS=Androgen Insensitivity Syndrome. Taken from (Rajpert-De Meyts, 2006).

These male reproductive disorders can manifest at birth (cryptorchidism and hypospadias) or in young adulthood (low sperm count and TGCT) and are either already common and/or are increasing in incidence in the Western world (Sharpe, 2003). There is also a variable penetrance of these disorders such that a low sperm count is the most common, then cryptorchidism, and hypospadias and TGCT is the rarest.

1.5.3 Animal model for TDS

Due to the high/increasing frequency of TDS disorders and the severity of TGCT, a way to study how such dysgenesis occurs has been sought. As TDS probably involves complex cell-cell interactions in the fetal testis, transgenic mice are unlikely to provide a suitable model for this human disease. However phthalate exposure of fetal rats *in utero* has been shown to result in a TDS-like phenotype in male offspring and may therefore offer new insights into TDS origins.

Phthalates are ubiquitous environmental chemicals primarily used as plasticizers (such as in the production of polyvinyl chloride) and are found in a vast array of products used by humans in daily life (personal care products, food containers, numerous "fabrics" of modern society and medical devices) (reviewed in Rudel et al., 2009). Human biomonitoring studies have detected variable levels and mixtures of phthalates in urine samples, illustrating the level of human exposure to phthalate esters (Heudorf et al., 2007; Wittassek et al., 2007). The effects of these phthalates on human health are still unknown. However, exposure to these phthalates, in particular to Di (n-Butyl) Phthalate (DBP) and Di (2-EthylHexyl) Phthalate (DEHP), in fetal rats results in males with a TDS-like phenotype. This has led to a variety of phthalate studies being performed on rodents, including mixtures of phthalates, variable doses and timings, and has raised the question of whether phthalate effects might be important in human TDS. This review will focus on *in utero* exposure to DBP, as it is the phthalate treatment that has been optimised for the studies in this thesis.

1.5.3.1 In utero DBP exposure

Exposure of fetal male rats to DBP *in utero* can induce a range of reproductive disorders including cryptorchidism, hypospadias, impaired spermatogenesis and reduced fertility and so has provided a useful model to study possible mechanisms of human TDS (Barlow et al., 2003; Ema et al., 1998; Ema et al., 2000; Fisher et al., 2003; Mylchreest et al., 1998; Mylchreest et al., 1999). Crucially, DBP exposure does not lead to TGCT in rats, although there are reported acute and long term GC effects (Ferrara et al., 2006). The postnatal TDS-like changes resulting from *in utero* DBP exposure are probably not due to a single mechanism but may result from effects on Leydig, Sertoli and/or GCs.

In the testes of DBP exposed rats, fetal Leydig cells produce less testosterone and INSL3, effects which are probably responsible for the cryptorchidism and hypospadias in offspring. In addition, fetal Leydig cells become abnormally aggregated resulting in areas of focal dysgenesis postnatally, and postnatally can be

found within seminiferous cords (Fisher et al., 2003; Mahood et al., 2005). These areas of focal dysgenesis include Sertoli cells and are similar to dysgenetic areas found in the testes of human TGCT patients (Hoei-Hansen et al., 2003; Holm et al., 2003; Skakkebaek et al., 2003).

In addition to being present in focal dysgenetic areas, DBP exposed Sertoli cells are reduced in number by around 50% by the end of gestation, though this number recovers by adulthood (Hutchison et al., 2008a; Hutchison et al., 2008b; Scott et al., 2008). DBP exposed animals often exhibit areas in their testes postnatally in which seminiferous cords are present that contain Sertoli cells only and these may still appear immature (Fisher et al., 2003; Hutchison et al., 2008a), which are again similar to what is seen in testes of men with TGCT (Hoei-Hansen et al., 2003; Holm et al., 2003; Skakkebaek et al., 2003).

Whilst DBP exposure does not induce TGCT or CIS cells, there are effects on GCs. These include induction of abnormal multinucleated gonocytes, delayed entry into quiescence and reduction in GC number (Ferrara et al., 2006; Fisher et al., 2003). These changes combined with the Sertoli cells effects may explain the reduced sperm count and infertility in adulthood. These GC effects and the general similarity of abnormal features in DBP exposed rats to these in men with TGCT suggest that the effects of DBP exposure on GC development warrants further investigation.

1.5.3.2 In vitro models for phthalate effects

In order to examine the direct effects of phthalates on testis development, several studies have been performed on *in vitro* cultured testes. The advantage of such *in vitro* techniques is that it removes the maternal and fetal metabolism and endocrinology from interfering with investigations of chemical exposures (reviewed in Livera et al., 2006). In addition it provides a way to study human fetal testis exposure to phthalates (Hallmark et al., 2007; Lambrot et al., 2009).

These *in vitro* manipulations have mainly used DEHP and its active metabolite mono (2-EthylHexyl) phthalate (MEHP), with effects in the rat described on mitotically active gonocytes (Chauvigne et al., 2009; Li and Kim, 2003), as well as effects on Leydig cells but not on Sertoli cells (Chauvigne et al., 2009), as well as differing reports on inhibition of testosterone production (Chauvigne et al., 2009; Stroheker et al., 2006). Recent work using human testes showed an MEHP induced reduction in gonocyte numbers but not on steroidogenesis (Lambrot et al., 2009).

In vitro manipulations using the active metabolite of DBP, monobutyl phthalate (MBP) have also been attempted using both rat (e_r19.5-21.5) and human fetal testis explants (Hallmark et al., 2007). In rat fetal testis explants, 48 hours *in vitro* treatment with MBP failed to match *in vivo* DBP exposure effects on Leydig aggregation and testosterone production (Mahood et al., 2005). MBP treatment also had no effect on testosterone production in the human fetal testis explants (Hallmark et al., 2007).

In vitro manipulation of fetal rat testes at a time point after cord formation (e_r14.5) therefore has potential utility especially for studying early phthalate effects on GCs and can be investigated to complement *in vivo* DBP exposure experiments on GCs.

1.6 General Aims of Thesis

There is currently no accepted animal model for TGCT/CIS and this has severely hampered progress in understanding how the disease arises in humans, especially as it is impossible to study the origin of CIS cells in the human. More generally there is little known about the process of fetal germ cell differentiation, how this is regulated and what might perturb these processes and lead to CIS. A more thorough understanding of these fetal events is essential if the origin of CIS cells is to be elucidated. In the DBP exposed rat model, testes show evidence of altered GC differentiation and a somatic cell environment similar to what is reported for TGCT and as such may provide a tool to gain some of the insight that is required.

The general aim of this thesis was to obtain new insights into regulation and dysregulation of fetal GC development in the rat and the susceptibility of these processes to disruption by DBP or other factors. The first step was to characterise normal fetal GC development in the rat testis and ovary (Chapter 3), and then to investigate how these normal processes are disrupted after DBP exposure in the fetal rat testes (Chapter 4). As DNA methylation is one of the key development processes that fetal GCs undergo in fetal life, this was investigated further in relation to DBP exposure and DNA methylation inhibition (Chapter 5). *In vitro* studies using testis explants were also examined to see if they were useful in providing an additional tool to investigate fetal GC development and phthalate exposure (Chapter 6).

2 General Materials and Methods

2.1 Animal work

Animal work was performed using Wistar rats and carried out in accordance with the UK Home Office Animal Experimentation (Scientific Procedures) Act 1986 under project licence 60-3259. Wistar rats, originally purchased from Harlan UK, were bred within our own animal facility to generate stock under the supervision of Mark Fisken, who provided the day-to-day animal husbandry and performed the majority of licensed procedures. Some licensed procedures were performed under my personal licence 60-10976.

2.1.1 Welfare conditions

Within our animal facility, animals were housed in a room with a fixed 12 hours per day light cycle (from 7am-7pm), with the temperature kept between 20-25°C and an average humidity of 55%. Animals were housed in clear sided, solid bottom cages with food (Soy-free, SDS, Dundee, Scotland) and fresh tap water available *ad libitum.* In normal circumstances, male and female rats were housed separately, so that females were typically kept in groups of six and stud males housed individually. For mating, a single male and female were placed in a cage with a mesh grid bottom, so that the copulatory plug could fall to a tray below and be recorded.

2.1.2 Timed-mating

Due to the importance of knowing the gestational stage in the present studies, timed-mating was used to ascertain the date of conception of pregnant rats. Organised by Mark Fisken, one male and female were placed together in a mesh grid bottomed cage at the end of the working day (approximately 4pm), as mating usually takes place at night. The following morning, the tray beneath the cage examined was for evidence of mating (the copulatory plug). Should a copulatory plug be found, mating was presumed to have occurred and the date was recorded and designated as embryonic day (e)0.5. As female rats have a 4-5 day oestrus cycle, mating may not occur for up to 5 days. Once a mating is assumed to have happened, the male is removed and the pregnant female was usually housed singly. To reduce the risk of

non-pregnancy, and wasted animals, whenever possible proven fertile males and females were used, that were sexually mature at least over 10 weeks old and usually around 3 months of age.

2.2 In vivo treatments

The chemicals administered to pregnant female rats for studies *in vivo* were Di (n-Butyl) Phthalate (DBP) via oral gavage, and 5-aza-2'deoxycytidine (AZC) via intraperitoneal injection, given alongside their respective control vehicles. In addition, to label proliferating cells, some pregnant female rats and postnatal males were treated with 5-Bromo-2'deoxyuridine-5'-monophosphate (BrdU), via intraperitoneal injection 1.5 hours prior to kill.

2.2.1 Di (n-Butyl) Phthalate (DBP)

DBP was administered daily by oral gavage using a 10-12cm long 15-16G blunt ended steel gavage cannula (Medicut, Sherwood Medical Industries Ltd., UK), attached to a disposable plastic 1 ml syringe (B-D Plastipak), usually between 9.00-10.30am. Pregnant dams were weighed prior to dosing to calculate the correct volume of chemical to be administered. Post-treatment, animals were regularly checked for signs of discomfort or toxicity.

The dose of DBP (Sigma) used for the present studies was 500mg/kg bodyweight per day, as this dose has been optimised in this research group to induce a high incidence of TDS-like disorders. This *in utero* DBP500 exposure results in Leydig cell aggregation and multinucleated gonocytes in the fetal testes and focal dysgenetic areas in adulthood (Fisher et al., 2003; Mahood et al., 2005; Mylchreest et al., 1998). The treatment window used most commonly involved starting dosing at e13.5 until either birth or killing, although in some experiments other treatment windows were used. An early window of treatment from e13.5 to e15.5 only (EW), a middle window of treatment was from e15.5 to e17.5 (MW) and an extended window involved starting treatment at e11.5 instead of e13.5 (Ext). These treatments are summarised in Table 2.1. As with the previous *in vivo* DBP studies, DBP was diluted with corn oil (supermarket bought) to the 500mg/kg bodyweight dose. It was

assumed that DBP and corn oil had similar densities (1g/ml), so that making up a dose to be given at 1ml/kg bodyweight, involved adding 5ml DBP to 5ml corn oil. Fresh DBP/corn oil mixes were made for each study and kept in glass airtight containers (to prevent additional phthalate leaching from a plastic container) and kept at room temperature. Upon completion of a DBP study, any remaining DBP/corn oil was disposed of. In DBP studies, control animals received 1ml/kg bodyweight corn oil per day.

Table 2.1 Summary of maternal DBP treatments and collection ages used in the studies in this thesis.

Dose (ml DBP/kg bodyweight)	Treatment window	Abbrev.	Collection ages
500	e13.5-e20.5	Std/ DBP500	e14.5, e15.5, e17.5, e19.5, e21.5, D4, D6, D8, D10, D15, D25, Adult
500	e11.5-e20.5	Ext	e21.5, D6
500	e13.5-e15.5	EW	e17.5, e19.5, e21.5, D6
500	e15.5-e17.5	MW	e17.5, e21.5

2.2.2 5-aza-2'deoxycytidine (AZC)

AZC is an analogue of the DNA nucleotide cytidine, that cannot become methylated and can inhibit DNA methylation by two mechanisms; either it can substitute cytidine during DNA replication and then that nucleotide cannot be methylated, or it can bind to DNA methyl transferases and directly inhibit their action (Christman, 2002). AZC (Sigma) was administered in 2ml/kg saline (0.9% NaCl, w/v) on e16.5 via intraperitoneal injection, with the aim that one dose of AZC towards the end of germ cell (GC) proliferation (Section 3.3.5) would cause AZC to become incorporated into the GC genome prior to *Oct4* gene silencing (~e17.5), while minimizing the side-effects of global methylation inhibition in the developing rat fetus. Two doses of AZC alone were used, 5mg/kg bodyweight and 10mg/kg

bodyweight. The 10mg/kg dose of AZC was also combined with DBP treatment from e13.5 until collection, as summarised in Table 2.2. The AZC doses of 5mg/kg bodyweight and 10mg/kg bodyweight were chosen as having had been used previously in Wistar rats to inhibit methylation and produced acceptable levels of fetal mortality (Lu, 1998).

Table 2.2 Summary of maternal AZC±DBP treatment and collection ages used in the studies in this thesis.

AZC Dose (mg/kg bodyweight)	I.P. inj.	DBP Dose (ml/kg bodyweight)	Treatment window	Abbrev.	Kill age
5	e16.5	-	-	AZC5	e17.5, e19.5
10	e16.5	-	-	AZC10	e17.5, e19.5
10	e16.5	500	e13.5-e20.5	AZC+DBP	e17.5, e19.5

2.2.3 5-Bromo-2'deoxyuridine-5'-monophosphate (BrdU)

BrdU is an analogue of the DNA nucleotide thymidine. If BrdU is present during DNA replication, it can substitute thymidine and become incorporated into newly synthesised DNA strands. The incorporation of BrdU can be detected by BrdU specific antibodies and allows the identification of proliferating cells. By counting BrdU labelled and unlabelled nuclei of identified cell types allows the proliferation index to be calculated, by expressing the number of proliferating cells as a percentage of the total number of that cell type (Section 2.8.3).

BrdU (Sigma) was administered via intraperitoneal injection at approximately 1.5 hours prior to kill. The BrdU dose used was 100mg/kg bodyweight in 2ml/kg saline (0.9% NaCl, w/v). To aid solubilisation of BrdU, the saline is first heated to boiling point in the microwave before the BrdU was added, the mixture was then left to cool to room temperature before being injected into animals.

2.3 Necropsy procedure

Pregnant dams and postnatal males were killed by inhalation of carbon dioxide followed by cervical dislocation under Schedule 1 of the Animal (Scientific Procedures) Act 1986. Fetuses were then removed from pregnant dams and placed in ice-cold phosphate buffered saline (PBS, Section 2.13), while older fetuses (e19.5 and e21.5) were decapitated before being placed in ice-cold PBS.

2.3.1 Gross dissection

In pregnant dams, after cervical dislocation the rat was placed on her back, and the abdomen cut open to reveal the uterine horns. The uterus was then removed, and each fetus removed from its amniotic sac and the umbilical cord severed. Fetal bodyweight and anogenital distance (at e19.5 and e21.5 ages) were then recorded and the fetuses stored and transported in PBS on ice to the dissection area, to avoid degeneration of the fetal tissue. In postnatal males, after cervical dislocation the bodyweight and anogenital distance were recorded, as described in Section 2.3.2, and a thorough examination was made for hypospadias and cryptorchidism. Postnatal males were then cut open to examine and weigh the testes and other internal male reproductive tissues. Tissues collected from postnatal males at this point were preserved as described in Section 2.3.5.

2.3.2 Fetal bodyweight and testis weight

Pups taken at e19.5 and e21.5 were wiped clean to remove excess tissue and labelled using permanent marker, so that the bodyweight and testis weight for each individual animal could be recorded. Fetuses were then weighed, using an electronic analytical balance (Handy H110, Sartorius), before being decapitated and placed in PBS.

2.3.3 Fine dissection

Testes or ovaries were removed from fetuses under a binocular dissecting microscope (Leica, MZ6). Illumination of tissue during dissection was provided using a transilluminated stage and lighting from external cold lights (Leica CLS 150x). Fetuses collected at e14.5 were immersed in PBS during dissection, while older ages were placed on their backs on a moistened paper towel bed to allow stable

dissection. The fetal abdomen was cut open just below the umbilical cord, and the abdominal cavity examined to find the gonads, which were generally located between the kidneys and bladder, depending on the gestational age. Gonads and attached mesonephros or ducts were then carefully removed and placed in chilled PBS in a separate petri dish for microdissection. By e14.5, cord structures are visible in the fetal testis using the transilluminated stage, this made identification of testes at e14.5 and e15.5 easier. At later ages the testis is much larger than the fetal ovary and was located lower in the abdomen. Fetuses collected at e13.5 were fixed in Bouin's for 30 minutes, discussed in Section 2.3.5, prior to fine dissection to strengthen the tissue so that gonads could be removed.

2.3.4 Microdissection

Gonads from fetuses at e13.5, e14.5 and e15.5 were collected with the mesonephros attached for *in vitro* experiments or for fixation, whilst the mesonephros was removed for frozen samples. In testes and ovaries from older animals, the fetal 'epididymis' and efferent ducts were removed using disposable plastic 1ml syringes fitted with 25G needles (Monoject, sterile needles, 0.5mm x 25mm) attached as scalpels.

2.3.5 Tissue preservation

Generally, one gonad from each fetus was frozen and the other fixed using Bouin's solution. The frozen gonads, trimmed of ducts/mesonephros, were placed in individually labelled 1.5ml Eppendorf tubes and frozen on dry ice, before being stored at -80°C. The fixed gonads were individually fixed by immersion in Bouin's solution (Section 2.13) in at least 10 times their own volume for a time dependent on the collection age; 30 minutes for e14.5 and e15.5, and 1 hour for older fetal ages. Bouin's solution is a formaldehyde based fixative that works by forming cross-links between proteins and aldehydes that produces a stable structure without losing or damaging antigenic sites. Bouin's is well established for preserving both embryonic and endocrine tissues. After a suitable fixation time, gonads were then transferred to 70% ethanol, and weighed using an electronic analytical balance (Handy H110, Sartorius).

Testes from postnatal males were preserved in a similar manner, with some slight differences. Testes to be frozen were de-capsulated and macerated to allow more efficient freezing. The length of time testes were fixed in Bouin's solution was dependent on the postnatal age at collection; 6 hours for testes from adult animals, and 3 hours for testes from younger animals. Generally halfway through fixation time, testes would be cut in half with a razorblade to aid fixation.

2.3.6 Fixed tissue processing

Once Bouin's fixed tissue had been transferred to 70% ethanol, it was processed by the histology department of the MRC Human Reproductive Sciences Unit, Edinburgh. Briefly, the tissue was processed through a series of graded alcohols using the 18 hour automated cycle on a Leica TP-1050 (Leica UK Limited, UK) tissue processor, and then embedded into molten paraffin wax by hand. These wax blocks were then allowed to cool and then stored at room temperature prior to sectioning (Section 2.6.2).

2.4 GC sorting from whole testis

In an attempt to isolate GC DNA from whole testis DNA (Section 5.3.3), a protocol was developed to isolate GCs from the whole testis. Previously, this has been done successfully in the postnatal testis of mice and primates (von Schonfeldt et al., 1999). The chosen method for cell sorting was to use Magnetic-activated cell sorting (MACS), which required only two stages; making a single cell suspension from whole testis and then using magnetic beads and antibodies to isolate GCs from that cell suspension.

2.4.1 Single cell suspension

To develop this protocol (adapted from in-house protocols from L. O'Hara and G. Cowan), excess rats from postnatal day 0 (birth) were used. These animals were killed and their testes dissected out, as described in Sections 2.3.1-2.3.4, except filter sterilised PBS (FS-PBS, Section 2.13) was used to reduce bacterial contamination of cell sorting. Testes from 4-5 rats were decapsulated and extensively macerated in 4.5ml of FS-PBS to break up the tissue using disposable plastic 1 ml syringes fitted

with 25G needles (Monoject, sterile needles, 0.5mm x 25mm). 500µl of 1mg/ml collagenase (Roche) was then added to the testes to help break cellular adhesion. The resulting 5ml solution was transferred into a flat-bottomed glass tube, and incubated at 32°C in a shaking waterbath for 15 minutes. 200µl of 1mg/ml DNase (Roche) was then added to the suspension, which was returned to the waterbath for a further 15 minutes. The resulting cellular solution was transferred to a 15ml Falcon tube and centrifuged for 5 minutes at 3000 rpm, and the supernatant was replaced with 1ml FS-PBS and the pellet resuspended. This washing of the pellet was repeated twice more. The cellular pellet was then resuspended in 500µl trypsin (0.5mg/ml trypsin in 0.2mg/ml EDTA, Roche), 4.5mls FS-PBS and 200µl DNase, and incubated at 32°C in a shaking waterbath for 5 minutes, to further break down cellular adhesion. The cell mixture was then dispersed using a 1ml pipette and filtered through a 70µm mesh filter (Millipore), to remove any remaining clumps of tissue. This cell mixture was then centrifuged for 5 minutes at 3000 rpm and washed in FS-PBS, twice more, before being finally resuspended in 1ml FS-PBS+0.1%BSA+10% normal sheep serum. At this point the cell suspension was counted using a haemocytometer (usually ~5 million cells/ml were present) and examined to make sure it consisted of single cells. Cells were left to rest/recover at 32°C in a lightly shaking waterbath for 1 hour prior to cell sorting.

2.4.2 Magnetic bead preparation

Whilst the single cell suspension was resting, the sheep anti-mouse antibody conjugated magnetic Dynabeads (Invitrogen) were prepared for cell sorting. Dynabeads were mixed within their container and 30µl was removed into an autoclaved 1.5ml Eppendorf tube. This tube was placed in a magnetic rack for two minutes, so that Dynabeads would separate from the storage solution, which was then removed. The beads were then removed from the magnet and resuspended in 1ml FS-PBS, before being returned to the magnet for a further two minutes to wash the beads. This wash was repeated again, until finally the beads were resuspended in 30µl FS-PBS. This prepared approximately 10 million Dynabeads for MACS, a slight excess beyond the target 4 beads per GC.

2.4.3 Magnetic-activated cell sorting (MACS)

From the 1ml single cell suspension, 500µl was removed and stored at -80°C as the Unsorted (US) fraction. The remaining 500µl solution was incubated with 2µg anti-SSEA1 antibody (Abcam, ab16285) for 1 hour at 4°C. Anti-SSEA1 proved to be the most efficient for MACS, though other GC surface antigens were attempted (e.g. cKIT, CD9, CD44). A GC surface antigen had to be used as whole, unlysed cells were present in the solution. After incubation with the antibody, the cell solution was washed by gently centrifuging at 1000rpm for 10 minutes and discarding the supernatant, before resuspending in 500µl FS-PBS. This wash was repeated twice more to remove any unbound antibody, leaving only the antibody bound to the GCs. 30µl of the prepared Dynabeads were then added to the cell solution, which was incubated for 30 minutes at 4°C on a gentle rocker, to allow the anti-mouse Dynabeads to mix throughout the solution and bind to the antibody labelled GCs. The cell solution was then placed in a magnetic rack for 2 minutes to separate the Dynabeads (and attached cells) from the cell solution. The cell solution was then removed and stored at -80°C as the Unbound (UB) fraction. The Dynabeads were then removed from the magnetic rack and resuspended in FS-PBS and stored at -80°C as the Bound (B) fraction. These cell fractions were then used for RNA analysis (Section 2.11).

2.5 In vitro culture

2.5.1 Testis explant preparation for in vitro culture

Testes with attached mesonephros were dissected out of e14.5 aged fetuses from untreated dams, as described in Section 2.3.3. Care was taken to remove testes and mesonephros without damage to ensure more successful *in vitro* culture. These testis explants were then cultured for between 48-72 hours with either no treatment or treatments designed to disrupt fetal testis development. The culture media and equipment used for these testis explants were optimised in this laboratory by Nina Hallmark (Hallmark et al., 2007).

2.5.2 Tissue culture conditions

Once testis explants were isolated from fetuses, experiments were performed in a sterile class 2 microbiological safety cabinet (BioMAT-2, MAT, Lancashire, UK), using standard aseptic techniques. Culture media was prepared as detailed below:

Stock Media: 500ml DMEM/F12 (Gibco Invitrogen Ltd.)
5ml Penicillin/Streptomycin (Sigma)
2.5ml Amphotericin (Sigma)

Culture Media: 48.5ml Stock Media (above)
1ml Sodium Pyruvate (Sigma)
0.5ml ITS liquid media supplement (Sigma)
1.5mg Bovine serum albumin (Sigma)

Once culture experiments were prepared, they were kept humidified and incubated using a HERACell 150 CO_2 incubator, for 48-72 hours in 95% air, 5% CO_2 and 37°C conditions (the temperature of *in situ* fetal testes).

2.5.3 Culture contamination

Testis explant *in vitro* cultures were at risk of contamination from a variety of microorganisms during dissection and culture preparation, so in addition to aseptic techniques being used wherever possible, anti-microbial agents were added to the media. The anti-microbials used were Penicillin/Streptomycin (Sigma; antibiotics) and Amphotericin (Sigma; antifungal), these were chosen as having been routinely used in cultures in-house and had not shown any adverse affects on cultured tissues.

2.5.4 Culture set up

Culture well inserts (Millicell 0.4 μm, Millipore, UK) were placed in 24 well culture plates (Corning, NY), 400μl of culture media (pre-warmed to 37°C) was then added to each well, 200μl within the insert and 200μl outside the insert. Testis explants were then placed onto the porous membranes of the culture well insert, with a maximum of 4 explants per insert. If testis explants were to be treated, chemical treatments would then be added to the culture well, in volumes/concentrations

described in Section 2.5.2, with half the volume within the insert and the other half outside the insert.

Every 24 hours, 200µl of culture media (and treatment) in the insert was replaced with fresh pre-warmed culture media (and treatment). 45 minutes to 1 hour prior to the end of the culture period, 200µl of culture media was removed and replaced with pre-warmed culture media containing an excess of BrdU (approximately 10µg/ml), and *in vitro* cultures were then returned to the incubator. At the end of the culture period, testis explants were carefully removed from inserts and either fixed in Bouin's for 30 minutes or snap frozen on dry ice, before being archived at -80°C. After 30 minutes of Bouin's fixation, testis explants were transferred to 70% ethanol and were processed into paraffin wax blocks, as described in Section 2.3.6.

2.5.5 Culture treatments

If testis explants were treated *in vitro*, the concentrations of treatment compounds in the culture media that were used are summarized in Table 2.3. For monobutyl phthalate and cyclopamine treatment, solvents were necessary and equivalent volumes of these were added to the media of the corresponding controls. These doses had previously been optimised within the laboratory.

Table 2.3 Summary of chemical treatments added to *in vitro* fetal testis explants.

Chemical Treatment	Source	Solvent	Target Conc.	Vol in 400 µl culture media
MBP	TCI, Europe	DMSO	1 x 10^{-3}M	10µl
DMSO	Sigma	-	-	10µl
Cyclopamine	In-house gift from Dr Axel Thomson	Ethanol	25µM	8µl
Ethanol	VWR International	-	-	8µl

2.5.5.1 Monobutyl phthalate (MBP)

MBP is the active metabolite of DBP, and has been used on both human and rat fetal testis explants to examine the effects of phthalate treatment directly (Hallmark et al., 2007). In that study, MBP treatment *in vitro* on e19.5 aged rat testis explants failed to

match observations *in vivo* of DBP exposure on Leydig cells and steroidogenesis. The present studies were more focussed on GC development and it was hoped that use of earlier aged testis explants treated with MBP would match *in vivo* effects. A high dose of 10^{-3}M MBP was used to maximise potential treatment effects. MBP was dissolved in dimethyl sulfoxide (DMSO, Sigma) as a solvent, so that an equivalent volume of DMSO was used as a control treatment.

2.5.5.2 Cyclopamine (Cyc)

Cyc is a steroidal alkaloid that inhibits the Hedgehog signalling pathway. Briefly, Hedgehog ligand inhibits the PTCH1 receptor, which removes the repression of SMO, which then stimulates transcription factors to induce the expression of certain genes. Cyc inhibits Hedgehog signalling by binding and blocking the SMO protein and so prevents the Hedgehog signal being transduced. In the mouse testis, DHH is thought to be produced by the Sertoli cell and acts through the PTCH1 receptor on the Leydig cell surface and other interstitial cells (Bitgood et al., 1996). In *Dhh* knock-out mice, fetal Leydig cells fail to differentiate and postnatally adult Leydig cells are lacking (Clark et al., 2000; Yao et al., 2002). *In vitro* mouse gonad organ culture using Cyc has showed that blocking DHH signalling in early testis development prevented Leydig cell differentiation (Yao et al., 2002).

Cyc was used in these experiments to investigate a chemical treatment that has many effects *in vivo* beyond the testis which limits utility in *in vivo* testis investigations, and one that could disrupt signalling between Sertoli cells and Leydig cells. Cyc treatment *in vitro* was performed at 25μM concentration with ethanol (EtOH) as a solvent, with an equivalent volume of EtOH used as a control treatment.

2.6 Protein investigations

2.6.1 Immunohistochemical (IHC) analysis

The major method to investigate protein expression in this thesis was through the use of specific antibodies on individual sections of Bouin's fixed tissue, in order to visualize both the localization and level of protein expression. The basic system used to perform this antibody detection is described below:

- Tissue sections were dewaxed and re-hydrated
- Antigen retrieval, if required for specific primary antibody
- Blocking of non-specific antigens and detection enzymes
- Primary antibody incubation
- Primary antibody detection using an amplification system
- Primary antibody visualization using colour reaction
- Counterstaining of non-stained tissue

During each IHC analysis, control slides were generated by incubating slides with normal serum instead of primary antibody to ensure IHC staining was succesful.

2.6.2 Sectioning

Tissue collected and fixed (Section 2.3.5) was embedded in wax blocks (Section 2.3.6) for sectioning. Wax blocks were chilled on ice for 30 minutes prior to sectioning; to harden the wax and aid cutting. Using a hand operated microtome (RM 2135, Leica), 5μm thick sections were then cut and floated onto warm (45-50°C) water. This enabled smooth unwrinkled wax sections to be placed on slides. If needed, sections were floated on 30% industrial methylated spirit (IMS, Fischer Scientific) prior to the water. Charged glass slides (SuperFrost Plus, Menzel GmbH & Co.) that were pre-labelled with animal codes and ages (automated slide labeller, Leica IP S) were used to ensure that tissue data was recorded on each slide. Once wax sections were placed on the individual slide, they were allowed to dry overnight in a metal rack in a 50°C oven.

2.6.3 Dewaxing and re-hydration

Slides were initially dewaxed by submerging them in Xylene for 5 minutes (twice), before being re-hydrated by being passed through a series of alcohols. These alcohols were: absolute alcohol (twice), 95% alcohol, 80% alcohol and finally 70% alcohol, spending 20 seconds in each. After 70% alcohol, slides were rinsed in tap water, prior to either antigen retrieval or blocking.

2.6.4 Antigen retrieval

In most cases, to allow antibody recognition in fixed tissue, antigen retrieval was performed. This is necessary as fixation with Bouin's, a formaldehyde based fixative, causes protein cross-links that can hide antigenic sites from antibody detection. Antigen retrieval breaks these cross-links, revealing the antigen sites (Shi et al., 1993). If antigen retrieval was required, dewaxed and re-hydrated slides were immersed in 2L of boiling citrate retrieval buffer, (0.01M citrate buffer, pH 6.0, Section 2.13), within a Tefal Clipso pressure cooker. The pressure cooker was then sealed and pressure set to the highest setting. Slides were pressure cooked for 5 minutes at maximum pressure, as evidenced by a continuous jet of steam from the cooker lid. Then the pressure was released and the entire pressure cooker removed from the heat. Slides and buffer were left to cool for 15-20 minutes, then additional tap water was added to cool slides to room temperature, before being blocked.

2.6.5 Blocking

After dewaxing, re-hydration and optional antigen retrieval, slides were incubated in 3% (vol/vol) hydrogen peroxide (VWR) in methanol for 30 minutes to block any endogenous peroxidase activity within the tissue; this prevents any non-specific background staining. Slides were then rinsed for 5 minutes in tap water followed by two 5 minute washes in Tris buffered saline (TBS, Section 2.13). Once the methanol/hydrogen peroxide was washed off, serum blocking was performed. Using an ImmEdge pen (Vector Laboratories, Inc. Burlingame, CA), a circle was drawn around the tissue section on each slide. This produced a hydrophobic barrier that ensured maximum coverage of sections with reagents, as well as aiding visualization of smaller sections.

Serum blocking was performed using normal serum (Diagnostics Scotland) diluted 1:5 in TBS with 5% bovine serum albumin (BSA, Sigma), this was done to block any non-specific binding sites and so reduce background staining. The serum used for blocking was dependent on the species the secondary antibody was raised in, such that rabbit serum would be used for blocking if a rabbit raised anti-mouse secondary antibody was used for detection.

2.6.6 Primary antibodies

After 30 minutes of blocking, serum was replaced with the primary antibody/serum solution for the IHC detection. Primary antibodies were diluted in normal serum/TBS/BSA, as described in Table 2.4 and then incubated overnight at 4°C in a humidity chamber.

Table 2.4 Details of primary antibodies used, and dilution used in single IHC.

Antibody	Source	Retrieval	Species	Dilution
AMH	Santa Cruz, CA	No	Goat	1:1000
BrdU	Fitzgerald industries, MA	Yes	Sheep	1:1000
cKIT	Santa Cruz, CA	Yes	Rabbit	1:50
CYP11A	Chemicon	No	Rabbit	1:300
DAZL	AbD Serotec	Yes	Mouse	1:300
DMRT1	Gift from David Zarkower, MN	Yes	Rabbit	1:2000
DNMT1	Abcam, Cambridge	Yes	Rabbit	1:50
DNMT3A	Abcam, Cambridge	Yes	Rabbit	1:250
DNMT3L	Abcam, Cambridge	Yes	Rabbit	1:100
OCT4	Santa Cruz, CA	Yes	Goat	1:100
PTCH1	Abcam, Cambridge	Yes	Rabbit	1:250
PTCH1	Santa Cruz, CA	Yes	Goat	1:200
SMA	Novocastra	No	Mouse	1:1000
SOX9	Santa Cruz	Yes	Goat	1:1000
VASA	Abcam, Cambridge	Yes	Rabbit	1:200
3β HSD	Gift from Ian Mason, Edinburgh	No	Rabbit	1:2000
5MeC	Abcam, Cambridge	Section 2.6.6.1	Sheep	1:250

2.6.6.1 5-methyl cytidine (5MeC)

IHC staining for 5MeC required a slightly altered protocol to allow the methylated cytidine residues to be detected by the antibody. Slides for 5MeC staining were dewaxed, rehydrated and blocked in methanol/hydrogen peroxide as normal. Then slides underwent a digest using 1mg/ml pepsin (Sigma) solution with 3% acetic acid (vol/vol) (BDH), for 15 minutes at 37°C using a water bath. After the pepsin digest, slides were incubated in 2M hydrochloric acid (VWR) for 20 minutes at 37°C. Slides were then serum blocked and the protocol continued as described in Section 2.6.7.

2.6.7 Secondary antibodies

After incubation overnight with the primary antibody at 4°C, the primary antibody was removed and the slides underwent two 5 minute washes in TBS to remove any of the unbound primary antibody from the slide. A biotinylated secondary antibody to the species the primary antibody was raised in, was diluted in the same type of serum used in the serum blocking step, as described in Table 2.5. The antibody/serum mix was then added to the slides, which were incubated at room temperature for 30 minutes. After this incubation time, the antibody/serum mix was removed from the slides which then underwent two 5 minute washes in TBS.

Table 2.5 Details of secondary antibodies and dilutions used for both single and double IHC.

Secondary Antibody	**Source**	**Dilution**
Rabbit anti-mouse biotinylated	DAKO, Cambridge	1:500
Rabbit anti-sheep biotinylated	Vector Labs, CA	1:500
Rabbit anti-goat biotinylated	Vector Labs, CA	1:500
Swine anti-rabbit biotinylated	DAKO, Cambridge	1:500
Goat anti rabbit biotinylated	Vector Labs, CA	1:500

To amplify the biotinylated secondary antibody signal, a streptavidin-horseradish peroxide (HRP) enzyme conjugate was used, where the streptavidin binds to the

biotin on the antibody and the HRP causes detection. Streptavidin-HRP was prepared by adding 1µl solution (Vector Labs) to 1ml TBS (1:1000 dilution). The final step in antibody detection was to expose the slides to a chromogenic substrate (DAB) (Section 2.6.9) that undergoes a colour change reaction in the region where the primary antibody had bound.

2.6.8 Double IHC

In order to perform GC proliferation index analysis (Section 2.8.3), and to calculate the percentage of GCs expressing OCT4 or DMRT1 (Section 2.8.4), or simply to examine two proteins in the same section, double IHC was performed requiring two different detection systems. To perform double IHC, primary antibody concentrations were adjusted, as described in Table 2.6.

Table 2.6 Details of primary antibodies used, and dilution used in double IHC.

Antibody	Source	Retrieval	Species	Dilution
AMH	Santa Cruz, CA	No	Goat	1:500
BrdU	Fitzgerald industries, MA	Yes	Sheep	1:500
DAZL	AbD Serotec	Yes	Mouse	1:100
DMRT1	Gift from David Zarkower, MN	Yes	Rabbit	1:1000
OCT4	Santa Cruz, CA	Yes	Goat	1:50
SMA	Novocastra	No	Mouse	1:500
VASA	Abcam, Cambridge	Yes	Rabbit	1:200

To perform double IHC, after chromogen detection of streptavidin-HRP the slides were not counterstained and mounted (Sections 2.6.10-2.6.11) but underwent two further 5 minute washes in TBS. After these washes, slides underwent a second serum blocking step as described (Section 2.6.5) for 30 minutes, before incubation overnight at 4°C with the second primary antibody to be used.

After overnight incubation with the second primary antibody, slides underwent two 5 minute washes in TBS before being incubated for 30 minutes with a second

antibody/serum mix, in the same manner as for single IHC. After another two 5 minute washes in TBS, slides were exposed to a different detection method, avidin conjugated alkaline phosphatase enzyme (DAKO). Avidin-alkaline phosphatase was diluted 1µl in 200µl TBS and incubated on the slides for 30 minutes at room temperature. Following two further 5 minute washes in TBS, slides were exposed to the Fast Blue chromogenic detection system (Section 2.6.9), such that brown DAB staining would visualize the first antibody and blue/purple Fast Blue staining would visualize the second antibody on the same tissue section.

2.6.9 Chromogen detection

Chromogen detection using either 3,3 DiAminoBenzidine (DAB) or Fast Blue was used to visualise the location within a tissue section at which the primary antibody had bound to its specific protein.

DAB was diluted from its concentrated form using a kit from DAKO, just prior to use. Upon application to slides, HRP action on DAB causes brown staining of tissue within 30 seconds to 5 minutes, depending on the primary antibody. After colour development, DAB was removed and the slides were washed in tap water for 5 minutes to prevent further development.

Fast Blue was made just prior to use by adding 1mg Fast Blue salt (Sigma), stored at -20°C to 1ml Fast Blue buffer (Section 2.13), stored at 4°C. This solution was then thoroughly mixed and filtered through a 0.2µm filter before being applied to the slides. Upon application to the slide, alkaline phosphatase action on Fast Blue solution causes blue/purple staining in tissue after around 20-30 minutes of development, which required the slides were kept in the dark. After colour development, Fast Blue solution was removed and slides were washed in PBS (Section 2.13) to prevent further development. If Fast Blue staining was performed, slides were not dehydrated or counterstained with haematoxylin, as Fast Blue is soluble in alcohol and staining would be lost. Instead, after washing in PBS, slides were mounted using glass coverslips (VWR International) and Permafluor aqueous mounting fluid (Beckham Coulter).

2.6.10 Counterstaining

Slides were counterstained using haematoxylin (Section 2.13) for 5 minutes, to ensure saturation of binding sites. Excess haematoxylin was then rinsed off by submerging slides in tap water, before being transferred to 1% acid alcohol (Section 2.13) for 10-20 seconds, to remove any non-specific background staining. Acid alcohol was then rinsed off by tap water and slides then transferred to Scott's tap water (Section 2.13), an alkaline solution, for 20 seconds. In this alkaline environment, haematoxylin staining of nuclei turned blue. Scott's tap water was then rinsed off by transferring slides to tap water again.

2.6.11 Dehydration and mounting

After counterstaining with haematoxylin, slides were dehydrated by passing them through a series of increasing concentrations of alcohol for 20 seconds at a time, going from 70% to absolute alcohol. Slides were then cleared by two 5 minute washes in Xylene, before being mounted using glass coverslips (VWR International) and Pertex mounting medium (Cell Path, Hemel Hampstead, UK), a solvent based glue. Once slides were mounted, the sections could be imaged (Section 2.6.13) and analysed (Section 2.8).

2.6.12 Terminal deoxynucleotidyl transferase dUTP nick end labelling (TUNEL)

In the last phase of apoptosis there is massive DNA fragmentation, which the TUNEL assay detects by labelling the terminal ends of nucleic acids (Negoescu et al., 1998). By using IHC to detect the labelled DNA strands, it is possible to visualize apoptotic cells in a tissue section. The TUNEL assay required a modified IHC protocol. Slides for TUNEL IHC were dewaxed, rehydrated and blocked in methanol as normal (Sections 2.6.3-2.6.5), but after methanol blocking slides underwent two 5 minute washes in PBS (Section 2.13). At this point slides were placed on ice and exposed to the TUNEL reaction solution of 1µl TdT (Roche), 5µl Dig-11-dUTP (Roche) in 1ml TUNEL reaction buffer (Section 2.13). Temporary coverslips (GelBond Film) were then placed on slides to prevent dehydration whilst slides were incubated at 37°C for 30 minutes to allow the TUNEL reaction to occur. After 30

minutes, slides underwent two 5 minute washes in PBS, before serum blocking (using normal rabbit serum (NRS)/BSA/PBS) for 10 minutes at room temp. Slides were then incubated with anti-Dig primary antibody (raised in Sheep, from Roche) diluted 1:100 in NRS/BSA/PBS, for 90 minutes at room temperature. After primary antibody incubation, slides underwent two 5 minute washes in PBS, before incubation with the secondary antibody, rabbit anti-sheep biotinylated, diluted in NRS/BSA/PBS as described in Table 2.5). From this point, IHC detection continued as described for DAB staining in Sections 2.6.7-2.6.9.

2.6.13 Imaging

Images were taken of mounted slides stained with IHC by using a Provis microscope (Olympus Optical AX70, London, UK) fitted with a DCS330 digital camera (Eastman Kodak, NY). Images were then edited using PhotoshopCS2 9.0 (Adobe Systems Inc, CA).

2.7 Immunofluorescent IHC

In order to investigate colocalization of GC proteins DAZL and VASA, and early testis proteins SOX9 and DMRT1 in Chapter 3, immunofluorescent IHC detection was used in a similar manner to standard IHC. Slides to be examined by immunofluorescence were prepared as described (Sections 2.6.3-2.6.5) until the serum blocking stage, where normal serums were diluted in 1:5 in PBS instead of TBS, and all washes in TBS washes were replaced with PBS.

2.7.1 First primary antibodies

After serum blocking, slides were incubated overnight at 4°C with the primary antibodies for either VASA diluted in swine serum/PBS (1:200), or DMRT1 diluted in swine serum/PBS (1:1000). After incubation overnight with the primary antibody, slides underwent two 5 minute washes in PBS to remove any of the unbound primary antibody from the slide. A swine anti-rabbit biotinylated secondary antibody was diluted in the swine serum/PBS 1:500. This secondary antibody/serum mix was then added to the slides, which were then incubated at room temperature for 30 minutes. After this incubation time, the antibody/serum mix was removed from the slides and

they underwent two 5 minute washes in PBS. From this point onwards, slides were kept in the dark to prevent bleaching of fluorescent signal.

2.7.2 Detection of first primary antibody

After PBS washes, slides were incubated with streptavidin conjugated to a fluorescent label that emits signal at a wavelength of 546 nm (Molecular Probes, Leiden, Netherlands), diluted 1:200 in PBS, for 60 minutes. Slides then had two 5 minute washes in PBS, before blocking in rabbit serum/PBS for 30 minutes.

2.7.3 Second primary antibodies

After the second serum blocking step, slides were incubated overnight with the second primary antibody, either DAZL diluted in rabbit serum/PBS (1:100), or SOX9 diluted in rabbit serum/PBS (1:500). After overnight incubation, slides were washed twice in PBS for 5 minutes, before being incubated for 30 minutes at room temperature with either a rabbit anti-goat HRP conjugated antibody (to detect SOX9) diluted 1:500 in rabbit serum/PBS, or rabbit anti-mouse HRP conjugated antibody (to detect DAZL) diluted 1:500 in rabbit serum/PBS. Slides then underwent two 5 minute washes in PBS.

2.7.4 Detection of second primary antibody

To detect the HRP conjugated secondary antibody, the tyramide signal amplification system (TSA, Perkin Elmer) was used, where the HRP catalyzes the deposition and binding of a labelled tyramide adjacent to the location of the HRP conjugated secondary antibody. Slides were incubated for 10 minutes with Tyramide-Cy5 diluted 1:50 with the supplied buffer. This resulted in VASA or DMRT fluorescing green, and DAZL or SOX9 fluorescing red. To remove any excess background tyramide staining, slides underwent two final 5 minute washes in PBS.

2.7.5 Counterstaining and imaging

To counterstain the immunofluorscent slides, the nuclear stain 4',6-diamidino-2-phenylindole (DAPI; Sigma) was used. Slides were incubated with DAPI diluted 1:1000 in PBS for 10 minutes, before being mounted using Permafluor (Section 2.6.8). These mounted slides were stored at 4°C in the dark to prevent loss of

fluorescence. Images were captured using an LSM 510 Meta Confocal microscope (Carl Zeiss).

2.8 Image analysis

To quantify GC number in a testis and to calculate the GC proliferation index and the percentage of GCs expressing either OCT4 or DMRT1, specialised stereological image analysis of IHC stained slides was performed. These investigations were achieved using a microscope fitted with a camera and motorised stage (Prior Scientific Instruments Ltd., Cambridge, UK), and ImagePro 6.2 computer software (Media Cybernetics, Wokingham, Berkshire, UK).

2.8.1 Calculation of GC number per testis

Sections of testis were IHC stained for either DAZL or VASA protein to label GC cytoplasm and then used to calculate GC number per testis using standard stereological techniques. This was of particular interest in relation to determining how *in utero* DBP exposure may be reducing GC number. IHC stained sections were examined under oil immersion using a Zeiss ×63 EC Plan objective fitted to a Zeiss Imager A1 microscope. The number of fields that were counted depended on the size of the testis section, but was usually between 30-60 random fields to ensure a percentage standard counting error below 5%. Fields were counted by recording points falling over GC nuclei, which was then expressed as a percentage of the total points counted, giving the percentage nuclear volume occupancy. This measurement of percentage nuclear volume was converted to absolute nuclear volume (of GCs) per testis by multiplying by testis weight, determined at collection (Section 2.3.2), or derived for testes collected at e14.5, e15.5 and e17.5 (Section 2.8.2). The testis weight (mg) is assumed to be equivalent to total testis volume (mm^3), as shrinkage was assumed to be minimal and the specific gravity of tissue is close to 1.

$$\text{Absolute volume } (mm^3) = (\%\text{ volume occupancy}/100) \times \text{testis weight (mg)}$$

GC absolute nuclear volume per testis can be converted into the GC number per testis, if mean nuclear volume of GC is calculated. The same IHC stained slides were again examined under oil immersion using a Zeiss ×63 EC Plan objective, and using the Stereology tool of ImagePro 6.2 (Media Cybernetics, Wokingham, Berkshire,

UK) the centre of a GC nucleus was selected, and then three lines from this centre were used to generate three diameter measurements (μm). From these diameter measurements the nuclear volume was calculated by the software, which assumed nuclei were spherical. As GC nuclei were broadly spherical, this was a good estimate of GC nuclear volume. At least 90 GC nuclei per testis section were measured in this manner, and the mean nuclear volume was then calculated. The number of GCs was then calculated by dividing the GC absolute volume by the mean GC nuclear volume:

$$\text{Number of cells (millions)} = \frac{\text{Absolute volume } (mm^3)}{\text{mean nuclear volume } (\mu m^3)} \times 1000 \text{ (to account for mg to } \mu m^3)$$

In this way, GC number of the whole testis was calculated from a single testis section. It should be noted that the Sertoli cell counts performed by H. Scott and S. Auharek, discussed in Section 4.3.1, were generated using the same method except using staining for WT-1 to identify Sertoli cells.

2.8.2 Calculating volume/weights of fetal testes

Testes taken from pups younger than e19.5 were too small to be weighed accurately using the electronic analytical balance (Handy H110, Sartorius). Therefore, in order to generate an approximate testis weight to compare control and DBP exposure for GC number, two different methods were used.

2.8.2.1 Calculating volume/weights of e17.5 testes

The weights of e17.5 testes used in this thesis were calculated by H. Scott during her thesis studies using the following method based upon Cavalieri's Principle. Briefly, an average weight/volume for control and DBP exposed testes was calculated by using three control and three DBP exposed testes that were each serially sectioned (Section 2.6.2). Then the first section, every fifth section and the final section were stained with haematoxylin to visualize the section. Each serial section was then measured for area, using Image-Pro Plus 4.5.1 software (Media Cybernetics, Wokingham, Berkshire, UK) at x10 magnification. As illustrated in Fig 2.1, the areas of adjacent sections (Section A and B,) were averaged and then multiplied by the

distance between them (Distance C), to give the volume. This was calculated for all serial sections to get an overall volume (μm^3), equal to weight (mg).

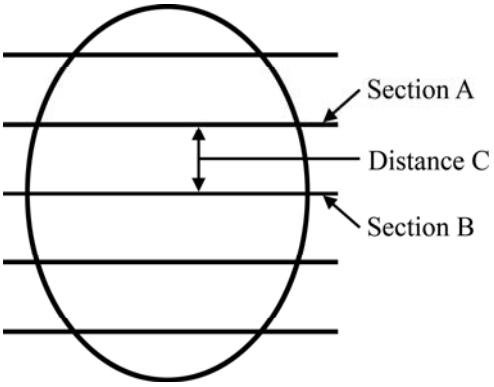

Figure 2.1 Representation of how testis volume at e17.5 was calculated. Taken from (Scott, 2007).

2.8.2.2 Calculating volume/weights of e14.5 and e15.5 testes

The H. Scott method for calculating testis weight was deemed unsuitable for testes taken from pups at e14.5 and e15.5, as serial sectioning is not as efficient at younger ages with smaller testes and haematoxylin staining of every fifth slide was viewed as too wasteful for the limited sections available from these ages. Instead, to calculate an average weight/volume for control and DBP exposed testes, three control and three DBP exposed litters at each age were used. During collection (prior to processing), images were taken of dissected testes from each male of these litters using Leica FireCam. These images were then analysed using ImagePro 6.2, to measure the dimensions of the each testes in each litter, as shown in Fig 2.2.

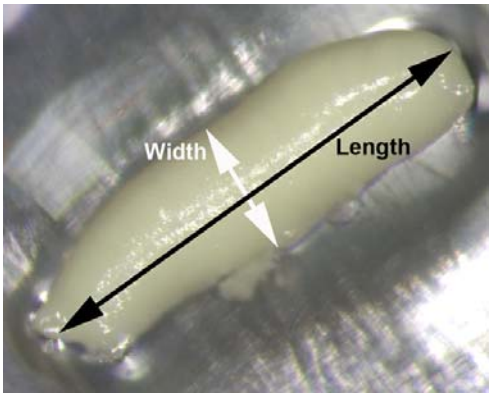

Figure 2.2 Photograph illustrating how e14.5 and e15.5 testes were measured to calculate testis weight.

At e14.5 and e15.5, the testis is broadly cylindrical so that the equation for calculating the volume of a cylinder was used to calculate testis volume (μm^3), equal to weight (mg). With testis width as an approximation of cylinder diameter.

$$\text{Volume of a cylinder } (\mu m^3) = \pi \times \text{radius}^2\ (\mu m^2) \times \text{length}\ (\mu m)$$

In this way, average testis weight at e14.5 and e15.5 was calculated and used to generate GC number data (Section 2.8.1) for these ages.

2.8.3 GC proliferation index

The proliferation index was calculated as the percentage of GCs that were positively stained for the proliferation marker BrdU (Section 2.2.3). This was calculated by double IHC staining for both a cytoplasmic GC marker (VASA or DAZL) and BrdU, before image analysis using a microscope with camera and motorised stage (Prior Scientific Instruments Ltd., Cambridge, UK), and ImagePro 6.2 computer software (Media Cybernetics, Wokingham, Berkshire, UK) as above. Between 30-60 random fields were counted, depending on the size of the testis, to generate a percentage standard error below 5% for counting. In each field, the number of BrdU-positive and BrdU-negative GCs were counted. From this data the GC proliferation index was calculated as follows:

$$\text{GC Proliferation Index} = \frac{\text{Number GCs expressing BrdU}}{\text{Total number GCs}} \times 100$$

2.8.4 Percentage of OCT4 or DMRT1 expressing GCs

To calculate the percentage of OCT4 expressing GCs at e17.5 in Section 4.3.1.3, or DMRT1 expressing GCs at e19.5 in Section 4.3.1.6, a similar method was used for determining the proliferation index, except using OCT4 or DMRT1 expression instead of BrdU.

2.8.5 GC position at postnatal day 6

At postnatal day 6, the position of GCs within the seminiferous cords was investigated as discussed in Section 4.3.3.4. By using double IHC for SMA to

identify the PTMCs and the GC marker VASA (Section 2.6.8), GC position was classed as centrally located, if no GC cytoplasm was touching the basal lamina, or basally located, if the whole GC was located at the basal lamina, or some of the cytoplasm was touching the basal lamina. This position was then calculated as a percentage, in a similar manner to the proliferation index (Section 2.8.3).

2.9 Western immunoblotting

Western immunoblotting was attempted during the course of these thesis studies, but failed to be an efficient use of animal material and few antibodies worked sufficiently well, therefore no Western blots are presented in the results Chapters. In brief, protein was extracted from frozen testis tissue by homogenization in RIPA buffer and then quantified using the Biorad assay (Bio-Rad, California, US). From this quantification, the sample volume needed to contain 10μg protein was determined which would then be loaded into sample wells after NuPAGE (Invitrogen, California, US) preparation. Samples were be loaded into a 10% NuPAGE Bis-Tris gel (Invitrogen), and fitted loaded into a gel tank containing 1x NuPAGE MOPS SDS running buffer (Invitrogen). The gel was run at 200V for 50 minutes, before being removed and transferred to a nitrocellulose Immobilon FP membrane (Millipore). After transferring, the membrane was washed and blocked to prevent non-specific protein binding using Odyssey blocking buffer (Li-Cor Biosciences, Cambridge, UK). The membrane would then be incubated with the primary antibody of interest and a loading control. These antibodies would be detected by fluorescently labelled secondary antibodies that were visualized using the Li-Cor Odyssey system and software (Li-Cor Biosciences).

2.10 DNA investigations

To investigate the methylation status of the *Oct4* gene in the fetal testis (Section 5.3.3), a series of DNA investigations were undertaken. This involved extraction of DNA from whole testes, quantification of the DNA extracted followed by bisulphite treatment of the DNA, before a standard PCR amplification of three regions of the *Oct4* promoter. These three regions were then sequenced and analysed.

2.10.1 DNA extraction

DNA was extracted from frozen whole testes from e19.5 and pooled (3-4) whole testes from e15.5 using a QIAamp DNA Micro extraction kit (Qiagen, Crawley, UK), utilising the manufacturer's solutions and the protocol for isolation of genomic DNA from tissue. Briefly, 180µl ATL buffer was added to frozen testes in 1.5ml tubes, and equilibrated to room temperature before 20µl Proteinase K was added and the mixture pulse vortexed. Samples were incubated overnight at 56°C to ensure complete lysis. After incubation, 200µl AL buffer was added and the solution pulse vortexed. Then 200µl of 96-100% EtOH was added and the tube thoroughly vortexed again. The entire solution was then transferred to a QIAamp MinElute column, and centrifuged for 1 minute at 8,000 rpm. The column was moved to a fresh 2ml collection tube, and 500µl of AW1 buffer was used to wash the column by centrifuging for 1 minute at 8,000 rpm. The column was again moved to a fresh 2ml collection tube, and 500µl of AW2 buffer was used to wash the column by centrifuging for 1 minute at 8000 rpm. The column was then transferred to another fresh 2ml collection tube and centrifuged for 3 minutes at full speed (14000 rpm) to dry the membrane. DNA was eluted from the column by adding 20µl nuclease free water, and then incubated for 2 minutes at room temperature, before centrifugation for 1 minute at full speed to collect the extracted DNA solution. DNA concentrations were measured using the Nanodrop spectrophotometer (Section 2.10.2). DNA was stored at -20°C before use.

2.10.2 DNA quantification

To quantify the extracted DNA, the Nanodrop-1000 spectrophotometer (Nanodrop Technologies, Delaware, USA) was used. 1.5µl sample was pipetted directly onto the measurement pedestal and the amount of 260nM UV light absorbed by the sample was measured and the Beer-Lambert law was used to calculate the concentration of the light absorbing molecule (DNA or RNA). To examine the purity of the sample, the Nanodrop also measured the amount of 280nM UV light absorbed, as this was absorbed by impurities such as proteins, salts and solvents. By using the ratio of 260nM:280nM, the purity of the DNA sample can be ascertained and values between 1.9-2.1 were acceptable for further use.

2.10.3 Bisulphite treatment of DNA

Bisulphite treatment of testis DNA was performed using the EZ DNA Methylation-Gold kit (Zymo Research Corp.). Bisulphite treatment causes the conversion of unmethylated cytidine to uracil, whilst methylated cytidine residues are unaltered. This converts methylation status into changes in the DNA sequence that can be identified by subsequent sequencing. The protocol and reagents used were provided by Zymo Research Corp. Briefly, 200ng DNA extracted and quantified as in Sections 2.10.1-2.10.2, was added to 130µl CT Conversion Reagent in a 0.2ml PCR tube. Samples were placed in a thermal-cycler for 10 minutes at 98°C, and then incubated for 2.5 hours at 64°C, before storage at 4°C. Samples were loaded into a Zymo-Spin IC column, containing 600µl M-Binding buffer and the resulting solution mixed by gentle inverting. The column was then centrifuged for 30 seconds at full speed (14,000 rpm). The column was then washed by adding 100µl M-Wash buffer and centrifuged for 30 seconds at full speed. Then 200µl M-Desulphonation buffer was incubated in the column at room temperature for 15 minutes. After incubation, the column was centrifuged for 30 seconds at full speed, followed by two washes using 200µl M-Wash buffer and centrifugation for 30 seconds at full speed. Finally, 10µl M-Elution buffer was directly added to the column matrix, and the column was added to a 1.5ml collection tube, and centrifuged briefly at full speed to elute the converted DNA. DNA was stored at -20°C before use.

2.10.4 PCR amplification of converted DNA

Bisulphite converted DNA was amplified for three regions of the rat *Oct4* gene promoter and proximal enhancer that contained several possibly methylated CpG dinucleotides. These regions were chosen based on the importance of methylation of the promoter and proximal enhancer regions in silencing of *Oct4* gene in both mice and human (Deb-Rinker et al., 2005; Freberg et al., 2007; Hattori et al., 2004). The primers were designed using MethPrimer (http://www.urogene.org/methprimer/index1.html), based on the Primer3 system that takes into account the conversion of cytidine residues by bisulphite treatment. The details of the primers used to amplify the three regions are shown in Table 2.7.

Table 2.7 Details of primers used to amplify bisulphite converted whole testis DNA.

Region of *Oct4* gene	**Forward Primer 5' → 3'**	**Reverse Primer 3' → 5'**
Promoter	GGGTTTTATGGTGTAGAGA TTTTTT	TCAACCTATATCCAAAACCA AAACTA
Mid proximal enhancer	TAATGGGATTTTGGAGGATT TTTA	CTCAAACCCAAATACCCCTA CTT
Far proximal enhancer	TTTAATTTGTTTATTGTGGG GAAGT	CACCCAACCCTTATATAAAA ATCCT

The DNA was amplified using the Platinum PCR SuperMix (Invitrogen), using 45µl Platinum PCR SuperMix, 2µl forward primer (200nM), 2µl reverse primer (200nM) and 1µl of converted DNA, so that the final PCR reaction was 50µl. This solution was mixed together in 0.2ml sterile thin walled PCR tubes (VWR International) and placed in a thermo-cycler with the following cycle times:

	94°C for 2 minutes
Then 35 cycles of	94°C for 30 seconds
	55°C for 30 seconds
	72°C for 1 minute

The amplified DNA product was then stored at 4°C prior to purification using the QIAquant PCR purification kit (Qiagen, Crawley, UK) and ran on a standard 1% agarose gel to check the success of the amplification.

2.10.5 Sequencing of converted DNA

Purified PCR product and PCR region primers were sent to the MRC Human Genetics Unit, Edinburgh for sequencing to be performed. The resulting sequence data was analysed using Vector NTI Version 10 software (Invitrogen), and the methylation status of CpG dinucleotides recorded.

2.11 RNA investigations

To investigate the relative mRNA expression levels of genes in the fetal rat testis, both during normal development and after DBP exposure, Q-RT-PCR was performed

using the Taqman system. This involved extraction of RNA from whole testes, quantification of the RNA extracted, followed by conversion to cDNA, before the Q-RT-PCR reaction and analysis.

2.11.1 RNA extraction

RNA was extracted from frozen whole testes using the RNeasy Micro kit (Qiagen, Crawley, UK), using the manufacturer's solutions and the protocol for purification of total RNA from animal tissue. Briefly, 350µl RLT lysis buffer was added to frozen testes that were then homogenized using a hand homogenizer (Kontes Pellet Pestle) on ice. After homogenization 350µl EtOH was added, and the lysate was then transferred into RNeasy mini columns and centrifuged for 15 seconds at 10,000 rpm. The flow through was then reloaded onto the column to maximise yield, before being centrifuged again for 15 seconds at 10,000 rpm. The resulting flow through was then discarded. The columns were then washed to remove impurities by adding 350µl RW1 buffer and centrifuged for 15 seconds at 10,000 rpm. On column DNase digestion was performed by incubating DNase (10µl DNase 1 stock and 70µl RDD buffer) for 15 minutes at room temperature. After incubation, 350µl RW1 buffer was added and the column was centrifuged for 15 seconds at 10,000 rpm. The column was then transferred to a new collection tube and 500µl RPE buffer was added before the column was centrifuged for 15 seconds at 10,000 rpm. 500µl 80% EtOH was then added to the column, which was centrifuged for 2 minutes at 10,000 rpm. The column was then transferred to a fresh collection tube and spun for 2 minutes at full speed to allow the membrane to dry. The RNA was then eluted by adding 20µl RNase-free water directly onto the membrane and then incubating at room temperature, followed by centrifugation for 1 minute at 10,000 rpm to collect the RNA. RNA concentrations were measured using the Nanodrop spectrophotometer, as described in Section 2.10.2 for RNA instead of DNA, and then stored at -80°C.

2.11.2 Preparation of cDNA for Taqman analysis

Due to the limited amount of RNA extracted from fetal tissues (~100ng/µl), the VILO cDNA synthesis kit (Invitrogen) was used to maximise the number of cDNA

preparations that could be made. This reaction system converted total RNA, including ribosomal RNA, as in the Taqman assay 18S (ribosomal RNA) is used as the internal positive control. Each cDNA synthesis 20µl reaction mixture was performed in 0.2ml sterile thin walled PCR tubes (VWR International), set up as follows:

5x VILO reaction Mix	4µl
10x Superscript Enzyme Mix	0.25µl
RNA (100ng/µl)	1µl
Nuclease free H_2O	14.75µl

The reagents were mixed together and placed in a thermo-cycler with the following cycle times:

25°C for 10 minutes

42°C for 60 minutes

85°C for 5 minutes

2.11.3 Quantitative RT-PCR

To asses the relative levels of RNA expression, Q-RT-PCR was carried out using the Taqman system devised by Applied Biosystems, using primers and probes designed using the Universal Probe library system (Roche). The principle of the Taqman system is that a probe was assigned for each reaction, so that it anneals to the cDNA between the forward and reverse primers of the gene of interest. Each probe consists of a reporter dye at the 5' end, 6-carboxyfluorescein (FAM), and a quencher dye at the 3'end, 6-carboxy-tetramethyl-rhodamine (TAMRA). The proximity of the quencher suppresses the fluorescence of the reporter. So whilst the probe is intact, no fluorescence occurs. During the Taqman amplification, the probe becomes cleaved through the action of the Taq polymerases moving in a 5' to 3' direction, this releases FAM dye and the fluorescent activity is recorded. This is repeated for every cycle, so that fluorescent activity increases every time the probe is cleaved, which is proportional to the amount of PCR product created. With each cycle the fluorescent activity is measured quantitatively by the sequence detection system.

2.11.4 Primer Design

Primers were designed for each gene of interest using the free Universal ProbeLibrary assay design centre at http://www.roche-applied-science.com/sis/rtpcr/upl/ezhome.html. For each gene of interest, this enabled design of the primer sequences and provided the number of the probe compatible from the Universal ProbeLibrary (Roche). The primers were then purchased from MWG Biotech, London, UK, which were then diluted to 20μM with nuclease free water. Table 2.8 summarizes the primer sequences and Universal Probe Library probes used in these present studies.

Table 2.8 Taqman primer sequences and Universal ProbeLibrary probe number.

Gene	**Forward Primer 5' → 3'**	**Reverse Primer 3' → 5'**	**UPL Probe Number:**
Amh	CTGGACACCGTGCCTTTC	CACTGTGTGGCAGGTCCTC	98
Boris	GAAGAAAAAGAAAGATGCGGTCT	GAGATCCGGCTCAGCATTT	82
Dazl	GCTCAGTTCATGATGCTGCT	ATGCTTCGGTCCACAGATTT	110
Dmnt1	CGATGACGATGAAAAGGACA	GTCTCCGTTTGGTGGCTAGA	26
Dmnt3A	AACGGAAGCGGGATGAGT	TGCAATCACCTTGGCTTTCT	75
Dmnt3L	GAGGGTGTGGAGCAACATTC	GCTCTTCCTTAGGGGTCAGG	41
Dmrt1	CAGAAGCCAAAGCAAGTGTG	AGCTGCTGGAGAGGGAAAC	129
Oct4	GAAGTTGGAGAAGGTGGACC	CCTTCTGCAGGGCTTTCATA	95
Ptch1	CAAAGCTGACTACATGCCAGA	GCGTACTCTATGGGCTCTGC	64
Smo	CAGGAGCTCTCCTTCAGCAT	CATTGAGTTCAAAAGCCAAACC	94
Vasa	CATTCAGAAGAGGTGGGAGAGA	TGCTGGTTTCCTAGAACCAAA	77
3β hsd	GACCAGAAACCAAGGAGGAA	CTGGCACGCTCTCCTCAG	105

2.11.5 Q-RT-PCR reaction

Samples to be analysed using the Taqman system were run in triplicate on a 96 well MicroAmp optical reaction plate (Applied Biosystems). For each sample, a tube containing the following was prepared, totalling 45µl:

2x Express Supermix	22.5µl
Forward primer (20µM)	0.45µl
Reverse primer (20µM)	0.45µl
Universal Probe (10µM)	0.45µl
18s (primers 1.33µM, probe 5.3µM)	0.3375µl
cDNA (Section 2.11.2)	4.5µl
Nuclease free H_2O	16.3125µl

Each Taqman reaction mixture was vortexed and then divided into three wells, with 15µl in each. When each sample was loaded, the entire plate was sealed with a MicroAmp optical adhesive cover (Applied Biosystems) and then loaded onto the ABI 7900 sequence detection system.

2.11.6 Analysis of results – comparative Ct method

The Taqman RT-PCR system provided the results as an amplification plot, which showed the amount of reporter dye/fluorescence generated during amplification and that is proportional to the amount of PCR product formed. The FAM Ct value was the cycle number at which the fluorescence rises above the threshold level, representing when the amount of amplified DNA becomes significant above the background level. This threshold level was determined at a point during the exponential increase of the PCR product. The FAM Ct value was dependent on the original amount of target mRNA in the reaction mixture, such that a difference in Ct value by one compared to a reference sample equated to a two-fold difference in RNA in the initial reaction mixture. 18S ribosomal RNA was used as an internal control, to adjust for mRNA variation between samples.

By analysing the differences in FAM Ct value compared to a reference control (usually adult rat testis or ovary), relative changes in RNA expression of the target

gene were calculated using the comparative Ct method. This required the calculation of the ΔCt value, which was the difference between the FAM Ct and the 18S Ct value for each of the three 15µl reaction wells for each sample. From these triplicates, the mean ΔCt for that sample was calculated. Using the mean ΔCt, the ΔΔCt was then calculated, which was the difference between the mean ΔCt of each sample compared to the mean ΔCt of the reference sample. In most cases, the reference sample was either adult rat testis total RNA or adult rat ovary total RNA, purchased from Applied Biosystems. However for some analyses, where the gene could not be detected in adult RNA, a fetal sample collected and processed in-house was used as the reference sample.

The amount of amplified target was calculated as $2^{-\Delta\Delta Ct}$, which was based on the mathematical equation for the exponential amplification of the PCR reaction $X_n = X_0 \times (1+E_x)^n$, where X_n is the number of target molecules at the threshold at cycle n, X_0 is the initial number of target molecules, $(1+E_x)$ is the efficiency of the target amplification and n is the number of cycles. If the efficiencies of the target and internal control reactions are equal, the $2^{-\Delta\Delta Ct}$ value provided a measure of relative quantification, showing the fold increase or decrease in mRNA expression in samples, in relation to the reference sample, which always has a $2^{-\Delta\Delta Ct}$ value of one.

2.11.7 Primer validation

Use of the Universal Probe Library assay design centre to design primers ensures that primers meet the necessary criteria for Taqman assay use. However if further validation was required for use with the comparative CT method, a five-fold series of diluted cDNA (made from rat testis total RNA) was run in triplicate whilst maintaining the concentrations of the other reagents. From the triplicate of each sample, the mean ΔCt was calculated. This value should be the same for each concentration, reflecting the dilution of both gene of interest and 18S (internal control). Plotting of mean ΔCt against log transformed initial cDNA concentrations should also generate a horizontal line.

2.12 Statistical analysis

Values are expressed as means ±SEM, and data were analysed using Student's unpaired *t* test, comparing between ages, between testis and ovary or between control and treated, using GraphPad Prism (version 5, GraphPad software Inc., San Diego, CA). In Figures 3.7 and 4.18, analysis of variance was performed using ANOVA followed by Bonferroni's multiple comparison test between each set of results using GraphPad Prism (version 5, GraphPad software Inc., San Diego, CA). Asterisks were used to denote any statistically significant differences, using the following criteria: * $P<0.05$, ** $P<0.01$ and *** $P<0.001$.

2.13 Commonly used solutions

Acid alcohol:
70% EtOH
1% concentrated HCl

Bouin's solution:
Purchased from Triangle Biomedical Sciences Ltd, Lancashire, UK.

Citrate buffer:
42.02g Citric acid monohydrate; Sigma)
1.9L distilled H_2O
Make up to 2L and pH to 6, using concentrated NaOH
Use at 0.01M, diluting 1:10 in distilled H_2O

Harris's Haematoxylin:
2.5g Haematoxylin + 25ml absolute alcohol
50g aluminium potassium sulphate + 500ml distilled H_2O
Combine solutions and boil
Add 1.25g mercury oxide
Cool solution on ice then filter
Add 4ml glacial acetic acid/100ml Haematoxylin

Fast blue buffer:
12.1g Tris (VWR International)
950ml distilled H_2O
Make up to 1L and pH to 8.2 using concentrated HCl
Take 98ml of this solution and add
20mg Napthol AS-MX phosphate
2ml Dimethyl formamide

PBS:
1 tablet of PBS concentrate (Medicago, Sweden)
1L distilled H_2O

Scott's Tap water:	10g Potassium chloride
	100g Magnesium sulphate
	Dissolved in 5L tap water
TBS:	60.5g Tris (Sigma)
	87.6g NaCl (Sigma)
	300ml Hydrochloric acid (BDH) 300ml
	Adjust to pH 7.4 using concentrated HCl
TUNEL buffer:	6ml of 0.5M Tris/HCl pH7.2
	100ml distilled H_2O
	2.99g Na Cacodylate
	0.195g CoCl
	Store at 4°C

3 Germ cell development during the last week of fetal life in the rat

3.1 Introduction

Studies of germ cells (GC) and gonad formation in the mouse, as reviewed in Section 1.3, have identified the series of events that GCs undergo during embryogenesis. In summary, specification as primordial GCs occurs around e_m7.25 (Ginsburg et al., 1990), long before the gonads are formed at e_m11 (Capel, 2000), GCs then migrate through the hindgut and arrive at the gonad around e_m11 (Molyneaux et al., 2001). As GCs migrate, they undergo several rounds of proliferation and express genes associated with pluripotency, which continues in the early gonad. Depending on the somatic environment of the gonad, GCs will begin differentiation into a gonocyte in the testis or an oocyte in an ovary. Proliferation stops as GCs either become arrested in mitosis or meiosis between e_m12.5 and e_m13.5, and enter a quiescent state until postnatal resumption of gametogenesis (McLaren, 2003). During this same time period, GCs undergo global demethylation and begin the epigenetic reprogramming required in postnatal life. Each of these varied processes can become dysregulated which would be expected to have serious postnatal consequences. In the human testis, such dysregulation of fetal GC function is suggested to alter GCs differentiation and result in the carcinoma in situ (CIS) cell, the pre-malignant precursor to testicular germ cell tumours (TGCT).

To investigate the processes of early GC proliferation and differentiation in the rat and their susceptibility to disruption with the aim of giving insights that might be relevant to CIS, a thorough investigation into GC development in the fetal rat gonad was undertaken. Using the processes identified from mouse studies, the timings and specifics of fetal GC development in the gonad were described in detail for both the testis and ovary in the rat. As dysregulated GC differentiation is thought to be the major factor in CIS origin, a particular focus on GC differentiation formed the basis of these investigations.

3.2 Materials and Methods

3.2.1 Animals

Briefly, control animals were collected at e13.5, e14.5, e15.5, e17.5, e19.5 and e21.5 and gonads dissected out (Section 2.3-2.3.4). Gonads were either fixed in Bouin's and processed for immunohistochemical analysis, or stored at -80°C for RNA analysis.

3.2.2 Immunohistochemical (IHC) analysis

Briefly, IHC staining (Section 2.6) was performed on processed and sectioned fetal testes and ovaries as summarised in Table 3.1. The number of fetal testes and ovaries used for IHC was a minimum of 5 testes or ovaries in each age group and came from a minimum of three different litters.

Table 3.1 Details of antibodies used in Chapter 3.

Antibody	Source	Retrieval	Species
AMH	Santa Cruz, CA	No	Goat
BrdU	Fitzgerald industries, MA	Yes	Sheep
DAZL	AbD Serotec	Yes	Mouse
DMRT1	Gift from David Zarkower, MN	Yes	Rabbit
OCT4	Santa Cruz, CA	Yes	Goat
SOX9	Santa Cruz	Yes	Goat
VASA	Abcam, Cambridge	Yes	Rabbit

Additional IHC analyses were performed to calculate the GC number in fetal testes (Sections 2.8.1-2.8.2.2) and GC proliferation index (Section 2.8.3).

3.2.3 Immunofluorescent IHC

Briefly, immunofluorescent IHC staining (Section 2.7) was performed on processed and sectioned testes for colocalization of GC proteins DAZL and VASA, and for early testis proteins SOX9 and DMRT1. Images were taken using a LSM 510 Meta

Confocal microscope and settings were maintained between sections examined to produce comparable images (Section 2.7.5). The number of testes used for immunofluorescent IHC was a minimum of 5 testes in each age group and came from a minimum of three different litters.

3.2.4 RNA analysis

Briefly, RNA isolated from frozen testes or ovaries was converted into cDNA (Section 2.11.2) and Taqman quantitative RT-PCR performed (Section 2.11.5), to establish quantitative mRNA expression levels. The genes investigated, and primers used, are listed in Table 3.2.

Table 3.2 Taqman primers and Universal Probe Library probes used in Chapter 3.

Gene	**Forward Primer 5' → 3'**	**Reverse Primer 3' → 5'**	**UPL Probe Number:**
Dazl	GCTCAGTTCATGATGCTGCT	ATGCTTCGGTCCACAGATTT	110
Dmrt1	CAGAAGCCAAAGCAAGTGTG	AGCTGCTGGAGAGGGAAAC	129
Oct4	GAAGTTGGAGAAGGTGGACC	CCTTCTGCAGGGCTTTCATA	95
Vasa	CATTCAGAAGAGGTGGGAGAGA	TGCTGGTTTCCTAGAACCAAA	77

3.3 Results

3.3.1 Primordial germ cell migration

In the fetal rat, the earliest age that gonads could be visually identified and successfully removed during micro-dissection was embryonic day (e)13.5. At this age, there were no gross morphological differences between the sexes. To identify if sexual differentiation had initiated by e13.5, immunohistochemical (IHC) staining for SOX9 was performed as it is upregulated in pre-Sertoli cells and is a primary event in testis formation. It was used to establish the sex of the e13.5 gonad (Fig 3.1A and B). To determine if GC migration into the gonad had occurred by e13.5,

double IHC staining for the pluripotency factor OCT4 and the GC specific marker DAZL was performed (Fig 3.1C and D).

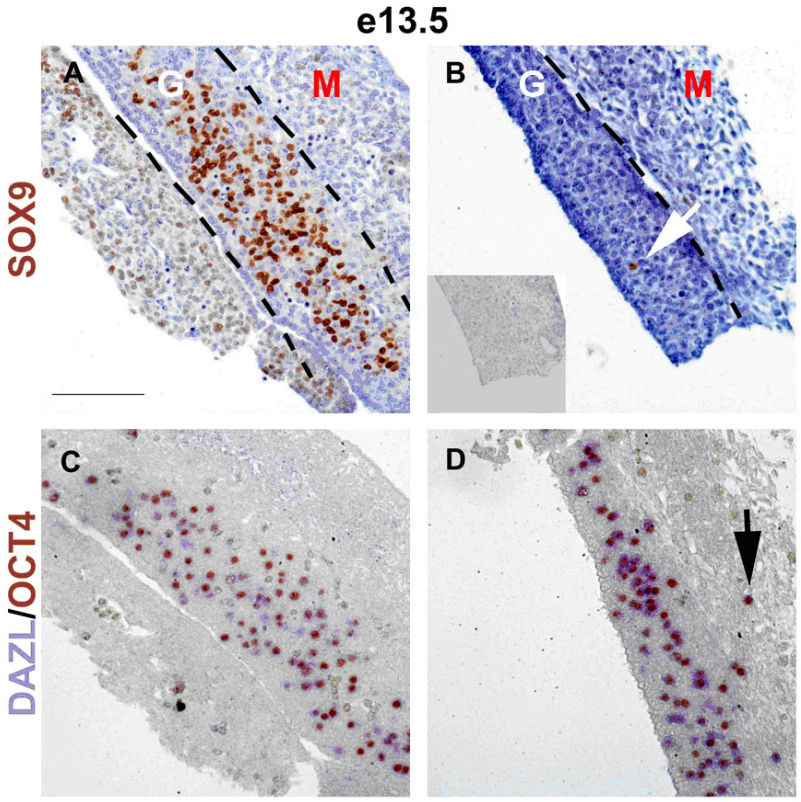

Figure 3.1 Panels A and B show representative photomicrographs of immunostaining for SOX9 in e13.5 fetal rat gonads (Dab = brown). Panels C and D show representative photomicrographs of DAZL (Fast blue = blue) and OCT4 (Dab = brown) in the same e13.5 fetal rat gonads as shown in A and B. White arrow depicts an isolated SOX9 cell in a presumptive ovary. In Panels A and B, G=gonad and M=mesonephros. Black arrow depicts isolated mesonephric GC. Insert in panel B shows a negative control for SOX9. Scale bar in panel A represents 100µm.

By e13.5, GC migration into the gonad is nearly completed in the fetal rat, with only isolated single GCs remaining in the mesonephros (Fig 3.1D) and by e14.5 GCs were only detected in the gonad (data not shown).

Expression of the GC protein VASA was also investigated at e13.5 and was barely detectable by IHC (data not shown). Similarly, the Sertoli cell protein Anti Müllerian Hormone (AMH) was also undetectable by IHC at e13.5, identifying this time point as around the time of sexual differentiation in the fetal rat. Due to the difficulty in

obtaining tissue from fetuses younger than e13.5 and the observation that GC migration into the gonad is more or less completed by e13.5, younger ages were not investigated.

3.3.2 Sexual differentiation and seminiferous cord formation

By e14.5, in contrast to e13.5, there was a clear sexual dimorphism of the gonads. This was evident during microdissection as an increased gonad size and conspicuous cord formation which gave the testes a "striped" appearance in contrast to ovaries. To examine this further, IHC for AMH was performed on e14.5 fetal rat testis sections and showed that AMH was detectable at this age, as the Sertoli cells become organised around GCs into seminiferous cords, as shown in Fig 3.2. Fetal rat ovaries showed no AMH staining in fetal life, as demonstrated by the insert in Fig 3.2B.

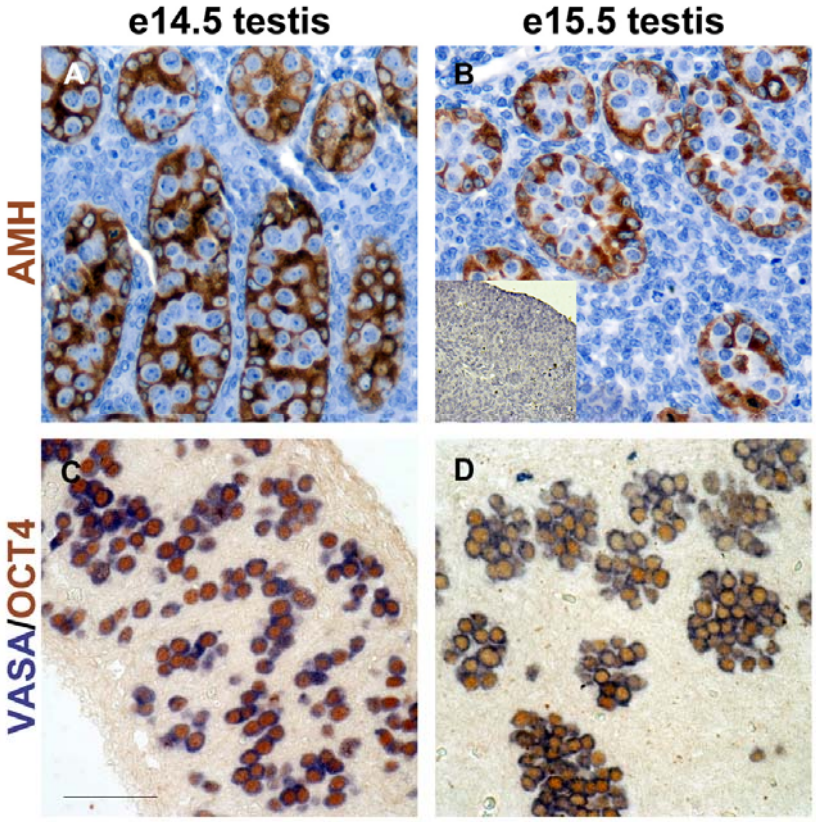

Figure 3.2 Representative photomicrographs of immunostaining for AMH in e14.5 fetal rat testis in panel A and, e15.5 fetal rat testis in panel B (Dab = brown). Panels C and D show representative photomicrographs of VASA (Fast blue = blue) and OCT4 (Dab = brown) in the e14.5 fetal rat testis (C) and e15.5 fetal rat testis (D). Insert in panel B shows negative staining for AMH in the e15.5 fetal rat ovary. Scale bar in panel C represents 50µm.

3.3.3 Germ cell distribution and protein expression

In the e14.5 fetal rat testes, the GC specific markers OCT4, VASA and DAZL were expressed (Fig 3.2 and data not shown) in the all GCs. In the fetal rat ovary at e14.5, similar GC protein expression was seen (data not shown). Between the ages of e14.5 and e15.5, the arrangement of GCs in the early seminiferous cords changed from a more 'single cell' distribution (Fig 3.2C) to central aggregation (Fig 3.2D). GC aggregations remain in the fetal rat testis until e21.5, and will be discussed in greater detail in Section 4.3.1.8. For the clarity of figures in the rest of this chapter, e14.5 gonads show the same GC protein expression patterns as e15.5 gonads unless otherwise stated.

3.3.4 Germ cell increase in the developing gonad

Having examined the early events of GC migration and seminiferous cord formation in the fetal rat, GC number in the developing gonad was investigated using IHC staining for VASA or DAZL to label GCs for counting, as shown in Figs 3.3 and 3.4. Due to the small size of the rat ovary throughout fetal life, reliable measurements of ovarian weight could not be obtained. As gonad weights are crucial for the determination of GC number (Section 2.8.1), GC counts were only performed on fetal testes, shown in Fig 3.3. The overall change in GC number in the developing gonad is illustrated in Fig 3.4, contrasting the difference between rat testes and ovaries.

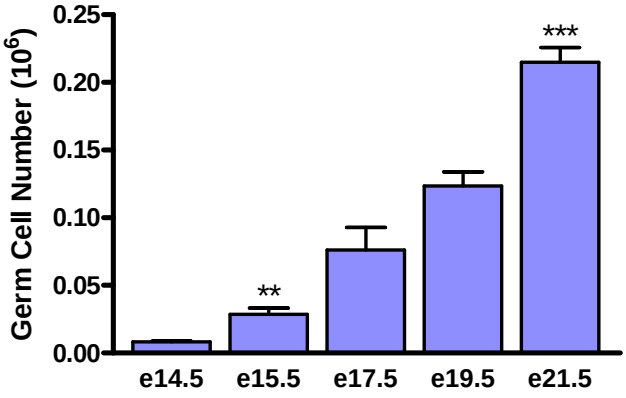

Figure 3.3 Number of germ cells in testes of animals between e14.5 and e21.5 (n=8 for e17.5, n=5 for others). Values are means ± SEM. Student's unpaired *t* test was performed, ** P<0.01 between e14.5 and e15.5, ** P<0.001 between e19.5 and e21.5.

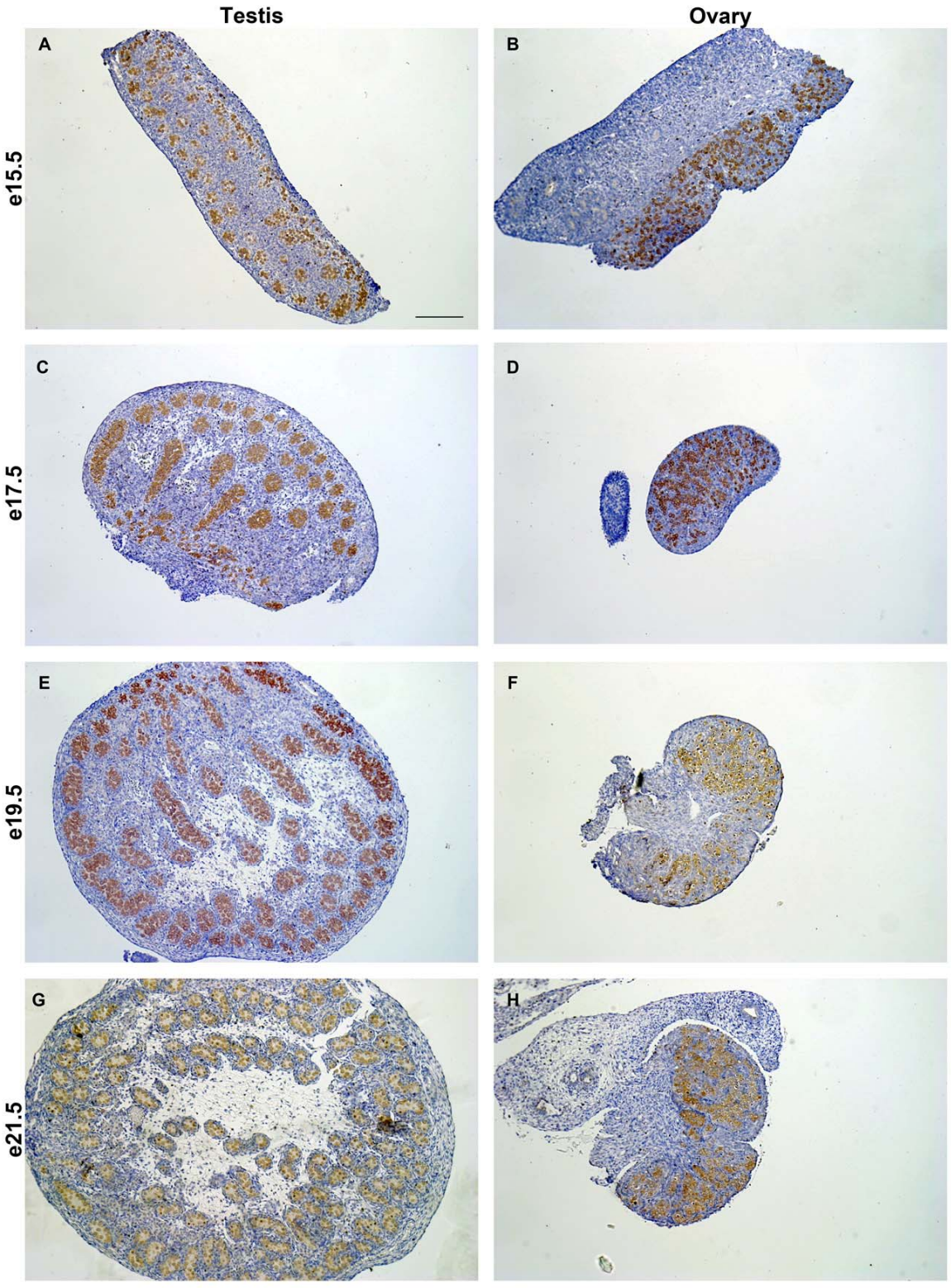

Figure 3.4 Representative photomicrographs of immunostaining for VASA (Dab = brown) in fetal testis (left) and ovary (right) from e15.5 (top) through to e21.5 (bottom). Scale bar in panel A represents 100µm.

Fig 3.3 shows how the number of GCs increased in the fetal rat testis over time, with a significant increase between e14.5 and e15.5, and again between e19.5 and e21.5. This increase in GC number was visualised (Fig 3.4), by VASA IHC and also illustrates the morphological changes that occur in the last week of fetal life in the rat. The fetal testis becomes much larger, especially in comparison to the ovary after e15.5. This increase in testis size has been studied with respect to the contribution of increasing number of the different somatic cell types of the testis (as quantified in (Hutchison et al., 2008; Scott et al., 2008) for Wistar rats that were kept, collected and analysed in the same manner as this thesis. In addition, Fig 3.4 shows that VASA IHC staining of GCs remained relatively constant during e15.5-21.5, in comparison to both OCT4 (Fig 3.6) and DAZL (Fig 3.9).

3.3.5 Germ cell proliferation index

To further examine the increase in GC number, GC proliferation was examined in the fetal rat gonads by performing double IHC staining for Bromo deoxyuridine (BrdU) and DAZL. As described in Section 2.2.3, BrdU labels proliferating cells in the developing fetus and when combined with the GC marker DAZL allowed proliferating and non-proliferating GCs to be identified and the determination of the GC proliferation index (Fig 3.5).

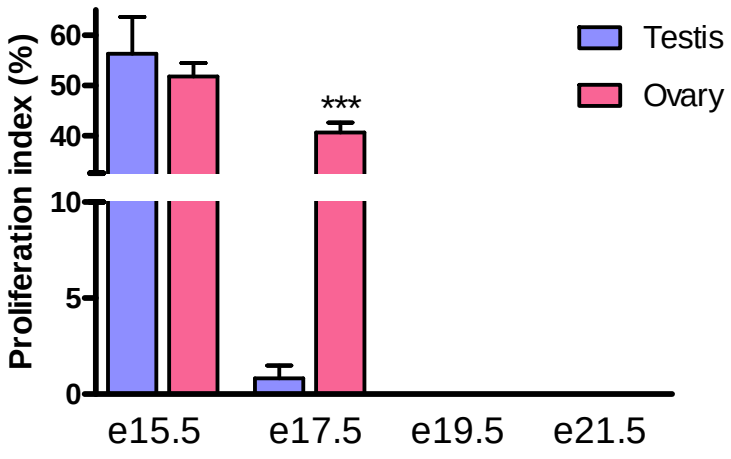

Figure 3.5 Germ cell proliferation index of fetal rat testes (blue bars) and ovaries (pink). n=5 for each age and sex, except for e15.5 ovary where n=6. Student's unpaired *t* test was performed, *** P<0.001 between testis and ovary.

GC proliferation was high in both the ovary and testis at e15.5, but at e17.5 GC proliferation in the testis had dropped to near zero whereas it remained high in the ovary. In both testis and ovary, no proliferating GCs were observed after e19.5, showing a difference in timing of cessation of GC proliferation (entry into quiescence) between testis and ovary.

However as described in Fig 3.3, GC number continued to increase after e17.5 when proliferation was completed. This is most likely due to differential errors in determining testis weights/volumes (Section 2.8.2) at the different fetal ages. This will be discussed in greater detail in Section 4.3.1, with respect to DBP exposure.

3.3.6 OCT4 expression in the developing gonad

As discussed in Sections 1.3.3, the pluripotency gene Octamer-binding transcription factor 3/4 (*Oct4*) is an early PGC marker in the mouse that is lost as GCs differentiate. To examine *Oct4* expression in the fetal rat, double IHC for OCT4 and VASA was performed (Fig 3.6).

Previously in this Chapter, IHC staining of OCT4 was shown to be present in GCs of both sexes at e13.5 (Fig 3.1C and D) and e14.5 (Fig 3.2) and remained in all GCs at e15.5 but declined thereafter. By e17.5 there was a mix of OCT4+ and OCT4- GCs (Fig 3.6C and D) and by e19.5, OCT4 expression was undetectable in all GCs, indicating loss of pluripotency (Fig 3.6E and F and data not shown for e21.5). In the e17.5 fetal rat ovary, there was relatively fewer OCT4+ GCs compared to the testis, as highlighted in Fig 3.6D.

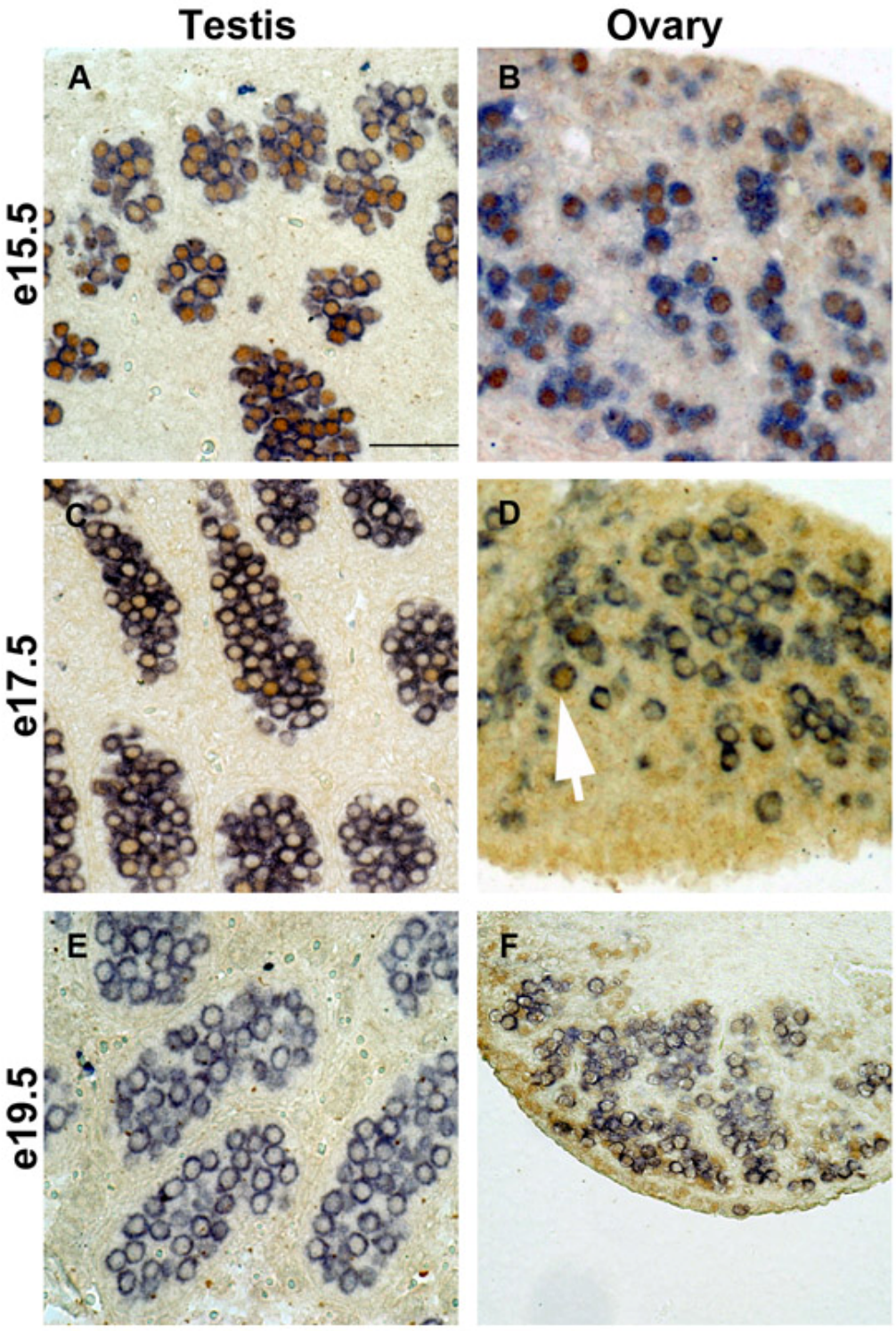

Figure 3.6 Representative photomicrographs of immunostaining for OCT4 (Dab = brown) and VASA (Fast blue = blue) in fetal testis (left) and ovary (right) from e15.5 (top) to e19.5 (bottom). White arrow depicts an OCT4 positive, VASA positive ovarian GC. Scale bar in panel A represents 50µm.

To complement IHC analysis of OCT4, *Oct4* mRNA levels were quantified over the same time period using Taqman (Section 2.11) for the testis (Fig 3.7) and ovary (Fig 3.8). As different control values were used to generate the following graphs, care should be taken when comparing these two figures. It should also be noted that whole testes or ovary were used for RNA extraction, not isolated cell types.

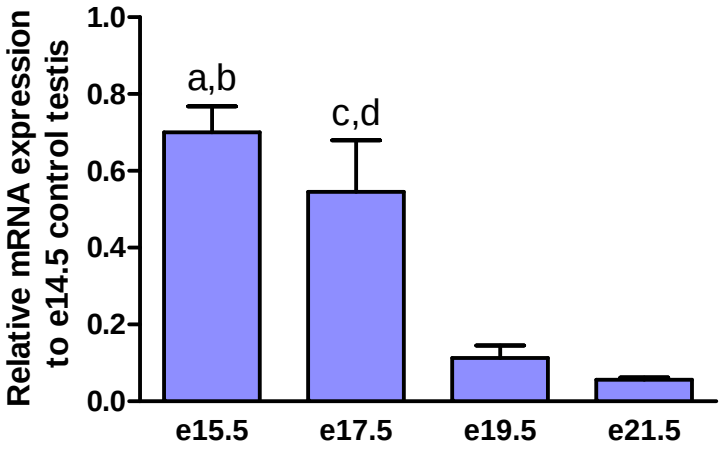

Figure 3.7 Quantitative analysis of *Oct4* mRNA levels in fetal rat testis at e15.5, e17.5, e19.5 and e21.5, (n=6 for each age). Values are means ± SEM. ANOVA followed by Bonferroni's multiple comparison test was performed. a= *** P<0.001 between e15.5 and e19.5, b= *** P<0.001 between e15.5 and e21.5, c= ** P<0.01 between e17.5 and e19.5 and d= ** P<0.01 between e17.5 and e21.5.

In the fetal rat testis, relative *Oct4* expression decreased over time, reducing significantly between e15.5-e17.5 and e19.5-e21.5 (Fig 3.6). Interestingly, *Oct4* mRNA was still detectable in e19.5 and e21.5 testes when OCT4 was no longer detectable by IHC. This may indicate that transcriptional mechanisms do not regulate OCT4 protein levels alone in the rat testis. In this Taqman assay, *Oct4* mRNA was also detectable in adult rat control testes in which OCT4+ cells are also undetectable by IHC (adult RNA purchased from Applied Biosciences, data not shown).

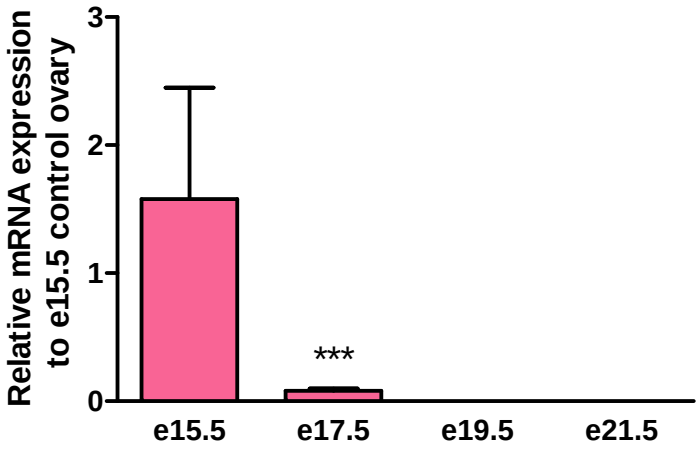

Figure 3.8 Quantitative analysis of *Oct4* mRNA levels in fetal rat ovary at e15.5, e17.5, e19.5 and e21.5, (n=6 for e15.5 and e17.5, n=5 for e19.5 and n=3 for e21.5). Values are means ± SEM. Student's unpaired *t* test performed on log transformed values, *** P<0.001 between e15.5 and e17.5.

In the fetal rat ovary, *Oct4* mRNA reduced between e15.5 and e17.5 and became undetectable at and beyond e19.5 in this assay, closely mirroring the OCT4 IHC results in Fig 3.6. In addition *Oct4* mRNA was not detected in the adult rat ovary (purchased from Applied Biosciences). Whilst it is important not to over-analyse, this sex-specific difference in *Oct4* expression profile over time may indicate both that different *Oct4* gene regulation occurs between the sexes in the rat.

3.3.7 DAZL expression in the developing gonad

Deleted in Azoospermia Like (*Dazl*) is a GC-specific gene, which is important in both male and female fertility, described in more detail in Sections 1.3.5-1.3.6. IHC analysis of DAZL during the last week of fetal life in the fetal rat gonad was performed (Fig 3.9).

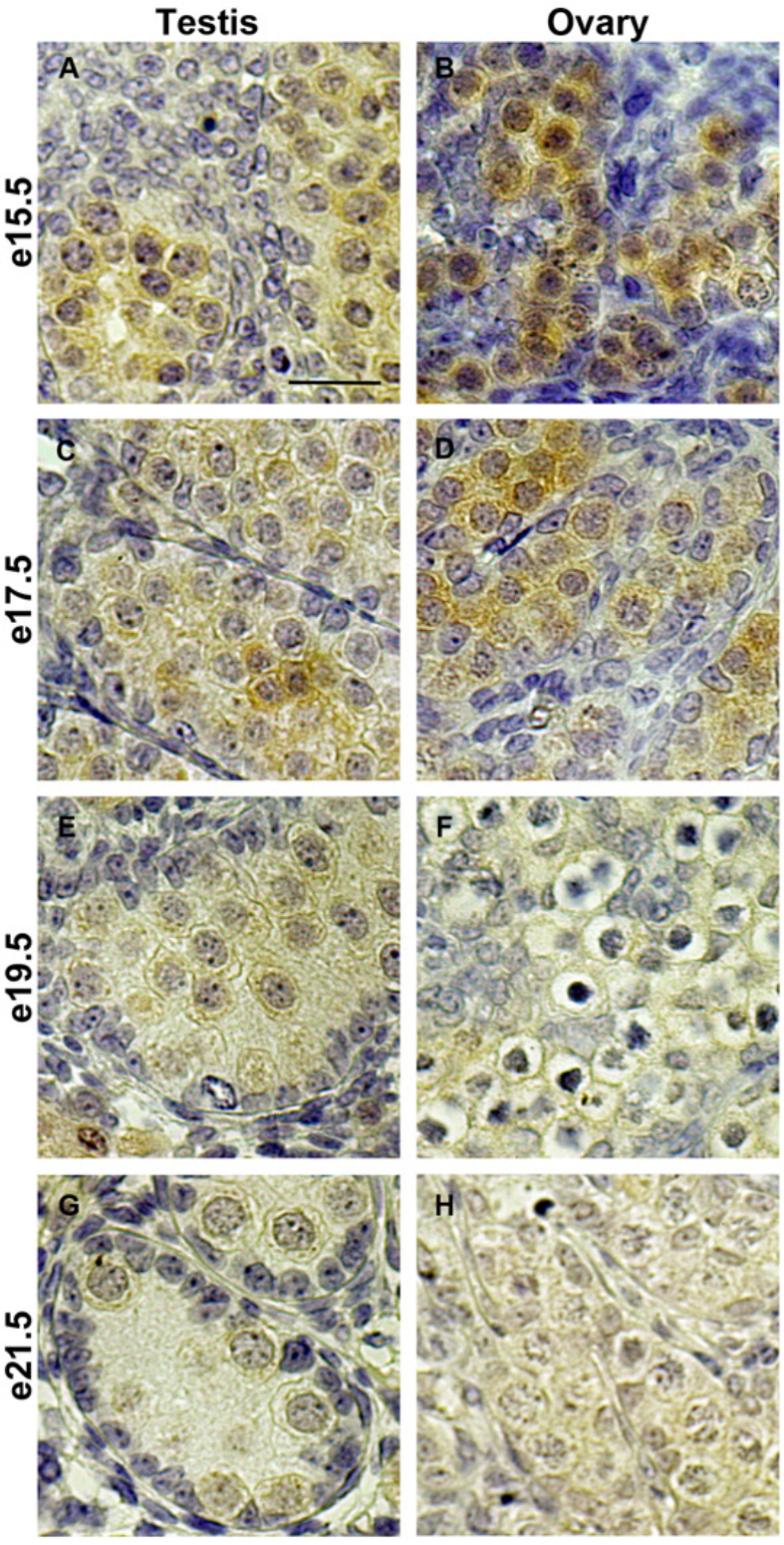

Figure 3.9 Representative photomicrographs of immunostaining for DAZL (Dab = brown) in fetal testis (left) and ovary (right) from e15.5 (top) through to e21.5 (bottom). Scale bar in panel A represents 50µm.

DAZL staining was intense in GCs at e15.5 and e17.5 but became weaker (but still detectable) at e19.5 and e21.5 for both ovary and testis. A similar reduction in DAZL in GCs has not been previously reported in other species, so this may be a rat-specific change. Attempts to quantify this reduction level of DAZL protein by Western blot proved unsuccessful, meaning that this potentially interesting aspect of DAZL expression cannot be confirmed.

Dazl gene expression was also examined using mRNA analyses by Taqman in the testis (Fig 3.10) and ovary (Fig 3.11). As with all Taqman analyses in this Chapter, whole gonads were used to extract RNA and different controls (adult gonads) were used for ovarian and testicular samples.

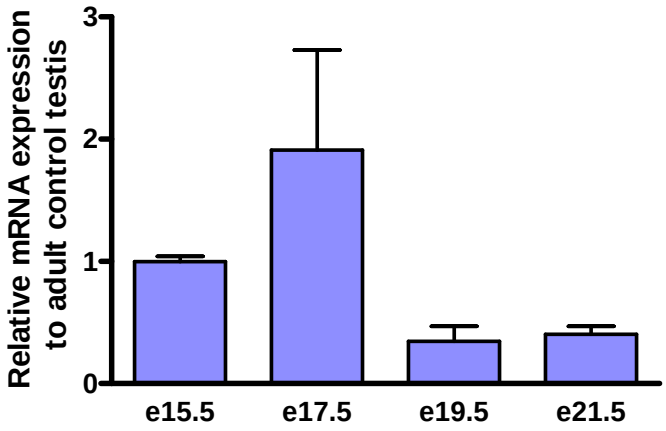

Figure 3.10 Quantitative analysis of *Dazl* mRNA levels in fetal rat testis at e15.5, e17.5, e19.5 and e21.5, (n=6 for each age). Values are means ± SEM. No statistically significant differences.

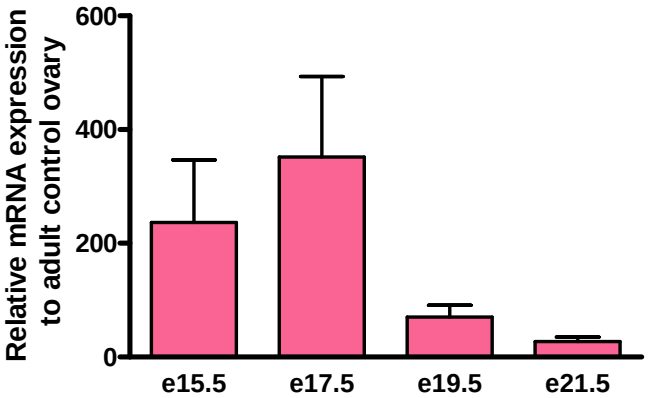

Figure 3.11 Quantitative analysis of *Dazl* mRNA levels in fetal rat ovary at e15.5, e17.5, e19.5 and e21.5, (n=6 for e15.5 and e19.5, n=5 for e17.5 and e21.5). Values are means ± SEM. No statistical significant differences.

Relative *Dazl* mRNA expression for both fetal testis and ovary shared a similar profile, with a slight increase between e15.5-e17.5 and then a decrease from e19.5 onwards, which supports the DAZL IHC results. Of note is that relative *Dazl* expression in the fetal rat ovary (Fig 3.11) is much higher than in the adult rat ovary (reference control), especially in comparison to the fetal versus adult testis comparison (Fig 3.10).

3.3.8 VASA expression in the developing gonad

Mouse Vasa Homologue (*Vasa*) is a GC-specific gene that is necessary for postnatal spermatogenesis. IHC analysis of VASA in the fetal rat gonad showed that it is barely detectable at e13.5 (data not shown), but from e14.5 until adulthood it remained a GC-marker that was not lost during differentiation (e.g. OCT4) and did not show variable expression over time (e.g. DAZL), as illustrated earlier in Fig 3.4. This makes it an important GC-specific gene to analyse as a relative "constant" in relation to these other genes, especially in regard to relative mRNA expression studies. *Vasa* mRNA expression was examined in the fetal testis (Fig 3.12 A and B) and ovary (Fig 3.13). Further analysis at each age to adjust for GC content of whole testis was performed by dividing by estimated GC number (Fig 3.3) and testis weight (Section 2.8.2) to determine how individual GC *Vasa* mRNA expression changed over time, and are shown in Fig 3.12B.

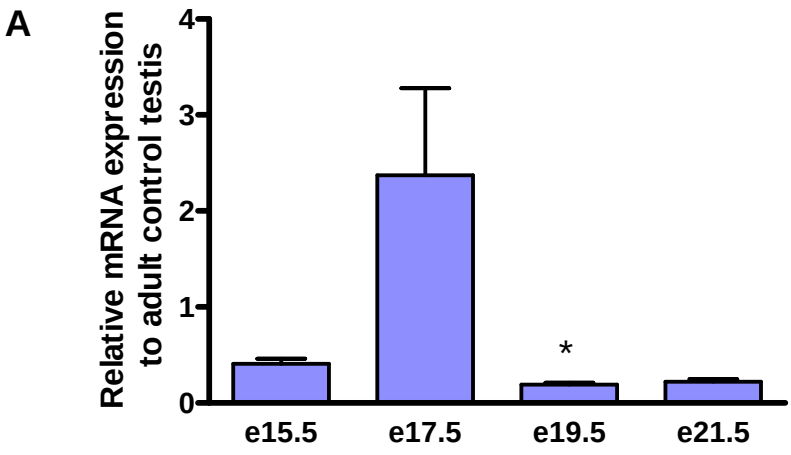

Figure 3.12 **A:** Quantitative analysis of *Vasa* mRNA levels in fetal rat testis at e15.5, e17.5, e19.5 and e21.5, (n=6 for each age). Values are means ± SEM. Student's unpaired *t* test was performed, * P<0.05 between e17.5 and e19.5.

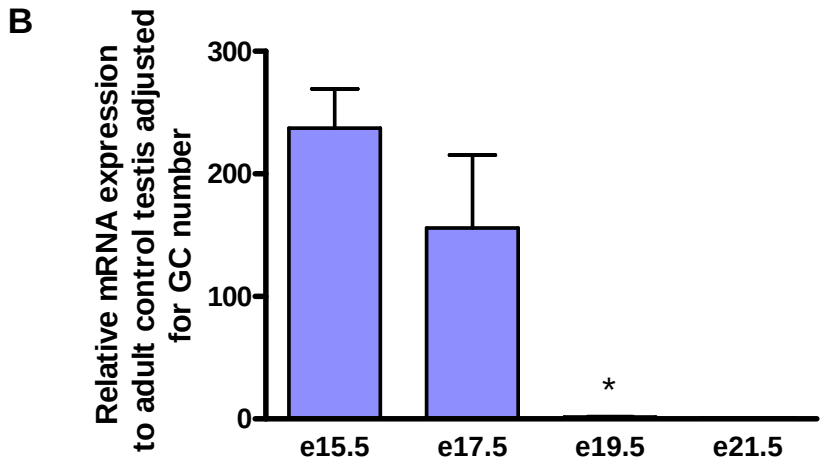

Figure 3.12 **B:** Quantitative analysis of *Vasa* mRNA levels in fetal rat testis at e15.5, e17.5, e19.5 and e21.5, (n=6 for each age) adjusted for GC number and testis weight. Values are means ± SEM. Student's unpaired *t* test was performed, * P<0.05 between e17.5 and e19.5.

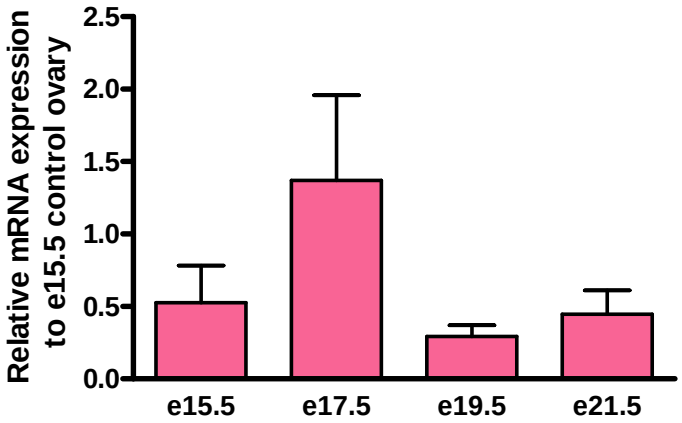

Figure 3.13 Quantitative analysis of *Vasa* mRNA levels in fetal rat ovary at e15.5, e17.5, e19.5 and e21.5, (n=6 for e17.5 and e21.5, n=5 for e15.5 and n=4 for e19.5). Values are means ± SEM. No statistically significant differences.

Relative *Vasa* mRNA levels in both sexes shared a similar pattern to *Dazl*, with an insignificant increase at e17.5 followed by a reduction afterwards. Adjusting for GC number supported the reduction of *Vasa* mRNA per GC from e15.5 to e21.5.

3.3.9 DAZL and VASA co-expression in the testis

To identify if DAZL and VASA stain different sub-populations of GCs in the fetal testis with IHC, co-localization immunofluorescent IHC for DAZL and VASA

protein was performed (Section 2.7) and visualized by confocal microscropy (Fig 3.14).

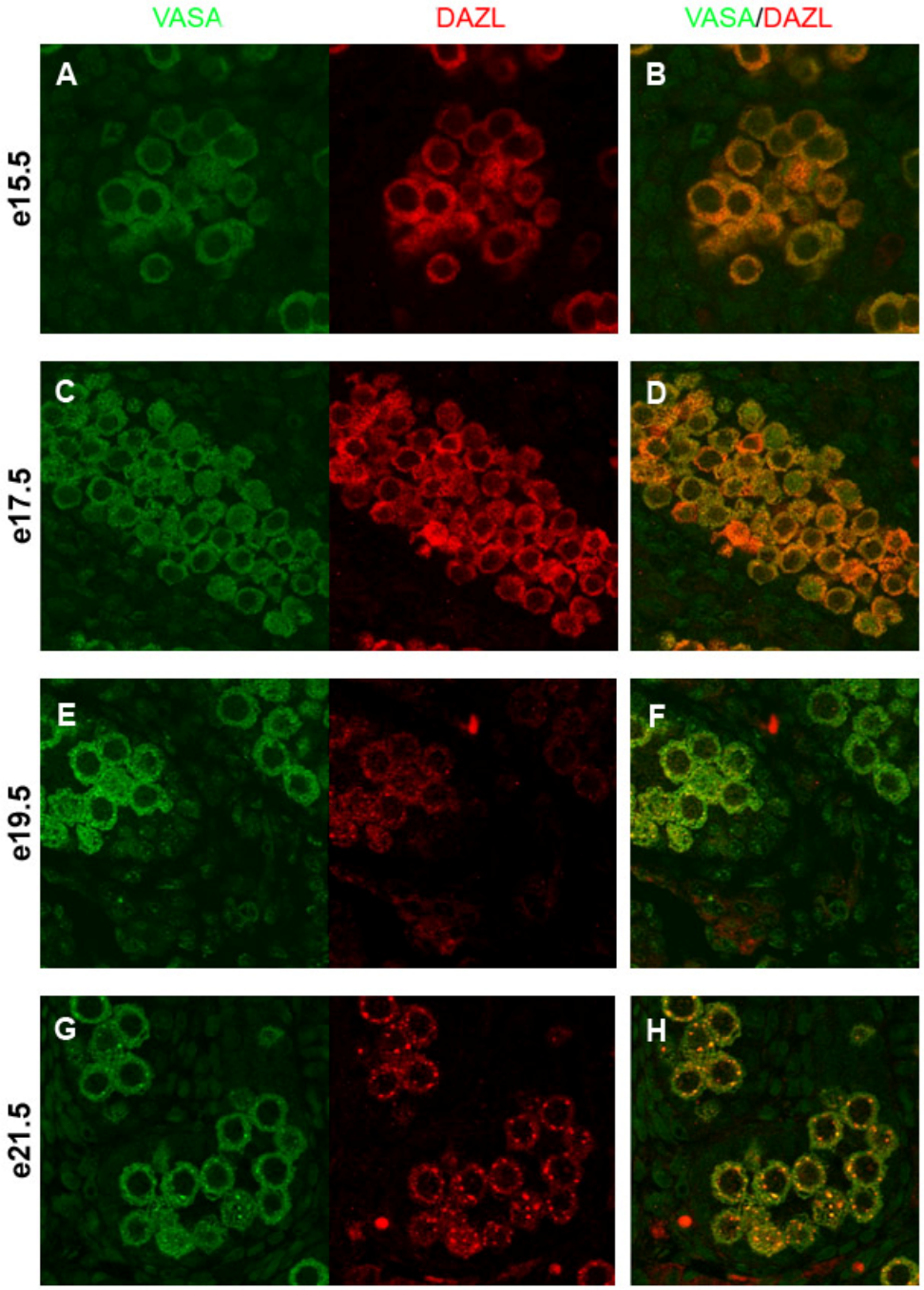

Figure 3.14 Representative confocal photomicrographs of immunostaining for VASA (green) and DAZL (red) in fetal rat testis at e15.5 (A and B), e17.5 (C and D), e19.5 (E and F) and e21.5 (G and H). Panels on the left side show individual staining for VASA and DAZL, and the panel on the right shows the merged image to highlight co-localization.

Throughout the last week of fetal life in the testis DAZL and VASA protein co-localized, even both exhibiting the slightly punctate expression at e19.5 and e21.5. As with DAZL IHC analysis alone (Fig 3.9), there was a reduction in DAZL protein visualized at e19.5 and e21.5 compared to the younger ages. Whilst it is possible this observation could be a result of differences in acquisition during the confocal imaging, the maintenance of settings between slides and ages make this unlikely.

DAZL and VASA co-localization was also examined during postnatal testis development, as shown in Fig 3.15. In early postnatal testis development, DAZL and VASA protein continued to co-localize. However in the adult rat, defined as over 3 months old in these studies, a difference in DAZL and VASA localization can be seen as DAZL expression is only expressed in spermatogonia and spermatocytes at the base of the tubule, and is lost as GCs proceed into spermatogenesis.

From these co-localization studies, DAZL and VASA can be used as interchangeable GC markers for these studies which are focused only on fetal and early postnatal testis development.

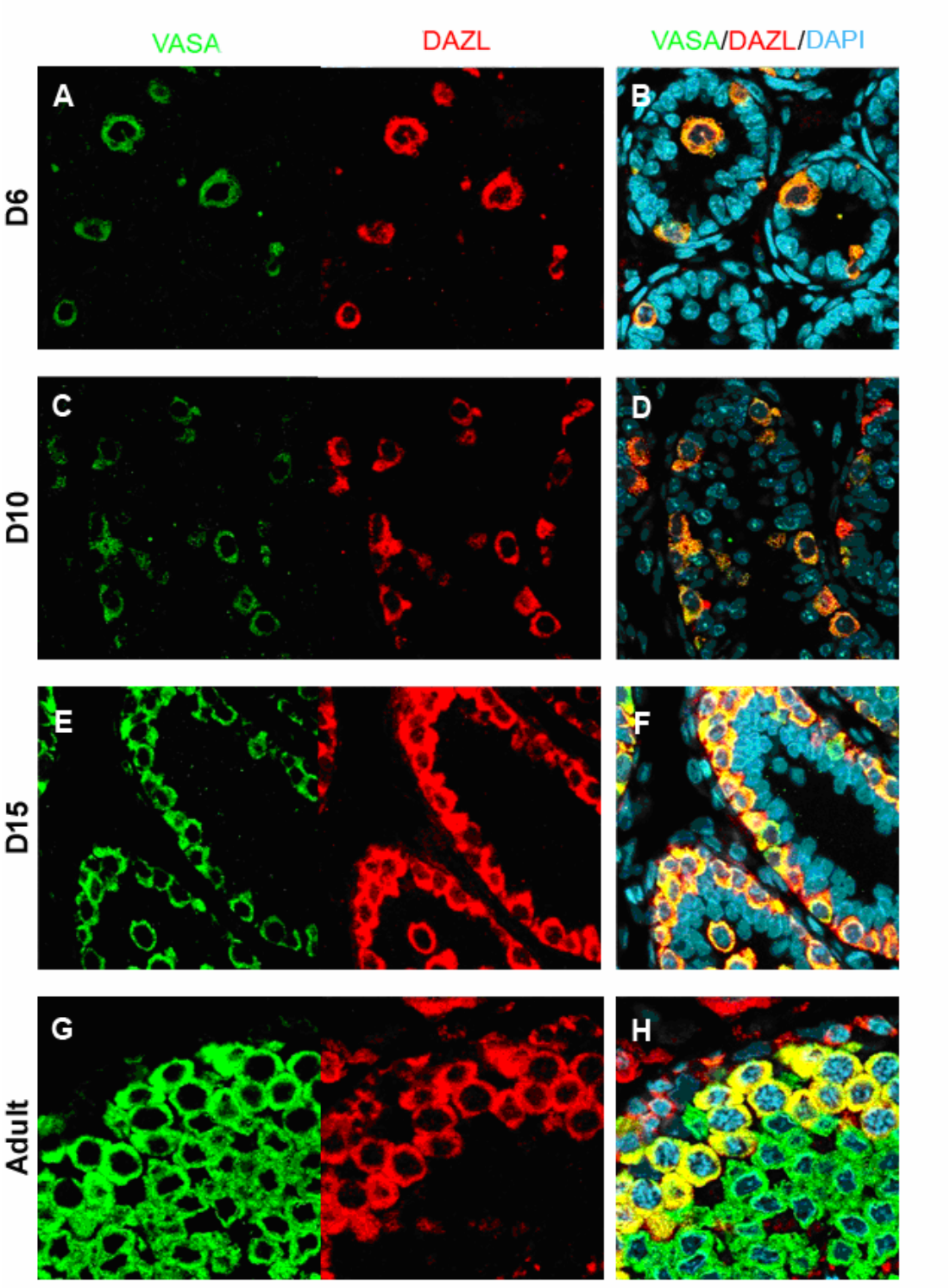

Figure 3.15 Representative confocal photomicrographs of immunostaining for VASA (green), DAZL (red) and DAPI (blue) in rat testis at postnatal day(D) 6 (A and B), D10 (C and D), D15 (E and F) and adulthood (G and H). Panels on the left side show individual staining for VASA and DAZL, and the panel on the right shows the merged image to highlight co-localization and DAPI (blue) nuclei staining. Note DAPI staining has been turned off in the two lefthand panels.

3.3.10 DMRT1 expression in the developing gonad

Doublesex- and mab-3 related transcription factor 1 (*Dmrt1*), a gene that is important in postnatal testis differentiation. As described in Section 1.2.2.2, *Dmrt1* is expressed in both Sertoli and GCs of the fetal mouse testis and remains expressed in the testis into adulthood (Raymond et al., 2000). In contrast in the fetal mouse ovary *Dmrt1* expression was absent after e_m15.5 and undetectable in the adult mouse ovary (Raymond et al., 1999a). This suggests an importance for *Dmrt1* in both fetal GC development and in the postnatal testis. In the fetal rat gonads, DMRT1 expression was examined by IHC during the last week of fetal life in both testes in ovary as shown in Fig 3.16.

In the fetal rat ovary, DMRT1 expression was GC-specific at e15.5-e17.5 but became undetectable after e19.5. In the fetal rat testis, a more complex pattern of DMRT1 protein expression was evident, with both Sertoli and GCs staining strongly until e19.5, when DMRT1 expression was switched off in GCs, similar to the ovary (Fig 3.16 E and F). These findings agree with the mouse studies, in which it has been shown that expression in Sertoli cells and in GCs may be driven by different promoter regulation (Lei et al., 2009).

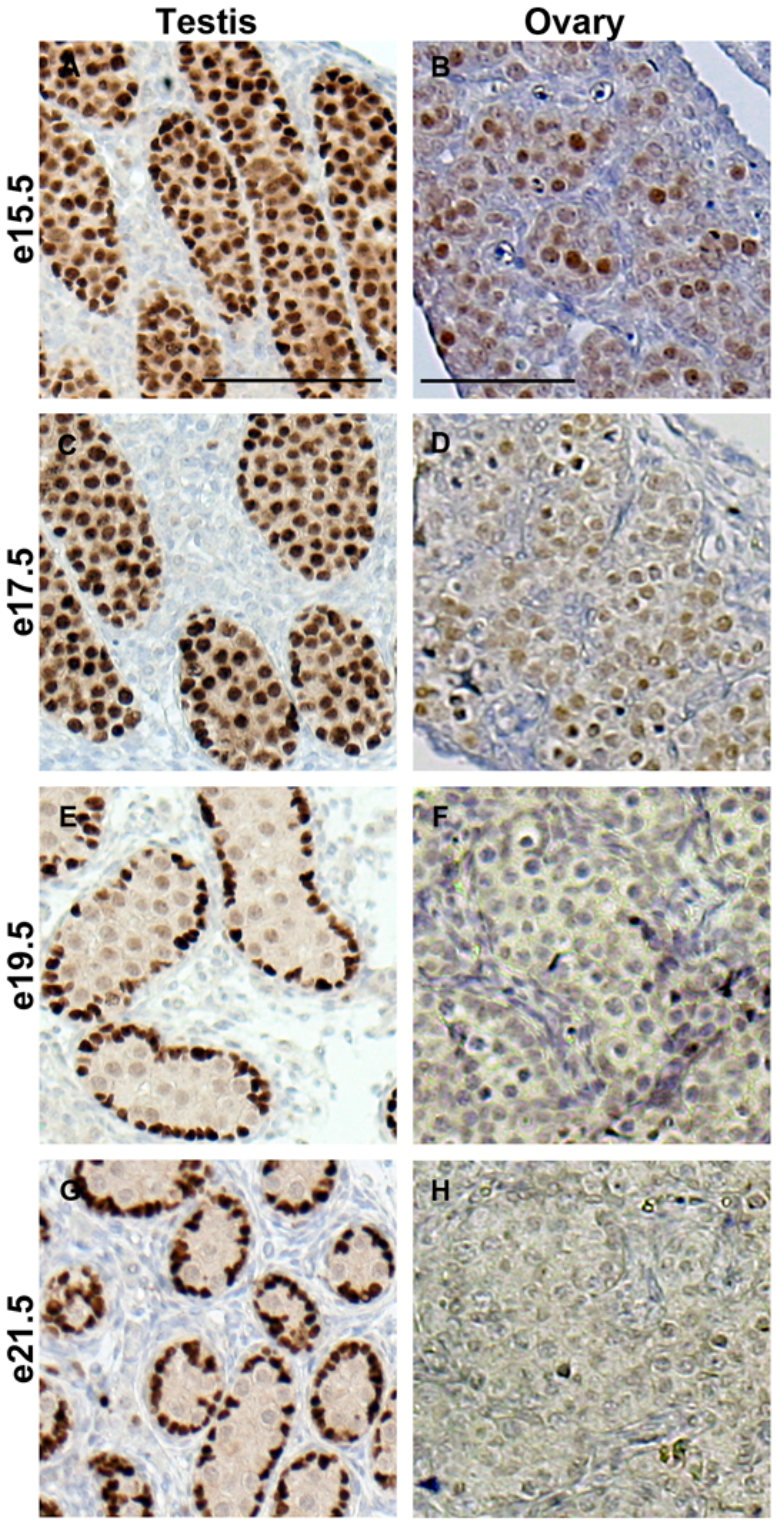

Figure 3.16 Representative photomicrographs of immunostaining for DMRT1 (Dab = brown) in fetal rat testis (left) and ovary from e15.5 (top) through to e21.5 (bottom). Scale bar in panel A represents 50µm for the testes panels. Scale bar in panel B represents 50µm for the ovarian panels.

Dmrt1 mRNA analysis was performed in fetal rat testis and ovary, in Figs 3.17 and 3.18 below. As with all Taqman analyses, whole gonads were used to extract RNA and different controls were used for ovarian and testicular samples.

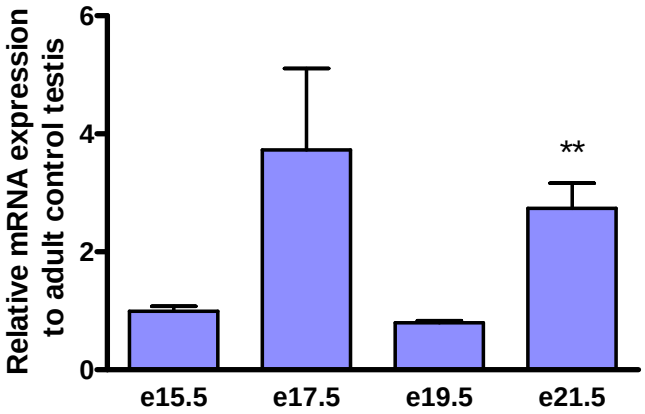

Figure 3.17 Quantitative analysis of *Dmrt1* mRNA levels in fetal rat testis at e15.5, e17.5, e19.5 and e21.5, (n=6 for each age). Values are means ± SEM. Student's unpaired *t* test was performed, ** P<0.01 between e19.5 and e21.5.

In the fetal rat testis, *Dmrt1* expression changes were confounded by both Sertoli and GC expression being detected at e15.5-e17.5. Nevertheless, the reduction at e19.5 is likely due to silencing of GC-specific *Dmrt1*, and the significant rise at e21.5 may be due to the substantial increase in Sertoli cell number by the end of gestation (Scott et al., 2008).

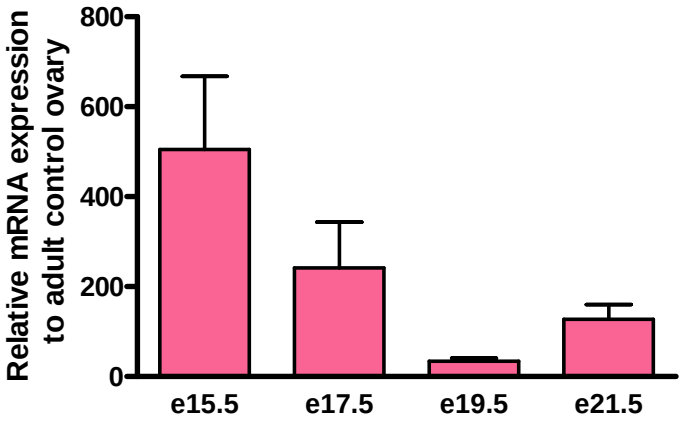

Figure 3.18 Quantitative analysis of *Dmrt1* mRNA levels in fetal rat ovary at e15.5, e17.5, e19.5 and e21.5, (n=6 for each age). Values are means ± SEM. No statistically significant differences.

In the fetal rat ovary, without somatic cell *Dmrt1* expression, GC specific *Dmrt1* was still detectable (background noise) after e19.5 and even showed some evidence of an increase at e21.5. As with several other GC genes in the ovary, there was a much higher level of relative expression compared to the (control) adult rat ovary (Fig 3.18).

To identify if DMRT1 expression was differentially expressed in Sertoli and GCs in the early fetal testis, confocal microscopy of e13.5 testes was performed with double IHC staining for SOX9 and DMRT1 as shown in Fig 3.19.

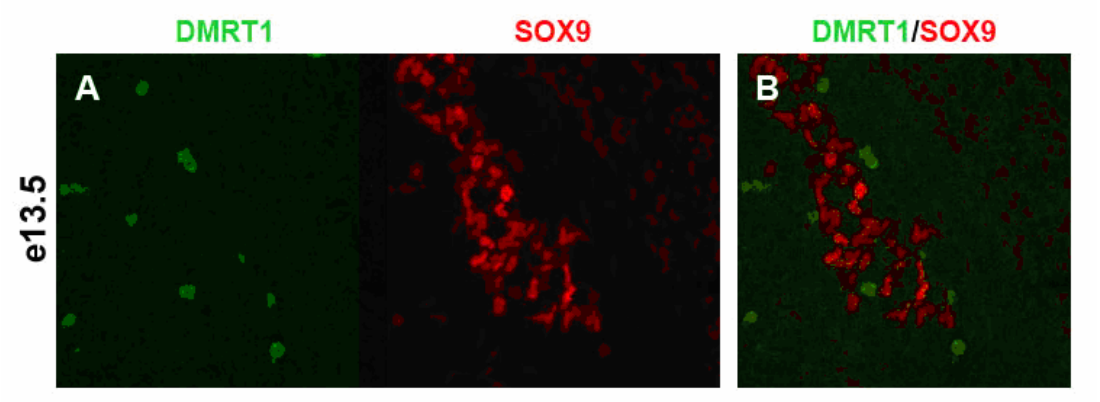

Figure 3.19 Representative confocal photomicrographs of immunostaining for DMRT1 (green) and SOX9 (red) in e13.5 fetal rat gonad (A and B). Panel A shows individual staining for DMRT1 and SOX9, and panel B shows the merged image to highlight the lack of co-localization.

At e13.5 in the rat fetal testis (SOX9+), DMRT1 was detected in presumptive GCs and not in the SOX9+ pre-Sertoli cells. This suggests that initial GC expression of DMRT1 is not induced in the same way as in Sertoli cells and follows the pattern observed in the fetal rat ovary where GCs alone expressed DMRT1. At present, it is unknown if GCs express DMRT1 earlier in development or if it is induced upon entry into the gonad.

3.3.11 Germ cell/pluripotency associated genes

During the course of this thesis, several other GC or pluripotency genes were also investigated, particularly in the fetal rat testis in relation to DBP exposure (Chapter 4). These genes were suggested by the literature, conferences or from personal discussions with other researchers. Many of these genes and/or their encoded

proteins were unable to be investigated in the fetal rat due to failure of antibodies to work or showed a vastly differing expression pattern from what has been reported in the mouse or human. Some genes showed no difference in expression during the last week of fetal life and/or with DBP exposure, and were therefore of less interest for the studies in this thesis. Table 3.3 below provides a brief summary of these attempts.

Table 3.3 Summary of germ cell and pluripotency associated genes investigated.

Gene	Function	Tech tried	Result	Selected References
Klf4	Pluripotency factor, also expressed in TGCT	IHC and Taqman	Did not work	Godmann et al 2009, Takahashi et al 2007
Dppa2	Pluripotency factor, expressed then lost in PGCs	IHC and Taqman	Did not work	Maldonado-Saldivia et al 2007
Ssea1	Early stem cell marker, expressed in PGCs of human fetal gonad then lost	IHC and Confocal	Did not work	Kerr et al 2008
Ssea3	Early stem cell marker	IHC	Did not work	Brimble et al 2007
Ssea4	Early stem cell marker	IHC	Did not work	Brimble et al 2007
Plap	PGC marker retained in TGCT	IHC	Leydig cell expression	Molyneaux et al 2001, Koshida et al 1996
Cd9	GC surface marker and spermatogonial stem cell niche	IHC and Confocal	Did not work	Kanatsu-Shinohara et al 2004
Gcna	GC marker after arrival in gonad until meiosis	IHC and Confocal	Did not work	Enders and May 1994
Tex14	Maintains male GC intercellular bridges	Confocal	GC specific but unaltered with DBP	Greenbaum et al 2006, Greenbaum et al 2009
Fgf2	Growth factor that signals in Sertoli cells and in spermatogenesis	IHC	GC specific but unaltered with DBP	Gomzalez-Herrara et al 2006
Fgfr2	Growth factor receptor involved in early sex determination	IHC	Non specific staining, unaltered with DBP	Schmahl et al 2004, Kim et al 2007
E-cad	Adhesion protein, involved in TGCT	IHC	Leydig cell expression	Batistatou et al 2005
p53	Apoptotic protein, involved in several cancers	IHC	Leydig cell expression	Renaud et al 2007
p63	Apoptotic protein, involved in TGCT and normal ovary	IHC	Postnatal GC expression, unaltered with DBP	Suh et al 2006, Emanuel et al 2006
Cxcl12	Chemokine involved in GC migration and TGCT	IHC	Non specific staining, unaltered with DBP	Molyneaux et al 2003, Gilbert et al 2009
Cxcr4	Chemokine receptor involved in GC migration and TGCT	IHC	Non specific staining, unaltered with DBP	Molyneaux et al 2003, Gilbert et al 2009

3.4 Discussion

The aim of this chapter was to characterise GC development in the fetal rat gonad using the variety of studies previously published for the mouse as a basis for comparison (as reviewed in Section 1.3). This was to provide understanding of how fetal GC development occurs, how it is regulated and to identify targets for dysregulation that could be investigated with regard to fetal DBP exposure and Testicular Dysgenesis Syndrome in Chapter 4.

In the fetal rat, the majority of GC migration into the developing gonad was completed at e13.5 and finished by e14.5. At e13.5 the gonads are in the beginnings of sexual differentiation, as no seminiferous cords were visible and only increased SOX9 expression was detected. SOX9 is upregulated in pre-Sertoli cell nuclei by testis specific SRY expression and is one of the earliest markers of sex differentiation. 24 hours later at e14.5 in a fetal rat testis, AMH was expressed in the Sertoli cells which have become organised around the GCs to form the seminiferous cords. In the e14.5 fetal ovary, the GCs were comparatively disorganised.

By e15.5 in the fetal rat gonad, GCs show very little developmental change since e14.5, with the exception of their central aggregation within the seminiferous cords. This aggregation could be an active feature or could simply reflect clonal expansion of the proliferating GCs. GCs within the fetal rat ovary do not show any strong aggregation until around e19.5. In both fetal testis and ovary, GC proliferation was high during early gonad formation (at both e14.5 and e15.5 ~50%). The early events of GC migration, cord formation and GC proliferation in the fetal rat testis are similar to that described for the mouse, just on a different time scale.

The proliferation index of GCs in the fetal gonads was reducing at e17.5 and by e19.5 and e21.5 no proliferating GCs were found in either the testis or ovary. Interestingly, the GC proliferation index was significantly different between the sexes at e17.5, with ~40% of ovarian GCs still proliferating, compared to ~2% of GCs in the testis. As GC proliferation initiates during migration (in the mouse) and is

independent of the sex of the GC, this sex dependent difference at e17.5 must be due to the somatic environment regulating GC proliferation.

One other possibility for the observed difference at e17.5, is that a proliferation index does not calculate the actual number of proliferating GCs but instead labels the percentage of GCs that are in S phase during the time between BrdU injection and collection (1.5hours) and not the actual number of GCs that are proliferating. This leaves the option that there might be the same number of proliferating GCs in an ovary and testis if there are fewer GCs in an e17.5 rat ovary. However, such a significant difference in proliferation index and visual comparison of GC number in e17.5 testes and ovaries makes this possibility highly unlikely. A more likely explanation is that this difference in proliferation index is a reflection of the difference in the timing of commitment to spermatogenesis in the testis that occurs earlier than commitment to oogenesis (meiotic arrest) in the ovary. If GCs require a somatic signal to end their proliferation, the later initiation of meiotic control, possibly through retinoic acid exposure (reviewed in Section 1.3.4), would explain this sex specific difference in GC proliferation index at e17.5.

The disparity between the end of GC proliferation and the observed increase in GC number in the fetal testis is hard to reconcile and is most likely due to an error in calculating GC number, because of differences in determining testis weight/volume. This will be discussed in more detail, and with regard to DBP exposure in Section 4.3.1 and Section 4.4.

Investigation of fetal GC differentiation was performed by examining several key GC genes and how both protein and mRNA expression changed over time, as early GC markers are lost and markers of more mature GCs are initiated. The early GC marker OCT4 was investigated and found to be expressed in all fetal rat GCs from e13.5 until e17.5 at which point some GCs had lost OCT4 expression. After e19.5 OCT4 was lost in all GCs and was not detected postnatally. This pattern of OCT4 expression was similar in GCs of both fetal testes and ovaries, except at e17.5 when fewer OCT4 positive GCs were observed the fetal ovary, which matches a sex

difference in OCT4 expression reported in the fetal mouse ovary. In the fetal mouse ovary, once *Stra8* is expressed *Oct4* expression becomes down regulated (Menke et al., 2003), possibly induced by retinoic acid (RA) exposure (Bowles and Koopman, 2007). mRNA analysis of *Oct4* matched the protein expression pattern, but showed an interesting difference between the ovary and testis. In both the adult and fetal rat testis, *Oct4* mRNA was detectable in the absence of OCT4 protein, whereas *Oct4* mRNA was not detected in the fetal ovary after e19.5 or in the adult rat ovary. Whilst it is important not to over-interpret such results, this observed difference in *Oct4* expression profile over time may indicate that different gene regulation occurs between the sexes in the rat. The reduced but continued detection of *Oct4* mRNA in the male rat suggests that both post transcriptional control and promoter silencing are involved in OCT4 protein expression. If it is RA that induces *Oct4* down regulation, as in *in vitro* ES studies (Li et al., 2007; Pikarsky et al., 1994), then this difference in *Oct4* expression regulation would be needed as RA may be degraded in the fetal testis by CYP26B1 enzyme action (Bowles et al., 2006). If there is indeed a difference (possibly due to differing RA levels) in how *Oct4* expression is regulated between the testis and ovary, this may also occur in the human testis, where it could play a role in how *Oct4* expression is retained into CIS and TGCT.

DMRT1 is another GC gene for which protein expression is switched off in the GCs during fetal life at ~e19.5, although it remains expressed in the Sertoli cells. Analysis of *Dmrt1* mRNA in the testis was complicated by its Sertoli cell expression, but there was a reduction in mRNA coincident with loss of GC protein expression and the significant increase in mRNA at e21.5 is likely due to the increase in Sertoli cell numbers at this age (Scott et al., 2008). In the fetal rat ovary, in which DMRT1 was only detected in GCs, *Dmrt1* mRNA expression was reduced at e19.5 but showed a slight increase at e21.5 and was also detectable in the adult rat ovary. This is interesting as mice knockouts for *Dmrt1* suggest that its expression is not required for normal ovarian function, but otherwise the present results in the rat match reports of *Dmrt1* in the mouse (Lei et al., 2007; Raymond et al., 1999).

Markers of more mature GCs such as VASA and DAZL were found to be expressed in all GCs during the last week of fetal life in both the testis and ovary, with VASA initiating later than DAZL and remaining relatively constant. DAZL expression showed a possible reduction at e19.5 and e21.5 in both testis and ovary, a change which has not been described in the mouse. However, postnatally DAZL expression increased and co-localized with VASA until adulthood. mRNA analysis for both *Vasa* and *Dazl* showed a similar pattern of expression levels in fetal rat testes and ovaries, with highest expression at e17.5 followed by a sharp reduction at e19.5.

As with all the Taqman analyses of mRNA levels, the whole gonad is used for RNA isolation, resulting in a mix of cellular origins for the mRNA pool relative to both the expression from each cell and the ratio of cell types in the gonad. This means that the high level of *Vasa* and *Dazl* expression at e17.5 could be due to an increase in GC expression of these genes or due to the relatively high GC contribution to the whole gonad at this age (as visible in Fig 3.3C and D). Whilst the fetal rat testis increased in size over time due to increase in number of Sertoli, Leydig and other cell types, the fetal rat ovary did not. As the relative mRNA expression pattern was the same in the fetal testis and ovary, the similar reduction in expression at e19.5 is more likely due to reduced GC mRNA expression. The continued levels of VASA protein expression observed after e19.5, when mRNA levels were reduced, indicates that VASA protein is not being actively degraded and is relatively stable at these ages.

During the mRNA analyses of the fetal rat ovary, some genes were undetectable in the adult ovary or showed highly increased expression in fetal life relative to the adult ovary (e.g. *Dazl* Fig 3.10 and *Dmrt1* Fig 3.17). This could be due to the high level of GC activity for these genes in the fetal ovary when compared to the adult ovary, or is due to the relatively small GC contribution to the adult ovary. In contrast, the adult rat testis contains a high number of GCs, in a variety of steps of development through spermatogenesis, and highlights that many of the GC genes investigated in fetal life are still expressed in the adult testis.

In summary, GC development is similar in both fetal rat testis and ovary, with some small differences (OCT4 expression at e17.5) and some major (meiotic/mitotic arrest). These similarities highlight the importance of the somatic environment of the gonad in fetal life in both determining the sex-specific development of the GC and supporting their subsequent development into a gonocyte or oocyte. By examining the events of fetal GC development in the rat, we have identified several processes that could become dysregulated with DBP exposure, and these events are summarised in Fig 3.20 (note that GC apoptosis is discussed in Chapter 4 and methylation in Chapter 5).

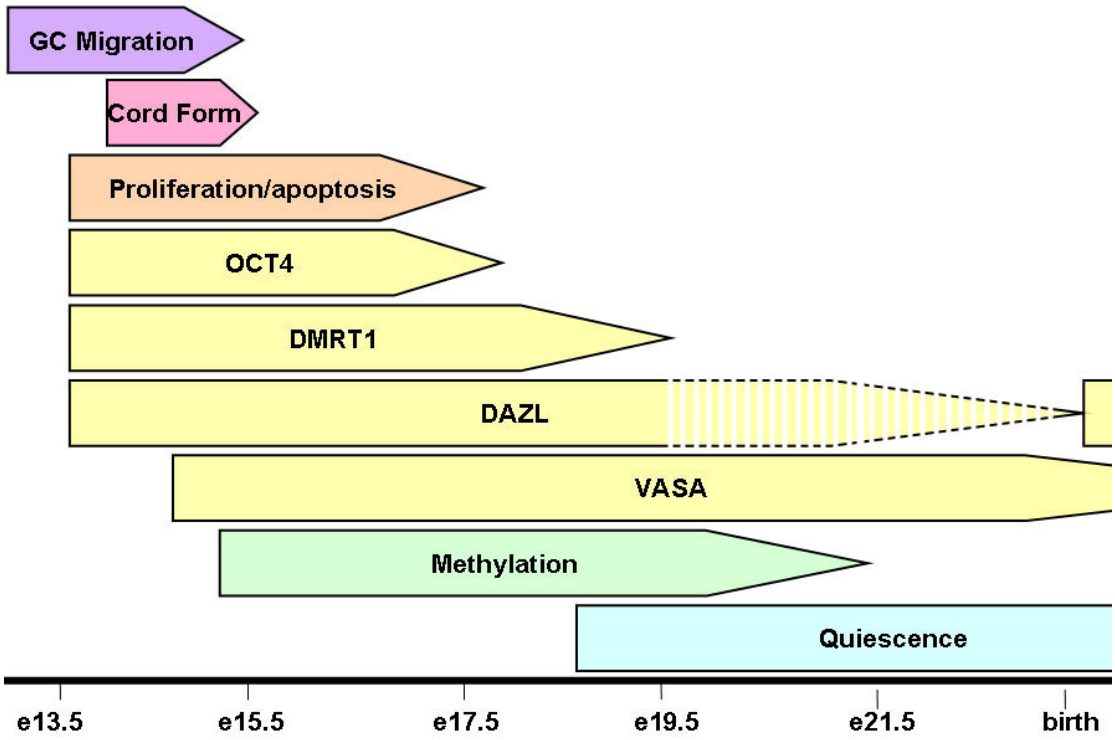

Figure 3.20 Summary of the different events of fetal GC development investigated in this thesis, with timings for the fetal rat.

Since the start of the studies comprising this thesis, new understanding about fetal and early postnatal GC development in the human has been published and has highlighted some important and fundamental differences between rat and human fetal GC organization and development. As described in Section 1.3.5.1, human GCs

show sub populations of GCs (e.g. differentiated and non-differentiated) within any individual seminiferous cord, in comparison with the largely synchronised GC populations observed within an individual seminiferous cord in the rat (Gaskell et al., 2004). Further examination has identified separate OCT4+, VASA+ and DAZL+ GC sub populations within seminiferous cords in the fetal human testis (Anderson et al., 2007). In the fetal rat testis, it is only at e13.5 that GCs do not express DAZL and VASA proteins (barely detectable) at the same time, and sub populations of germ cells that only expressed OCT4 were never observed. These species differences have further been highlighted by comparison to the marmoset (Mitchell et al., 2008), which shows a similar "unsynchronised" pattern of GC development to the human, with GCs only expressing OCT4 persisting into neonatal life and the existence of distinct sub populations of GCs within individual seminiferous cords. Based on these comparisons, GC development in the fetal rat may have limited usefulness as a model for GC development in the human, but these differences may account for the absence of CIS cells and TGCT in the rat.

4 The effect of exposure in utero to Di (n-Butyl) Phthalate on fetal germ cell development

4.1 Introduction

Having established the normal process of germ cell (GC) development during the last week of fetal life in the rat in Chapter 3, the effects of *in utero* Di (n-Butyl) Phthalate (DBP) exposure on this pattern was investigated. DBP exposure during fetal life of the rat produces several reproductive defects in the male, including cryptorchidism, hypospadias, impaired spermatogenesis and reduced fertility and is used as an animal model for human Testicular Dysgenesis Syndrome (TDS, discussed in more detail in Section 1.5) (Fisher et al., 2003). Whilst DBP exposure does not induce the most severe aspect of TDS, Carcinoma in Situ (CIS) cells or testicular germ cell tumours (TGCT), a previous study showed that DBP exposure can alter fetal rat GC development, resulting in significantly reduced GC number prior to birth and postnatal consequences (Ferrara et al., 2006). In addition, *in utero* DBP exposure causes areas of focal dysgenesis and seminiferous cords containing only immature Sertoli cells in the postnatal rat testis, which are features similar to those found in human testes with TGCT (Hoei-Hansen et al., 2003; Mahood et al., 2005; Skakkebaek et al., 2003; Hutchison et al., 2008a).

The aim of this chapter was first to examine in detail how DBP exposure *in utero* altered GC development in the fetal rat testis, by investigating GC number, proliferation, apoptosis, differentiation (observed through changes in protein expression) and aggregation/migration in testes from control and DBP exposed animals. Then, different time windows of *in utero* DBP exposure were examined to gain more insight into when and how DBP exposure caused its effects on GC development. Finally, early postnatal testes were examined to determine the consequences of *in utero* DBP effects on fetal GC development for postnatal GC development after DBP exposure had ceased.

4.2 Materials and methods

4.2.1 Animals and in vivo treatments

Briefly, pregnant Wistar rats were treated with DBP or corn oil and collected at fetal and postnatal ages, as described in Section 2.2 and summarized in Table 4.1.

Table 4.1 Summary of maternal DBP treatments and collection ages used in Chapter 4.

Dose (ml DBP/kg bodyweight)	Treatment window	Abbrev.	Collection ages
500	e13.5-e20.5	Std/ DBP500	e14.5, e15.5, e17.5, e19.5, e21.5, D4, D6, D8, D10, D15, D25, Adult
500	e11.5-e20.5	Ext	e21.5, D6
500	e13.5-e15.5	EW	e17.5, e19.5, e21.5, D6
500	e15.5-e17.5	MW	e17.5, e21.5

Testes from control and DBP exposed animals were dissected out (Section 2.3-2.3.4) and were either fixed in Bouin's and processed for immunohistochemical analysis, or stored at -80°C for RNA analysis.

4.2.2 Immunohistochemical (IHC) analysis

Briefly, IHC staining (Section 2.6) was performed on processed and sectioned fetal testes as summarised in Table 4.2. The number of fetal testes used for IHC was a minimum of 5 testes in each age and treatment group and came from a minimum of three different litters.

In addition to standard single and double IHC, TUNEL IHC for apoptotic cells was performed as described in Section 2.6.12. Several IHC analyses were performed to calculate the GC number in fetal testes (Sections 2.8.1-2.8.2.2), GC proliferation

index (Section 2.8.3), the percentage of OCT4 or DMRT1 expressing GCs (Section 2.8.4) and GC position at postnatal day (D)6 (Section 2.8.5).

Table 4.2 Details of antibodies used in Chapter 4.

Antibody	Source	Retrieval	Species
BrdU	Fitzgerald industries, MA	Yes	Sheep
cKIT	Santa Cruz, CA	Yes	Rabbit
DAZL	AbD Serotec	Yes	Mouse
DMRT1	Gift from David Zarkower, MN	Yes	Rabbit
OCT4	Santa Cruz, CA	Yes	Goat
SMA	Novocastra	No	Mouse
VASA	Abcam, Cambridge	Yes	Rabbit

4.2.3 RNA analysis

Briefly, RNA isolated from frozen testes was converted into cDNA (Section 2.11.2) and Taqman quantitative RT-PCR performed (Section 2.11.5), to establish quantitative mRNA expression levels. The genes investigated, and primers used, are listed in Table 4.3.

Table 4.3 Taqman primers and Universal Probe Library probes used in Chapter 4.

Gene	Forward Primer 5' → 3'	Reverse Primer 3' → 5'	UPL Probe Number:
Dazl	GCTCAGTTCATGATGCTGCT	ATGCTTCGGTCCACAGATTT	110
Dmrt1	CAGAAGCCAAAGCAAGTGTG	AGCTGCTGGAGAGGGAAAC	129
Oct4	GAAGTTGGAGAAGGTGGACC	CCTTCTGCAGGGCTTTCATA	95
Vasa	CATTCAGAAGAGGTGGGAGAGA	TGCTGGTTTCCTAGAACCAAA	77

4.3 Results

4.3.1 Germ cell counts after DBP exposure

As described above, previous studies of the effects of DBP exposure on fetal rat germ cell (GC) development had identified that DBP induced a significant reduction in GC number at embryonic day (e)21.5 (Ferrara et al., 2006). To examine in detail when this reduction occurs, GC counts at e14.5, e15.5, e17.5, e19.5 and e21.5 were performed on sections of control and standard DBP exposed fetal rat testes (as outlined in Table 4.1) by immunohistochemical (IHC) staining for VASA or DAZL, as described in Section 2.8.1. These GC counts are presented in Fig 4.1.

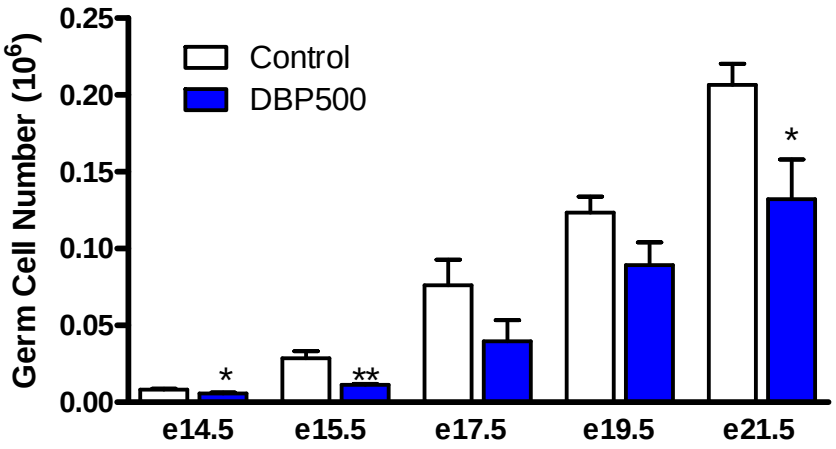

Figure 4.1 Number of germ cells in testes of control and DBP exposed animals between e14.5 and e21.5 (n=8 for control e17.5, n=5 for others). Values are means ± SEM. Student's unpaired *t* test was performed, * P<0.05, ** P<0.01 between control and DBP exposed.

The previously reported significant reduction in GC number at e21.5 was confirmed, and a pattern of consistently reduced GC number with DBP exposure was observed at every age investigated. There was also a significant early reduction in GC number with DBP exposure at e14.5 and e15.5, suggesting an early origin for this consistent reduction in GC number with DBP.

In testes from both control and DBP exposed animals, GC number increased during the last week of fetal life, even though GC proliferation no longer occurs in the fetal rat testis after e17.5 (Fig 3.5). The increase in GC number after GC proliferation has ceased may therefore be artificial and result from errors in the accuracy of using three different methods to determine testis weight (Section 2.8.2). Beyond e17.5, there is a large increase in numbers of somatic cells, in particular Sertoli cells, which can clearly be seen in the left panels of Fig 3.4. Whilst stereology is an accurate way to calculate cell number it is possible that as the testis weight increased so much between e17.5 and e19.5 and is used as a multiplier to generate GC number, an over-estimation of GC number may have occurred. This is discussed in more detail in Section 4.4. To illustrate this increase in other testicular cell types and to examine if DBP exposure altered the ratio of Sertoli cells to GCs, Sertoli cell counts (performed by S. Auharek and H. Scott) were combined with GC counts at e17.5, e19.5 and e21.5 to generate Fig 4.2.

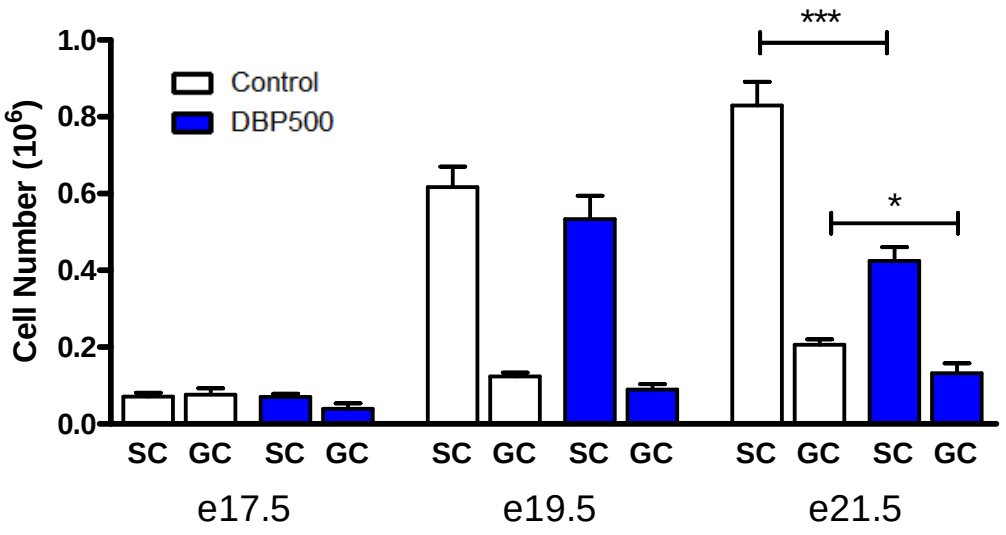

Figure 4.2 Number of Sertoli cells (SC) and germ cells (GC) in testes from control and DBP exposed animals at e17.5, e19.5 and e21.5 (n=5-19). Values are means ± SEM. Student's unpaired *t* test was performed, * P<0.05, *** P<0.001 between control and DBP exposed.

At e17.5, Sertoli cell number and GC number were relatively similar but as Sertoli cell number increased from e19.5 onwards, relatively speaking GC number did not. DBP exposure significantly decreased both Sertoli cell number and GC number at e21.5, but did not significantly alter the ratio of GC to Sertoli cells (data not shown).

4.3.1.1 GC proliferation after DBP exposure

Having established that GC number was consistently reduced at each age with DBP exposure, it was suspected that altered GC proliferation by DBP exposure may explain this reduction. This was investigated by double IHC staining for Bromo deoxyuridine (BrdU) and DAZL. As described in Section 2.2.3, BrdU labels proliferating cells and when combined with GC marker DAZL, allowed a GC proliferation index to be generated, as shown in Fig 4.3.

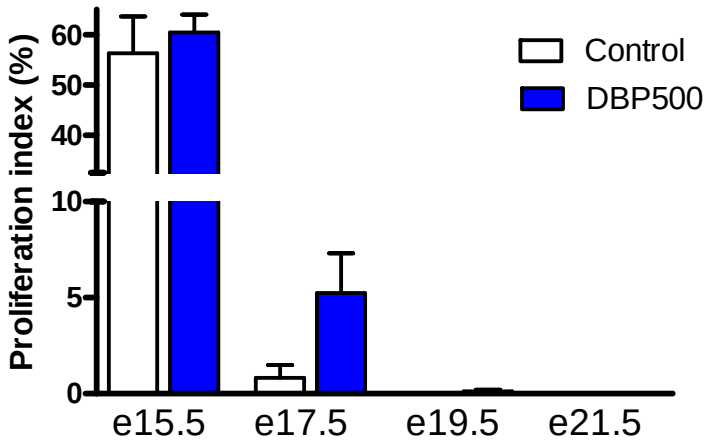

Figure 4.3 Germ cell proliferation index in testes of control and DBP exposed animals at e15.5, e17.5, e19.5 and e21.5 (n=5). Values are means ± SEM. No statistically significant differences.

GC proliferation index was high in both control and DBP exposed testes at e15.5, and then reduced markedly at e17.5 to zero levels at e19.5-e21.5 in controls. At e17.5, DBP exposure increased average GC proliferation compared to controls, but not significantly, and rare single proliferating GCs were also identified at e19.5 in

DBP exposed animals. This suggested that DBP exposure was prolonging GC proliferation.

To reconcile this observed increase in GC proliferation over time with the observed decrease in GC number with DBP exposure, the number of proliferating GCs was calculated for testes from control and DBP exposed animals at e15.5, e17.5, e19.5 and e21.5, as shown in Fig 4.4.

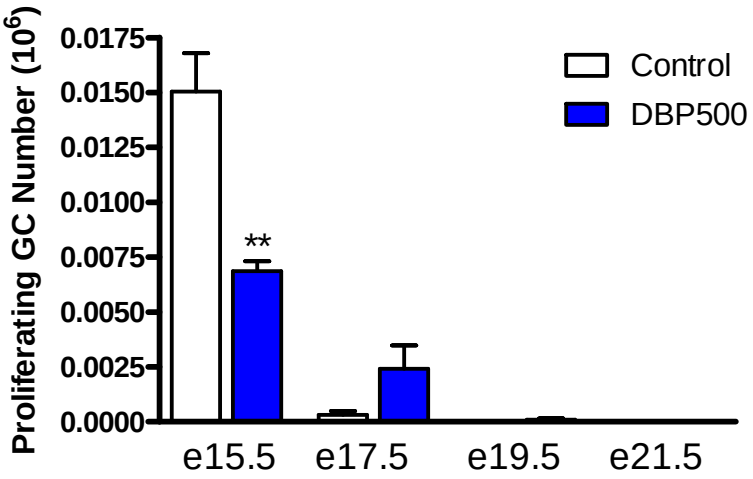

Figure 4.4 Total proliferating germ cell number in testes from control and DBP exposed animals at e15.5, e17.5, e19.5 and e21.5 (n=5). Values are means ± SEM. Student's unpaired *t* test was performed, ** P<0.01 between control and DBP exposed.

By calculating the number of proliferating GCs in the fetal rat testis it became clear that even though GC proliferation was prolonged, the significant reduction in proliferating GC number at e15.5 means that GC number cannot recover to control levels. This result implied that the consistent reduction observed in Fig 4.1 is due to an initial effect/reduction in GC number that occurred prior to e14.5 or e15.5, and must be a very early effect as this is only 24 hours after the first DBP exposure at e13.5.

During the process of generating the GC counts, it was observed that GC nuclear volume increased as the GCs were developing during the last week of fetal life. To investigate if DBP exposure altered this aspect of GC development, mean nuclear GC volumes were calculated for testes from control and DBP exposed animals between e14.5 and e21.5, as shown in Fig 4.5.

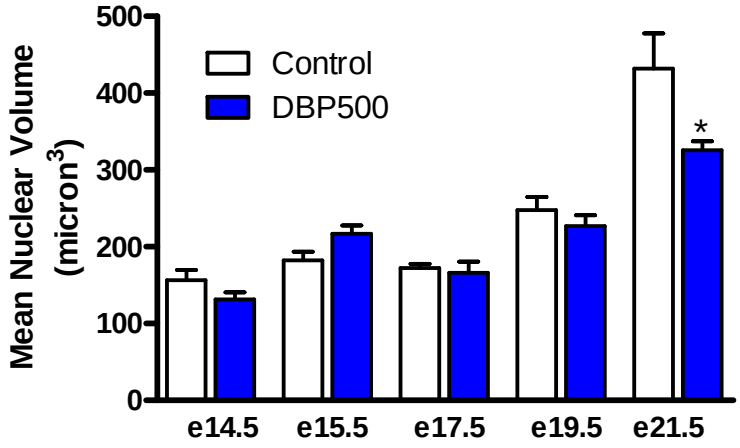

Figure 4.5 Germ cell mean nuclear volume in testes from control and DBP exposed animals between e14.5 and e21.5 (n=5). Values are means ± SEM. Student's unpaired *t* test was performed, * P<0.05 between control and DBP exposed.

GC mean nuclear volume increased between e14.5 and e21.5, and especially beyond e19.5 and was not affected by DBP exposure until e21.5, when a significant reduction was found. This may be due to DBP exposure delaying an increase in nuclear size during GC development, or that DBP exposure is directly preventing GC nuclear expansion at e21.5.

4.3.1.2 Apoptosis analysis after DBP exposure

To investigate if the reduction in GC number resulting from DBP exposure was due to an increase in GC apoptosis, the apoptosis assay TUNEL was performed on fetal rat testes from control and DBP exposed animals, as described in Section 2.6.12. The results are summarized in Fig 4.6.

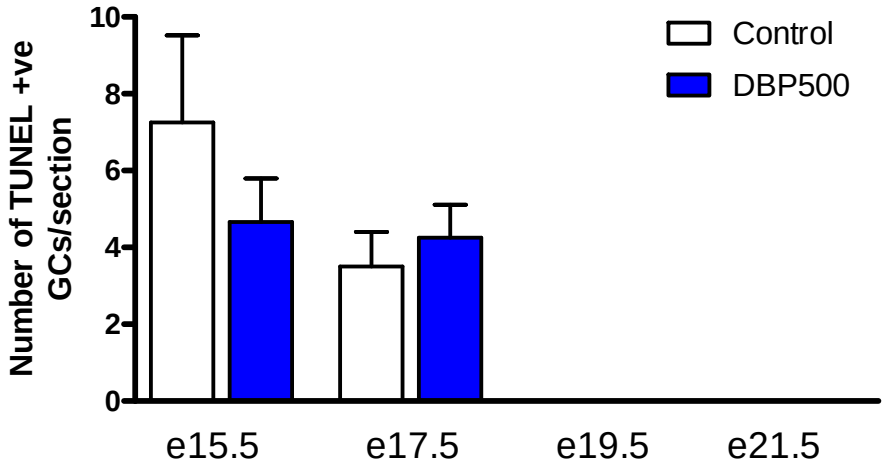

Figure 4.6 Number of apoptotic germ cells in testes from control and DBP exposed animals at e15.5, e17.5, e19.5 and e21.6 (n=6). Values are means ± SEM. No statistically significant differences.

GC apoptosis in the fetal testis was low at e15.5 and e17.5 with only around 5 TUNEL positive GCs in a complete testis cross-section, and by e19.5 and e21.5 no TUNEL positive GCs were detected. Examination of e13.5 control and DBP exposed testes (8 hours after oral gavage) showed no greater increase in TUNEL+ GCs (data not shown). Therefore DBP exposure had no significant effect on the number of apoptotic GCs, suggesting that DBP does not cause an increase in GC apoptosis, at least not at the ages examined.

4.3.1.3 OCT4 expression after DBP exposure

As discussed in Section 1.3.3, the pluripotency factor Octamer-binding transcription factor 3/4 (OCT4) is an early PGC marker in the mouse, whose expression is reduced as fetal GCs differentiate. In previous studies using the DBP rat model, OCT4 expression was reported to be affected by DBP exposure (Ferrara et al., 2006). To confirm this and to quantify this DBP effect, IHC for OCT4 and VASA was performed (Fig 4.7) and the percentage of OCT4 positive GCs determined, as shown in Fig 4.8.

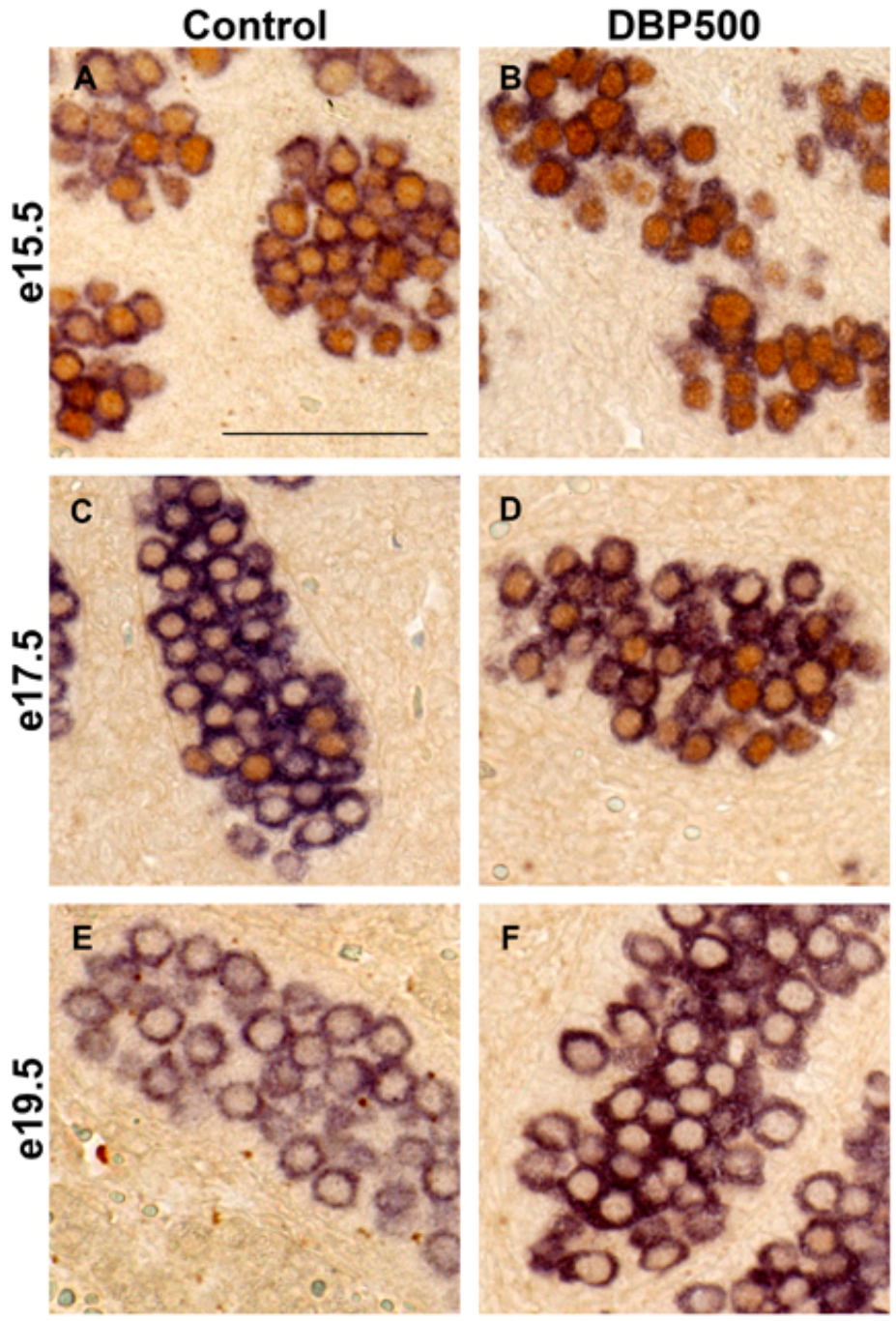

Figure 4.7 Representative photomicrographs of immunostaining for OCT4 (Dab = brown) and VASA (Fast blue = blue) in fetal rat testes from control (left) and DBP500 exposed animals (right) from e15.5 (top) through to e19.5 (bottom). Scale bar in panel A represents 50µm.

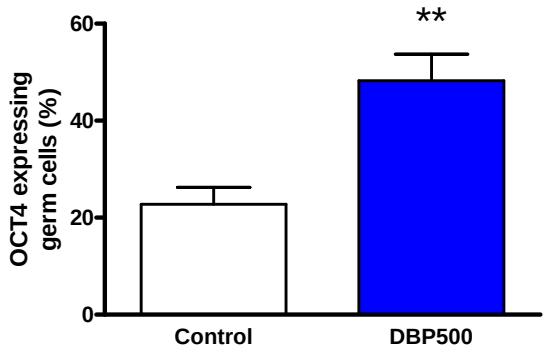

Figure 4.8 Percentage of OCT4 expressing germ cells in e17.5 fetal rat testes from control and DBP exposed animals (n=6). Values are means ± SEM. Student's unpaired *t* test was performed, ** P<0.01 between control and DBP exposed.

At e17.5 there was a significant increase in the percentage of GCs expressing OCT4 after DBP exposure. As OCT4 expression is lost during the last week of fetal life, this result suggested that DBP exposure delayed but did not prevent the loss of OCT4 protein expression. To examine how *Oct4* mRNA expression was altered by DBP exposure, Taqman analysis was performed on testes from control and DBP exposed animals at e15.5, e17.5, e19.5 and e21.5 are shown in Fig 4.9A. Further analysis at e17.5 to adjust for GC content of whole testis was performed by dividing by estimated GC number (Fig 4.1) and testis weight (Section 2.8.2) and are shown in Fig 4.9B.

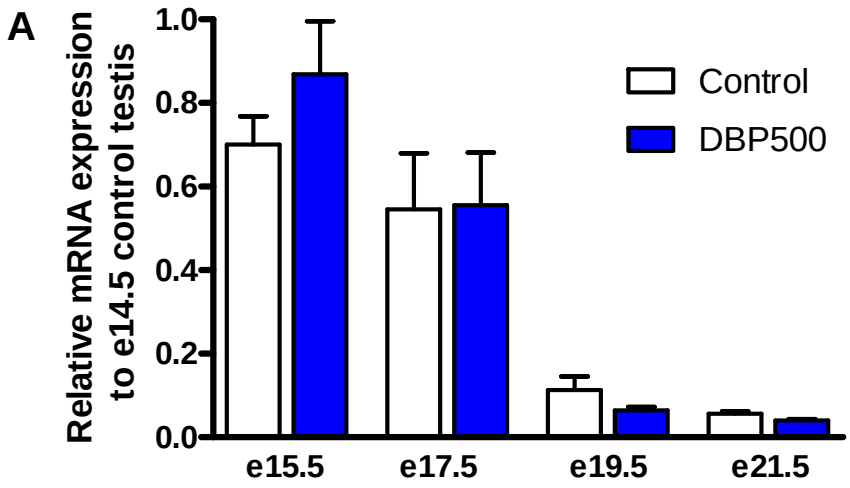

Figure 4.9 **A:** Quantitative analysis of *Oct4* mRNA levels at e15.5, e17.5, e19.5 and e21.5 in fetal rat testes from control and DBP exposed animals (n=6). Values are means ± SEM. No statistically significant differences.

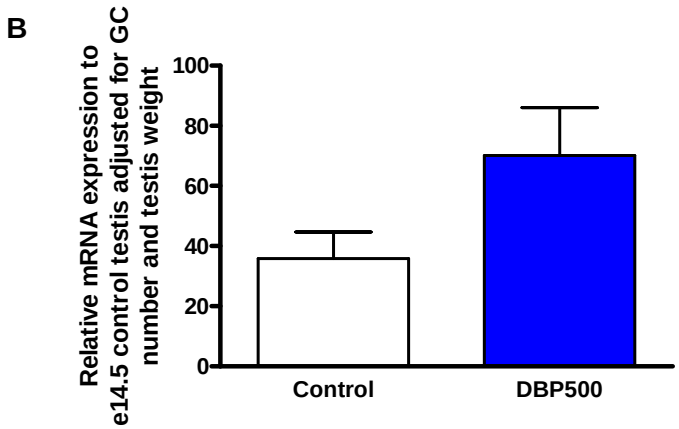

Figure 4.9 **B:** Quantitative analysis of *Oct4* mRNA levels at e17.5 in control and DBP exposed animals (n=6) adjusted for GC number and testis weight. Values are means ± SEM. No statistically significant differences.

Oct4 mRNA expression diminished over time in the fetal testis and, unlike the IHC result in Figs 4.7 and 4.8, was not altered by DBP exposure at e17.5. As GC number is reduced after DBP exposure, the similar *Oct4* mRNA levels observed at e17.5 in control and DBP exposed animals could be due to the fewer GCs individually expressing higher levels of *Oct4* mRNA than in controls. When *Oct4* mRNA levels at e17.5 were adjusted for GC number and testis weight, an increase in mRNA expression between control and DBP exposed testes was observable but not significant.

4.3.1.4 DAZL expression after DBP exposure

Deleted in Azoospermia Like (*Dazl*) is a GC-specific gene, which is described in more detail in Sections 1.3.5-1.3.6. During normal GC development in the fetal rat, DAZL expression is reduced in GCs after e17.5, discussed in Section 3.3.7. To examine if DBP exposure altered the expression of DAZL, IHC analysis of DAZL expression was performed during the last week of fetal life in the testes from control and DBP exposed animals (Fig 4.10).

As described in Section 3.3.7 and Fig 4.10, DAZL protein was expressed throughout the last week of fetal life, and appeared to be reduced at e19.5 and e21.5. In contrast, DBP exposure resulted in a persistence of stronger DAZL expression at e19.5

compared with control testes, although this was less evident at e21.5. Attempts to quantify these differences in level of DAZL protein by Western blot proved unsuccessful.

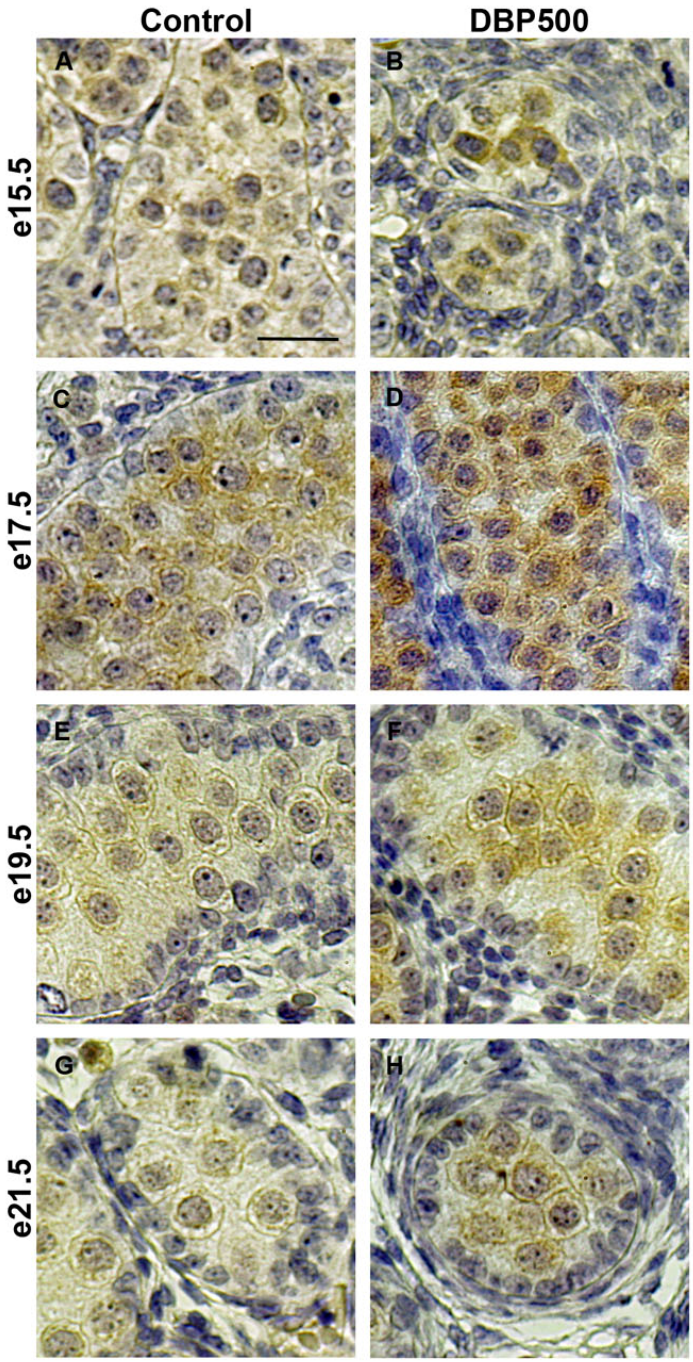

Figure 4.10 Representative photomicrographs of immunostaining for DAZL (Dab = brown) in fetal rat testes from control (left) and DBP500 exposed (right) animals from e15.5 (top) through to e21.5 (bottom). Scale bar in panel A represents 50µm.

Dazl gene expression was also examined after DBP exposure using mRNA analyses by Taqman on testes from control and DBP exposed animals at e15.5, e17.5, e19.5 and e21.5, shown in Fig 4.11.

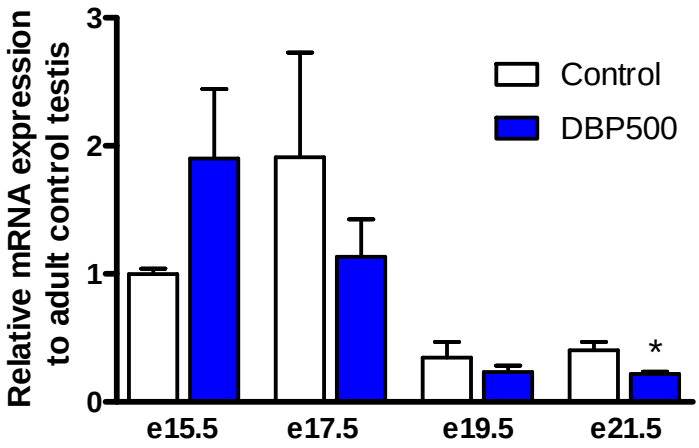

Figure 4.11 Quantitative analysis of *Dazl* mRNA levels at e15.5, e17.5, e19.5 and e21.5 in fetal rat testes from control and DBP exposed animals (n=6). Values are means ± SEM. * P<0.05 between control and DBP exposed.

Dazl mRNA levels showed a slight increase at e15.5 after DBP exposure, and at e17.5, e19.5 and e21.5 DBP exposure produced a reduction in *Dazl* mRNA expression, although this was only significant at e21.5. This decrease in *Dazl* mRNA may be due to the reduction in GC number at these ages.

4.3.1.5 VASA expression after DBP exposure

Mouse Vasa Homologue (*Vasa*) is a GC-specific gene that is necessary for postnatal spermatogenesis. In normal fetal rat testes, as described in Section 3.3.4, VASA was expressed in all GCs from e14.5 onwards. To examine if DBP exposure altered this expression, IHC analysis of VASA was undertaken in the fetal testes from control and DBP exposed animals during the last week of fetal life. DBP exposure had no effect on VASA protein expression (data not shown). *Vasa* mRNA expression was also examined for a DBP exposure effect at e15.5, e17.5, e19.5 and e21.5, shown in Fig 4.12.

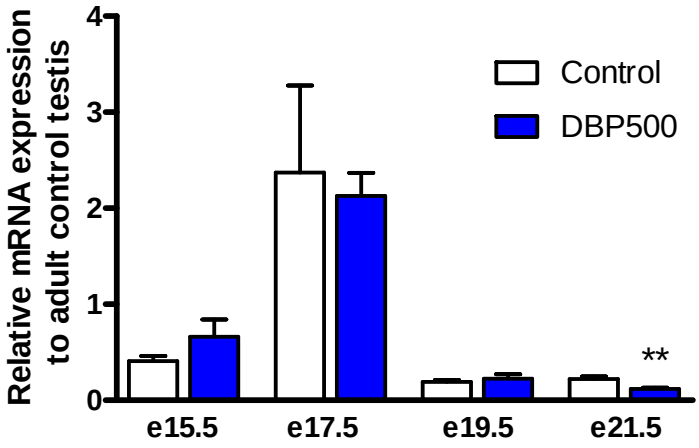

Figure 4.12 Quantitative analysis of *Vasa* mRNA levels at e15.5, e17.5, e19.5 and e21.5 in fetal rat testes from control and DBP exposed animals (n=6). Values are means ± SEM. ** P<0.01 between control and DBP exposed.

Vasa mRNA expression was unaltered by DBP exposure until e21.5, when there was a significant reduction. As with *Dazl* mRNA expression, this could be due to each GC expressing less *Vasa* or as a consequence of fewer GCs at e21.5 after DBP exposure. However, GC number is consistently reduced at each age examined (Fig 4.1) whilst *Vasa* expression is only reduced at e21.5, so it is possible DBP exposure is only effecting *Vasa* expression at e21.5 or that a significant reduction in GC number (at e21.5) is required for a significant reduction in *Vasa* expression levels to be detected.

4.3.1.6 DMRT1 expression after DBP exposure

Dmrt1 is a gene that is essential for postnatal testis function in the mouse, as described in Sections 1.2.2.2 and 1.3.5. In the fetal rat testis, as discussed in Section 3.3.10, DMRT1 protein is expressed in both Sertoli cells and GCs during the last week of fetal life. DMRT1 expression is diminished in GCs at e19.5 and is no longer detectable by e21.5. To examine if DMRT1 expression is altered by DBP exposure, IHC for DMRT1 was performed on testes from control and DBP exposed animals from e17.5 onwards, as shown in Fig 4.13.

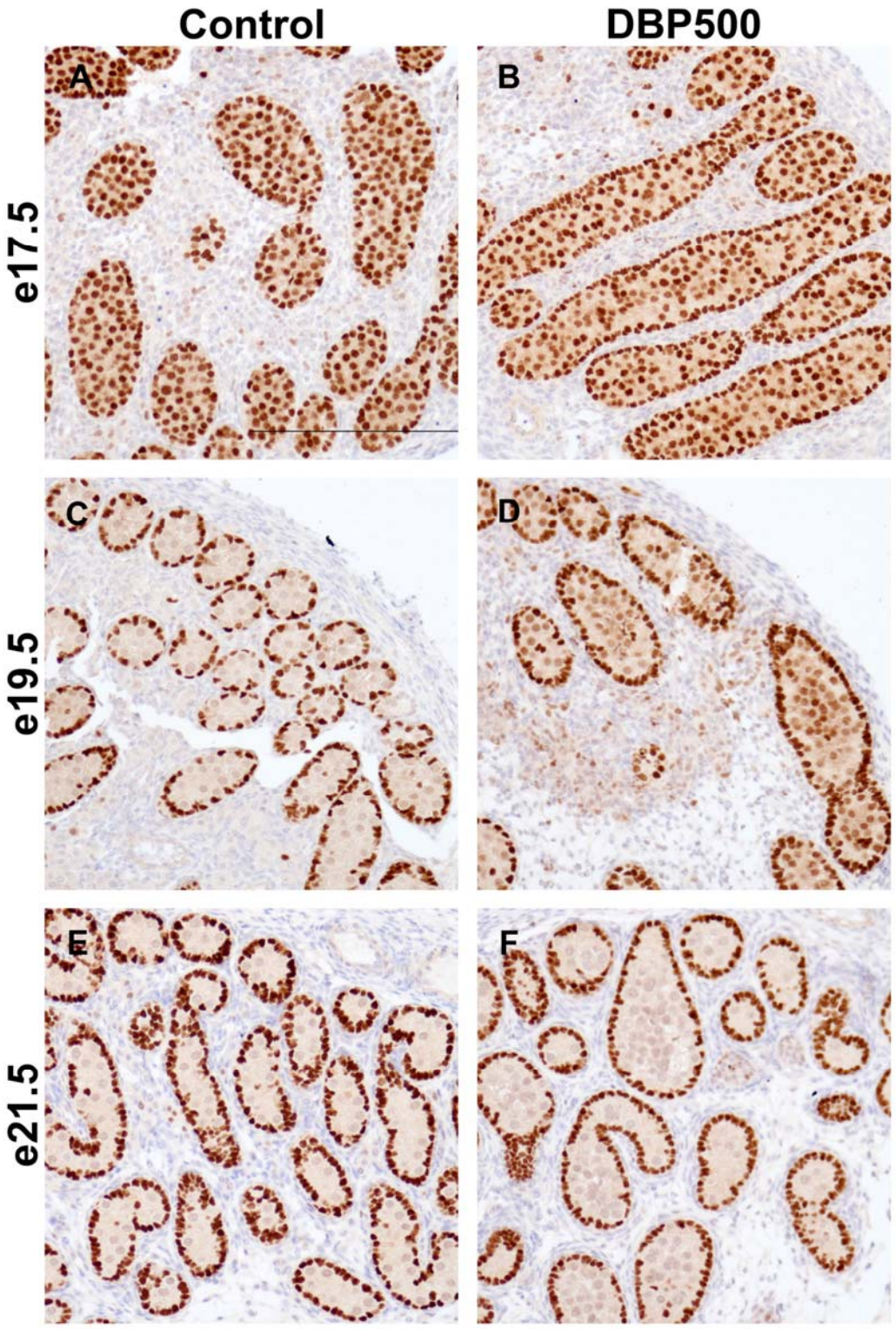

Figure 4.13 Representative photomicrographs of immunostaining for DMRT1 (Dab = brown) in fetal rat testes from control (left) and DBP500 exposed (right) animals from e17.5 (top) through to e21.5 (bottom). Scale bar in panel A represents 100µm.

DMRT1 GC expression in controls was pronounced at e17.5 but was virtually absent at later ages. In DBP exposed animals, this pattern was altered as many GCs still expressed DMRT1 at e19.5 and even at e21.5 there were still occasional GCs positively staining for DMRT1. To quantify the proportion amount of GCs expressing DMRT1 at e19.5, double IHC for VASA and DMRT1 was undertaken to ensure that DMRT1 expressing cells could be identified as GC or Sertoli cell. The percentage of DMRT1 positive GCs was calculated and is shown in Fig 4.14.

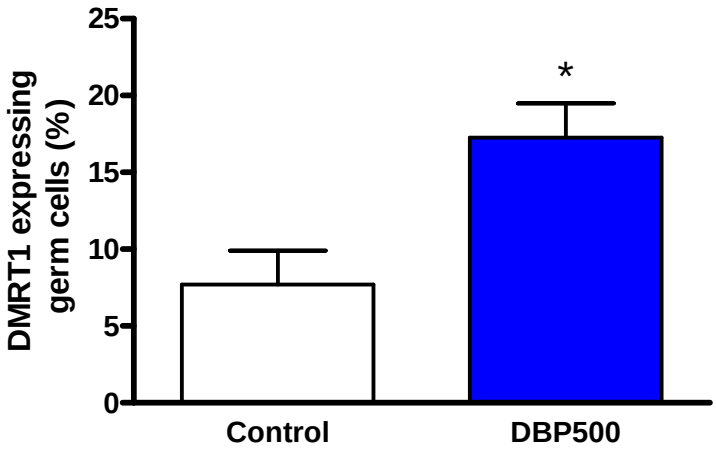

Figure 4.14 Percentage of DMRT1 expressing germ cells in e17.5 fetal rat testes from control and DBP exposed animals (n=4). Values are means ± SEM. Student's unpaired *t* test was performed, * P<0.05 between control and DBP exposed.

There was a significantly higher percentage of GCs expressing DMRT1 at e19.5 in DBP exposed animals, suggesting that, as with OCT4, DBP exposure delayed the loss of GC-specific DMRT1 expression but did not prevent it. To examine if this is delay in *Dmrt1* loss was observable at the mRNA level, Taqman mRNA analysis was performed on testes from control and DBP exposed animals, and is shown in Fig 4.15.

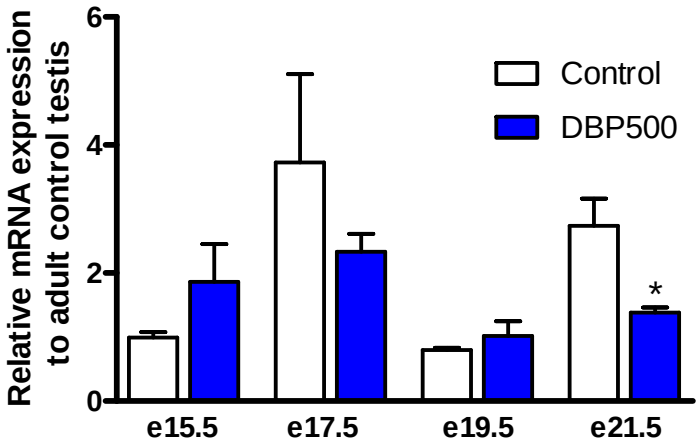

Figure 4.15 Quantitative analysis of *Dmrt1* mRNA levels at e15.5, e17.5, e19.5 and e21.5 in fetal rat testes from control and DBP exposed animals (n=6). Values are means ± SEM. * P<0.01 between control and DBP exposed.

As DMRT1 is also expressed in Sertoli cells as well as in GCs, *Dmrt1* mRNA levels per testis will not accurately reflect just GC expression. There was no significant increase in *Dmrt1* mRNA expression induced by DBP exposure at e19.5, which could be due to the combined effect of fewer GCs and Sertoli cells at this age. At e21.5, *Dmrt1* mRNA expression levels was significantly reduced in DBP exposed animals, most likely due to the reduction in both GC and Sertoli number (Fig 4.2) that was observed with DBP exposure at this age.

4.3.1.7 cKIT expression after DBP exposure

cKIT is the cell surface receptor for the KIT ligand, which is essential for GC migration into the gonad in the mouse, as well as for GC survival and proliferation, as discussed in Section 1.3.2. To examine the pattern of cKIT expression in fetal rat testes, and whether DBP exposure altered this pattern, IHC for cKIT was performed on testes from control and DBP exposed animals at e15.5, e17.5 and e19.5, as shown in Fig 4.16.

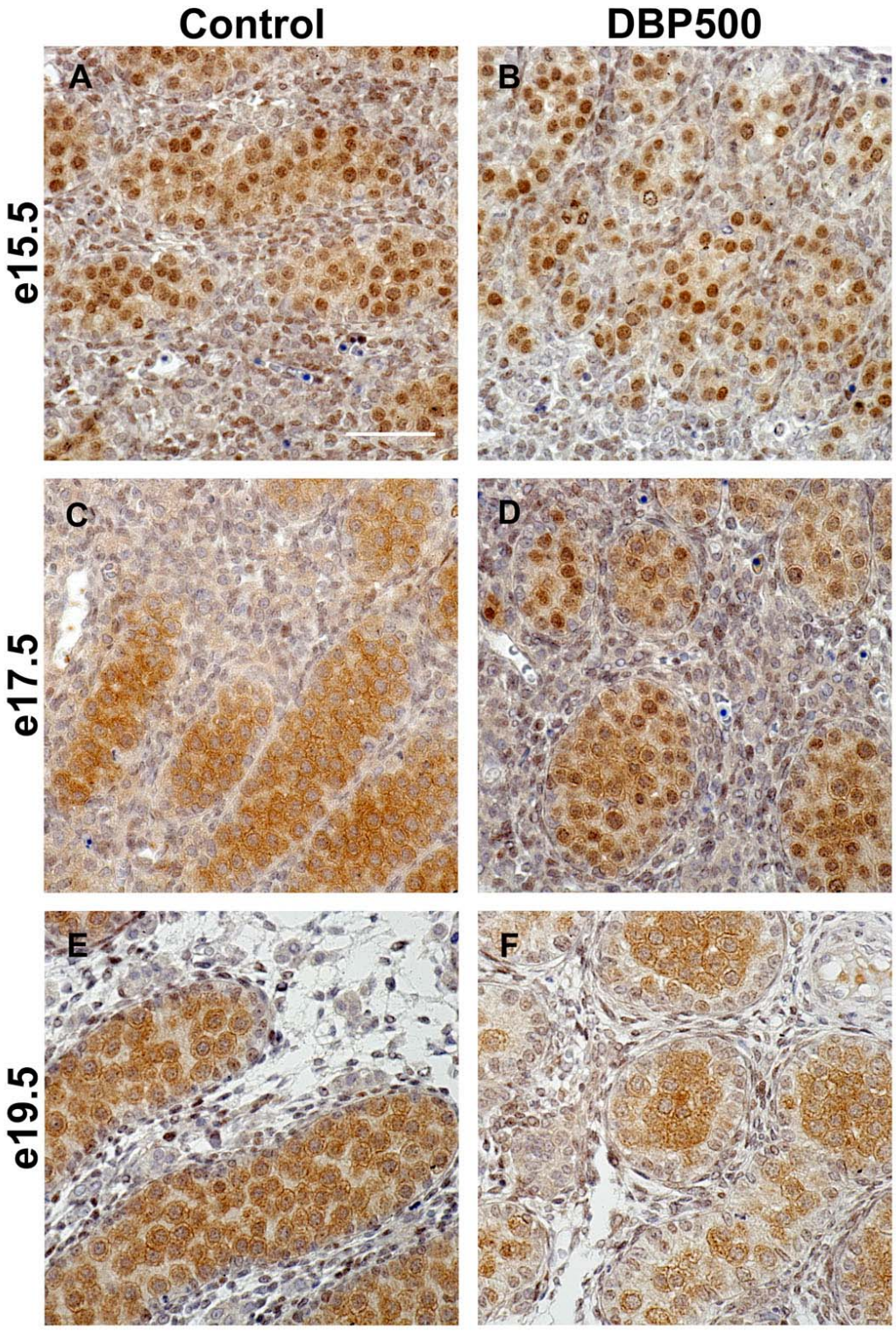

Figure 4.16 Representative photomicrographs of immunostaining for cKIT (Dab = brown) in fetal rat testes from control (left) and DBP500 exposed (right) animals from e17.5 (top) through to e19.5 (bottom). Scale bar in panel A represents 50µm.

According to the IHC, there was a change in cKIT localisation during GC development, changing from predominantly nuclear at e15.5 to more cytoplasmic/cell membrane localisation at e19.5. DBP expression did not prevent this change in localisation, but seemed to delay the change, most noticeable at e17.5 where there were more GCs with nuclear cKIT staining compared to controls. As cKIT is normally described as a cell membrane associated protein, working as a receptor for KIT ligand, the observation of nuclear expression at some ages was unexpected (Matsui et al., 1990). A different antibody for cKIT (from DAKO, A4502) was also used for IHC and produced a perinuclear pattern of expression that was unaltered by DBP exposure. Based on these results, the localisation of expression of cKIT remains uncertain in the fetal rat testis. However, if cKIT is not detected in Fig 4.16, the antibody is clearly binding to an antigen with a GC-specific expression pattern that is altered/delayed by DBP exposure.

4.3.1.8 Prenatal germ cell aggregation/migration

As described in Section 3.3.3, GCs in the testis show an aggregation centrally in the seminiferous cords that begins at e15.5 until e19.5 when the GCs disaggregate and begin to migrate down to the basal lamina. To identify if this process of GC disaggregation was affected by DBP exposure, double IHC for SMA (to identify the basal lamina) and VASA was performed and is shown in Fig 4.17.

In e21.5 DBP exposed animals, the GCs did not disaggregate and remained centrally located in the seminiferous cords. In addition, as previously described in detail (Ferrara et al., 2006), DBP exposure increased the occurrence of multinucleated gonocytes (MNG), as highlighted in Fig 4.17D.

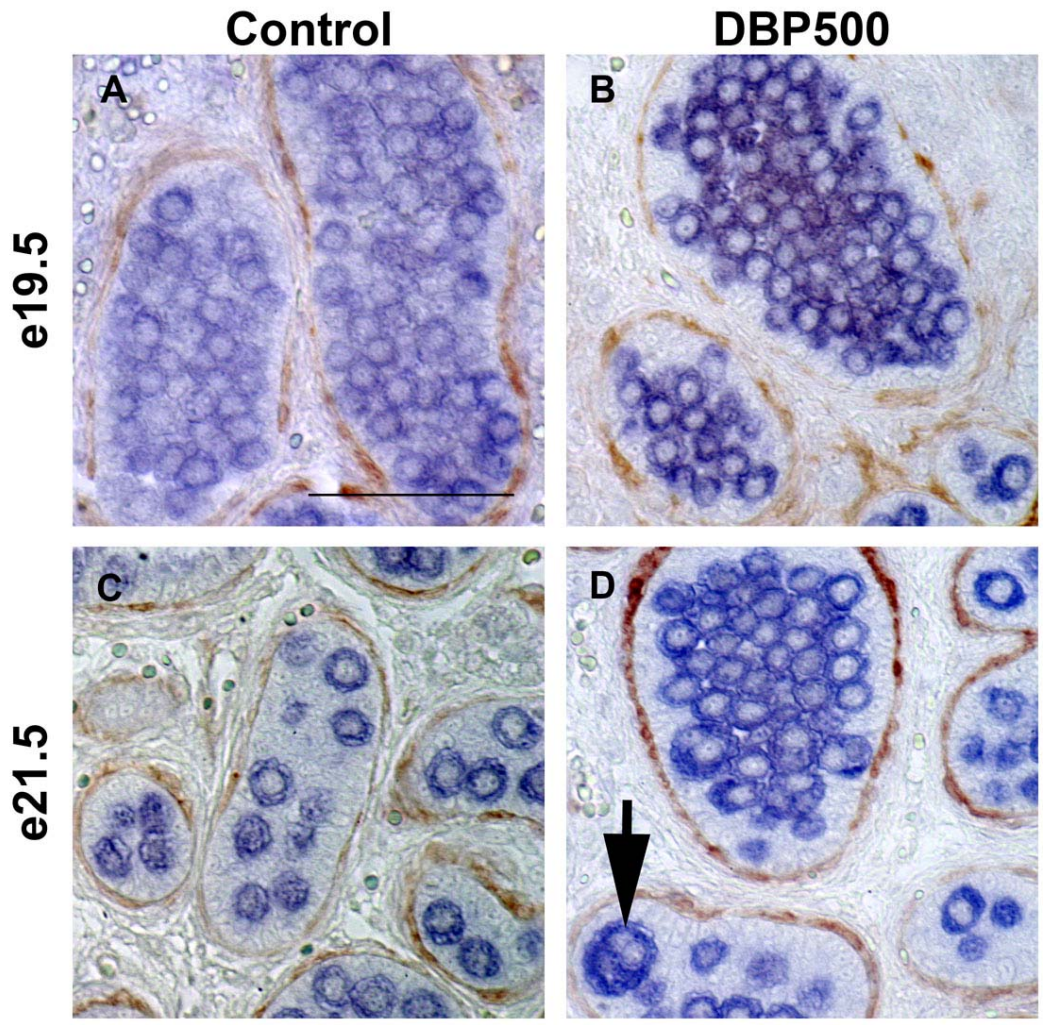

Figure 4.17 Representative photomicrographs of immunostaining for SMA (Dab = brown) and VASA (Fast blue = blue) in fetal rat testes from control (left) and DBP500 exposed animals (right) from e19.5 and e21.5. Scale bar in panel A represents 50µm. Black arrow depicts a MNG.

In summary, DBP exposure from e13.5-e21.5 delayed fetal GC development when compared to controls, as exhibited by prolonged proliferation, delayed increase in GC nuclear size, prolonged OCT4, DMRT1 and possibly DAZL expression and delayed GC disaggregation at e21.5. That GC development is delayed but not stopped may explain why CIS like cells are not produced by DBP exposure in the rat model of TDS.

4.3.2 Effect of different time windows of DBP exposure on GC development

Having established how *in utero* DBP exposure from e13.5-e20.5 altered several aspects of GC development in the fetal rat testis, several different time windows of DBP exposure were investigated with the aim of elucidating the crucial time points when DBP exposure affects GCs. These different treatment windows are discussed in Section 4.2 above, but in brief they were: an extended exposure window of e11.5-20.5 (Ext), an early exposure window of e13.5-e15.5 (EW) and a middle exposure window of e15.5-e17.5 (MW). For the rest of this chapter the exposure window of e13.5-e20.5 is termed as the standard DBP exposure window (Std).

As GC number in the fetal rat testis at e21.5 was significantly reduced with the standard DBP exposure, the effect of DBP exposure windows on GC number was investigated at e21.5. This is shown in Fig 4.18.

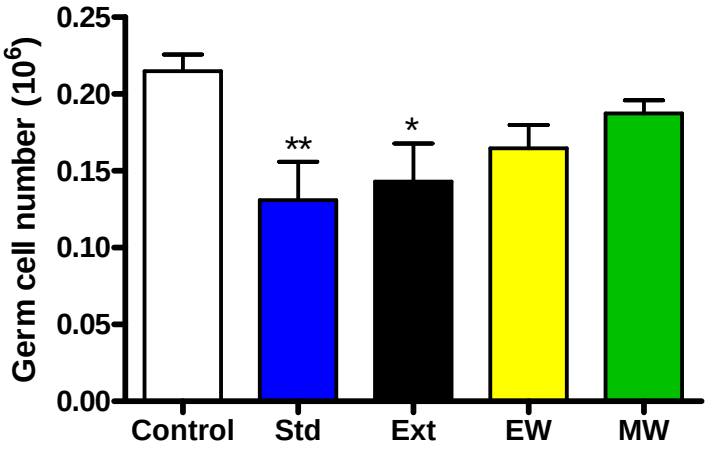

Figure 4.18 Number of germ cells at e21.5 in testes from control and DBP exposed animals after different DBP exposure time windows (n=5-8). Values are means ± SEM. ANOVA followed by Bonferroni's multiple comparison test was performed, * P<0.05 between control and Ext DBP exposure, ** P<0.01 between control and Std DBP exposure.

The extended exposure window (Ext) caused a significant reduction in GC number by e21.5, but was not significantly different than that induced by the standard DBP exposure, suggesting that earlier DBP exposure than e13.5 had no greater effect on

GC number. The early exposure window (EW) also reduced GC number by e21.5, but not to the same extent as did the standard DBP exposure window. The middle exposure window did not have a significant effect on GC number at e21.5.

As size of the GC nuclei was also reduced at e21.5 with the standard DBP exposure window (Fig 4.5), the effects of the other exposure windows on GC nuclear volume was also investigated, as shown in Fig 4.19.

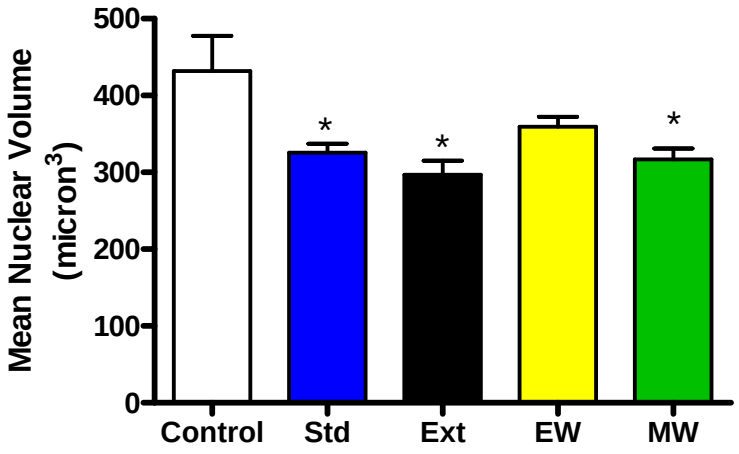

Figure 4.19 Germ cell mean nuclear volume at e21.5 in testes from control and DBP exposed animals in different exposure time windows (n=5-6). Values are means ± SEM. Student's unpaired *t* test was performed, * P<0.05 between control and DBP exposed.

The mean nuclear volume of GCs at e21.5 in the extended and middle DBP exposure time windows showed the same significant reduction in GC nuclear volume as seen with the standard DBP exposure window. The early exposure window did not produce a significant reduction in GC nuclear volume at e21.5. This result suggested that the altered GC endpoints described require DBP exposure at different times, instead of one time period of DBP exposure being responsible for all of the DBP exposure effects observed.

4.3.2.1 OCT4 expression after DBP exposure in different time windows

As previously described in Section 4.3.1.3, OCT4 protein expression was prolonged with standard DBP exposure, such that at e17.5 significantly more GCs expressed OCT4 in testes from DBP exposed animals. To examine if this DBP effect was due to exposure within a certain time window, the percentage of OCT4+ GCs at e17.5 was calculated for animals exposed to DBP in the EW and MW using double IHC for OCT4 and VASA. This analysis is shown in Fig 4.20.

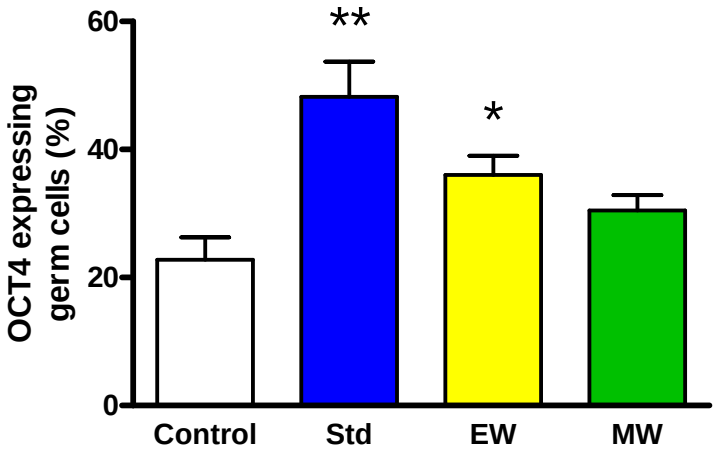

Figure 4.20 Percentage of OCT4 expressing germ cells in e17.5 fetal rat testes from control and DBP exposed animals after DBP exposure in different time windows (n=6). Values are means ± SEM. Student's unpaired *t* test was performed, * P<0.05, ** P<0.01 between control and DBP exposed.

The early exposure window produced a significant increase in the number of OCT4+ GCs at e17.5, although this was not as large an increase as found with the standard DBP exposure. The middle DBP exposure time window had no effect on numbers of OCT4 expressing GCs. This suggested that DBP exposure during e13.5-e15.5 is crucial to alter OCT4 expression whereas continued DBP exposure between e15.5-e17.5 enhances the delay in loss of OCT4 expression.

4.3.2.2 DMRT1 expression after DBP exposure in the early time window

Having established that the early exposure window was the more important exposure time to induce a GC differentiation delay; based on OCT4 expression, the effect of DBP exposure in the early time window on DMRT1 expression at e19.5 was investigated. As described above in Section 4.3.1.6, standard DBP exposure prolonged DMRT1 expression in GCs at e19.5 resulting in a significant increase in the percentage of GCs expressing DMRT1. The same analysis was performed for the EW as well, as shown in Fig 4.21. Exposure to DBP only in the early window (e13.5-e15.5) increased the percentage of GCs expressing DMRT1, but not to the same degree as the standard DBP window and not significantly.

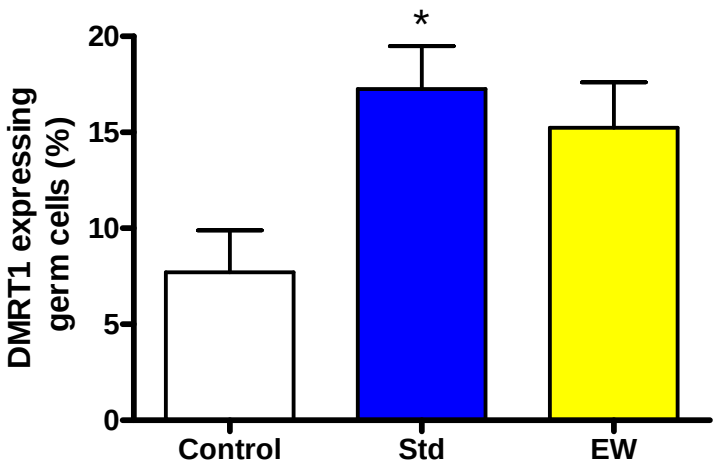

Figure 4.21 Percentage of DMRT1 expressing germ cells at e19.5 in fetal rat testes from control and DBP exposed animals from different exposure time windows (n=4-6). Values are means ± SEM. Student's unpaired *t* test was performed, * P<0.05 between control and DBP exposed**.**

These results using different DBP exposure time windows have identified that shorter exposure windows can alter GCs as in the standard DBP exposure time window, although the magnitude of effect tended to be smaller. It also suggested that DBP exposure prior to e13.5 had no greater effect than did the standard DBP

exposure and that exposure e13.5-e15.5 is the crucial exposure time for GC number reduction and delay in GC differentiation (OCT4 and DMRT1 expression).

4.3.3 Early Postnatal Consequences of DBP exposure

Having identified that DBP exposure induced a delay in fetal GC development, and the effects of different fetal DBP exposure windows on that delay, the postnatal development of GCs after fetal DBP exposure was examined. As previous studies (Ferrara et al., 2006) of fetal DBP exposure on rat GCs had identified significant reductions in GC number at postnatal day (D)6 and D15 that recovered by adulthood (over 3 months of age), the early events of postnatal GC development were focussed upon as most likely to show effects of the DBP induced GC delay.

4.3.3.1 DMRT1 expression in the postnatal testis

DMRT1 is essential for postnatal development in the mouse testis, where it is expressed in both Sertoli and GCs (Raymond et al., 2000). Having established that DMRT1 expression is absent in GCs at around e19.5 and is altered by DBP exposure in the fetal rat testis, several postnatal ages were examined to identify the GC re-expression pattern of DMRT1 in the rat. At D4, GCs did not express DMRT1 in controls (data not shown) but by D6 GCs begin to express DMRT1, this can be seen in Fig 4.22.

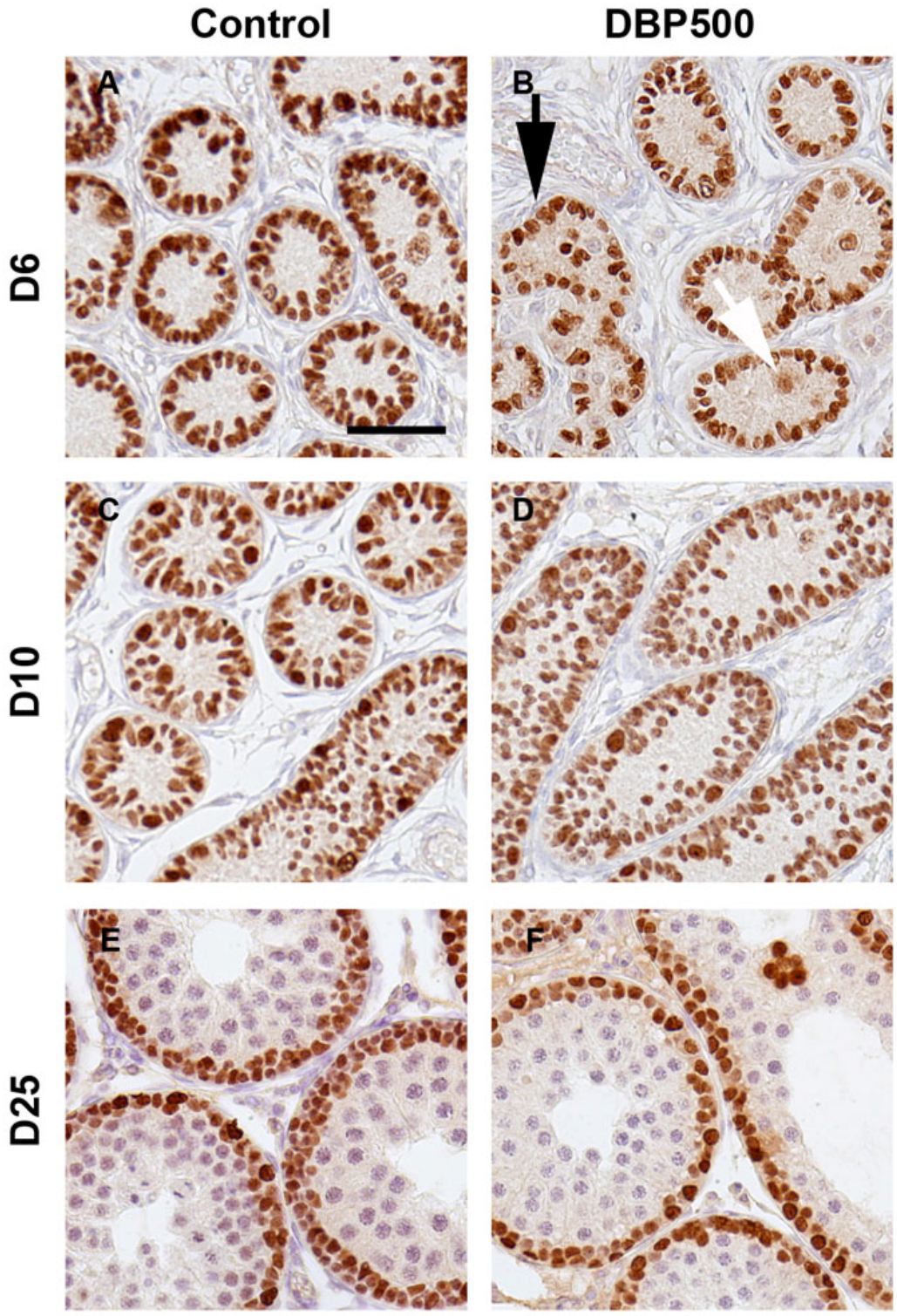

Figure 4.22 Representative photomicrographs of immunostaining for DMRT1 (Dab = brown) in postnatal rat testes from control (left) and DBP exposed (right) animals from D6 (top) through to d25 (bottom). Scale bar in panel A represents 50µm. Black arrow depicts a dysgenic area, white arrow depicts a GC in Panel B.

At D6 in controls, the GCs began to re-express DMRT1 and to migrate from the centre of the cords, discussed further in Section 4.3.3.4. DMRT1 then remained expressed in all GCs until D25, when expression was confined to the spermatogonia (as well as Sertoli cells). Fetal DBP exposure appeared to result in fewer GCs expressing DMRT1 at D6. To clarify this impression double IHC for DMRT1 and VASA was performed, as shown in Fig 4.23.

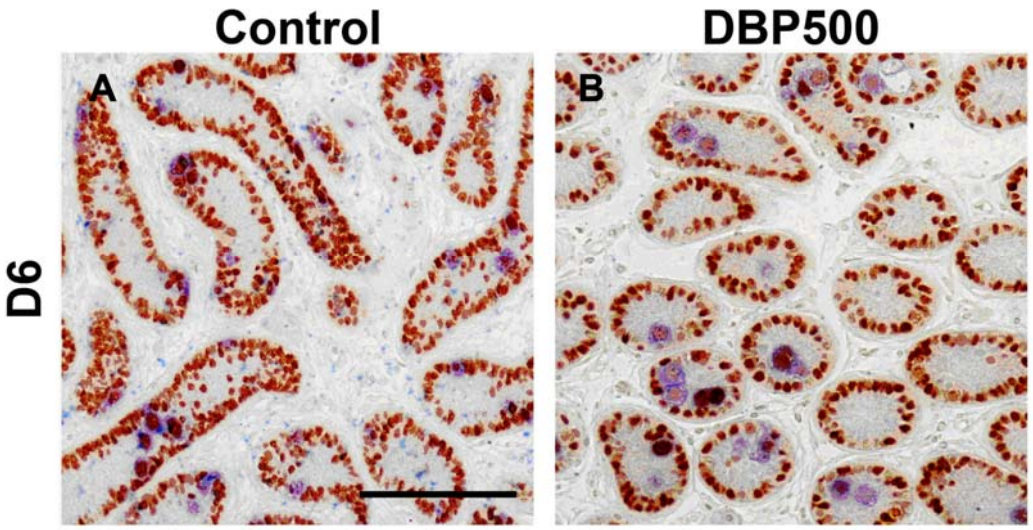

Figure 4.23 Representative photomicrographs of immunostaining for DMRT1 (Dab = brown) and VASA (Fast blue = blue) in postnatal rat testes from control (left) and DBP500 exposed animals (right) at D6. Scale bar in panel A represents 100µm.

Fetal DBP exposure did not prevent the re-expression of DMRT1in GCs postnatally at D6, but did seem to reduce the number of GCs expressing DMRT1. To quantify this possible DBP effect, the percentage of DMRT1 expressing GCs at D6 was calculated and the results shown in Fig 4.24. Fetal DBP exposure did significantly reduced the percentage of GCs expressing DMRT1 at postnatal D6, showing that the DBP induced delay in GC development continued into early postnatal life.

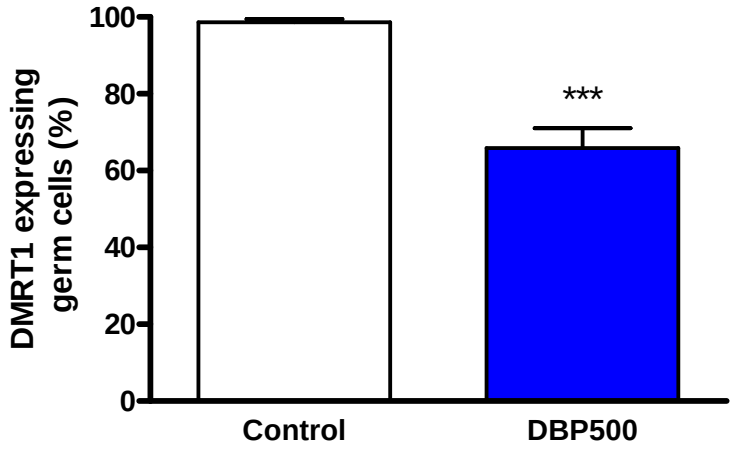

Figure 4.24 Percentage of DMRT1 expressing germ cells at D6 in postnatal rat testes from control and DBP exposed animals (n=4). Values are means ± SEM. Student's unpaired *t* test was performed, *** P<0.001 between control and DBP exposed.

To investigate if the different exposure windows of DBP could produce the same postnatal GC effect, D6 testes from early time window DBP exposed animals (EW, e13.5-e15.5) and extended window exposed animals (Ext, e11.5-e21.5) were also quantified for DMRT1 expression in GCs in Fig 4.25.

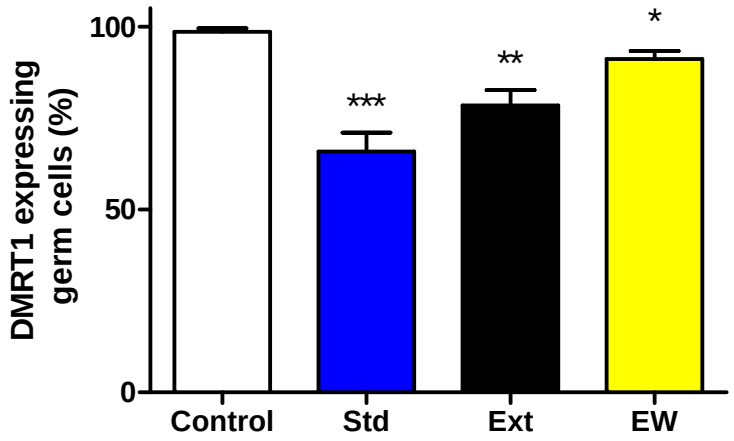

Figure 4.25 Percentage of DMRT1 expressing germ cells at D6 in postnatal rat testes from control and DBP exposed animals from different exposure time windows (n=4). Values are means ± SEM. Student's unpaired *t* test was performed, * P<0.05, ** P<0.01, *** P<0.001 between control and DBP exposed.

The different DBP exposure time windows all resulted in a significant reduction in the percentage of GCs expressing DMRT1 at D6, but the effect was largest for the standard DBP exposure window. The less significant reduction observed with the extended exposure window is most likely due to the variability of DBP effects and the relatively low "n" number.

4.3.3.2 Postnatal germ cell number

As previously reported, DBP exposure reduced GC number at D6 (Ferrara et al., 2006), so to examine if the different DBP exposure windows could reproduce this effect, GC counts were performed on D6 testes from control and standard, early and extended time window DBP exposed animals, and results are shown in Fig 4.26.

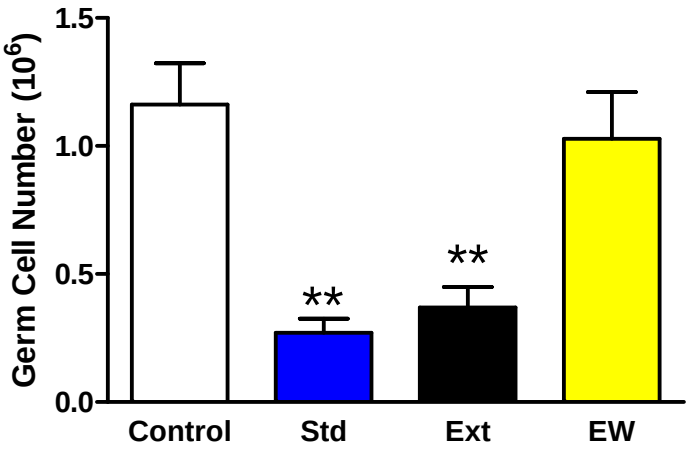

Figure 4.26 Number of germ cells at D6 in testes from control and DBP exposed animals from different DBP exposure time windows (n=4). Values are means ± SEM. Student's unpaired *t* test was performed, ** P<0.01 between control and DBP exposed.

The extended exposure window reduced GC number to a similar level as did the standard DBP exposure window, whilst DBP exposure in the early window did not. This may be a reflection of the fact that the EW exposed testes used for this analysis did not show the same severe reduction in testis size at D6 as the Std or Ext DBP

treatment windows. Whilst this may be due to EW DBP exposed testes somehow recovering from the significant reduction in GC number with EW DBP exposure at e21.5 (Fig 4.18), it is more likely due to the variability of *in vivo* tissue and the relatively low "n" number used to calculate GC number.

4.3.3.3 Postnatal resumption of germ cell proliferation

As postnatal GC numbers are reduced after fetal DBP exposure, changes in their proliferation were investigated as a possible cause of this reduction. GC Proliferation indices were calculated for postnatal D6, D8 and D10 testes in control and standard window DBP exposed animals, and results are shown in Fig 4.27.

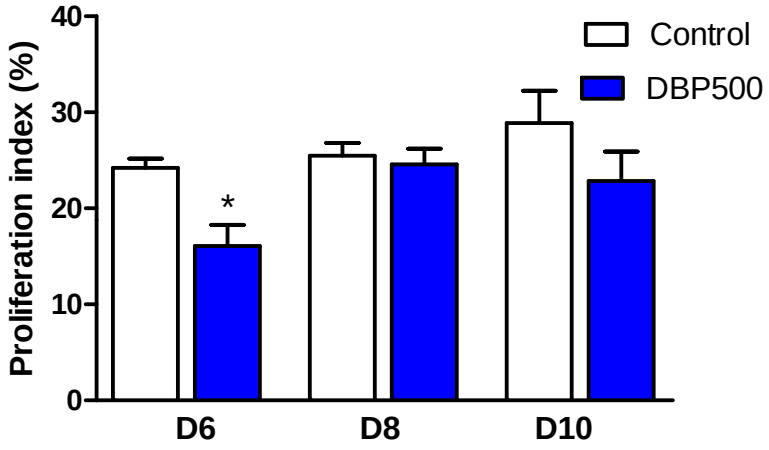

Figure 4.27 Germ cell proliferation index in testes from control and DBP exposed animals at D6, D8 and D10 (n=4-5). Values are means ± SEM. Student's unpaired *t* test was performed, * P<0.05 between control and DBP exposed.

DBP exposure only significantly reduced the GC proliferation index at D6, possibly indicating that the postnatal initiation of proliferation has been delayed by DBP exposure, providing another postnatal GC effect for which development is delayed but not prevented.

4.3.3.4 Postnatal germ cell migration

As fetal GCs in DBP exposed animals showed a delayed disaggregation/migration at e21.5, the postnatal GC migration to the basal lamina was investigated for a possible DBP exposure effect. Double IHC for VASA and SMA, used to identify the basal lamina, was performed on D6 testes and is shown in Fig 4.28

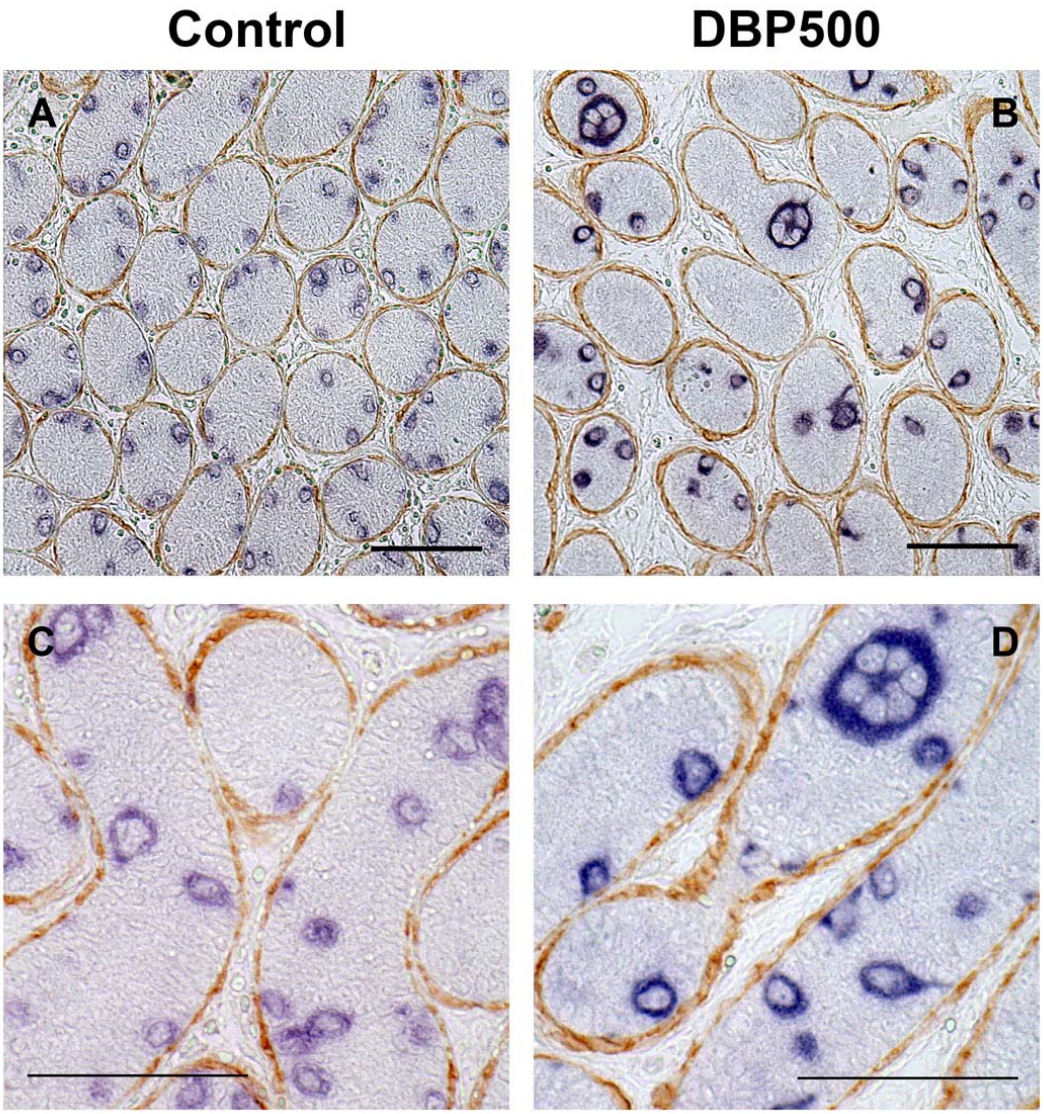

Figure 4.28 Representative photomicrographs of immunostaining for SMA (Dab = brown) and VASA (Fast blue = blue) in postnatal rat testes from control (left) and DBP exposed animals (right) at D6. Scale bars represent 50µm.

In addition to an increased incidence of multinucleated gonocytes (MNG) in testes of DBP exposed animals, the position of GCs within the seminiferous cords seemed to be more centrally located than in controls at D6. To quantify this, the percentage of GCs in either basal or central positions within the cords was evaluated, as described in Section 2.8.5, and results are shown in Fig 4.29.

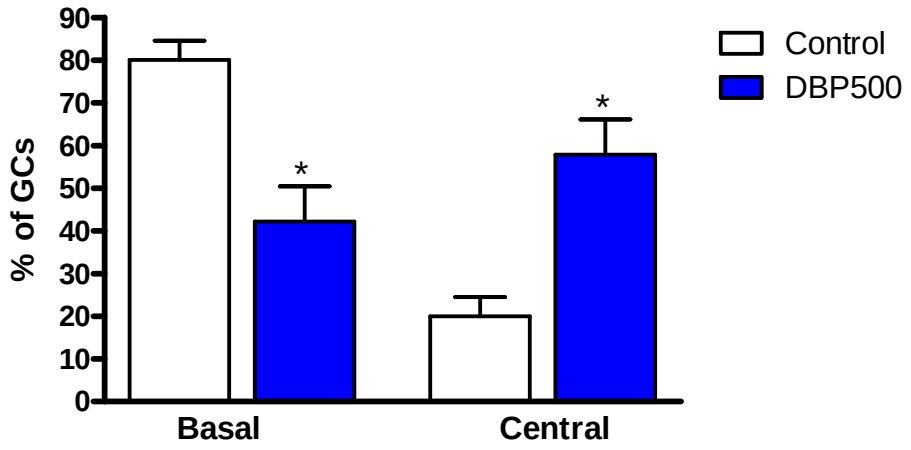

Figure 4.29 Percentage of germ cells in basal or central seminiferous cord positions at D6 in testes from control and DBP exposed animals (n=3). Values are means ± SEM. Student's unpaired *t* test was performed, * P<0.05 between control and DBP exposed.

In testes from DBP exposed animals at D6, there is a significant increase in the percentage of GCs located centrally within the seminiferous cords compared to controls, once again indicating a delay in GC migration. As mouse studies have identified that DMRT1 is essential in GCs for postnatal GC migration to the basal lamina, the delay in re-expression of DMRT1 may be involved in this delay (Kim et al., 2007). However, there were DMRT1- GCs at the basal lamina and DMRT1+ GCs centrally located (Fig 4.22), suggesting no consistent relationship between DMRT1 expression and GC location in the cords at D6.

4.3.3.5 Later postnatal consequences of DBP exposure

As previously reported (Ferrara et al., 2006), fetal DBP exposure significantly reduced GC number at D15. This was examined in the present study using VASA IHC to identify GCs for enumeration in D15 testes from control and DBP exposed animals, and a similar reduction was seen, as shown in Fig 4.30.

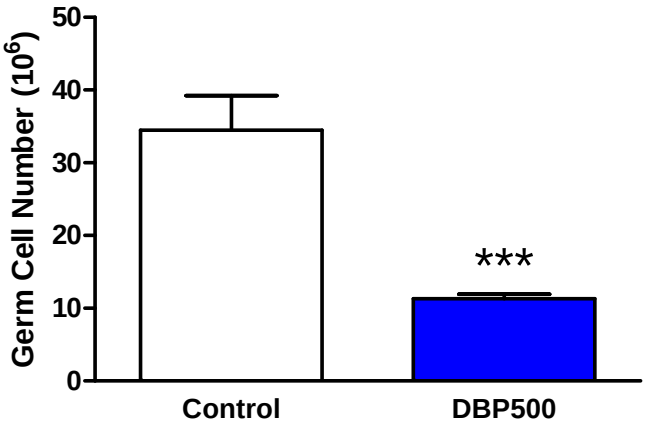

Figure 4.30 Number of germ cells at D15 in testes from control and DBP exposed animals (n=6). Values are means ± SEM. Student's unpaired *t* test was performed, *** P<0.001 between control and DBP exposed.

In analysing the D15 testes there was an observable difference in the position of GC in the seminiferous cords, as visualized by VASA IHC on testes from control and DBP exposed animals (Fig 4.31).

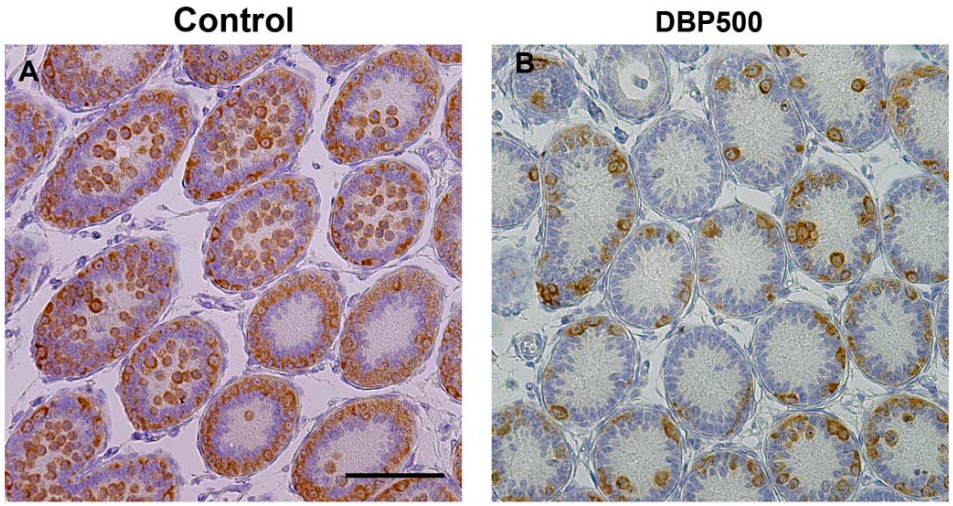

Figure 4.31 Representative photomicrographs of immunostaining for VASA (Dab = brown) in postnatal rat testes from control (left) and DBP exposed (right) animals at D15. Scale bar in panel A represents 50µm.

At D15, the reduction in number of GCs in testes of DBP exposed animals was clearly visible and GCs were located sparsely around the base of the seminiferous cords. In D15 control testes, GCs were beginning to enter meiosis (differentiate), and, in doing so, to move to the centre of the cords. This showed again that the fetal DBP exposure continued to delay GC development at least 15 days after DBP exposure had ended.

4.4 Discussion

The aim of this chapter was to determine how DBP exposure *in utero* could alter the process of germ cell (GC) development in the fetal rat testis, as described in Chapter 3. To that end GC number, proliferation, apoptosis, differentiation (observed through changes in protein expression) and aggregation/migration were examined in testes from control and DBP exposed animals. In addition, the effect of different DBP exposure time windows on GC development was examined to gain more insight into when DBP exposure causes its effect(s). Finally, early postnatal GC development was investigated to determine if altered GC development continued after DBP exposure was over.

Having established the normal pattern of GC development within the fetal rat testis in Chapter 3, the first aspect of this investigation was to thoroughly examine how these GC events were altered by *in utero* DBP exposure. Using previous work on the effects of DBP exposure on GCs as a starting point (Ferrara et al., 2006), which showed that GC number was significantly reduced by e21.5, GC number was calculated throughout fetal testis development for control and DBP exposed animals to identify when the significant reduction in GC numbers induced by DBP at e21.5 occurs. At every fetal age investigated, GC number was consistently reduced in the testes of DBP exposed animals, but this reduction was only significant in early testis development (e14.5 and e15.5) and just prior to birth (e21.5).

Problematically, GC number was shown to also increase after the established end of GC proliferation around e17.5 (Fig 3.5) in both control and DBP exposed animals.

This apparent increase after e19.5 is most likely due to differential errors in determining GC number at different ages. Whilst stereology is a well established technique to accurately determine cell numbers, in this case the huge increase in testis size/weight between e17.5 and e19.5 (which is a multiplier to calculate cell number per testis, Section 2.8.1) is a key factor in determining final GC number. In this regard, 3 different methods of determining testis weight were used according to age, with directly determined individual testis weights only being undertaken at e19.5 and e21.5, making GC number at e19.5 and e21.5 probably the most accurate. It seems likely that differential errors in determining testis weight/volume at the different ages explains the apparent increase in GC numbers beyond e17.5. However this chapter is focussed on DBP exposure effects and not on how GC number increases over time. Therefore, at each age comparison of GC number between testes from control and DBP exposed animals is valid and this showed a consistent reduction in GC numbers due to DBP exposure, which is the most important aspect of Fig 4.1.

Other factors that may be involved in errors in determining GC number are that there is inherently high variability with *in vivo* animal work and that, as shown in Fig 4.5, the mean nuclear volume of GCs changes substantially during testis development, which is also a potential source of error when comparing GC number at different ages. In fact DBP exposure seemed to cause a significant reduction in mean nuclear volume at e21.5 compared to control GCs, suggesting either delayed GC development or that DBP exposure is directly preventing GC nuclear expansion. Despite these technical reservations, there is no doubt that DBP exposure reduces GC number, in agreement with previously published data on GC number at e21.5 (Ferrara et al., 2006). This reduction in GC number is supported by similar reported reductions in GC number after *in vitro* phthalate exposure (MEHP) in neonatal mouse testes (Li and Kim, 2003) and in fetal human testes (Lambrot et al., 2009).

To try and determine how DBP induced a reduction in GC number, both GC proliferation and apoptosis were examined. The GC proliferation index was not

significantly altered by DBP exposure, but in testes from DBP exposed animals there was a noticeable increase in proliferating GCs at e17.5 and even isolated rare proliferating GCs at e19.5, neither of which were observed in controls. This suggested that instead of reducing GC proliferation as might have been suspected, GC proliferation was continuing for longer in DBP exposed animals. By combining GC number and the proliferation index data, the total number of proliferating GCs was calculated and this showed a significant reduction in testes from DBP exposed animals at e15.5. Therefore, even though GC proliferation was prolonged, GC number could not recover to control levels following the early reduction in their numbers. This suggested that the entry of GC into quiescence was being delayed by DBP exposure. This may be the result of a delay in time taken to complete each GC division, or a delay in the change from primordial GC division to regulation by the somatic environment, or a delay in the somatic signalling that regulates the entry into mitotic arrest (Monk and McLaren, 1981).

When GC apoptosis was examined by TUNEL staining, there was no significant difference between testes of control and DBP exposed animals, with only a few cells on each section staining TUNEL+. The lack of DBP effect and the general low level of GC apoptosis suggested that the consistent reduction in GC number observed with DBP exposure is not due to increased apoptosis, at least not at the ages investigated. However it is possible that, as collection of tissue occurred generally 24 hours after DBP dosing, any increase in GC apoptosis that might have occurred soon after treatment would no longer be evident at the time of collection. *In vitro* studies of MEHP treatment on fetal human testes has shown increased GC apoptosis (by cleaved caspase-3 detection) compared to controls (Lambrot et al., 2009). However, fetal mouse testes collected at e_m18 and cultured *in vitro* for 3 days with MEHP did not show an increase in GC apoptosis, whilst neonatal mouse testes collected at D3 and cultured in the same manner with MEHP did show a significant increase in apoptosis (Li and Kim, 2003). This may indicate that GCs are only susceptible to phthalate induced apoptosis at certain points in their development. This would fit

with the absence of evidence for any accumulative loss of GC as treatment progressed in the present studies.

There are several possible explanations for the consistent reduction in GC number after DBP exposure. As GC number is significantly reduced at e14.5, only 24 hours after the initial DBP dosing, this suggests that some early event of testis development is being disrupted. This is supported by findings involving DBP treatment in only an early time window, as discussed below. Unfortunately, no insights into what is causing this early effect have been identified in this thesis. But it is possible this early disruption could cause direct loss of GCs through phthalate induced apoptosis, as *in vitro* (Lambrot et al., 2009; Li and Kim, 2003), or through some indirect way that results in a reduction in GC number by e14.5, such as delaying the organisation of Sertoli cell and GC into cords, such that the program of GC development is initially delayed. As described above, it is also possible that DBP induced GC apoptosis may be being missed, or that it occurs at an early point in testis development (e.g. e13.5), when a relatively minor effect of DBP exposure may get multiplied by each subsequent round of GC proliferation and would lead to the observed major reduction in GC numbers by e21.5. In view of the observed reduction in GC number at e14.5 in DBP exposed animals, this sort of explanation seems most likely.

Having further investigated the reported reduction in GC number, the process of GC differentiation was examined for DBP exposure effects. For the purpose of this thesis, GC differentiation was viewed as the change in protein expression over time. Previous work on effects of DBP exposure on GCs in the fetal rat testis discovered that the pluripotency factor OCT4 appeared to be more highly expressed at e17.5 in the GCs of testes from DBP exposed animals compared to controls (Ferrara et al., 2006). This was confirmed in the present studies and the effect quantified. This showed that significantly more GCs expressed OCT4 at e17.5 in testes from DBP exposed animals, compared with controls, without a significant change in mRNA level in whole testes. This may be due to the fact that DBP exposure is having no

effect on mRNA expression at e17.5, or may reflect that there are fewer GCs in DBP exposed animals at e17.5 that are each expressing a higher level of *Oct4* mRNA than are individual GCs in control testes. As OCT4 expression in GCs in DBP exposed animals was absent by e19.5, as in controls, this suggested that DBP exposure was simply delaying the switching off of OCT4 expression, rather than preventing its switch off.

As described in Section 3.3.7, the expression of DAZL protein appeared to diminish in GCs after e19.5 but was still detectable at e21.5. In the testes of DBP exposed animals at e19.5 and e21.5, DAZL expression still diminished, as in controls, but possibly to a lesser extent than in control testes. Regrettably this could not be quantified by Western blot, so remains observational. When *Dazl* mRNA expression was examined there was no significant reduction in DBP exposed animals versus controls until e21.5, possibly reflecting the significant reduction in GC number at e21.5 in testes of DBP exposed animals. The possibly stronger expression of DAZL protein in GCs of testes from DBP exposed animals as compared to controls is most likely due to a DBP-induced delay in the silencing of DAZL.

Another GC marker investigated was VASA, which showed no change in protein localization or strength of expression (by IHC) between control and DBP exposed animals at any age. However, when *Vasa* mRNA was examined in control and DBP exposed animals it was significantly reduced in DBP exposed animals at e21.5, once again possibly reflecting the significant reduction in GC number at this time. However, GC number was consistently reduced in DBP exposed animals at each age investigated, but *Vasa* mRNA expression was only reduced at e21.5. This suggests that either DBP exposure reduced the individual GC expression of *Vasa* at e21.5, and by inference *Dazl* too, or that for a significant reduction in *Vasa* expression to be detected, a significant reduction in GC number must also be present.

In the fetal rat testis, DMRT1 was expressed in both GCs and Sertoli cells, but at around e19.5 most GCs have switched off DMRT1 expression until it resumes in

postnatal life. In the testes of DBP exposed animals at e19.5, there was a significant increase in the number of GCs that were continuing to express DMRT1, similar to the earlier delay in switching off of OCT4 expression. When *Dmrt1* mRNA expression levels were examined, they were complicated by mRNA expression from both GCs and Sertoli cells. At e21.5 there was a significant reduction in *Dmrt1* expression, but this is likely due to the significant reduction in both Sertoli and GCs at this age. At e19.5, when GCs are normally switching off DMRT1 protein expression, mRNA expression levels were similar in testes from control and DBP exposed animals, which may be due to individual GCs expressing more *Dmrt1* mRNA even though there are fewer GC in number in DBP exposed animals. In this way, GC-specific expression of DMRT1 is another aspect of GC development that showed a delay after DBP exposure.

When expression of cKIT protein was examined, a change in localization was discovered over time as expression went from predominantly nuclear to a more cytoplasmic/cell membrane staining. In the testes of DBP exposed animals there seemed to be a delay in the change in cKIT re-localization, so that at e17.5 cKIT expression remained nuclear in GCs from DBP exposed animals and cytoplasmic in GCs from controls. However, as cKIT protein is generally considered to be localized to the cell membrane the nuclear staining observed at earlier ages is puzzling and is potentially artifactual. Irrespective of this, the antibody to cKIT once again indicated that GC differentiation is delayed after DBP exposure.

Towards the end of fetal life in the rat, GCs begin to disaggregate from their central location in the cords and move gradually towards the basal lamina by e21.5. In testes from DBP exposed animals, GCs remained centrally aggregated at e21.5 although by postnatal life disaggregation has occurred, suggesting that DBP exposure is delaying this aspect of GC development. Related to this disaggregation is the appearance of multinucleated gonocytes (MNG) in the testes of DBP exposed animals at e19.5 and e21.5, which are presumably GCs that have become fused because of loss of intercellular bridges. The occurrence of MNGs is discussed in more detail elsewhere

(Ferrara et al., 2006), but interestingly DBP exposure at e19.5-e20.5 is sufficient to cause the appearance of MNGs at e21.5, suggesting that it is a late effect that is unconnected to GC proliferation. This late exposure to DBP (e19.5-e20.5) also resulted in central GC aggregation at e21.5 (data not shown), showing that this aspect can be induced late in gestation. One possible explanation for the failure of GCs to disaggregate at e21.5 is that this process involves Sertoli cell and GC interactions, so that Sertoli cell cytoplasm can invaginate between the GCs, which is delayed/prevented at e21.5 with DBP exposure (G. Hutchison, unpublished data).

In DBP exposed animals, the Sertoli cells are also significantly reduced in number at e19.5 and e21.5 compared to controls but not at e17.5 (Scott et al., 2008), and comparison of GC:Sertoli cell ratios in control and DBP exposed testes showed no significant difference at these ages (data not shown). This timing of Sertoli cell reduction at e19.5 and the early effects of DBP exposure on GC development suggests a limited involvement with Sertoli cells in the fetal GC effects after DBP exposure. However, if DBP is somehow interfering with Sertoli-GC interactions, it may explain both the early effect of DBP exposure on GC (reduced numbers) and why the disaggregation of GCs fails to occur later. As described above, GC effects of DBP exposure are noticeable by e14.5, 24 hours after initial exposure, so one possible explanation is that DBP exposure interferes with Sertoli-GC interactions during initial cord formation (which occurs by e14.5), causing the initial reduction in GC number and delaying all of the subsequent GC development. The use of an early window of DBP exposure from e13.5-e15.5 supported this conclusion, as described below. At e19.5, DBP exposure may also interfere with Sertoli-GC interactions and delay Sertoli cell invagination and cause the GCs to fail to disaggregate, which would match published data on DBP exposure only between e19.5-e20.5 (Ferrara et al., 2006). Regrettably this is just supposition, but the possible role of DBP on Sertoli-GC interactions warrants further work.

Having examined how DBP exposure from e13.5 onwards delayed GC development, different DBP exposure time windows were examined to gain more understanding

into how DBP exposure is affecting GC development and to possibly support some of the conclusions drawn from this previous data. Three different exposure time windows were used; an extended exposure window of e11.5-20.5(Ext), an early exposure window of e13.5-e15.5 (EW) and a middle exposure window of e15.5-e17.5 (MW).

The first aspect of GC development investigated using these different treatment time windows was GC number at e21.5. The results showed that the Ext DBP treatment window significantly reduced GC number by e21.5 to the same degree as did the standard DBP exposure window. The EW DBP treatment also showed a significant reduction in GC number, but not as great as with the standard DBP exposure window. The MW DBP treatment slightly reduced GC number at e21.5, but not significantly. This suggested that DBP exposure between e11.5-e13.5 had no greater effect on GC disruption than did treatment from e13.5, whilst treatment between e13.5-e15.5 was crucial to reduce GC number by e21.5. This time window corresponds with sex determination and seminiferous cord formation suggesting that this is the time when GCs are susceptible to DBP exposure, not when they are migrating into the gonad prior to e11.5.

When GC mean nuclear volume was examined at e21.5 for the different DBP treatment time windows, the Ext treatment window induced the same reduction in GC nuclear size as did the standard DBP treatment window, supporting the notion that earlier DBP exposure had no greater effect. The EW DBP exposure reduced GC nuclear size, but not significantly, whereas MW DBP exposure did significantly reduce GC nuclear size, suggesting that DBP exposure within the period e15.5-e17.5 is required for this particular GC effect. This would further suggest that the effects of DBP may not be due to a single event that permanently delays GC development in the manner observed for the standard DBP treatment window.

DBP induced prolongation of OCT4 expression at e17.5 was examined after treatment during the EW and MW time windows. In this instance, only the EW

treatment significantly increased the percentage of GCs expressing OCT4, but not as significantly as did the standard window DBP exposure. This suggests that the EW time period is the most important for delayed differentiation, whilst continued exposure is perhaps needed to maintain this delay. The use of these two windows of DBP exposure indicated that it is not a direct effect of DBP exposure on GCs at e17.5 that results in the increased OCT4+ GCs, as it was the EW DBP exposure rather than MW DBP exposure that caused the significant increase in OCT4+ GCs.

It was also examined whether EW DBP exposure significantly increased the percentage of DMRT1+ GCs at e19.5 similar to the standard DBP treatment window. EW treatment did cause an increase in DMRT1+ GCs, but not as significantly as did the standard DBP treatment, suggesting again that although early DBP exposure is required to induce these effects, their persistence requires prolonged DBP exposure.

In summary, DBP exposure earlier than e13.5 has no greater effect than does exposure from e13.5 and that no single short DBP exposure time window is sufficient to induce all of the GC effects induced by the standard DBP exposure treatment, although the EW has been identified as being more crucial for delayed GC differentiation than the MW.

Having examined the effects of DBP exposure on fetal GCs development, the postnatal consequences were then investigated. Previous work on the effects of fetal DBP exposure on postnatal GCs had identified that GC number was significantly reduced beyond puberty but was resolved by adulthood (Ferrara et al., 2006). To complement this observation the effect of both the standard and different DBP exposure time windows on early postnatal GC development was examined.

At postnatal day 6, GC number, the GC proliferation index, GC position and DMRT1 re-expression in the GCs were examined. DMRT1 is necessary in the mouse for correct postnatal testis development, as its knock-out in just the GCs results in their failure to migrate to the basal lamina postnatally (Kim et al., 2007). In the rat,

DMRT1 expression was switched off in the GCs at around e19.5 and then became re-expressed at around postnatal D6. The percentage of DMRT1+ GCs on D6 was significantly reduced by the standard DBP exposure, consistent with the notion that the DBP induced delay in GC development continued into early postnatal life.

In testes from standard window DBP exposed animals at D6, there was an increased percentage of GCs located centrally within the seminiferous cords, illustrating that migration to the basal lamina was also delayed. Whilst DMRT1 expression is related to GC migration to the basal lamina in the mouse, in the rat there was not a clear relationship between DMRT1 expression and GC position at D6.

The percentage of DMRT1+ GCs in testes from the Ext DBP exposure groups was significantly reduced but not to the same degree as occurred with the standard window DBP exposure. This is likely due to the inherent variability and low "n" number used in this experiment, rather than the Ext DBP treatment window having a lesser effect. With the EW DBP exposure window, the percentage of DMRT1+ GCs was also reduced at D6, showing that this brief early exposure window is causing a GC developmental delay, albeit not as severe as with the standard DBP exposure window.

At D6 GC number had been previously reported as significantly reduced after *in utero* DBP exposure (Ferrara et al., 2006), and was confirmed here. In addition, in D6 testes from animals from the Ext DBP treatment group, a similar significant reduction in GC number was found, as expected. However, D6 testes from EW DBP exposed animals did not show a significant reduction in GC number. As for most other aspects of GC development, this treatment was either partially or fully effective, compared with the standard treatment window, this disparity is unexplained. It could simply reflect the relatively low "n" numbers used, or it could mean that somehow GC number is recovering from the significantly reduced GC number observed with EW DBP exposure at e21.5. If so, this would have to involve an earlier resumption of GC proliferation. In this regard, when the GC proliferation

index was evaluated at D6, D8 and D10 for testes from control and standard DBP exposed animals, there was only a significant reduction at D6. This suggests that there is a delay in the resumption of proliferation in the postnatal testes of DBP exposed animals.

At D15 there was a significant reduction in GC number in testes from standard DBP exposed animals compared with controls, as well as a noticeable difference in GC location within the cords/tubules. In testes from control animals, GCs were beginning to enter meiosis (differentiate) and move into the centre of the cords, whilst in testes from DBP exposed animals GCs were sparse and were still mainly located at the basal lamina.

In summary of these postnatal investigations, several early postnatal events of GC development also showed a DBP induced delay that continued until at least D15. The Ext DBP exposure window had no greater effect on postnatal GC development, matching observations in fetal life. Furthermore, the EW DBP exposure window resulted in a less pronounced GC delay postnatally, once again matching data from the fetal studies. It should be noted that even with this early postnatal GC developmental delay, by adulthood GC numbers in DBP exposed rats have recovered to control levels in normally descended testes (Ferrara et al., 2006). However, the delayed GC development could have more subtle effects that might contribute to the reduced fertility in DBP exposed rats in adulthood, as delayed GC development may result in abnormal GCs.

In general summary of DBP exposure effects, the standard DBP exposure from e13.5-e21.5 delayed fetal GC development when compared to controls, as summarized in Table 4.4. That GC development is delayed but not stopped may explain why CIS like cells are not produced by DBP exposure in the rat model of TDS.

Table 4.4 Summary of effects of *in utero* DBP exposure from e13.5-e20.5 on GC development in the rat.

GC Process	**Effect of DBP exposure**
Number	Consistently reduced GC number from e14.5 until D15
Proliferation	Delayed end of proliferation and delayed postnatal resumption
Nuclear volume	Delayed or prevented expansion at e21.5
Apoptosis	No difference detected
OCT4 expression	Delayed switching off of OCT4 expression at e17.5
DAZL expression	Possible delay in reduction of DAZL expression at e19.5 and significant reduction in *Dazl* mRNA at e21.5
VASA expression	No difference in protein detected but significant reduction in *Vasa* mRNA at e21.5
Fetal DMRT1 expression	Delayed switching off of GC-specific DMRT1 expression at e19.5
"cKIT" expression	Possible delay in re-localization at e17.5
Fetal aggregation/ Migration	Delay in disaggregation and migration to basal lamina at e21.5, occurrence of MNGs
Postnatal DMRT1 Expression	Delayed re-expression of GC-specific DMRT1 expression at D6
Postnatal migration	Delayed migration to basal lamina
Meiosis	Delayed entry into meiosis at D15

5 Investigation of methylation as a potential mechanism for effects of Di (n-Butyl) Phthalate on germ cells

5.1 Introduction

DNA methylation is the addition of a methyl group to a CpG dinucleotide in the DNA, and is one of several mechanisms involved in epigenetic regulation of the genome, as reviewed in Section 1.4. In the mouse, fetal germ cells (GC) lose genomic methylation pattern during migration to the gonad, and then undergo gradual remethylation as a new genomic imprint is established (Oakes et al., 2007b). DNA methylation is also involved in gene silencing that occurs during cellular differentiation. As described in detail in Chapter 4, *in utero* exposure to Di (n-Butyl) Phthalate (DBP) alters several aspects of GC development and differentiation during the last week of fetal life in the rat testis, and in this chapter DNA methylation in the fetal testis was examined as a possible mechanism for DBP effects.

Three approaches were taken to investigate DNA methylation in the fetal rat testis after DBP exposure. First, it was examined how normal global methylation by the action of DNA methyl transferases occurred in the fetal rat testis and if this was disrupted by DBP exposure. Then the use of a chemical DNA methylation inhibitor was used to examine if GC differentiation could be prevented in the fetal rat testis, and whether DBP effects were altered when it was combined with methylation inhibition. Finally, gene specific methylation of the *Oct4* promoter was examined during the last week of fetal life, as OCT4 protein expression is altered by DBP exposure and the *Oct4* gene is regulated by promoter methylation in the mouse and human (Deb-Rinker et al., 2005; Freberg et al., 2007; Hattori et al., 2004).

5.2 Materials and methods

5.2.1 Animals and in vivo treatments

Briefly, pregnant Wistar rats were treated with DBP or corn oil from e13.5 onwards, or injected with 5-aza-2'deoxycytidine (AZC) or saline on e16.5, or a combination of both treatments (Section 2.2). These treatments and the ages of tissue collection are summarized in Table 5.1.

Table 5.1 Summary of maternal AZC and DBP treatments and collection ages used in Chapter 5.

AZC Dose (mg/kg bodyweight)	I.P. inj.	DBP Dose (ml/kg bodyweight)	Treatment window	Abbrev.	Kill age
-	-	500	e13.5-e20.5	DBP500	e15.5, e17.5, e19.5, e21.5
5	e16.5	-	-	AZC5	e17.5, e19.5
10	e16.5	-	-	AZC10	e17.5, e19.5
10	e16.5	500	e13.5-e20.5	AZC+DBP	e17.5, e19.5

Testes from control and AZC±DBP exposed animals were dissected out (Section 2.3-2.3.4) and were either fixed in Bouin's and processed for immunohistochemical analysis, or stored at -80°C for RNA analysis or bisulphite sequencing (Section 2.10).

5.2.2 Immunohistochemical (IHC) analysis

Briefly, IHC staining (Section 2.6) was performed on processed and sectioned fetal testes as summarised in Table 5.2. The number of fetal testes used for IHC was a minimum of 5 testes in each age and treatment group and came from a minimum of three different litters.

Table 5.2 Details of antibodies used in Chapter 5.

Antibody	Source	Retrieval	Species
DAZL	AbD Serotec	Yes	Mouse
DMRT1	Gift from David Zarkower, MN	Yes	Rabbit
DNMT1	Abcam, Cambridge	Yes	Rabbit
DNMT3A	Abcam, Cambridge	Yes	Rabbit
DNMT3L	Abcam, Cambridge	Yes	Rabbit
OCT4	Santa Cruz, CA	Yes	Goat
VASA	Abcam, Cambridge	Yes	Rabbit
5MeC	Abcam, Cambridge	Section 2.6.6.1	Sheep

In addition to standard single IHC, several IHC analyses were performed to calculate the percentage of OCT4 or DMRT1 expressing GCs (Section 2.8.4). Specialised IHC for 5-methyl cytidine (Section 2.6.6.1) and TUNEL for apoptotic cells (Section 2.6.12) was also performed in Chapter 5.

5.2.3 Bisulphite sequencing

To investigate the methylation status of the *Oct4* gene promoter and proximal enhancer in the fetal rat testis, whole testis DNA from 3x pooled (3-4) e15.5 control testes and 3x e19.5 control testes was isolated (Section 2.10.1) and converted by bisulphite treatment (Section 2.10.3) to alter the DNA sequence to allow methylation status of CpGs to be identified. The converted DNA was amplified (Section 2.10.4), sequenced and analysed for three regions of the *Oct4* gene promoter and proximal enhancer (Section 2.10.5).

5.2.4 GC sorting by MACS

To isolate GC DNA from whole rat testes, Magnetic-activated cell sorting (MACS) using a GC-specific cell surface antigen was performed (Section 2.4). Briefly, testes from postnatal day (D)0 were physically and enzymatically digested to produce a single cell suspension (Section 2.4.1), that was incubated with 2µg Anti-SSEA antibody (Abcam, ab16285) and prepared magnetic Dynabeads (Section 2.4.2). A magnet was then used to isolate the Dynabeads with attached GCs (Section 2.4.3).

Isolated cell fractions (Bound, Unbound and Unsorted) were then stored at -80°C for RNA or DNA analysis.

5.2.5 RNA analysis

Briefly, RNA isolated from frozen testes was converted into cDNA (Section 2.11.2) and Taqman quantitative RT-PCR performed (Section 2.11.5), to establish quantitative mRNA expression levels. The genes investigated, and primers used, are listed in Table 5.3.

Table 5.3 Taqman primers and Universal Probe Library probes used in Chapter 5.

Gene	**Forward Primer 5' → 3'**	**Reverse Primer 3' → 5'**	**UPL Probe Number:**
Amh	CTGGACACCGTGCCTTTC	CACTGTGTGGCAGGTCCTC	98
Boris	GAAGAAAAAGAAAGATGCGGTCT	GAGATCCGGCTCAGCATTT	82
Dazl	GCTCAGTTCATGATGCTGCT	ATGCTTCGGTCCACAGATTT	110
Dmnt1	CGATGACGATGAAAAGGACA	GTCTCCGTTTGGTGGCTAGA	26
Dmnt3A	AACGGAAGCGGGATGAGT	TGCAATCACCTTGGCTTTCT	75
Dmnt3L	GAGGGTGTGGAGCAACATTC	GCTCTTCCTTAGGGGTCAGG	41
Oct4	GAAGTTGGAGAAGGTGGACC	CCTTCTGCAGGGCTTTCATA	95
3β hsd	GACCAGAAACCAAGGAGGAA	CTGGCACGCTCTCCTCAG	105

5.3 Results

5.3.1 Global germ cell methylation

Studies in the mouse have shown that when germ cells (GC) arrive in the gonad, they have undergone global demethylation to provide a "blank epigenetic slate". The GCs then undergo establishment of new methylation patterns and genomic imprinting that is not complete until postnatal meiosis in the testis (Oakes et al., 2007b). To examine if similar demethylation and gradual remethylation occurs in the fetal rat testis, examination of the global methylation state of the GC genome during testis development was performed. Immunohistochemical (IHC) staining for 5-methyl cytidine (5MeC) was performed as described in Section 2.6.6.1, on testis sections from fetal rats during the last week of fetal life and the results are shown in Fig 5.1. Testes from both control and DBP exposed fetal rats were examined to see if DBP exposure altered global GC methylation.

The amount of staining for 5MeC in the nuclei gives a simple visualization of the degree of methylation of CpG dinucleotides in the genome of a cell. At embryonic day (e)15.5 and e17.5, the GCs showed noticeably less 5MeC staining than surrounding somatic cells, as highlighted in Fig 5.1A. This difference in 5MeC staining showed that at these ages GCs are globally demethylated in comparison to the somatic cells of the testis. Later in fetal life, GC nuclear staining for 5MeC increased until at e21.5, when GC nuclei appeared comparable to somatic nuclei.

This pattern of 5MeC staining showed the increasing level of methylation in the whole GC genome that occurred during GC development, as germ-line epigenetic imprinting patterns are being established and GC differentiation occurs. This pattern of 5MeC staining was unaffected by DBP exposure (Fig 5.1), suggesting that DBP exposure did not prevent global remethylation of the whole GC genome.

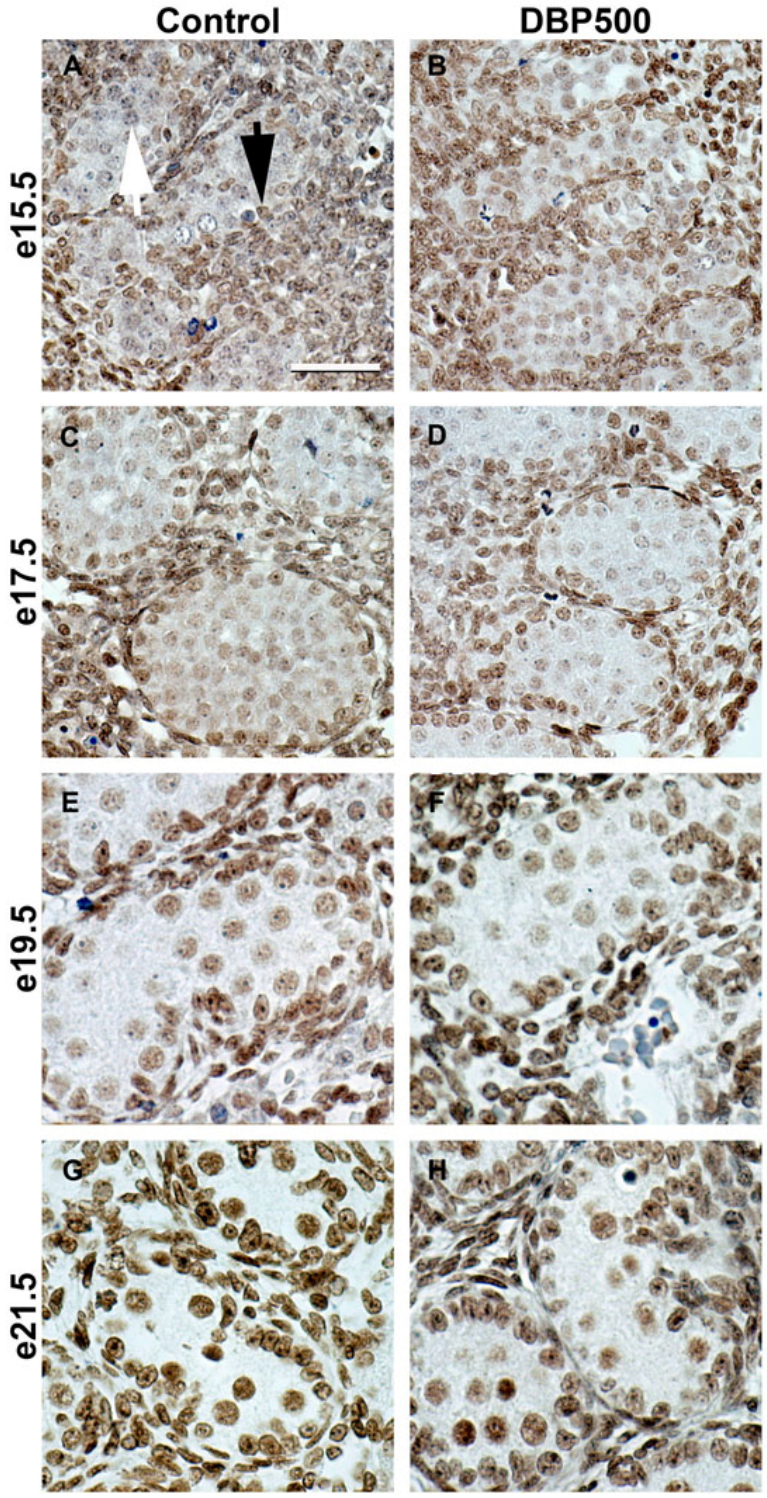

Figure 5.1 Representative photomicrographs of immunostaining for 5MeC (Dab = brown) in fetal rat testes from control (left) and DBP500 exposed animals (right) animals from e15.5 (top) through to e21.5 (bottom). Scale bar in panel A represents 50µm. White arrow depicts GC. Black arrow depicts Sertoli cell.

5.3.1.1 Methylation maintenance by DNMT1

Having established that the global methylation state of GCs increased during the last week of fetal life in the rat and that it was unaffected by DBP exposure, the expression levels of some of the enzymes involved in DNA methylation were then examined. DNA methyl transferase 1 (DNMT1) is the methyl transferase that is reported to perform the methylation of the newly synthesized hemi-methylated DNA strand during DNA replication and as such is responsible for maintaining DNA methylation patterns in the daughter cells after each mitotic replication, discussed in Section 1.4.4. IHC staining for DNMT1 showed protein expression in both somatic and GCs, but this was highly variable and unaltered by DBP exposure (data not shown). *Dnmt1* mRNA levels were examined by Taqman analysis, as described in Section 2.11, and shown in Fig 5.2.

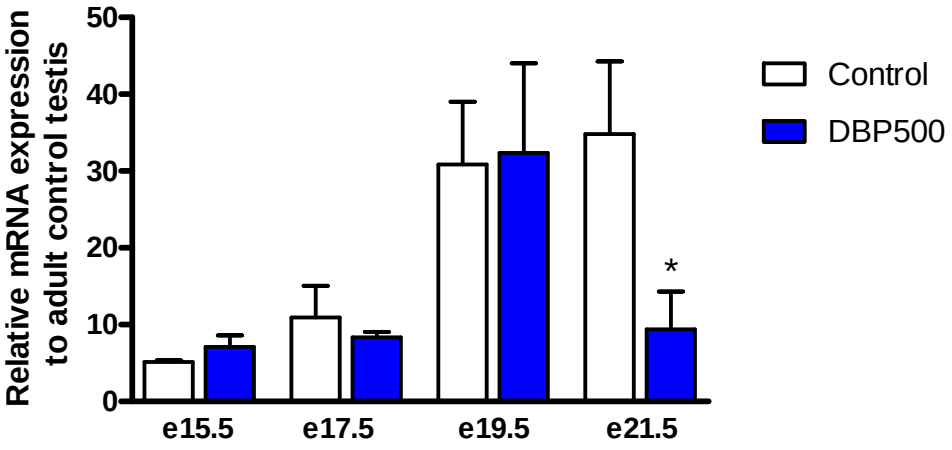

Figure 5.2 Quantitative analysis of *Dnmt1* mRNA levels at e15.5, e17.5, e19.5 and e21.5 in fetal rat testes. (n=6 for e15.5 and e17.5 testes, n=5 for e19.5 testes, n=4 for e21.5 control testes and n=6 for e21.5 DBP exposed testis). Values are means ± SEM. Student's unpaired *t* test was performed, * P<0.05 between control and DBP500 testes.

Dnmt1 expression increased during the last week of fetal life in the testis and consistently showed a higher level of expression than in the adult testis. DBP exposure had no affect on mRNA expression until e21.5.

As DNMT1 protein is detected in both soma and GCs and fulfils an essential role in maintaining methylation patterns during cellular replication, the DBP exposure effect at e21.5 is interesting. If *Dnmt1* is solely involved in methylation maintenance during DNA replication, the increased expression of *Dnmt1* after e19.5 (when no GCs are proliferating, Fig 3.5) may be due to the increase rise in somatic replication (Scott et al., 2008) and Fig 4.2), which is also altered by DBP exposure and which may explain the significant difference between control and DBP exposed testes at e21.5.

5.3.1.2 De Novo Methylation by DNMT3A and DNMT3L

De Novo methylation is the establishment of new methylation patterns on unmethylated DNA and is an important process in fetal GC development, as described in Sections 1.4.2-1.4.4. De novo methylation is thought to occur by the action of the DNMT3 family of DNMT3A, 3B and the non-catalytic 3L, with DNMT3A and 3L thought to be the most important in fetal GC methylation in the mouse (La Salle and Trasler, 2006). IHC staining was performed for DMNT3A on testes from both control and DBP exposed animals during the last week of fetal life, as shown in Fig 5.3.

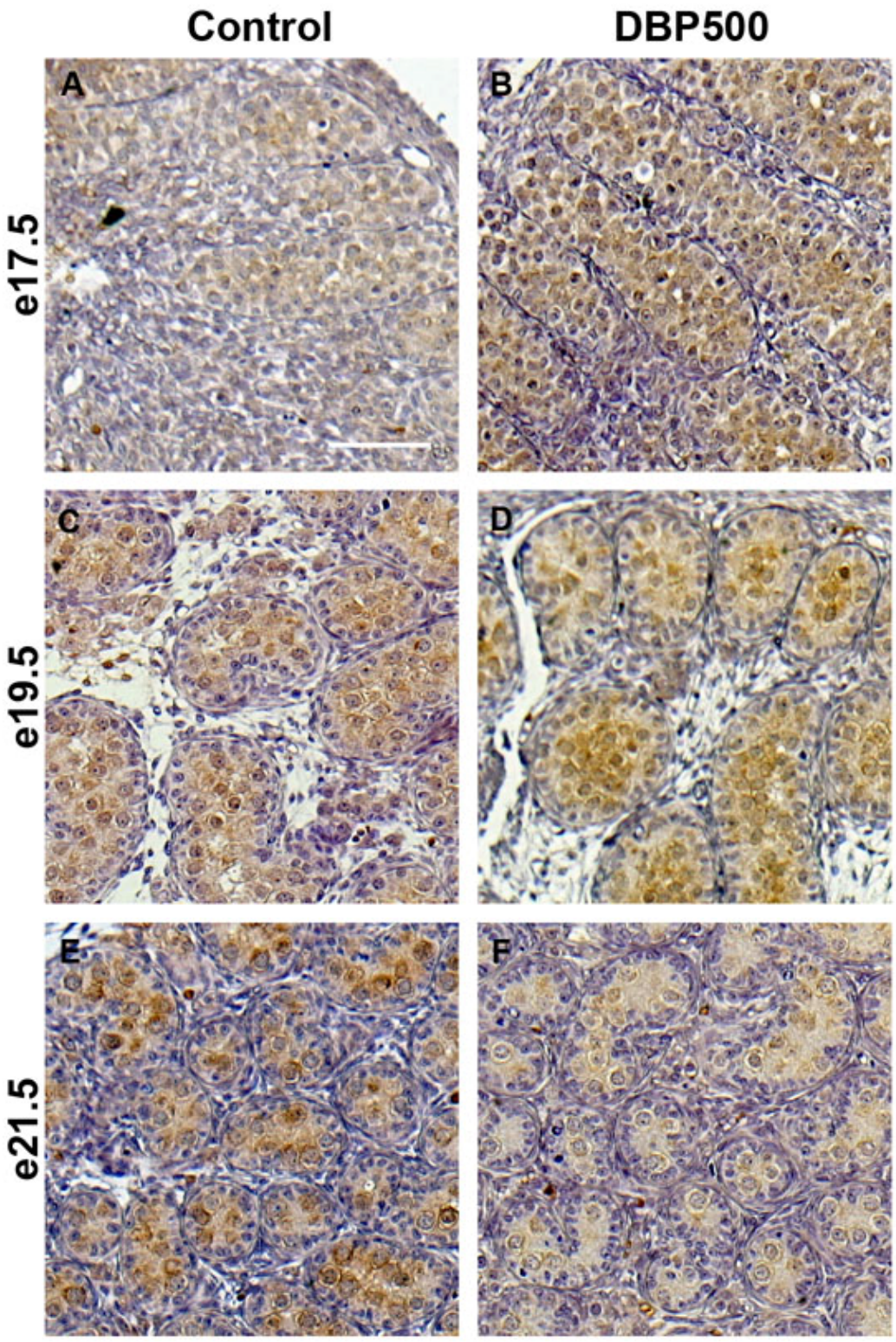

Figure 5.3 Representative photomicrographs of immunostaining for DNMT3A (Dab = brown) in fetal rat testis from control (left) and DBP500 exposed animals (right) from e17.5 (top) through to e21.5 (bottom). Scale bar in panel A represents 50µm.

IHC staining for DMNT3A on fetal rat sections showed expression is not confined to the nuclei of cells as might be expected for a DNA methyl transferase. DNMT3A staining was more highly detected in GCs and increased during GC development. In testes from DBP exposed animals, the expression of DNMT3A was unaltered until e21.5 when a slight reduction in staining was detected. This possible DBP effect on GC DNMT3A could not be quantified. *Dmnt3A* mRNA expression was then investigated by Taqman analysis, as shown in Fig 5.4.

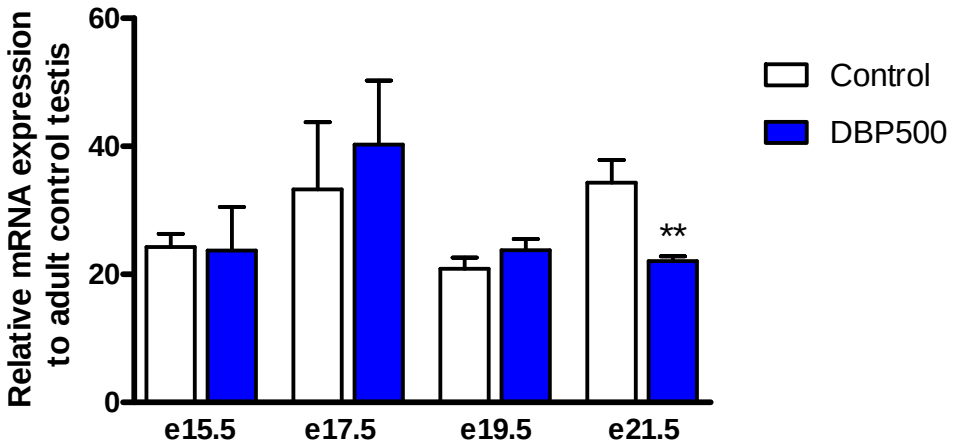

Figure 5.4 Quantitative analysis of *Dnmt3A* mRNA levels at e15.5, e17.5, e19.5 and e21.5 in fetal rat testes, (n=6 for each age and treatment). Values are means ± SEM. Student's unpaired *t* test was performed, ** P<0.01 between e21.5 Control and DBP500 testes.

As with *Dnmt1,* mRNA levels for *Dnmt3A* were much higher than in the adult testis and were unaltered by DBP exposure until e21.5, when a significant reduction of expression occurred.

DNMT3L is a non-catalytic member of the DNMT3 family that is thought to be involved in the regulation of DNMT3A and 3B activity (La Salle et al., 2004; La Salle and Trasler, 2006). Previous studies in the mouse have highlighted that DNMT3A and 3L are highly expressed in the testis and stimulate de novo methylation *in vitro* (Chedin et al., 2002). IHC staining for DNMT3L was examined in the fetal rat testis, as shown in Fig 5.5.

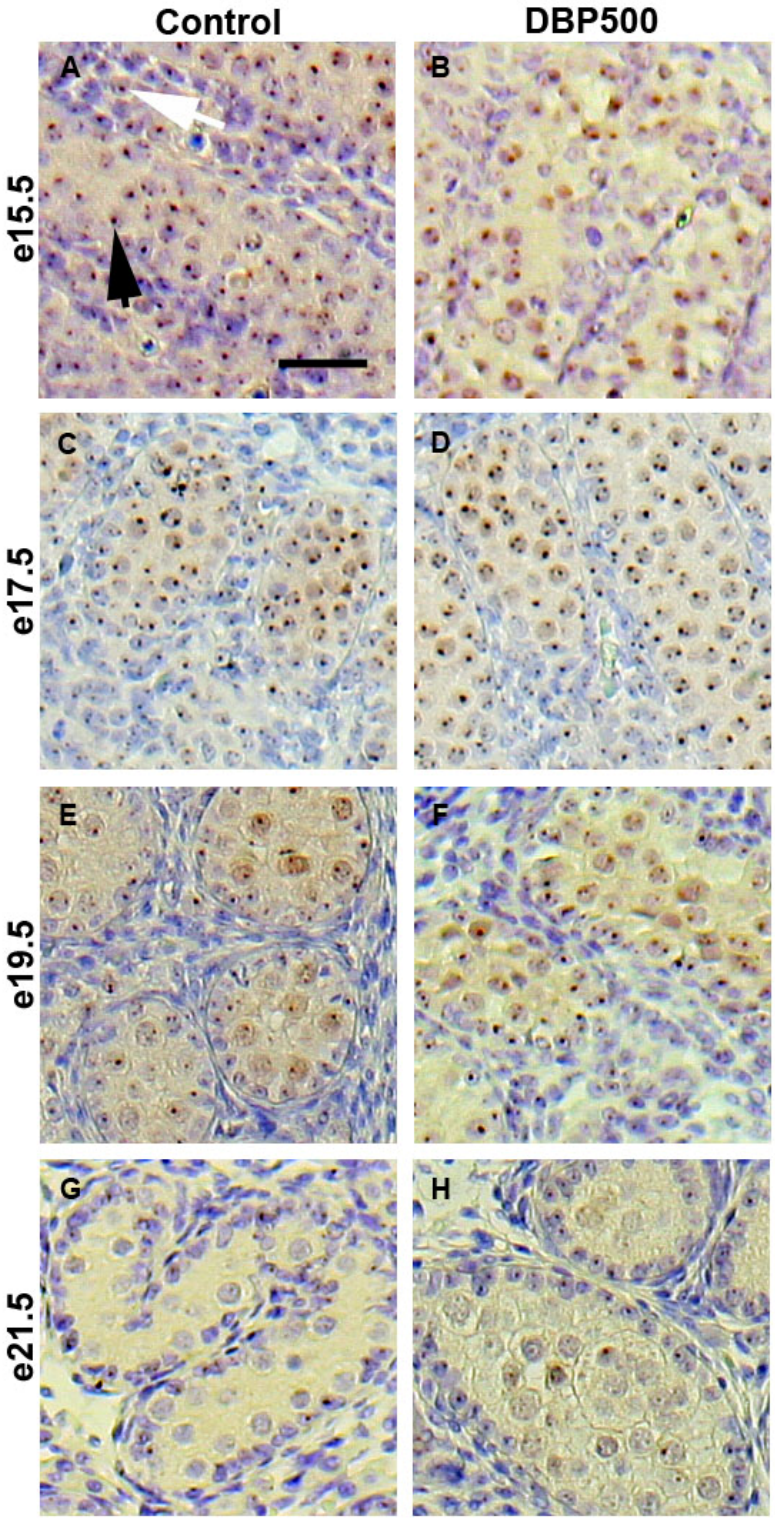

Figure 5.5 Representative photomicrographs of immunostaining for DNMT3L (Dab = brown) in fetal rat testis from control (left) and DBP500 exposed animals (right) from e15.5 (top) through to e21.5 (bottom). Scale bar in panel A represents 50µm. White arrow depicts somatic cell. Black arrow depicts GC.

DNMT3L expression varied during the last week of fetal life. At e15.5 and e17.5, DNMT3L was detected as one or two punctate dots within the nuclei of both somatic cells and GCs (highlighted in Fig 5.5 A). At e19.5, DMNT3L staining became more diffuse throughout the nuclei of the cells and by e21.5 DNMT3L expression was barely detectable in testes from control and DBP exposed animals. *Dnmt3L* mRNA expression levels were then investigated by Taqman to see if a similar expression pattern occurred, as seen in Fig 5.6.

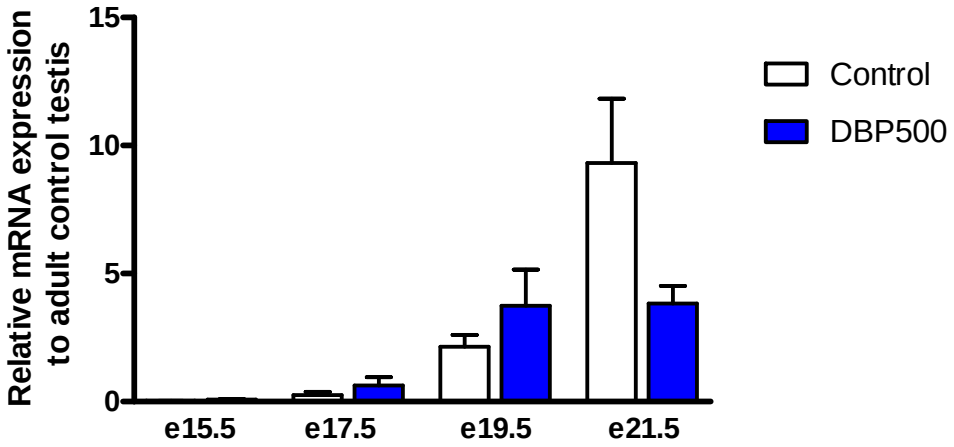

Figure 5.6 Quantitative analysis of *Dnmt3L* mRNA levels at e15.5, e17.5, e19.5 and e21.5 in fetal rat testes (n=6 for age and treatment). Values are means ± SEM.

Dnmt3L mRNA expression showed an increase over time in the fetal testis, in opposition to the IHC detection of the protein. Thus, at e21.5 mRNA was highly expressed but the protein was barely detectable. DBP exposure had no significant effect on *Dnmt3L* mRNA expression.

5.3.1.3 Regulation of imprinting sites by BORIS

Brother Of the Regulator of Imprinted Sites (BORIS) is a gene associated with both cancer and the testis in the mouse, in which it is involved in regulating imprinting sites in the fetal GCs and primary spermatocytes (Klenova et al., 2002; Loukinov et

al., 2002). BORIS binds to imprinting control regions, such as *Igf2*/*H19*, during male fetal GC development in the mouse and regulates histone modifications (Jelinic et al., 2006). To investigate the role of BORIS in the fetal rat testis, IHC staining was attempted for BORIS expression but was unsuccessful (data not shown). *Boris* mRNA analysis by Taqman was then investigated and is shown in Fig 5.7. This epigenetic imprinting regulator was highly expressed in the developing rat testis in comparison to the adult, and was unaltered by DBP exposure.

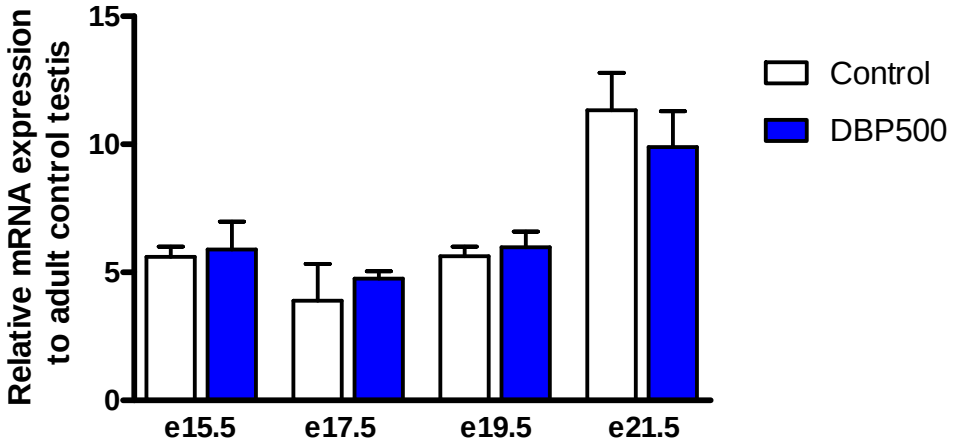

Figure 5.7 Quantitative analysis of *Boris* mRNA levels at e15.5, e17.5, e19.5 and e21.5 in fetal rat testes, (n=6 for each age and treatment). Values are means ± SEM.

5.3.2 Methylation inhibition by AZC with and without DBP

Having established how global methylation of GCs increased during fetal rat testis development and that this process was seemingly unaffected by DBP exposure, methylation inhibition was investigated to see if could disrupt GC development in a similar manner to DBP. The chemical methylation inhibitor 5-aza-2'deoxycytidine (AZC) was investigated using a single I.P. injection in the pregnant female rat at e16.5, as described in Section 2.2. Methylation inhibition by AZC is due to both direct inhibition of the DNA methyl transferases and through incorporation into DNA during replication as a modified cytidine that cannot itself become methylated. Injection at e16.5 with AZC was selected as a time when GCs are proliferating and before OCT4 expression begins to be lost (Figs 3.4, 3.5 and 3.6), so that AZC can

become incorporated into some GC genomes during replication and result in CpGs in the OCT4 promoter that cannot be methylated, so that OCT4 would continue to be expressed into the adult. A single dose was used to minimize the side effects of inhibiting methylation throughout the whole developing fetus. Two different doses of AZC alone (5mg/kg and 10mg/kg) were examined for GC effects, and the AZC 10 dose was also combined with DBP to see if methylation inhibition altered DBP effects. Methylation inhibition by AZC alone or with DBP unfortunately proved to be fatal, with no offspring from treated females surviving to e21.5.

However the effects on fetal GC development could still be investigated at e17.5 and e19.5, to provide some insight into the role of methylation in fetal rat GC development. An examination of some broad aspects of the fetal testis was performed by IHC to examine if methylation inhibition by AZC completely dysregulated the fetal testis, these are summarized in Table 5.4.

Table 5.4 Summary of methylation inhibition by AZC ± DBP on some aspects of testis development.

	Treatment		
	AZC5	**AZC10**	**AZC+DBP**
AMH	No change	No change	No change
VASA	No change	No change	No change
DAZL	No change	No change	No change
GC Proliferation	No change	No change	Same as DBP alone
GC TUNEL	No change	No change	No change

Global methylation in the fetal rat testes of the different maternal treatments was then investigated by IHC for 5MeC at e17.5 and e19.5, as shown in Fig 5.8 below.

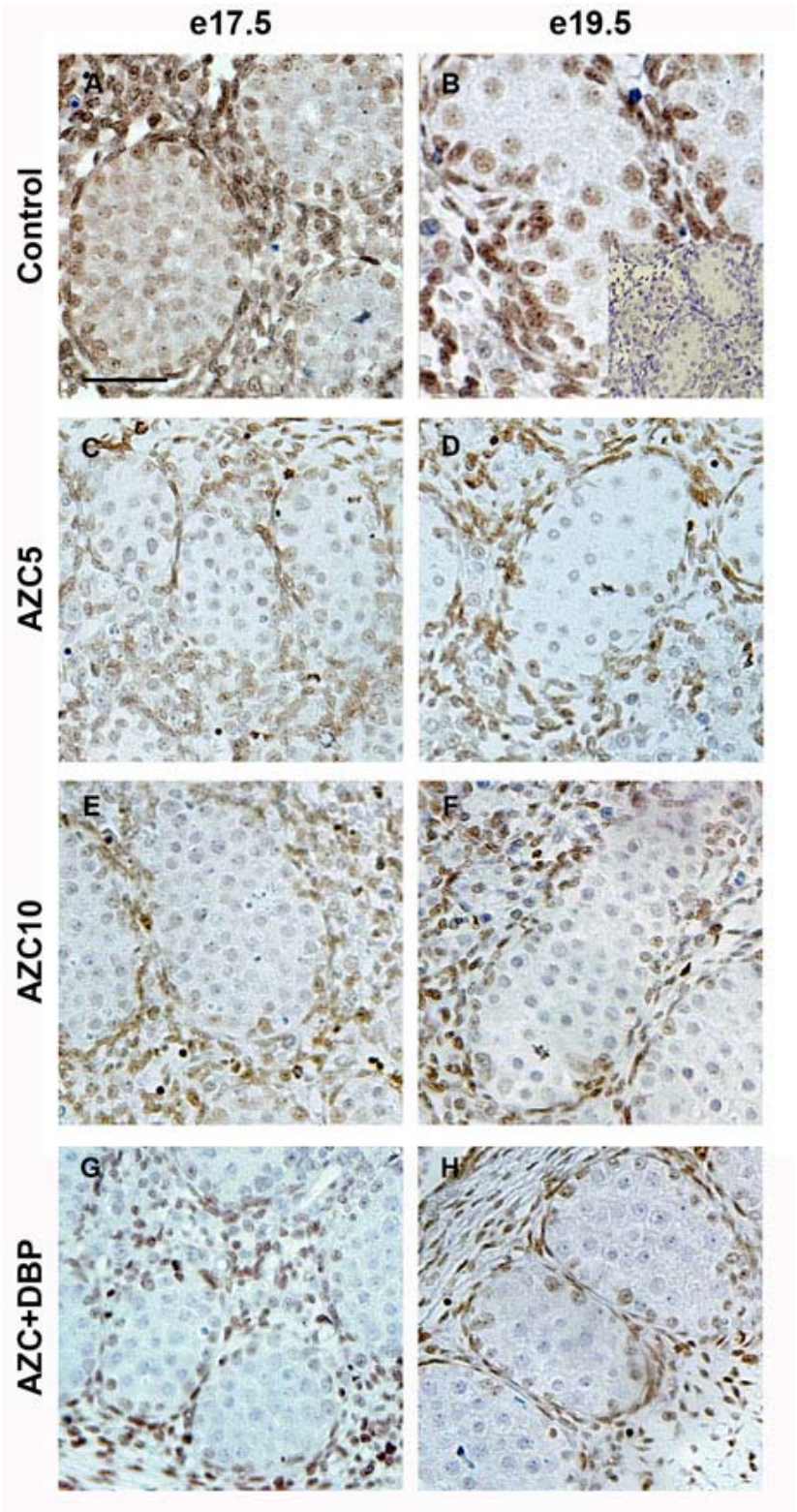

Figure 5.8 Representative photomicrographs of immunostaining for 5MeC (Dab = brown) in e17.5 (left) and e19.5 (right) fetal rat testes from control (A and B), AZC5 exposed (C and D), AZC10 exposed (E and F) and AZC+DBP exposed (G and H). Scale bar in panel A represents 50µm. Insert in panel B is a negative control for 5MeC.

In the testes of AZC ± DBP exposed animals, 5MeC staining was still present in the somatic cells of the testis and reduced in the GCs at both e17.5 and e19.5. This illustrated that methylation inhibition by AZC does not remove existing methylation in the somatic cells but does reduce global remethylation in the GCs at e19.5.

5.3.2.1 Effect of methylation inhibition by AZC on OCT4 expression

As the aim of the methylation inhibition study was to see if OCT4 expression could be altered by preventing methylation during GC development, examination of OCT4 protein by IHC was performed at e17.5 and e19.5 in testes from AZC±DBP exposed animals. In e17.5 testes from AZC ± DBP exposed animals, the percentage of OCT4 positive GCs was counted, as described in Section 2.8.4, and shown in Fig 5.9.

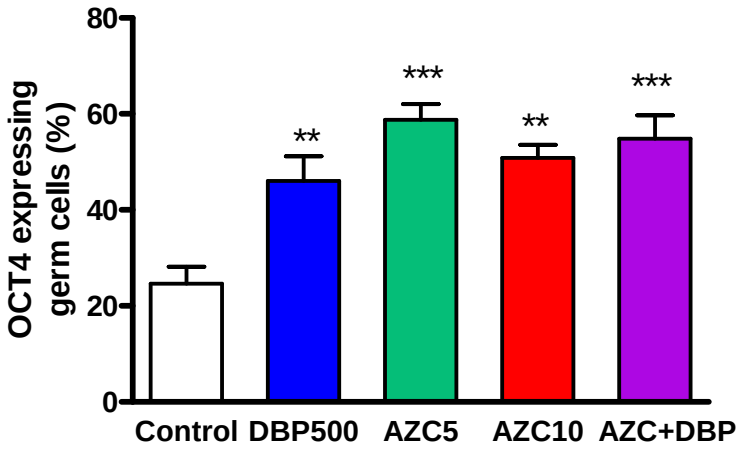

Figure 5.9 Percentage of OCT4 positive germ cells at e17.5 in testes from control (n=7), DBP500 (n=7), AZC5 (n=4), AZC10 (n=4) and AZC+DBP (n=4) treatment groups. Values are means ± SEM. Student's unpaired *t* test was performed, ** P<0.01 and *** P<0.001 between treatment and control.

Methylation inhibition at e16.5 by either dose of AZC caused a significant increase in the percentage of OCT4+ GCs at e17.5 compared to controls, with AZC5 treatment causing a slightly more significantly difference than AZC10. When AZC was combined with DBP exposure there resulted in a higher percentage of OCT4+ GCs than with DBP exposure alone. Importantly, the treatments were not

significantly different from each other, only when compared with control testes. It should also be noted that AZC did not cause the expression of OCT4 in non GCs.

To examine if the observed increase in OCT4+ GCs at e17.5 was due to prevention of promoter silencing and increased mRNA expression levels for *Oct4*, Taqman analysis was performed on e17.5 testes and e19.5 testes, as shown in Fig 5.10.

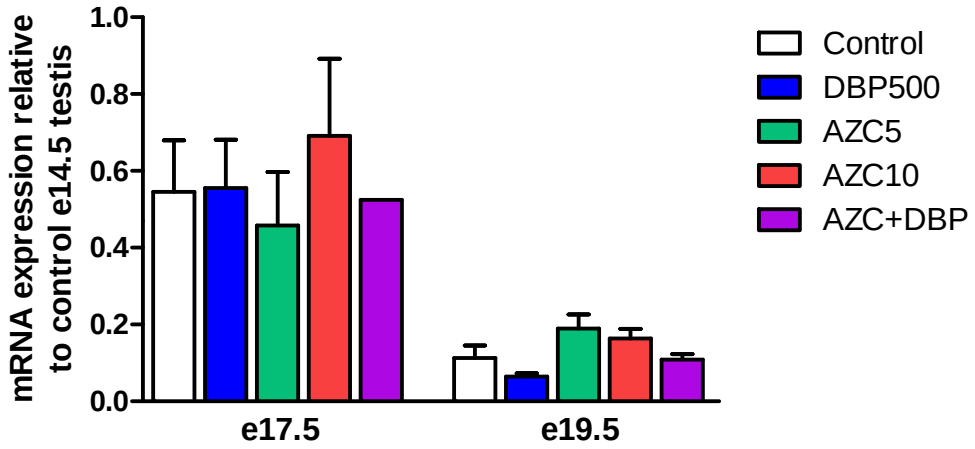

Figure 5.10 Quantitative analysis of *Oct4* mRNA levels in testes at e17.5 and e19.5 for Control (n=6 both ages), DBP500 (n=6 both ages), AZC5 (n=6 at e17.5, n=3 at e19.5), AZC10(n=3 at e17.5, n=6 at e19.5) and AZC+DBP(n=1 at e17.5, n=5 at e19.5) treatment groups. Values are means ± SEM. No significant differences within each age group.

In e17.5 testes, *Oct4* mRNA levels were unaltered by either AZC dose or when combined with DBP. In the e19.5 testes, *Oct4* mRNA levels had reduced noticeably from e17.5 levels, even with methylation inhibition by AZC treatment. This suggests that inhibiting methylation at e16.5 does not prevent *Oct4* promoter methylation, however a slight increase in *Oct4* mRNA can be seen.

Having examined OCT4 expression at e17.5, it was also examined if AZC-induced methylation inhibition allowed GCs to continue to express OCT4 after e17.5 by examining e19.5 testes for OCT4 expression by IHC. OCT4+ GCs were detected in 1 of 6 testes from AZC10 treated mothers, and in 1 of 5 testes from fetal rats exposed

to AZC+DBP, as shown in Fig 5.11. This expression was not present in every section of testis examined from the affected animals, suggesting that AZC exposure may delay the loss of OCT4 expression for longer than DBP, but did not prevent it.

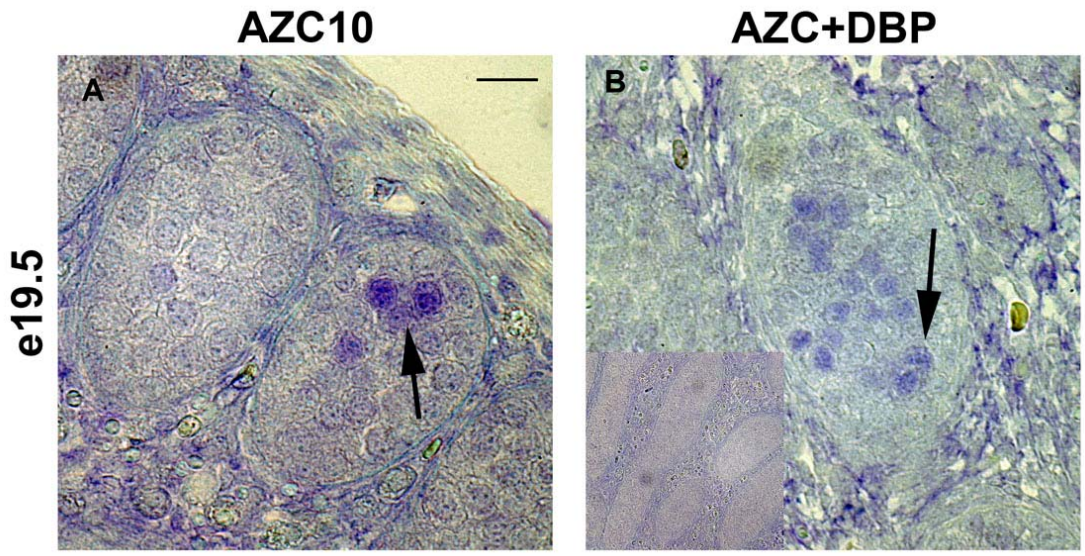

Figure 5.11 Photomicrographs of immunostaining for OCT4 (Fast blue = blue) in e19.5 fetal testes from AZC10 and AZC+DBP treated groups (A and B). Scale bar in panel A represents 50µm. Insert in panel B is a negative control for OCT4.

5.3.2.2 Methylation inhibition by AZC on DMRT1 expression

As described in Section 3.3.10, loss of DMRT1 expression in GCs is an event of GC differentiation that occurs around e19.5. To investigate if methylation inhibition by AZC altered DMRT1 expression in a similar way to OCT4, the loss of DMRT1 protein was examined by IHC at e19.5. The percentage of DMRT1+ GCs was calculated by examination of double IHC for VASA and DMRT1 in testes from animals exposed to AZC±DBP and is shown in Fig 5.12.

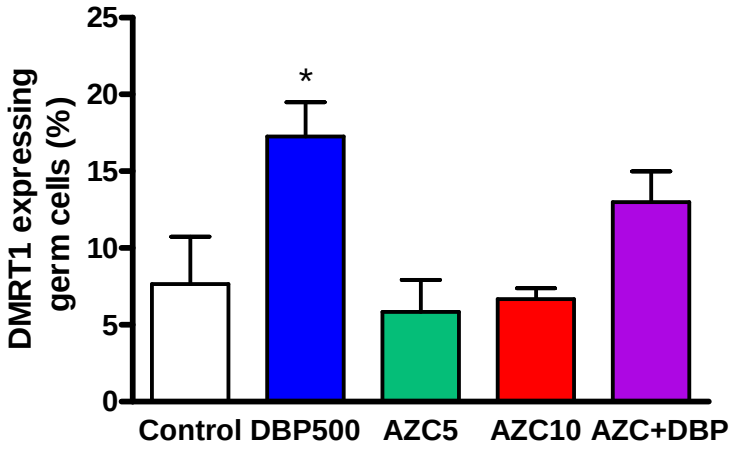

Figure 5.12 Percentage of DMRT1 positive germ cells at e19.5 in fetal testes from Control (n=3), DBP500 (n=4), AZC5 (n=3), AZC10 (n=9) and AZC+DBP (n=6) treatment groups. Values are means ± SEM. Student's unpaired *t* test was performed, * P<0.05 between treated and control.

In contrast to increased OCT4 expression in the GCs at e17.5, AZC exposure alone had no effect on the percentage of DMRT1+ GCs at e19.5 and when AZC was combined with DBP it showed a lesser effect than did DBP alone. This suggested that methylation inhibition by AZC at e16.5 has no effect on GC specific DMRT1 expression by e19.5.

5.3.3 Bisulphite sequencing of the OCT4 promoter

Having examined global methylation and methylation inhibition, gene specific methylation was then investigated. During the course of this thesis, *Oct4* expression has been of great interest as a gene that marks human CIS and is altered by DBP exposure in the rat, and therefore *Oct4* was chosen for promoter methylation investigation. In both human and mouse ES cells and iPS cells the *Oct4* gene is regulated by methylation of CpGs in the promoter region (Ben-Shushan et al., 1993; Takahashi et al., 2007; Yeo et al., 2007). To examine if *Oct4* expression in the fetal rat testis is regulated by methylation of the *Oct4* promoter, three regions of the *Oct4* promoter were examined by bisulphite sequencing to identify the methylation states of individual CpGs in these regions. The regions were selected due to the reported

importance of methylation in the regulatory regions of the promoter and proximal enhancer of the mouse and human *Oct4* gene (Deb-Rinker et al., 2005; Freberg et al., 2007; Hattori et al., 2004). To examine how methylation patterns might change during fetal GC development two different ages were used to extract whole testis DNA. These ages were chosen as times when OCT4 protein was expressed in all GCs at e15.5 and when OCT4 protein is not expressed in any GC at e19.5. The hypothesis was that at e15.5 the CpGs of the regulatory regions of the *Oct4* gene would be unmethylated as OCT4 is expressed, and that by e19.5 the CpGs will have become methylated as *Oct4* expression becomes silenced. Bisulphite sequencing was performed on the three regulatory regions and fetal ages, as described in Section 2.10. The results of this sequencing and analysis are presented diagrammatically in Fig 5.13.

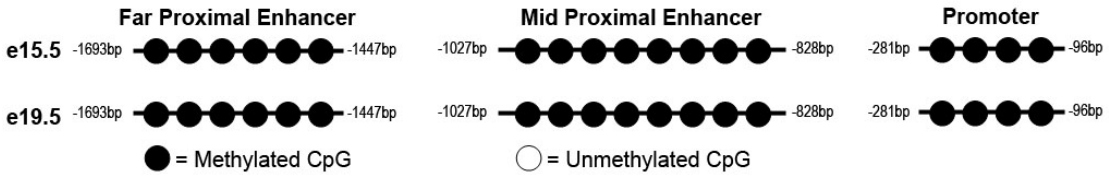

Figure 5.13 Summary of methylation status of CpGs for three regulatory regions of the rat *Oct4* gene at e15.5 and e19.5. (n=3 for each age)

At all the CpGs examined, they were methylated at e15.5 and remain methylated at e19.5. This is most likely due to the fact that the analysis used whole testis DNA and not isolated GC DNA. This means that the methylation of *Oct4* promoters in somatic cells is also being detected and any methylation change in GC DNA may be diluted out by somatic DNA and so undetected by sequencing.

As use of whole testis DNA for *Oct4* promoter methylation analysis was confounding, there was an attempt to isolate GCs from the whole testis and then perform bisulphite sequencing. Isolation of postnatal day (D)0 GCs by MACS and GC surface protein SSEA1, as described in Section 2.4, produced three fractions that were analysed for GC content. The three fractions were an Unsorted fraction (US) of testicular cells that were not incubated with anti-SSEA1, a Bound fraction (B) that

should contain only those cells that anti-SSEA1 and magnetic beads bound to and an Unbound fraction (UB) of those cells that did not bind anti-SSEA1. The aim of the MACS sorting was to produce a relatively pure GC population in the Bound fraction. To determine the content of each fraction, Taqman mRNA analysis for a GC gene (*Dazl*), a Sertoli cell gene (*Amh*) and a Leydig cell gene (*3β hsd*) was performed and shown in Fig 5.14.

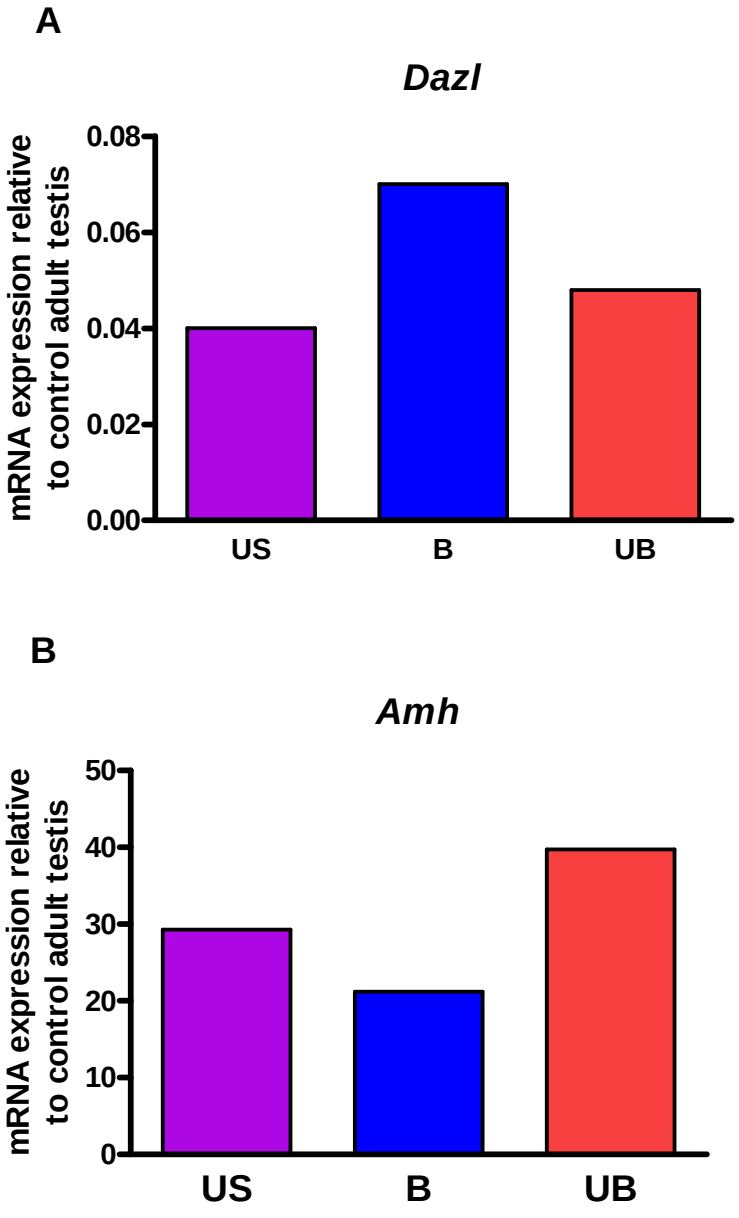

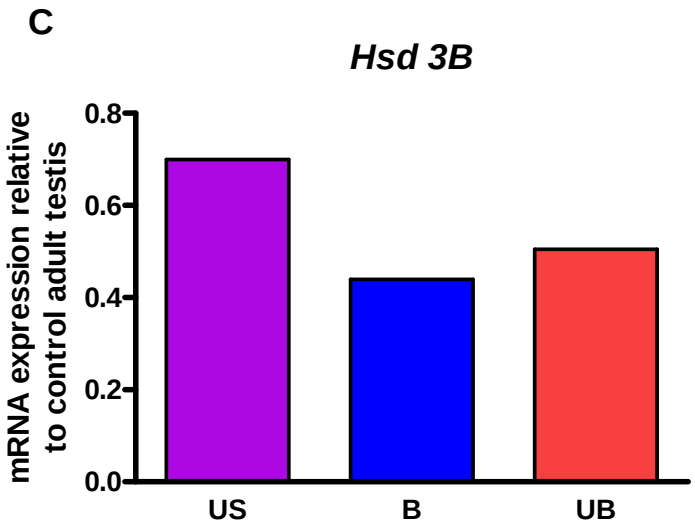

Figure 5.14 Quantitative analysis of mRNA levels in the three fractions produced by MACS of D2 testis (n=1). A shows relative *Dazl* mRNA levels, B shows *Amh* mRNA levels and C shows relative *Hsd 3β* levels.

This attempt at MACS to isolate GCs did not produce a pure GC population and only enriched GC content, as both *Amh* and *3β hsd* mRNA were detected in the bead bound fraction. This technique was therefore of limited use, as whole litters of fetal rats would be required to produce sufficient cells for sorting and it did not succeed in isolating GCs. Therefore it was decided not to pursue GC isolation and bisulphite sequencing any further in the fetal rat.

5.4 Discussion

The aim of this chapter was to investigate fetal GC DNA methylation during the last week of fetal life in the rat, especially as a mechanism that could be disrupted by DBP exposure. To that end three different approaches were used to investigate DNA methylation in fetal GCs; global methylation changes during the last week of fetal life, the effect of a chemical methylation inhibition on GC differentiation, and specific promoter analysis of a candidate gene.

The first approach was to examine the events of DNA methylation in fetal rat GCs in testes from control and DBP exposed testes. As in the mouse, migrating primordial

GCs lost their global DNA methylation in the rat, so that by e15.5 they appear un-methylated in comparison to somatic cell nuclei, as visualized by IHC staining for 5MeC. This IHC staining for methylated cytosine residues increased during the last week of fetal life, so that by e21.5 the nuclei of GC stained to the same degree as did the surrounding somatic cell nuclei. This time window of DNA methylation corresponds with the DBP exposure window used to generate the rat model for TDS, as described in detail in Chapter 4. However, the process of global GC remethylation was unaffected by DBP exposure based on staining for 5MeC. This loss and reacquisition of fetal GC methylation patterns is involved in the process of epigenetic imprinting, discussed in Section 1.4.2, and assuming the rat is similar to mouse (Oakes et al., 2007b), this process is not completed until spermatogenic meiosis. Failures in correct epigenetic imprinting often cause sub-fertility (Hammoud et al., 2009), like that reported with DBP exposure in rats (Fisher et al., 2003). So, while DBP exposure in fetal rat testes may not be altering global DNA methylation, it may be affecting the epigenetic imprinting. It should be noted that if DBP exposure was inducing a delay in remethylation, as is most likely given the evidence in Chapter 4, it would be unlikely to be observable by 5MeC staining, unless the delay was severe.

IHC for 5MeC is a very simple measurement of global DNA methylation level and is not informative about single gene methylation or more subtle changes in DNA methylation patterns. To further investigate the normal pattern of fetal GC DNA methylation, the expression of DNA methyl transferases (DNMTs) was examined.

The methylation maintenance enzyme DNMT1 was found to be expressed in every cell of the fetal rat testis, as would be expected from its crucial role in maintaining methylation in hemi-methylated DNA during cell division. IHC staining for DNMT1 was very variable, but showed no change in testes from DBP exposed animals. When *Dnmt1* mRNA levels were examined, expression noticeably increased at e19.5 and showed a significant reduction with DBP exposure at e21.5. This mRNA expression pattern is in line with the increase in somatic replication in the testis from e19.5 onwards. DBP exposure significantly reduced numbers of both Sertoli cells (Scott et

al., 2008) and GCs (Fig 4.1), which may explain this reduction in *Dnmt1* mRNA per testis.

Of more interest in fetal GC DNA methylation is de novo methylation, the acquisition of new methylation patterns, by the DNMT3 family (Okano et al., 1999; Suetake et al., 2004). The protein expression of DNMT3A by IHC was more highly detected in GCs and its expression increased over time. However, DNMT3A expression was not confined to the nuclei, as would be expected of a DNA methyl transferase, which may imply that localization to the nuclei is a factor in the regulation of de novo methylation by DNMT3A. When *Dnmt3A* mRNA expression was examined, the level of expression was fairly constant throughout fetal life, so that both protein and mRNA support the reported role of DNMT3A in de novo methylation that is occurring in the GCs during this time (Chedin et al., 2002; Suetake et al., 2004). DBP exposure only significantly reduced *Dnmt3A* expression at e21.5, which may be as a consequence of reduced GC number in the testes of DBP exposed animals at e21.5, or that at e21.5 GCs from DBP exposed animals are expressing less *Dnmt3A*. This reduction is more likely a GC only effect than that observed with *Dnmt1*, as DNMT3A protein was barely detectable in somatic cells.

DNMT3L is a non-catalytic member of the DNMT3 family, and is reported to be involved in the regulation of de novo methylation, even stimulating DNMT3A activity *in vitro* (Chedin et al., 2002). IHC staining identified that DNMT3L expression occurred as punctate dots in both GCs and somatic cells of the testis at e15.5 and e17.5, which changed into more diffuse nuclear staining by e19.5 and became barely detectable by e21.5. In testes from DBP exposed animals at e21.5, there was slightly more DNMT3L protein detected. Whilst this DBP effect could not be quantified, it may follow the general pattern of delayed GC development with DBP exposure, discussed in detail in Chapter 4. *Dnmt3L* mRNA expression levels were also examined and showed an increase in expression during the last week of fetal life, in stark contrast to the IHC result. This could be due to failure of the anti-DNMT3L antibody to detect the DNMT3L protein when it is bound to another member of the DNMT3 family, as such protein-protein interactions are how

DNMT3L may regulate de novo methylation (Jia et al., 2007). This explanation would tie in with the increased methylation (de novo) in GCs around e19.5 at the same time that DNMT3A expression was increasing in the GCs, as DNMT3A and 3L become bound and de novo methylate the GC genome. Alternatively there may be an mRNA processing delay, so that the DNMT3L protein levels only increase after e21.5, as de novo methylation and imprinting continues postnatally until meiosis.

The imprinting regulator, *Boris*, was also examined during the last week of fetal life in the rat. IHC for BORIS failed to work, but mRNA analysis was successful. The pattern of *Boris* mRNA expression showed a steady expression between e15.5-e19.5, and a small increase at e21.5. DBP exposure had no effect on *Boris* mRNA levels. In the mouse, *Boris* is expressed specifically in male GCs (Loukinov et al., 2002) and if it is GC-specific in the rat as well, the lack of DBP effect is interesting. The lack of an effect of DBP exposure on GC-specific *Boris* expression at e21.5 implies that the significant reduction at e21.5 observed with *Dnmt1* and *Dnmt3A* is due to a DBP-induced reduction in GC expression rather than a simple reduction in GC number. However, it is possible that the lack of reduction in *Boris* mRNA at e21.5 indicates that DBP exposure induced higher *Boris* expression in the fewer GCs present, though there is no other evidence to support this. Also of interest is that the mRNA expression levels of each *Dnmt* investigated and *Boris* were much higher than that of the adult testis control (used as the reference standard), highlighting the importance of DNA methylation in the fetal rat testis, and in particular the role of the DNMT3 family in de novo methylation.

In summarising the first approach, the effects of DBP exposure on fetal GC DNA methylation were limited, as global methylation was unaltered. However, as DBP exposure delays several aspects of GC development, discussed in Chapter 4, and significantly reduced the mRNA expression of *Dnmt1* and *Dnmt3A* expression at e21.5, it is still possible that there are effects on GC DNA methylation/imprinting that have not been detected.

The next approach was to use the chemical methylation inhibitor 5-aza-2'deoxycytidine (AZC, two doses of 5mg/kg and 10mg/kg), to see if inhibiting methylation altered GC development similar to that of DBP exposure. AZC (10mg/kg) exposure was also combined with DBP exposure between e13.5-e21.5, to see how methylation inhibition affected the established effects of DBP exposure on fetal GCs in the rat. Unfortunately, AZC exposure proved to be lethal to the fetus by e21.5 limiting the study of methylation inhibition to the ages of e17.5 and e19.5. At both these ages, the AZC exposed testes remained grossly normal (displaying continued proliferation and most of the correct cell-specific protein expression was retained). The detection of 5MeC by IHC showed that GCs in AZC±DBP exposed rats were relatively unmethylated compared to somatic cells and untreated controls, illustrating that normal global methylation had been maintained in the soma whilst methylation had been successfully inhibited in the GCs.

At e17.5, AZC±DBP exposure significantly increased the percentage of OCT4+ GCs in the fetal rat testis, but by e19.5 only rare GCs still expressed OCT4 and the mRNA level still reduced normally at e19.5. This suggests that AZC exposure delayed the loss of OCT4 expression in GCs but did not prevent it, similar to that observed with DBP exposure alone. When DMRT1 expression was examined at e19.5, AZC exposure did not increase the percentage of DMRT1+ GCs, in contrast to DBP exposure. This suggests that either *Dmrt1* does not become methylated or that the methylation inhibition is gone by the time GC-specific *Dmrt1* gene silencing is occurring. These results suggest that AZC exposure is most probably only inhibiting the DNMT enzymes and has not become incorporated into GC DNA. This transient inhibition would explain why OCT4 expression was affected, whilst DMRT1 was not (the inhibitory AZC having been cleared by e19.5). This also matches reports of AZC preferentially inhibiting DNMTs rather than becoming incorporated into DNA (Oakes et al., 2007b).

In summary, these studies into chemical methylation inhibition were originally conceived to produce a subset of GCs with *Oct4* promoters that could not become methylated, such that OCT4 expression would continue into adulthood. The failure

of AZC to become incorporated into the GC genome, and the rare number of OCT4+ GCs detected at e19.5, combined with the fetal mortality suggest that this method of inducing OCT4+ (CIS) cells in the rat is not a viable option. Whilst lower doses and different timings of AZC exposure may have a stronger effect on OCT4/DMRT1 expression, they would likely still prove to be lethal to the rat fetus.

The final approach to examine fetal GC methylation was gene-specific examination of the *Oct4* promoter. Three candidate regions of the *Oct4* promoter were examined by bisulphite sequencing for CpG methylation of whole testis DNA. It was hoped that with the relatively high GC content in an e15.5 testis combined with the fact that OCT4 is expressed in every GC at that age, a change in DNA methylation could be detected. And if any CpGs were unmethylated at e15.5, they would become methylated by e19.5 (when no GCs express OCT4), allowing this change to be investigated with regard to DBP exposure. Unfortunately, at both e15.5 and e19.5 all the CpGs investigated by bisulphite sequencing were fully methylated. This is most likely due to the somatic DNA present in the whole testis DNA used for sequencing, so that any subtle differences in DNA methylation in GC would be undetectable.

However, there are other possibilities for a lack of difference in CpG methylation between e15.5 and e19.5. It is possible that the wrong regions of the *Oct4* promoter were examined and that those chosen are not involved in methylation/gene silencing, even though in both human and mouse, methylation of the *Oct4* promoter and proximal enhancer regions regulates expression (Deb-Rinker et al., 2005; Freberg et al., 2007; Hattori et al., 2004). Alternatively, methylation of the *Oct4* promoter is not as important in the rat as it is in the mouse. A further alternative is that in the testis a different method of *Oct4* silencing occurs, due to a lack of retinoic acid induced silencing, as mentioned in Section 3.4 (Bowles and Koopman, 2007; Li et al., 2007). Furthermore, whilst methylation is important in *Oct4* expression in embryonic stem cells and induced pluripotency cells (Ben-Shushan et al., 1993; Takahashi et al., 2007; Yeo et al., 2007), there may be other mechanisms involved in the gonad.

As the presence of somatic DNA is the most likely reason for the result of *Oct4* promoter analysis and to attempt to remove this confounding factor, cell sorting to produce a pure GC population for bisulphite sequencing was attempted. However, the MACS protocol attempted was nowhere near good enough to commit the animal numbers required for robust analysis and could not be optimized during the course of this thesis. This is highly regrettable as the ability to isolate fetal rat GCs from a whole testis would allow a thorough investigation of both DBP exposure effects on GCs and how fetal GC DNA methylation occurs.

In conclusion, DBP does not alter global methylation of GCs in the rat, but does affect DNMTs and may have more subtle effects on imprinting sites that the techniques used were unable to detect. Methylation inhibition can prolong OCT4 protein expression in GCs, (but it is eventually removed) and causes fetal lethality. Bisulphite sequencing identified no changes in the *Oct4* promoter regions investigated for the whole testis, but could not be attempted on isolated GCs. Therefore, while the DBP exposure effects reported in Chapter 4 are not causing (or caused by) global DNA methylation changes, there may be gene-specific methylation delays and/or more subtle changes that could not be identified.

6 Studies on in vitro manipulation of fetal testis explants

6.1 Introduction

The process of fetal germ cell (GC) development in the rat and how that process can be disrupted by *in utero* exposure to Di (n-Butyl) Phthalate (DBP) has been discussed in Chapters 3 and 4. However the reported effects of *in utero* DBP exposure on the fetal rat testis are confounded by both the maternal and fetal metabolism and endocrinology, such that the direct action of phthalate exposure on the fetal testis alone is unknown. To investigate this further, several studies have isolated the fetal rat testis which has then been cultured *in vitro* with one or other presumptive active phthalate metabolites (Chauvigne et al., 2009; Hallmark et al., 2007; Li and Kim, 2003).

Previous *in vitro* culturing with the active metabolite of DBP, monobutyl phthalate (MBP) has been attempted on fetal rat testis from e19.5-21.5, but MBP treatment failed to match the steroidogenic suppressing effects observed with *in vivo* DBP exposure (Hallmark et al., 2007; Mahood et al., 2005). However that study was not focused on GC effects. In other phthalate *in vitro* studies, the use of testes from younger (e14.5) animals in *in vitro* culture has shown effects on GCs (Li and Kim, 2003; Livera et al., 2006). Therefore the utility of e14.5 fetal rat testis for *in vitro* manipulation with MBP was investigated for early phthalate effects on GCs and to complement the previously described *in vivo* DBP exposure experiments on GCs.

A further advantage of *in vitro* studies of fetal rat testis is that chemical treatments that are lethal or that severely damage wider aspects of embryogenesis *in vivo* can be used directly on the fetal testis. To take advantage of this, cyclopamine (Cyc) was used to bind and block SMO protein action treatment to block Hedgehog signalling, which is important in the mouse testis for Leydig cell differentiation and cord formation, as described in Section 1.2.3.3, was also investigated in e14.5 fetal rat testis explants.

6.2 Materials and methods

6.2.1 In vitro culture

Briefly, testes and mesonephros were removed from e14.5 fetuses collected from untreated dams (Section 2.3), and were then cultured for 48-72 hours (Section 2.5) with; either no treatment, with MBP (10^{-3}M) or DMSO control, or with cyclopamine (25μM) or ethanol control (Section 2.5.5). Half of the culture media was removed every 24 hours and replaced with fresh media and treatment. Then, 45 minutes to 1 hour before the end of culture time, culture media was replaced with media containing BrdU to enable cell proliferation analysis (Section 2.8.3). All media collected was stored at -80^{o}C for testosterone analysis.

At the end of the *in vitro* culture time, testis explants were either frozen or fixed (Section 2.3.5). Frozen testis explants were then homogenised and RNA extracted (Section 2.11.1) for Taqman quantitative RT-PCR (Section 2.11.3). Fixed testis explants were processed (Section 2.3.6) and sectioned (Section 2.6.2) for IHC analysis.

6.2.2 Immunohistochemical (IHC) analysis

Briefly, IHC staining was performed on processed and sectioned testis explants as summarised in Table 6.1. The number of testis explants used for IHC was a minimum of 6 testis explants in each treatment group and came from a minimum of three different culture experiments.

Additional IHC analyses were performed to calculate the GC proliferation index (Section 2.8.3) and the percentage of GCs expressing OCT4 (Section 2.8.4). Cell apoptosis was also examined using the modified IHC staining protocol for TUNEL (Section 2.6.12).

Table 6.1 Details of antibodies used in Chapter 6.

Antibody	Source	Retrieval	Species
AMH	Santa Cruz, CA	No	Goat
BrdU	Fitzgerald industries, MA	Yes	Sheep
CYP11A	Chemicon	No	Rabbit
DAZL	AbD Serotec	Yes	Mouse
DMRT1	Gift from David Zarkower, MN	Yes	Rabbit
OCT4	Santa Cruz, CA	Yes	Goat
PTCH1	Abcam, Cambridge	Yes	Rabbit
PTCH1	Santa Cruz, CA	Yes	Goat
3β HSD	Gift from Ian Mason, Edinburgh	No	Rabbit

6.2.3 RNA analysis

Briefly, RNA isolated from frozen testis explants was converted into cDNA (Section 2.11.2) and Taqman quantitative RT-PCR performed (Section 2.11.5), to establish quantitative mRNA expression levels. The genes investigated, and primers used, are listed in Table 6.2.

Table 6.2 Taqman primers and Universal Probe Library probes used in Chapter 6.

Gene	Forward Primer 5' → 3'	Reverse Primer 3' → 5'	UPL Probe Number:
Dazl	GCTCAGTTCATGATGCTGCT	ATGCTTCGGTCCACAGATTT	110
Oct4	GAAGTTGGAGAAGGTGGACC	CCTTCTGCAGGGCTTTCATA	95
Ptch1	CAAAGCTGACTACATGCCAGA	GCGTACTCTATGGGCTCTGC	64
Smo	CAGGAGCTCTCCTTCAGCAT	CATTGAGTTCAAAAGCCAAACC	94
3β hsd	GACCAGAAACCAAGGAGGAA	CTGGCACGCTCTCCTCAG	105

6.3 Results

6.3.1 Untreated in vitro testis explant culture

In order to investigate the viability of this *in vitro* culture system, an untreated 48 hour *in vitro* culture period was performed to examine if e14.5 testis explants could be cultured for that length of time and the testis develop reasonably normally under these conditions. Immunohistochemical (IHC) analysis of untreated testis explants was performed and compared to fetal rat testes collected at e16.5 to provide an *in vivo* comparison. The core developmental processes of fetal testis development that were examined in these untreated testes were; GC proliferation by double IHC staining for DAZL and BrdU, GC differentiation by double IHC for DAZL and OCT4, seminiferous cord structure by double IHC for DAZL and AMH and Leydig cell function by IHC staining for 3β HSD. These IHC examinations are summarized in Fig 6.1.

Testis explants cultured for 48 hours showed reasonably comparable development to *in vivo* e16.5 testes, though development was clearly not as good as *in vivo*. Untreated testis explants contained cells that continued to proliferate (both GCs and somatic cells), showed that normal GC differentiation occurred by the continued expression of OCT4, by the maintenance of seminiferous cord structure with Sertoli cells organized around the GCs, and Leydig cells continued to express the steroidogenic enzyme 3β HSD. This illustrated that after 48 hours of *in vitro* culturing, testis explants were still viable and did not degenerate and/or lose testicular organization. This supported the further use of *in vitro* testis explant cultures as an investigative tool.

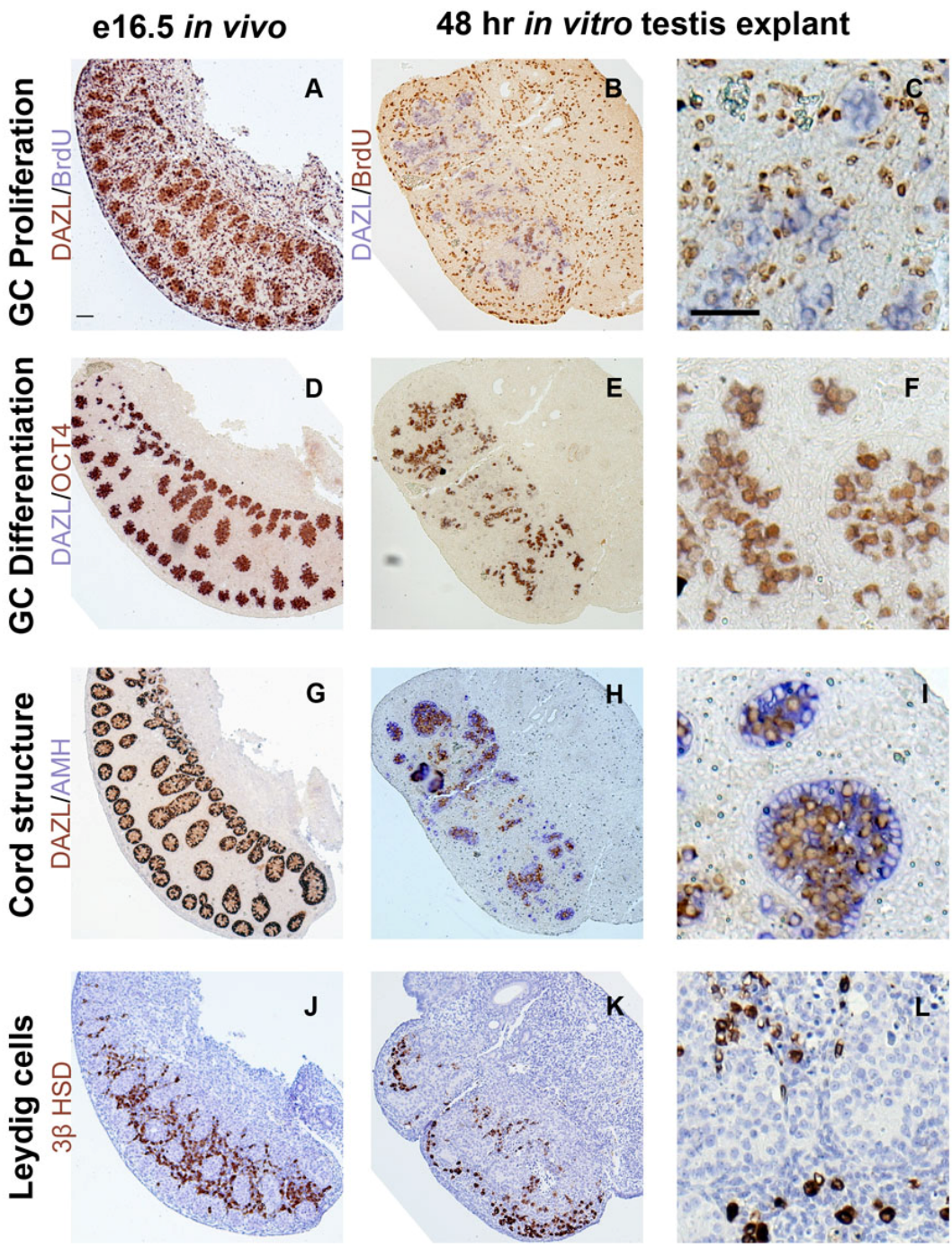

Figure 6.1 Representative photomicrographs of IHC staining from e16.5 fetal rat testis (left) and 48 hour *in vitro* cultured rat testis explants (middle and right) and magnified for detail (right). Panels A shows IHC staining for DAZL (Dab = brown) and BrdU (Fast blue = blue), B-C show IHC staining for BrdU (Dab = brown) and DAZL (Fast blue = blue). D-F show IHC staining for OCT4 (Dab = brown) and DAZL (Fast blue = blue). G-I show IHC staining for DAZL (Dab = brown) and AMH (Fast blue = blue). J-L show IHC staining for 3β HSD (Dab = brown). Scale bars in Panels A and C represents 50 μm.

6.3.1.1 Apoptosis in untreated testis explants

To examine if the level of apoptosis was increased in the untreated testis explants, TUNEL was performed as described in Section 2.6.12. The TUNEL IHC staining of 48 hours untreated testis explants is illustrated in Fig 6.2.

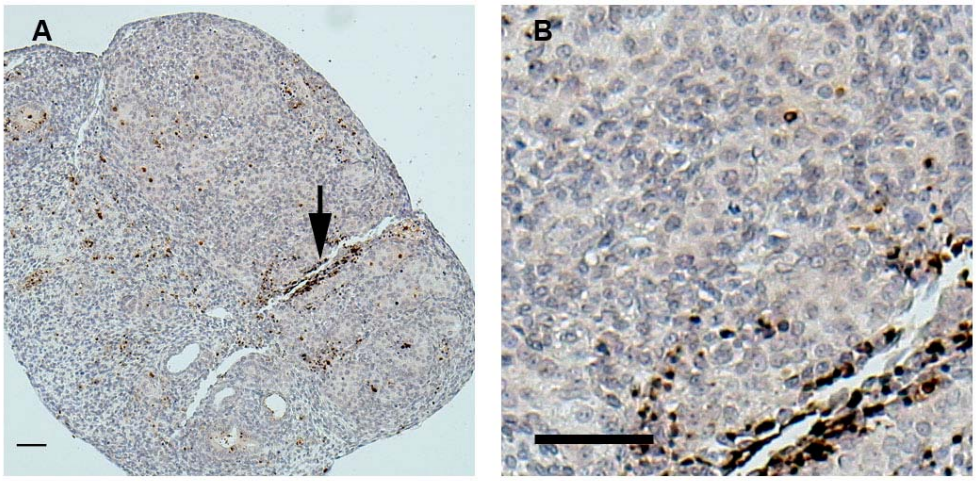

Figure 6.2 Representative photomicrographs of immunostaining for TUNEL in 48 hour untreated fetal rat testis explants (Dab = brown). Black arrow depicts damage during dissection. Scale bars represent 50μm.

There were a few TUNEL+ cells in the untreated testis explant after 48 hours of *in vitro* culture. There was increased TUNEL+ cells in areas where the testis has been damaged during extraction from the rat fetus, as highlighted in Fig 6.2A. This result indicated that the testis explant did not become obviously necrotic after 48 hours and that there was not widespread apoptosis.

6.3.2 In vitro MBP treatment of testis explants

6.3.2.1 Effect of MBP treatment for 48 hours on GC development

Having established the utility of the 48 hour cultures of fetal rat testis explants, the model was then investigated for chemical manipulation during the 48 hour culture period. The effects of DBP exposure on fetal GC development have been covered in Chapter 4, and it is believed that it is not DBP that acts *in vivo*, but rather the primary metabolite, MBP. Such *in vitro* investigations using MBP and MEHP have been attempted before, as described in Section 1.5.3.2. To investigate if MBP treatment of testis explants produced a similar effect to DBP exposure *in vivo*, e14.5 testis explants were cultured for 48 hours using the high (10^{-3}M) concentration, as optimized by Nina Hallmark (Hallmark et al., 2007), with DMSO used as the vehicle control. As with the untreated 48 hour *in vitro* cultures, the testis explants were analysed by IHC for the core developmental processes of fetal testis development including - GC proliferation by double IHC staining for DAZL and BrdU, GC differentiation by double IHC for DAZL and OCT4 and seminiferous cord structure by double IHC for DAZL and AMH. These IHC examinations are summarized in Fig 6.3.

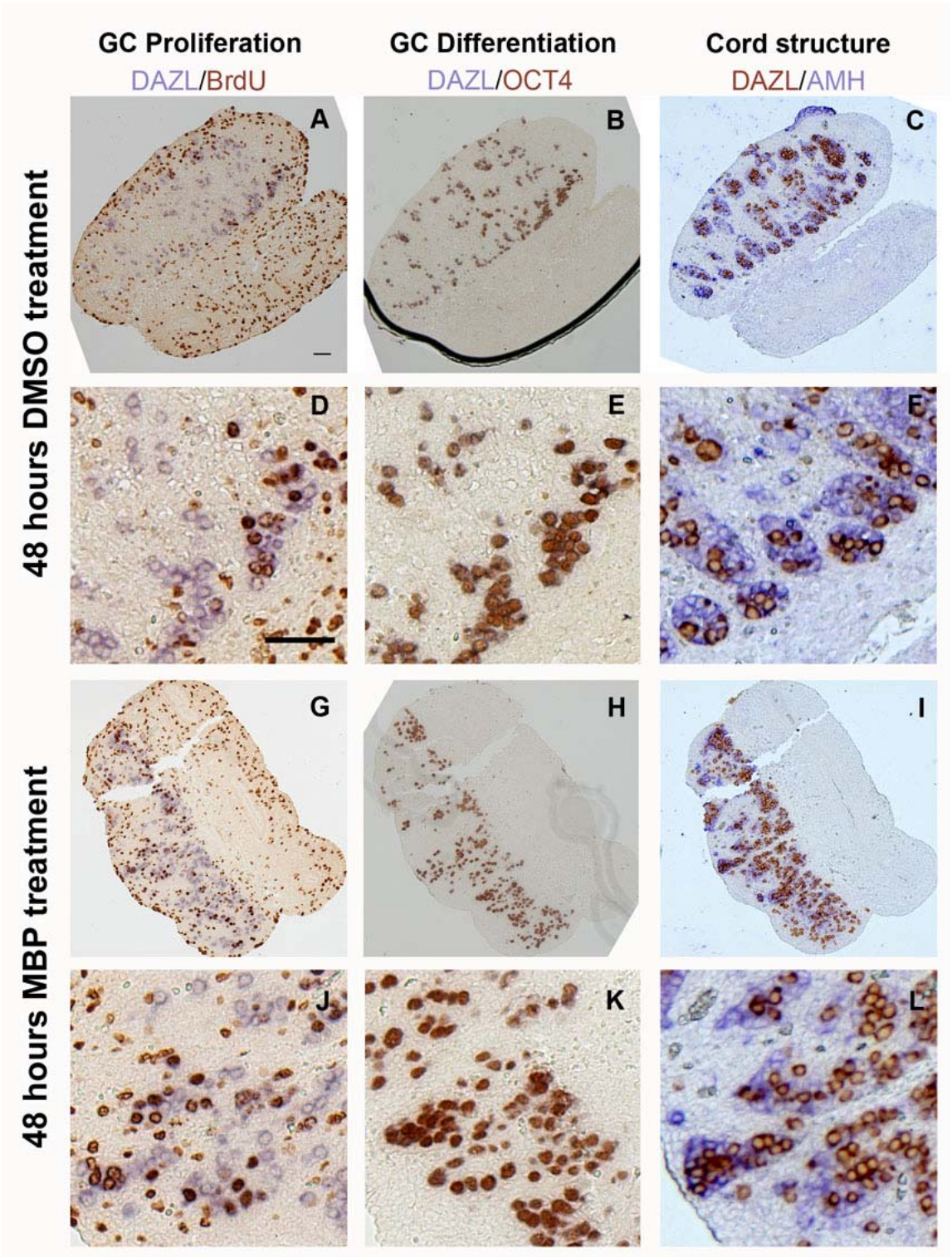

Figure 6.3 Representative photomicrographs of IHC staining from 48 hour *in vitro* cultured rat testis explants treated with DMSO (A-F) or MBP (G-L). Left-hand panels show IHC staining for BrdU (Dab = brown) and DAZL (Fast blue = blue). Middle panels show IHC staining for OCT4 (Dab = brown) and DAZL (Fast blue = blue). Right-hand panels show IHC staining for DAZL (Dab = brown) and AMH (Fast blue = blue). Scale bars in Panels A and D represent 50 µm.

As in the untreated testis explants, *in vitro* treatment with MBP or DMSO did not prevent GC proliferation, GC differentiation or organization into seminiferous cords. As GC number could not be calculated from testis explants, an MBP treatment effect on GC number, as occurs with *in vivo* DBP exposure (Section 4.3.1), could not be investigated. To investigate if *in vitro* MBP treatment altered GC proliferation as occurs after *in vivo* DBP exposure, the proliferation index for GCs was calculated as shown in Fig 6.4.

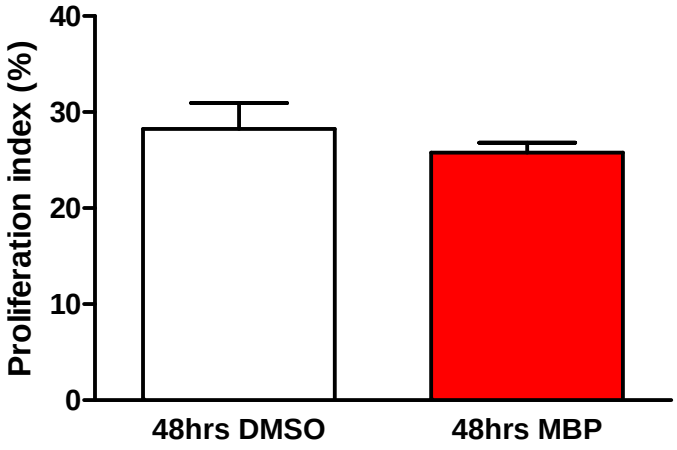

Figure 6.4 Germ cell proliferation index of fetal rat testis explants treated for 48 hours with DMSO or MBP, (n=4). Values are means ± SEM. No statistically significant difference.

48 hours of *in vitro* MBP treatment did not alter the GC proliferation index in testis explants in comparison to vehicle control. However, *in vivo* DBP exposure only caused effects on proliferation at e17.5, whilst these testis explants were comparable to e16.5 *in vivo* testes, so it may have been too early a time window for any effect to have been observed.

6.3.2.2 Effect of MBP treatment for 72 hours on GC development

As *in vivo* DBP exposure had effects on GC development at e17.5, an extended culture and treatment time to 72 hours was used to investigate if MBP treatment prolonged OCT4 expression as did DBP exposure *in vivo* (Section 4.3.1.3). Double IHC staining for OCT4 and DAZL was performed on 72 hour cultured testis explants with either DMSO or MBP treatment, as shown in Fig 6.5.

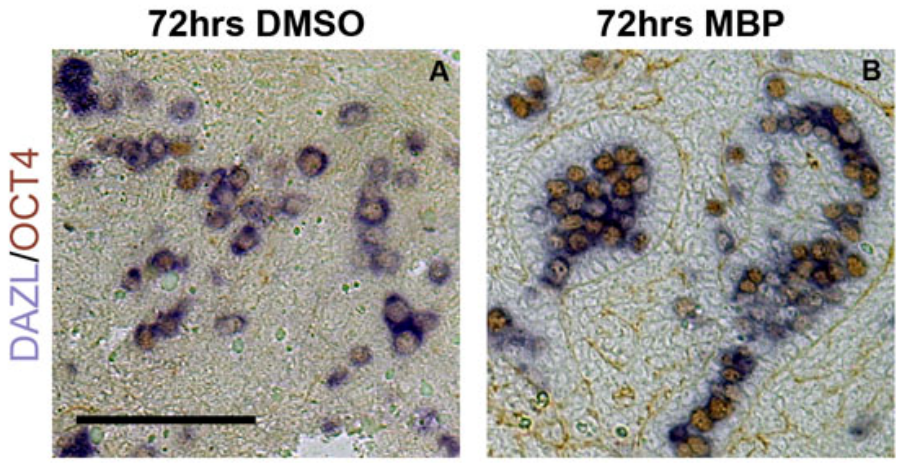

Figure 6.5 Representative photomicrographs of immunostaining for OCT4 (Dab = brown) and DAZL (Fast blue = blue) in 72 hour fetal rat testis explants treated with DMSO or MBP. Scale bar in panel A represents 50μm.

In both DMSO and MBP 72 hour treated testis explants, OCT4 expression was absent in some GCs after 72 hours, showing that the normal GC differentiation process was still occurring in the *in vitro* testis explants, and there was some evidence that MBP treatment might prolong OCT4 expression (Fig. 6.5). Therefore, quantification of the percentage of GCs expressing OCT4 after 72 hours in culture was performed and results shown in Fig 6.6.

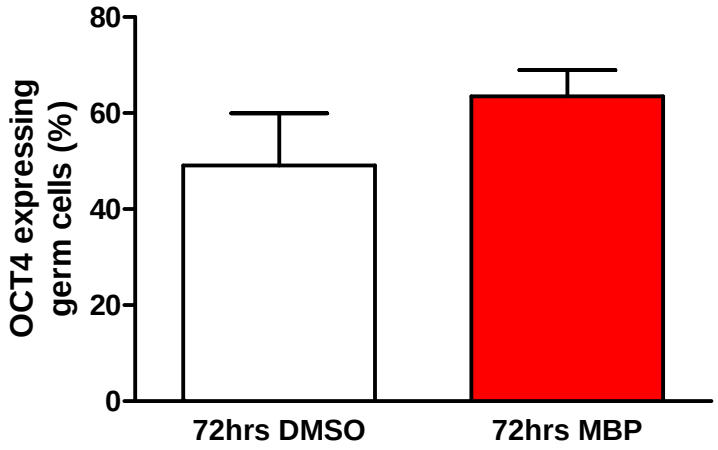

Figure 6.6 Percentage of OCT4 expressing germ cells in 72 hour fetal rat testis explants treated with DMSO or MBP, (n=6). Values are means ± SEM. No statistically significant differences.

There was no significant increase in the percentage of OCT4+ GCs in testis explants after 72 hours of *in vitro* MBP treatment, as compared to DMSO. However, there was high variability between testis explants as the percentage of OCT4+ GCs could vary in each treatment group between 10-90%. *Oct4* mRNA expression levels were then analysed by the Taqman system in 72 hour cultured fetal rat testis explants treated with DMSO and MBP, and results shown in Fig 6.7.

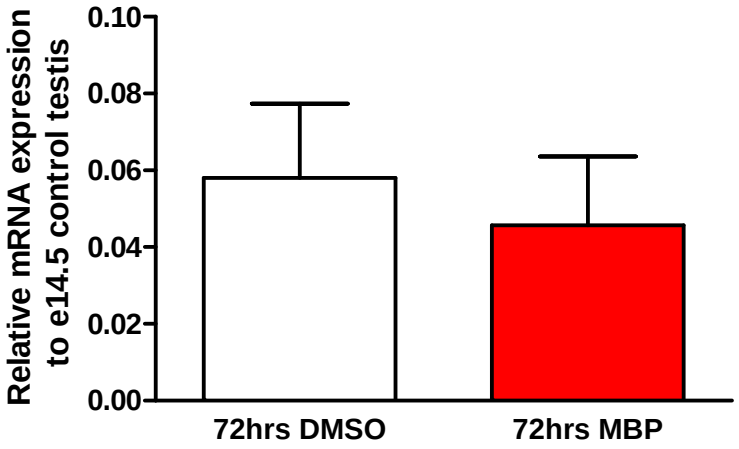

Figure 6.7 Quantitative analysis of *Oct4* mRNA levels in 72 hour fetal rat testis explants treated with DMSO or MBP (n=5). Values are means ± SEM. No statistically significant differences.

As with *Oct4* mRNA expression levels in testes from DBP exposed animals *in vivo* (Fig 4.9), 72 hours of MBP treatment did not significantly increase *Oct4* mRNA expression in comparison to vehicle control. As with the *in vivo* DBP exposure effect, this could be due to fewer GCs after 72hrs treatment with MBP that are each expressing more *Oct4* mRNA.

6.3.2.3 Effect of MBP treatment for 48 hours on Leydig cells

Having examined GC development with 48-72 hours of MBP treatment, Leydig cell development in the 48 hour cultured testis explants treated with DMSO or MBP were examined by IHC staining for 3β HSD, as shown in Fig 6.8.

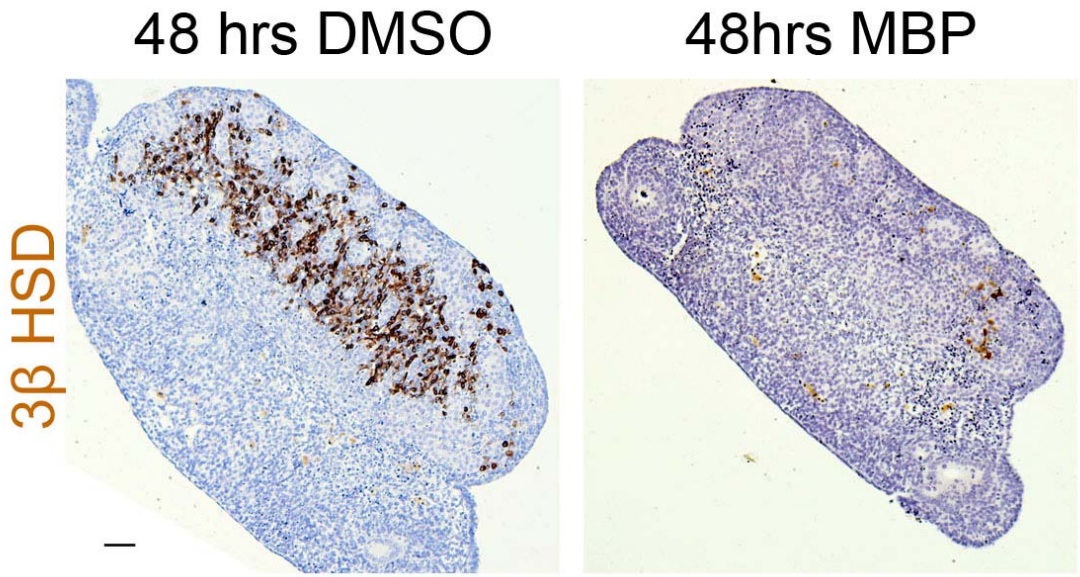

Figure 6.8 Representative photomicrographs of immunostaining for 3β HSD (Dab = brown) in 48 hour fetal rat testis explants treated with DMSO or MBP. Scale bar in panel A represents 50μm.

IHC staining for 3β HSD was severely reduced in testis explants after 48 hours of MBP treatment in comparison to DMSO vehicle control. IHC staining for another Leydig cell protein, the steroidogenic enzyme CYP11A also showed the same loss of

expression (data not shown). This suggested that MBP treatment severely reduced either Leydig cells or steroidogenesis after 48 hours. Culture media were assayed for testosterone, as described in (Fisher et al., 2003), but the results obtained were far too variable for useful analysis (1000 fold difference between similarly treated wells in the same culture experiment). To further examine the possible *in vitro* effect of MBP treatment, *3β hsd* mRNA levels were analysed by the Taqman system in 48 hours cultured testis explants treated with either DMSO or MBP, and results are shown in Fig 6.9.

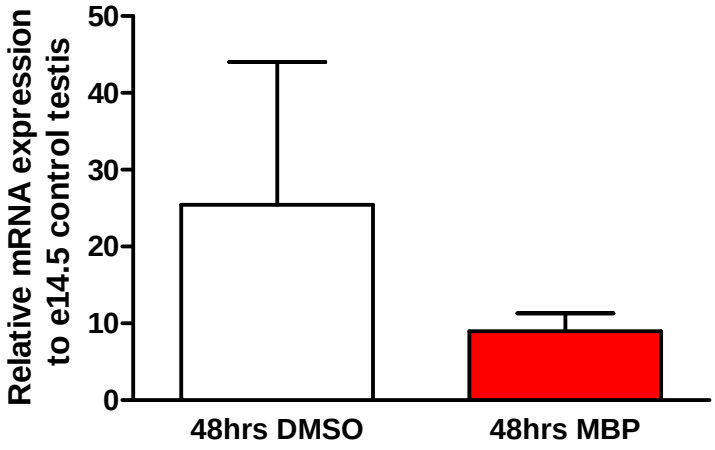

Figure 6.9 Quantitative analysis of *3β hsd* mRNA levels in 48 hour fetal rat testis explants treated with DMSO or MBP (n=5). Values are means ± SEM. No statistically significant differences.

There was no significant difference between MBP and DMSO treatment in *3β hsd* mRNA expression after 48 hours of *in* vitro culture, but it is likely that high variability in the expression level in DMSO treated testis explants may have masked an inhibitory effect of MBP treatment. This observation has led to other members of the research group examining early Leydig cell effects after *in vivo* DBP exposure.

6.3.3 In vitro treatment of testis explants with cyclopamine

Having established the utility of the 48 hour testis explant to be chemically manipulated, the model was then investigated for treatments that would not be possible *in vivo*, such as cyclopamine (Cyc) blockade of Hedgehog signalling. As described in Section 1.2.3.3, Desert Hedgehog signalling is important in fetal Leydig cell differentiation in the mouse (Clark et al., 2000; Yao et al., 2002). In *Dhh* null mice, there are also irregular cords by $e_m16.5$, and some GCs are found outside the cords (Clark et al., 2000), suggesting a role for Desert hedgehog signalling in cord formation. To examine if blocking Hedgehog signalling in the fetal rat testis affected cord formation and Leydig cells, e14.5 testes were cultured for 48 hours using cyclopamine at the 25 μM dosage, with ethanol (EtOH) used as the vehicle control. As with the untreated 48 hour cultures, the testis explants were analysed by IHC for the core developmental processes of fetal testis development including - GC proliferation by double IHC staining for DAZL and BrdU, seminiferous cord structure by double IHC for DAZL and AMH and Leydig cells by IHC for 3β HSD. These IHC examinations are summarized in Fig 6.10.

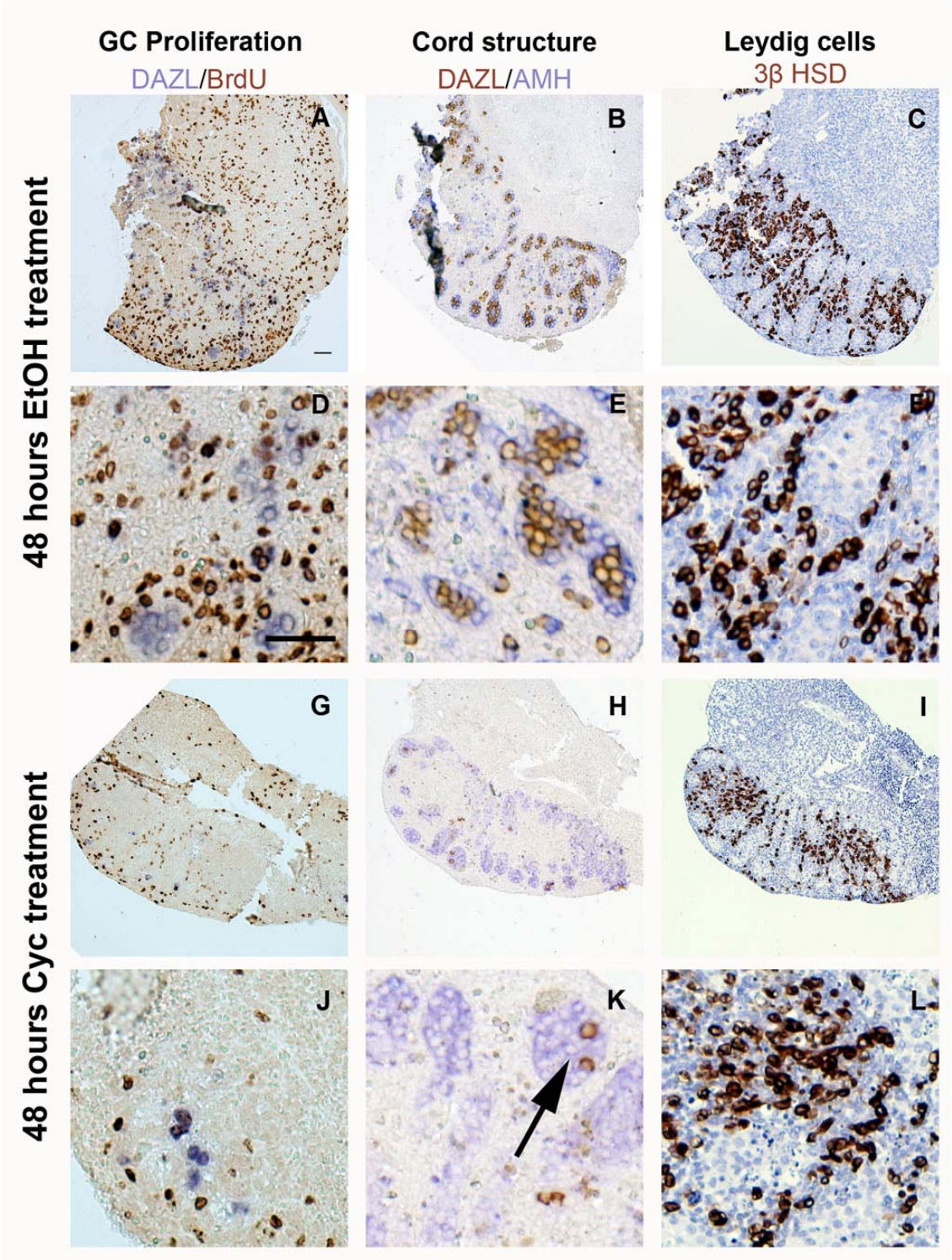

Figure 6.10 Representative photomicrographs of IHC staining from 48 hour *in vitro* cultured rat testis explants treated with EtOH (A-F) or Cyclopamine (Cyc) (G-L). Left-hand panels show IHC staining for BrdU (Dab = brown) and DAZL (Fast blue = blue). Middle panels show IHC staining DAZL (Dab = brown) and AMH (Fast blue = blue). Right-hand panels show IHC staining for 3β HSD (Dab = brown). Black arrow depicts reduced GCs in cords. Scale bars in Panels A and D represent 50 μm.

48 hours of *in vitro* treatment with EtOH or Cyc on testis explants did not prevent proliferation, or organization into seminiferous cords or Leydig cell expression development, based on 3β HSD immunoexpression. However a consistent reduction in GCs was detected in Cyc treated explants, highlighted (arrow) in Fig 6.10K. These remaining GCs continue to proliferate, as seen by the BrdU+DAZL+ cells present in Fig 6.10J. This was unexpected as Desert Hedgehog signalling has not been described as important in GC survival previously. To further examine if Cyc treatment altered both Leydig cell development and GCs, Taqman analysis for *3β hsd* and *Dazl* mRNA expression in testis explants cultured for 48 hours with EtOH or Cyc was performed, as shown in Fig 6.11 and Fig 6.12.

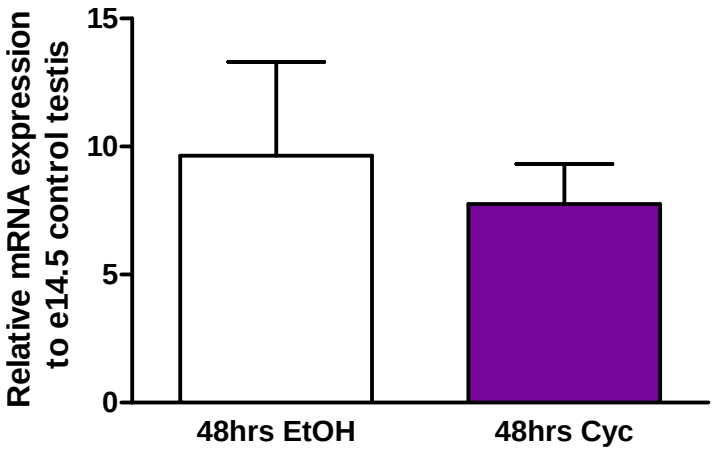

Figure 6.11 Quantitative analysis of *3β hsd* mRNA levels in 48 hour fetal rat testis explants treated with EtOH or Cyc (n=6). Values are means ± SEM. No statistically significant differences.

There was no significant difference in *3β hsd* mRNA expression in 48 hour cultured testis explants treated with Cyc, suggesting that blocking Desert Hedgehog signalling in the fetal rat testis did not alter *3β hsd* expression.

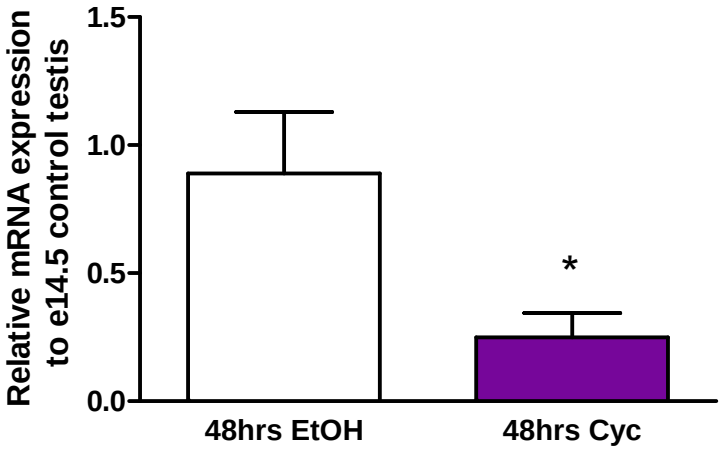

Figure 6.12 Quantitative analysis of *Dazl* mRNA levels in 48 hour fetal rat testis explants treated with EtOH or Cyc (n=6). Values are means ± SEM. * P<0.05 between EtOH and Cyc treated.

Forty eight hours of Cyc treatment significantly reduced *Dazl* mRNA expression in comparison to EtOH vehicle control. This matched the IHC staining result in Fig 6.10. To examine if this was just a reduction in DAZL expression, other GC markers (OCT4 and VASA) were examined by IHC in 48 hour *in vitro* cultured EtOH and Cyc treated testis explants and showed the same reduction in GCs (data not shown). To further investigate the role of Hedgehog signalling in the fetal rat testis, IHC staining for PTCH1 (the DHH receptor) using an antibody purchased from Abcam was performed on *in vivo* rat testes, as shown in Fig 6.13A and C. The staining detected with this Abcam antibody stained every cell in the rat testis at e16.5, before becoming more highly expressed in the cords than in the interstitium at e21.5. IHC staining using this antibody on postnatal rat testes showed GC specific staining at D25 and spermatogonial specific staining in adulthood (data not shown). This pattern of staining supported the Cyc treatment result, with GCs expressing PTCH1, but the IHC staining was consistently nuclear for a membrane receptor. To examine if this was true PTCH1 staining, a different antibody from Santa Cruz was used for IHC on e16 and e21.5 in vivo testes, shown in Fig 6.13B and D. This staining was more membrane bound and also seemed to be GC-specific, in fact IHC detection of

PTCH1 using the Santa Cruz was never found in Leydig cells at any age (fetal and postnatal), contradicting the reported role of DHH signalling in the testis.

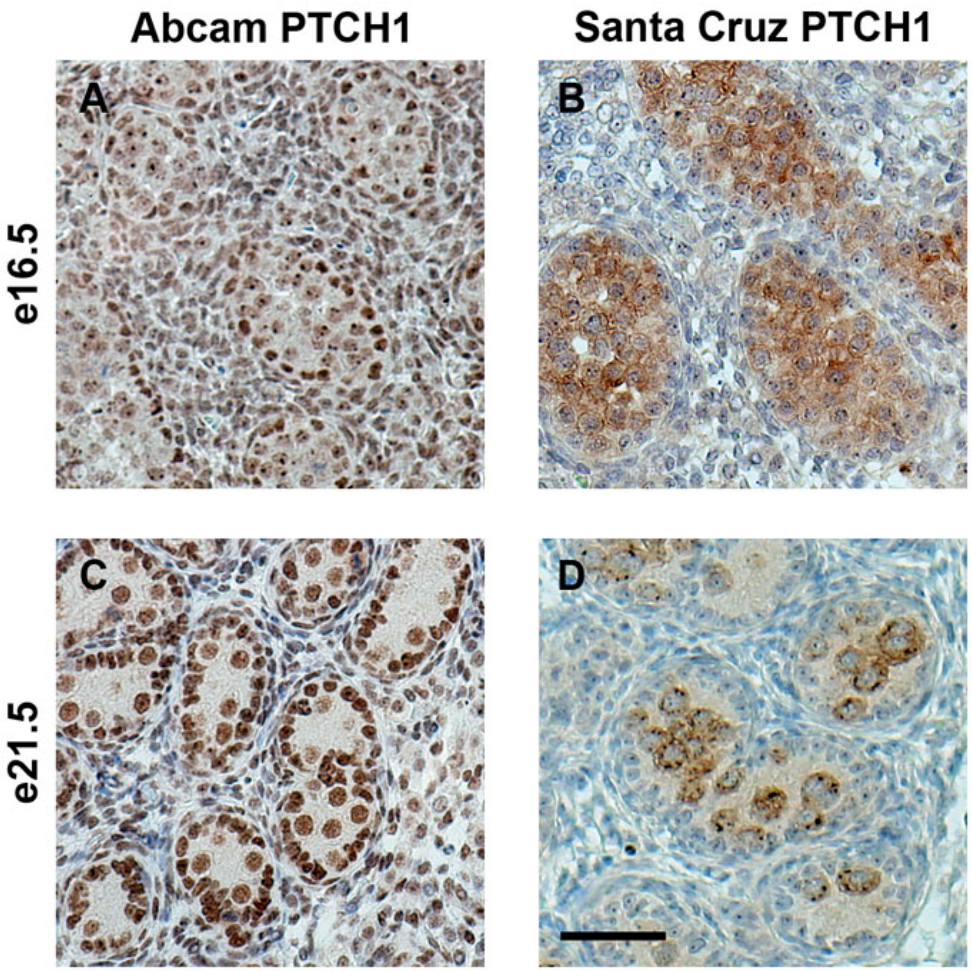

Figure 6.13 Representative photomicrographs of IHC staining using two antibodies to PTCH1 (Dab = brown) in fetal rat testes from e16.5 (A-B) and e21.5 (C-D). Antibody raised to PTCH1 purchased from either Abcam (left) or from Santa Cruz (right). Scale bar in Panel D represents 50 µm.

Due to the lack of consistency with reported PTCH1 expression by this IHC detection, it remains undetermined how PTCH1 protein is expressed in the fetal rat testis. IHC examination of the first downstream target after PTCH1, SMO was attempted but failed to provide convincing staining in the rat (data not shown).

This made the identification of which cells in the fetal rat testis were expressing the Hedgehog signalling proteins uncertain, and this would be vital in order to establish if there is a fundamental difference between rats and mice in the role of Hedgehog signalling in the fetal testis. Taqman mRNA analysis for *Ptch1* and *Smo* was then performed on testis explants after 48 hours of EtOH or Cyc treatment, as shown in Fig 6.14 and Fig 6.15.

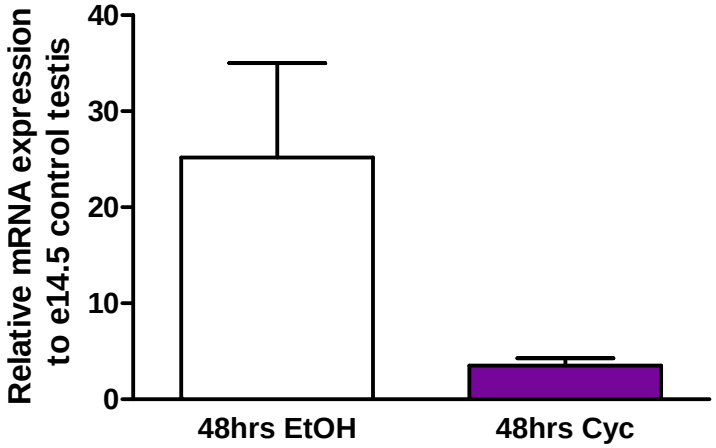

Figure 6.14 Quantitative analysis of *Ptch1* mRNA levels in 48 hour fetal rat testis explants treated with EtOH or Cyc (n=6). Values are means ± SEM. No statistically significant differences.

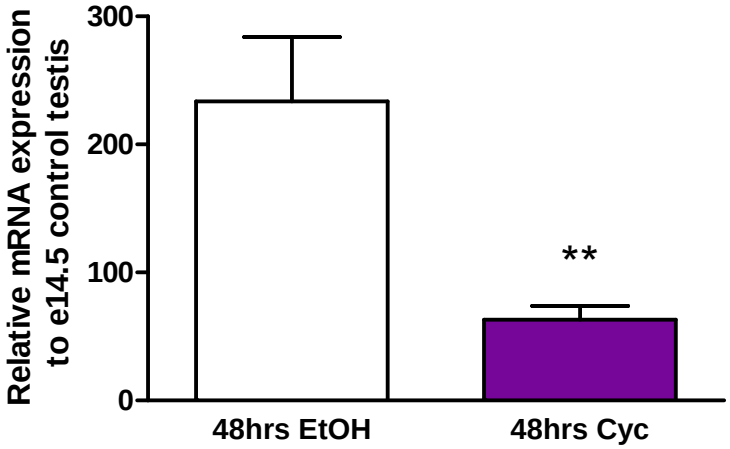

Figure 6.15 Quantitative analysis of *Smo* mRNA levels in 48 hour fetal rat testis explants treated with EtOH or Cyc (n=6). Values are means ± SEM. ** P<0.01 between EtOH and Cyc treated.

In cultured testis explants, 48 hours of Cyc treatment noticeably reduced *Ptch1* mRNA expression and significantly reduced *Smo* mRNA expression in comparison to EtOH vehicle control. This is similar to the reduction in *Dazl* mRNA expression shown in Fig 6.12. This may be due to a reduction in GCs, seen in Fig 6.10 and 6.12, if it is the GCs that are expressing *Ptch1* and *Smo* in the fetal rat testis. This is further evidence of a previously unreported role for Hedgehog signalling in GCs of the fetal rat testis.

6.4 Discussion

The aim of this chapter was to investigate if *in vitro* culture of isolated fetal rat testes, free from both maternal and fetal metabolism and endocrinology, could be used to support investigations into phthalate exposure and germ cell (GC) development. To that end, testis explants from e14.5 aged animals were cultured without treatment for 48 hours to examine how *in vitro* culturing affected testis development, before investigating the effects of *in vitro* chemical treatment with either monobutyl phthalate (MBP) or cyclopamine (Cyc) on testis explant development.

When testis explants from e14.5 aged animals were cultured for 48 hours without any chemical treatment, gross IHC examination showed that cells within the explants continued to proliferate (including GCs), continued to express cell-specific markers (for GC, Sertoli and Leydig) and Sertoli cells and GCs remained broadly organised into cord structures. When these testis explants were examined for apoptosis, an increased number of apoptotic cells were seen, as opposed to *in vivo* (data not shown) and were generally located around areas of damage that occurred during isolation. This demonstrated that the testis explants cultured for 48 hours did not become disorganised or lose structure, the different cell types appeared broadly functional, and could show somewhat similar development to e16.5 aged testes from *in vivo* animals.

It should be noted that a great degree of tissue variability was present after *in vitro* culture, with some testis explants appearing very similar to *in vivo* testes while some degenerated and appeared quite abnormal, although this could not be assessed until

after fixation and processing. Over the course of these thesis studies, dissection became more skilled and there was less variability, making this less of a negative factor. Usually to get around the variability of tissue, a careful IHC analysis was performed on each testis explant and those explants that had lost testis structure were excluded from any subsequent analyses. Another consideration is that whilst TUNEL analysis did not indicate widespread apoptosis, it was still increased compared to *in vivo*, raising the possibility that the testis explant is 'slowly dying' and therefore, with time, will become increasingly non-representative of the corresponding *in vivo* testis.

Having established that testis explants could be cultured *in vitro* for up to 48 hours and survive, they were then used to examine the effects of chemical disruption on a variety of aspects of testis development. As *in vivo* DBP exposure is of particular interest in this thesis, the active metabolite MBP was used as an *in vitro* chemical treatment to be investigated for similarities to *in vivo* DBP exposure on GC development (Chapter 4), and to determine whether *in vitro* phthalate studies could complement or replace in vivo studies.

After 48 hours of *in vitro* MBP treatment, testis explants continued to survive and cells continued to proliferate (including GCs), and all GCs remained OCT4+ and were organized into seminiferous cords, much the same as in untreated testis explants. With *in vivo* DBP exposure, there are limited GC effects observable early in testis development, mainly a significant reduction in GC number at e14.5 and e15.5, and an increase in proliferation index at e17.5. When *in vitro* MBP treatment for 48 hours was examined for similar effects, only the GC proliferation index could be reliably calculated, and was unaltered in comparison to DMSO controls. As there was only a DBP effect on GC proliferation at e17.5, it is possible that 48 hours of *in vitro* MBP treatment was simply too early a time point to observe an effect on the proliferation index.

GC number in testis explants was not calculated as testis explants could not be weighed, and variability between testis explants would make deriving weights

(Section 2.8.2.2) wholly inaccurate, as well as being highly labour intensive. Other studies on phthalate exposure have attempted to quantify GC number (Chauvigne et al., 2009; Li and Kim, 2003), but were deemed similarly labour intensive and limited to attempt here.

Of more interest in this study was to extend culture time and examine if a similar delay in loss of OCT4 expression, as seen with *in vivo* DBP exposure at e17.5, could be induced with in vitro MBP treatment. In MBP treated testis explants there were seemingly more OCT4+ GCs present than in DMSO controls, but when the percentage of OCT4+ GCs was quantified, no significant difference was found. This is most likely due to the variability in the treatment groups, where between 10-90% of GCs could be OCT4+. It should be noted that in both MBP and DMSO treated 72 hour cultured testis explants, the percentage of OCT4+ GCs was higher than *in vivo* at e17.5 (~20%, Fig 4.8), suggesting that delayed GC development was already occurring *in vitro*. When *Oct4* mRNA expression was examined in 72 hour testis explant cultures after exposure to MBP or DMSO, no difference in expression was observed, which may be due to MBP treatment having no effect on GC expression of *Oct4*, or possibly, as *in vivo* at e17.5 with DBP exposure (Fig 4.9), there are fewer GCs that are more highly expressing *Oct4* than in DMSO controls.

In vitro MBP treatment of testis explants failed to produce the same GC effects as reported after *in vivo* DBP exposure and therefore proved to be an inadequate tool in this regard, especially as testis explants are limited in what can be examined in terms of delayed GC development (DMRT1 at e19.5, GC aggregation at e21.5, MNGs at e21.5, reduced GC number). One of the other uses of *in vitro* culture is that different doses of phthalates can be used directly on testis explants (as attempted in Chauvigne et al., 2009; Li and Kim, 2003), however when GC effects in both controls and MBP treated explants were so variable, such dose response investigations would also be limited.

However, the testis explant experiments using MBP did yield one interesting result, with the identification of a possible phthalate effect on early testis development, as it

caused a dramatic reduction in 3β HSD and CYP11A1 expression after 48 hours of *in vitro* culture with MBP. This showed that MBP is either severely inhibiting steroidogenesis or differentiation of fetal Leydig cells, with presumably the same net effect. The limitations of *in vitro* testis explants become a factor again, as testosterone levels could not be reliably examined in MBP or DMSO treated culture media, making this MBP effect on steroidogenesis/Leydig cells observational. This early phthalate effect matches reported *in vivo* DBP exposure effects on Leydig cells, but at an earlier time than previously examined. This effect (of MBP on testis explants) is similar to what has been reported to occur in vivo after DBP exposure, but only at e15.5 (Hutchison et al., 2008).

Having established the relative merits and drawbacks of *in vitro* phthalate investigations to support *in vivo* studies, a chemical treatment that could not be attempted *in vivo* was then examined. Cyclopamine (Cyc) inhibits Hedgehog signalling through binding and blocking SMO protein action. *In vitro* treatment with Cyc has been used before on fetal mouse gonads to disrupt Leydig cell differentiation (Yao et al., 2002). Furthermore, in Desert Hedgehog null mice, both cord formation and Leydig cell development are disrupted (Clark et al., 2000). Therefore it was expected that Cyc treatment would disrupt seminiferous cords and Leydig cells in the fetal rat testis explants.

After 48 hours of *in vitro* Cyc treatment of testis explants, both seminiferous cord formation and Leydig cell steroidogenesis appeared unaltered in comparison to ethanol (EtOH) control treatment, when examined by both IHC and Taqman analysis. It is possible that this lack of effect of blocking Desert Hedgehog signalling in the fetal rat testis, when compared to the fetal mouse testis, may be due to the timing of Cyc treatment. Cyc only altered Leydig cell differentiation in mouse explants that were collected prior to $e_m12.5$, and after that time Cyc had no effect (Yao et al., 2002). This temporal aspect of Desert Hedgehog signalling may be similar in the rat, but testes from younger ages than e14.5 could not be dissected out in a manner suitable for *in vitro* culture.

Interestingly, after 48 hours of *in vitro* Cyc treatment of rat testis explants, a noticeable reduction in GCs was observed in comparison with EtOH treated controls. Previously, the only GC effect of blocking Desert Hedgehog signalling in the mouse testis was that some GCs were found outside of the cords, as a side effect of disrupted cord formation (Clark et al., 2000). However in the rat testis explants cultured for 48 hours with Cyc, GCs were all found within the cords and some were still proliferating (BrdU+). As GCs and Sertoli cells are organised into seminiferous cords by e14.5, the time of testis explant collection, the Cyc-induced loss of GCs was not due to disrupted cord formation, as that was relatively unaltered after 48 hours of *in vitro* Cyc treatment. Overall this suggests a possible role of Desert Hedgehog signalling from Sertoli cells (as in the mouse) that promotes GC survival in the fetal rat testis.

Attempts to further investigate the role of Desert Hedgehog signalling in the fetal rat testis were limited by inability to conclusively show that GCs express the Hedgehog signalling machinery (PTCH1 and SMO). The only support for GC expression of Hedgehog signalling molecules in the fetal testis was that mRNA levels for *Ptch1* and *Smo* were reduced in the whole testis to a similar degree as was the GC gene *Dazl*. In the postnatal (mouse) testis there is more evidence for a role of Desert Hedgehog signalling in spermatogenesis (Bitgood et al., 1996), and identification of PTCH1 and SMO in the meiotic and post meiotic GCs in the mouse testis (Morales et al., 2009) and the detection of a male GC-specific Patched-domain gene *Ptchd3*, the protein for which is found in the sperm of mice, rat and human (Fan et al., 2007).

Recently a study using fetal rat testis explants from e14.5 that were cultured up to three days in the presence of Cyc (at the same dose used here) or recombinant mouse Sonic Hedgehog has been performed (Brokken et al., 2009). In this study, no GC effects were reported, but the focus was more on Leydig cell effects and only a limited IHC analysis of the explants was performed. However after three days of culture, a significant reduction in *Ptch1* mRNA expression was reported with Cyc treatment, similar to reported here, as well as a significant reduction in both *3β hsd* and *Cyp11a* mRNA expression levels (Brokken et al., 2009). Taking all these factors

into account, any further conclusions about Desert Hedgehog signalling in fetal rat GCs remains a possibility but requires considerable further work.

These studies into Cyc treatment highlight both the strength and weakness of *in vitro* testis explants. Cyc treatment would not be possible *in vivo*, so blocking Hedgehog signalling in the developing fetal rat testis would be otherwise very hard to achieve. The data generated from Cyc treatment on testis explants has shown a clear reduction in GCs compared to controls and has suggested a possible new role of Hedgehog signalling in GCs that could not have been determined otherwise. Unfortunately, no further support could be generated from the testis explants and the same data contradicts several aspects of published work in the mouse and the rat (Brokken et al., 2009; Yao et al., 2002).

In summary, the MBP studies illustrate that *in vivo* studies are clearly a better way to examine testis development and disruption, whilst the Cyc studies illustrate the utility of testis explants when *in vivo* manipulation cannot be done. Generally the testis explants were useful in detecting gross changes caused by chemical treatment, such as MBP on 3β HSD and Cyc on GCs, that can be easily observed, but if more subtle changes are caused they may be missed due to the high variability. The inability to quantify GC number or testosterone levels from testis explants is also a consideration, though other groups have managed to collect reliable hormone data (Chauvigne et al., 2009; Hallmark et al., 2007; Lambrot et al., 2009; Li and Kim, 2003). Nevertheless, there is still considerable disagreement between the published data, for example phthalate effects on testosterone production on testis explants (Chauvigne et al., 2009; Stroheker et al., 2006), and this may reflect the inherent variability of the *in vitro* approach. In this regard, the notion that *in vitro* testis explants are a slowly dying tissue means that it will always have limited resemblance to the normal function of that tissue. However it remains the only way to disrupt certain aspects of testis development and allows a way to examine disruption on human tissue, which altogether makes *in vitro* testis explants a useful tool, but one that requires very careful application.

7 General discussion

The general aim of this thesis was to obtain new insights into regulation of fetal GC development in the rat and the susceptibility of these processes to disruption by DBP. As there is currently no accepted model for human CIS/TGCT, it was hoped that examining GC development in an animal model in which a TDS-like phenotype has been induced by DBP exposure might provide some insight into how perturbed fetal GC differentiation in the human can result in CIS cells and eventually TGCT. More generally, it was hoped that gathering more information on the process of fetal GC differentiation, especially in regard to methylation events in fetal life, might shed light on events that might predispose to CIS and/or to infertility in adulthood. In addition, *in vitro* fetal testis explants were evaluated as an additional tool to investigate early testis development, especially in regard to GC development.

To achieve these aims, normal GC development in the fetal rat testis and ovary was characterised, as described in Chapter 3, and identified a variety of events that could be investigated for possible DBP disruption. When the DBP exposure effects were examined in Chapter 4, a general pattern of delayed GC development was identified, which persisted into early postnatal life. In addition, it appeared that early exposure (between e13.5-e15.5) was a crucial time window in inducing the observed DBP exposure effects on GCs. Having thoroughly examined the effects of fetal exposure to DBP on GC development, the process of DNA methylation in the fetal testis was focussed upon as a possible mechanism for how DBP exposure may be exerting some of its effects, covered in Chapter 5. Examination of global DNA methylation in relation to DBP exposure showed no obvious DBP effect, whilst the relationship between methylation of the candidate gene *Oct4* and its protein expression was examined by chemical DNA methylation inhibition and bisulphite sequencing of the *Oct4* promoter region. Finally, *in vitro* studies using testis explants as an additional tool to investigate fetal GC development and phthalate exposure, described in Chapter 6, suggested a Leydig cell effect of phthalate exposure earlier than previously reported and a possible new role of Hedgehog signalling in fetal rat GCs.

When GC development was examined in both the fetal rat testis and ovary, it was found to be broadly similar with some small differences (OCT4 expression at e17.5) and some major (meiotic/mitotic arrest), which matched the published literature for the mouse (Bowles and Koopman, 2007). As well as providing the first data on these events for the rat, this characterisation detailed the processes and specific timings that were then examined for effects of *in utero* DBP exposure from e13.5 until birth. Two major effects of DBP on GC development were observed, which may be related or not. They were a consistent reduction in GC number at every age examined (even after only 24 hours of DBP exposure) and a delay in the timing of GC development.

The origin of the consistent reduction in GC numbers after DBP exposure seemed to be early in testis development, as a significant reduction in GC numbers was found by e14.5. Use of different exposure windows showed that starting DBP exposure earlier than e13.5 did not exacerbate this reduction in GC number and that DBP exposure after e15.5 did not significantly reduce GC number by e21.5. This indicated that DBP exposure between e13.5 and e15.5 is the crucial time when GC number reduction is established. This most probably occurred by increased GC apoptosis, but this was not directly shown. Phthalate exposure *in vitro* has been reported to increase GC apoptosis, but only at specific times (Lambrot et al., 2009; Li and Kim, 2003). It may be possible that fetal rat GCs are especially susceptible to DBP induced apoptosis between e13.5-e15.5, as no increased GC apoptosis was detected at e15.5 and e17.5. Associated with the reduction in GC number was altered GC proliferation after DBP exposure, which was increased at e17.5 in testes from DBP exposed animals compared with controls, and rare, single proliferating GCs were even observed at e19.5 in testes from DBP exposed animals. It was concluded that DBP exposure prolonged GC proliferation, but this increased proliferation could not recover final GC number in fetal life to control levels. The effect of DBP on GC proliferation may indicate a different explanation for the consistent reduction in GC number induced by DBP exposure, as it could be that DBP delays the progress of GC through the cell cycle. If DBP exposure was slowing down the GC cell cycle, a reduction in GC number would be observed as well as a prolonged detection of slower proliferating cells. However, as no difference in GC proliferation index was

observed at e15.5 between control and DBP exposed animals, as might be expected if DBP exposure slowed GC progress through the cell cycle, it is more likely that DBP exposure is instead delaying the end of GC proliferation. Further work is needed to identify the mechanisms underlying the early origin of reduced GC number after DBP exposure, for example by examining GC apoptosis at short time intervals after dosing with DBP on e13.5; these same samples could also be used to investigate if the progress of GC through the cell cycle is altered after DBP exposure.

The reduction in GC number after DBP exposure may be related to the described delays in GC development, as summarized in Table 4.4. Briefly, several processes of GC development showed a consistent, but transient, delay in their timings, such as the end of proliferation, the switching off of OCT4 and DMRT1 expression, “cKIT” localization and fetal GC disaggregation at e21.5. This consistent delay in fetal GC development after DBP exposure even continued into early postnatal life with delayed re-entry into proliferation, GC-specific re-expression of DMRT1, postnatal migration to the basal lamina at D6 and delayed entry into meiosis at D15. However, given enough time the GCs of DBP exposed animals managed to “catch-up” to control animals by adulthood (3 months old) (Ferrara et al., 2006). This consistent delay in so many aspects of GC development is very convincing evidence that *in utero* DBP exposure is somehow causing the endogenous GC program to run late, and that this effect is triggered by exposure during the period of initial cord formation.

As with the reduction in GC number throughout fetal life, the delay in GC development appeared to be an early event in testis development after DBP exposure. DBP exposure between e13.5-e15.5 resulted in a significant increase in OCT4+ GCs at e17.5, a noticeable increase in DMRT1+ GCs at e19.5, and significant decrease in DMRT1+ GCs at D6, though these delayed events were not as marked as with continued DBP exposure from e13.5 until birth. DBP exposure between e15.5 and e17.5 showed no significant induction of GC effects reported with standard DBP exposure, but did tend to show a slight change. These shorter windows of DBP exposure suggested that while delayed GC development in DBP exposed animals

originated from some event between e13.5-e15.5, continued DBP exposure after that point may be necessary to maintain and/or enhance this delay. As with the reduction in GC numbers, identification of the early event in GC development which DBP disrupts to cause this delay would be a major avenue of future investigation. This might also have relevance to CIS origins, as any process that can be perturbed and affect GC differentiation would be a step towards the block in differentiation that leads to CIS.

As the gross histology of e14.5 testes from DBP exposed animals was similar to e14.5 testes from control animals (though testes were slightly smaller) and seminiferous cord formation was not observed to be disrupted by e14.5 (data not shown), a subtle origin for both reduced GC number and delayed GC development is most likely. At such an early stage of testis development, relatively minor changes to GC development by DBP exposure could cause major consequences by the end of fetal life and postnatally. Investigating a possibly subtle change during the very early stages of testis development makes further *in vivo* investigations of DBP exposure a challenging task.

Ideally, *in vitro* manipulation of e14.5 fetal testis explants would be useful in trying to identify the origin of the DBP-induced delay in GC development. As described in Chapter 6, e14.5 testis explants can be cultured, but show a delayed development in longer culture times (i.e. a high percentage of OCT4+ GCs after 72 hours culture) and the high variability of morphology and phenotype may make identifying a subtle change difficult. However, improvements in the *in vitro* culture system that would allow e13.5 gonad pairs (to reduce tissue damage during extraction) to be cultured could provide a way to examine early testis development with MBP treatment. As seminiferous cords can be viewed using a transilluminated stage (during microdissection), cord formation between e13.5 and e14.5 could possibly be followed using live cell imaging, and examined for a possible MBP treatment effect.

The most obvious way to gain more insight into the early origin of DBP exposure effects on GCs would be to use narrower early windows of DBP exposure *in vivo*,

i.e. e13.5-e14.5 and e14.5-e15.5 and then examine the delay in switching off of OCT4 and DMRT1 and the effect on GC number at e21.5. This would hopefully identify if the early effect of DBP exposure was occurring prior to cord formation, which is complete by e14.5, or after. Should DBP exposure be required between e13.5 and e14.5 to cause disrupted GC development, this may explain the lack of MBP treatment effect on GCs in e14.5 testis explants in Chapter 6.

Whilst cord formation was not prevented in DBP exposed animals by e14.5, it is still possible that the early GC-Sertoli interactions and organization during cord formation may be susceptible to DBP interference, and that early interference may initiate the delay in GC development. This might be the most important area to investigate, as extended DBP exposure treatment has established that the GCs are only susceptible to DBP exposure once they have arrived in the gonad. The later event of GC disaggregation at e21.5 may provide a more convenient way to examine how GC-Sertoli interactions may be altered by DBP exposure effects, as illustrated by previous work on a late DBP exposure window from e19.5-e20.5 (Ferrara et al., 2006).

The importance of early exposure between e13.5-e15.5, when GCs are in the gonad but prior to reported DBP effects on other cell types (Hutchison et al., 2008b; Scott et al., 2008) suggests that the described effects of DBP exposure are a combination of both direct DBP exposure effect on the GCs and a necessity of the GCs to be present within the somatic environment of the gonad for DBP exposure to have an effect. Further work to identify how DBP exerts both the direct effect and indirect effect on GCs would be worth pursuing.

This thorough examination of GC development in the rat and DBP exposure encountered a few technical limitations, which if they could be overcome would provide further evidence of DBP exposure effects. For example, if the observed difference in DAZL protein reduction at e19.5 could be quantified, that would support the DBP induced delay in GC development. Taqman analysis was also limited by the use of whole testis RNA from control and DBP exposed animals, that

made it impossible to determine if a change in mRNA expression reflected a change in GC expression of that gene, or reflected a change in the number of cells expressing that gene (as happened for OCT4 at e17.5 in DBP exposed animals).

A major consequence of this thorough examination of GC development in the fetal rat is that it demonstrated fundamental differences in organisation and co-ordination of fetal GC development between rat/mouse and the human, as highlighted in recently published data on GC development in the human fetal testis (Anderson et al., 2007; Mitchell et al., 2008). These differences may account for why DBP exposure does not induce CIS/TGCT in the rat. As described in Section 3.4, fetal GCs within the human testis have heterogeneous sub-populations of GCs within individual seminiferous cords, whilst in the rat the seminiferous cords contain largely synchronised GC populations. In addition, there are sub-populations of OCT4+, VASA+ and DAZL+ GCs in the human, which were not found in the rat (Anderson et al., 2007). These differences probably reflect the differentiation of GCs in the human from one stage to another, whilst the comparatively rapid GC development in the rat may require quicker/more efficient GC differentiation. This difference between synchronised GC development in the rat and "unsychronised" GC development in the human may explain why CIS/TGCT were not induced with DBP exposure like the other TDS disorders. However the DBP exposure induced delay in rat GC development may provide some insight into the origin of CIS cells in the human, where a "delayed" GC may be a precursor to a "blocked" GC. As the described delay in rat GC development after DBP exposure is largely synchronised and isolated, "blocked in differentiation" GCs were not present, suggesting that rat GCs are more tightly regulated, either within the GC themselves or through external signals from the Sertoli cells or other GCs. In the human testis, where there are GC sub-populations and a lack of such synchronicity, it is more likely that if isolated GCs become delayed in development, it would be possible that a "block in differentiation" could occur, resulting in CIS.

If CIS is indeed the result of a developmentally delayed human GC that then becomes blocked from differentiating further, identification of the mechanisms

responsible for the early DBP-induced delay in GC development in the rat might enable the delay to be prolonged or enhanced and might then be capable of leading to CIS-like cells in the rat. Alternatively, a more appropriate animal model for human GC development than the rat could be used to investigate delayed differentiation and CIS cells. Recently, the marmoset has been described as an animal model with similar asynchronised fetal and neonatal GC development to the human (Mitchell et al., 2008), and has been examined for fetal and neonatal MBP exposure effects on testis development, with possible effects on OCT4 expression neonatally (McKinnell et al., 2009). Another option to investigate phthalate exposure on human GC development would be to use *in vitro* MBP treatment on fetal human testis explants, as previously attempted (Hallmark et al., 2007), but with a focus on GC development to compare with the results of MEHP on fetal human testis explants (Lambrot et al., 2009). However, if the rat is any guide, such *in vitro* studies may have to use 1st rather than 2nd trimester fetal human testis explants (unlike the studies to date), as it is possible that very early events are those susceptible to disruption to induce CIS cells; from studies of CIS cell protein expression patterns this is likely to be the case (Rajpert-De Meyts et al., 2003; van de Geijn et al., 2009).

One important aspect of CIS/TGCT that could be further investigated using the DBP exposure model of delayed GC development, is determining what is regulating the silencing of OCT4 expression in the fetal testis. In mouse and human ES (and iPS) cells, *Oct4* gene expression is related to promoter methylation that is regulated by retinoic acid (RA) signalling (Li et al., 2007; Yeo et al., 2007). In the fetal rat ovary, *Oct4* mRNA was significantly reduced around the time of meiotic induction supporting the role of RA in both initiating meiosis and silencing *Oct4* (Bowles et al., 2006; Bowles and Koopman, 2007). However, in the fetal testis, should the theory of RA signalling initiating GC meiosis be correct, RA would be absent, having been metabolised by CYP26B1, implying that another mechanism separate from RA signalling may be involved in *Oct4* silencing in the fetal testis. Use of the chemical methylation inhibitor AZC in Chapter 5 showed that inhibiting methylation can prolong the expression of OCT4 protein in GC until even e19.5, supporting the importance of methylation in the regulation of *Oct4* gene expression. Whilst

methylation may be important in *Oct4* gene expression, other forms of gene regulation (i.e. post-translational regulation) could also be occurring. This is a possibility as *Oct4* mRNA was still detected in both late fetal and postnatal rat testes, when OCT4 protein expression was completely absent, whereas in the ovary *Oct4* mRNA was never detected after e17.5. By taking advantage of the significant difference in OCT4 expression between testes from control and DBP exposed animals, a greater understanding of how *Oct4* expression is regulated in the absence of RA in the fetal testis would be a logical further study. Such insight into *Oct4* expression in the fetal testis would be of great interest with regard to the expression of OCT4 and the maintenance of pluripotency in human CIS cells.

Whilst *in utero* DBP exposure does not block GC differentiation and the observed delay in GC development eventually recovers to "normal" levels, DBP exposed males still have impaired spermatogenesis and reduced fertility (Fisher et al., 2003). This suggests that there may be subtle DBP exposure effects on GCs that have not so far been identified. One mechanism that is associated with reduced fertility is altered DNA methylation, especially at imprinted gene loci (Hammoud et al., 2009). The examination of DNA methylation for the first time in the fetal rat testis (Chapter 5) illustrated the importance of this process during testis development, with increased global methylation in GCs and high expression of DNA methyl transferases in comparison to the adult rat testis. Attempts to identify disrupted DNA methylation with DBP exposure were unsuccessful, but differences in timing and gene specific methylation would probably not have been detected. As GC development was consistently delayed after DBP exposure, it seems likely that GC de novo DNA methylation could also be delayed and if that delay was severe enough to cause aberrant genomic imprinting, this could lead to postnatal consequences such as reduced fertility.

To further investigate DNA methylation in regard to *in utero* DBP exposure, two approaches may be the most effective. First, examination of the methylation of imprinted genes in sperm from control and DBP exposed animals. Second, to use global comparative methylation analyses to look at the methylation of a wide variety

of genes in control and DBP exposed animals. By focussing on imprinted genes in sperm, the problems of somatic DNA contamination would be limited, and several imprinted genes have already been associated with altered methylation and reduced fertility to provide good target genes for investigation. Should global methylation differences between control and DBP exposed animals be examined, methods such as Restriction Landscape Genome Scanning (RLGS) would be a relatively simple way to compare groups. RLGS generates a 2 dimensional map of "spots" that are dependent on the methylation status of restriction sites and these maps can be used to visualise the methylation in a wide variety of genes in the sample. By comparing the "spot" maps between control and DBP exposed animals, or from different aged animals, regions that are differentially methylated could easily be identified and further examined (Costello et al., 2009).

If an efficient and robust method of isolating fetal rat GCs was developed, gene specific methylation investigations could be performed, as was attempted for *Oct4*. The ability to isolate fetal rat GCs would allow many questions about the DBP induced delay in GC development to be answered more clearly. For example, isolated GCs could be counted by a flow cytometer to determine the number of GCs in control and DBP exposed testes from any age, and isolated GCs could be used for Taqman analysis to determine if the DBP induced reductions in gene expression reflect a loss of mRNA or simply a loss of GCs.

In summary, the present studies have provided the first detailed analysis of GC development in the fetal rat and have identified the processes of GC development that are susceptible to disruption by DBP exposure. Whilst these effects of DBP exposure failed to provide specific new insight into the origin of human CIS/TGCT, they have identified processes that are of likely relevance to the origin of CIS cells, and have highlighted the potential vulnerability of very early GC development and differentiation to disruption by an environmental chemical such as DBP. DBP exposure delayed, but failed to ultimately block, GC differentiation in fetal life, and this delay continued into early postnatal life. The use of different DBP exposure time windows identified that early testis development was most susceptible to the effects

of DBP exposure on GCs. Although no direct evidence could be provided to show that altered DNA methylation was a mechanism via which DBP exposure affected GC development, studies using an inhibitor of methylation suggested this was a distinct possibility. Finally, *in vitro* culturing of testis explants was found to have limited utility for the study of fetal GC development and its manipulation in the rat, though further studies to refine techniques and reduce variability might improve this.

8 References

Adams, I. R. and McLaren, A. (2002). Sexually dimorphic development of mouse primordial germ cells: switching from oogenesis to spermatogenesis. *Development* **129**, 1155-64.

Adham, I. M. and Agoulnik, A. I. (2004). Insulin-like 3 signalling in testicular descent. *Int J Androl* **27**, 257-65.

Albrecht, K. H., Capel, B., Washburn, L. L. and Eicher, E. M. (2000). Defective mesonephric cell migration is associated with abnormal testis cord development in C57BL/6J XY(Mus domesticus) mice. *Dev Biol* **225**, 26-36.

Anderson, R., Copeland, T. K., Scholer, H., Heasman, J. and Wylie, C. (2000). The onset of germ cell migration in the mouse embryo. *Mech Dev* **91**, 61-8.

Anderson, R. A., Fulton, N., Cowan, G., Coutts, S. and Saunders, P. T. (2007). Conserved and divergent patterns of expression of DAZL, VASA and OCT4 in the germ cells of the human fetal ovary and testis. *BMC Dev Biol* **7**, 136.

Andersson, A. M., Toppari, J., Haavisto, A. M., Petersen, J. H., Simell, T., Simell, O. and Skakkebaek, N. E. (1998). Longitudinal reproductive hormone profiles in infants: peak of inhibin B levels in infant boys exceeds levels in adult men. *J Clin Endocrinol Metab* **83**, 675-81.

Anway, M. D., Cupp, A. S., Uzumcu, M. and Skinner, M. K. (2005). Epigenetic transgenerational actions of endocrine disruptors and male fertility. *Science* **308**, 1466-9.

Anway, M. D., Leathers, C. and Skinner, M. K. (2006a). Endocrine disruptor vinclozolin induced epigenetic transgenerational adult-onset disease. *Endocrinology* **147**, 5515-23.

Anway, M. D., Memon, M. A., Uzumcu, M. and Skinner, M. K. (2006b). Transgenerational effect of the endocrine disruptor vinclozolin on male spermatogenesis. *J Androl* **27**, 868-79.

Arango, N. A., Lovell-Badge, R. and Behringer, R. R. (1999). Targeted mutagenesis of the endogenous mouse Mis gene promoter: in vivo definition of genetic pathways of vertebrate sexual development. *Cell* **99**, 409-19.

Avilion, A. A., Nicolis, S. K., Pevny, L. H., Perez, L., Vivian, N. and Lovell-Badge, R. (2003). Multipotent cell lineages in early mouse development depend on SOX2 function. *Genes Dev* **17**, 126-40.

Baker, P. J., Sha, J. A., McBride, M. W., Peng, L., Payne, A. H. and O'Shaughnessy, P. J. (1999). Expression of 3beta-hydroxysteroid dehydrogenase type I and type VI isoforms in the mouse testis during development. *Eur J Biochem* **260**, 911-7.

Baltus, A. E., Menke, D. B., Hu, Y. C., Goodheart, M. L., Carpenter, A. E., de Rooij, D. G. and Page, D. C. (2006). In germ cells of mouse embryonic ovaries, the decision to enter meiosis precedes premeiotic DNA replication. *Nat Genet* **38**, 1430-4.

Barlow, N. J., Phillips, S. L., Wallace, D. G., Sar, M., Gaido, K. W. and Foster, P. M. (2003). Quantitative changes in gene expression in fetal rat testes following exposure to di(n-butyl) phthalate. *Toxicol Sci* **73**, 431-41.

Batistatou, A., Scopa, C. D., Ravazoula, P., Nakanishi, Y., Peschos, D., Agnantis, N. J., Hirohashi, S. and Charalabopoulos, K. A. (2005). Involvement of dysadherin and E-cadherin in the development of testicular tumours. *Br J Cancer* **93**, 1382-7.

Behringer, R. R. (1994). The in vivo roles of mullerian-inhibiting substance. *Curr Top Dev Biol* **29**, 171-87.

Ben-Shushan, E., Pikarsky, E., Klar, A. and Bergman, Y. (1993). Extinction of Oct-3/4 gene expression in embryonal carcinoma x fibroblast somatic cell hybrids is accompanied by changes in the methylation status, chromatin structure, and transcriptional activity of the Oct-3/4 upstream region. *Mol Cell Biol* **13**, 891-901.

Bendel-Stenzel, M., Anderson, R., Heasman, J. and Wylie, C. (1998). The origin and migration of primordial germ cells in the mouse. *Semin Cell Dev Biol* **9**, 393-400.

Besmer, P., Manova, K., Duttlinger, R., Huang, E. J., Packer, A., Gyssler, C. and Bachvarova, R. F. (1993). The kit-ligand (steel factor) and its receptor c-kit/W: pleiotropic roles in gametogenesis and melanogenesis. *Dev Suppl*, 125-37.

Best, D., Sahlender, D. A., Walther, N., Peden, A. A. and Adams, I. R. (2008). Sdmg1 is a conserved transmembrane protein associated with germ cell sex determination and germline-soma interactions in mice. *Development* **135**, 1415-25.

Biermann K, Göke F, Nettersheim D, Eckert D, Zhou H, Kahl P, Gashaw I, Schorle H and Büttner R. (2007). c-KIT is frequently mutated in bilateral germ cell tumours and down-regulated during progression from intratubular germ cell neoplasia to seminoma. *J Pathol.* **213**, 311-8.

Bitgood, J. J. and Rozum, J. J. (1996). Close linkage relationship of the Z-linked pop-eye and silver plumage color loci in the chicken. *Poult Sci* **75**, 1067-8.

Bortvin, A., Goodheart, M., Liao, M. and Page, D. C. (2004). Dppa3 / Pgc7 / stella is a maternal factor and is not required for germ cell specification in mice. *BMC Dev Biol* **4**, 2.

Borum, K. (1961). Oogenesis in the mouse. A study of the meiotic prophase. *Exp Cell Res* **24**, 495-507.

Bourc'his, D., Xu, G. L., Lin, C. S., Bollman, B. and Bestor, T. H. (2001). Dnmt3L and the establishment of maternal genomic imprints. *Science* **294**, 2536-9.

Bowles, J., Knight, D., Smith, C., Wilhelm, D., Richman, J., Mamiya, S., Yashiro, K., Chawengsaksophak, K., Wilson, M. J., Rossant, J. et al. (2006). Retinoid signaling determines germ cell fate in mice. *Science* **312**, 596-600.

Bowles, J. and Koopman, P. (2007). Retinoic acid, meiosis and germ cell fate in mammals. *Development* **134**, 3401-11.

Boyer, L. A., Mathur, D. and Jaenisch, R. (2006). Molecular control of pluripotency. *Curr Opin Genet Dev* **16**, 455-62.

Brennan, J. and Capel, B. (2004). One tissue, two fates: molecular genetic events that underlie testis versus ovary development. *Nat Rev Genet* **5**, 509-21.

Brennan, J., Karl, J. and Capel, B. (2002). Divergent vascular mechanisms downstream of Sry establish the arterial system in the XY gonad. *Dev Biol* **244**, 418-28.

Brennan, J., Tilmann, C. and Capel, B. (2003). Pdgfr-alpha mediates testis cord organization and fetal Leydig cell development in the XY gonad. *Genes Dev* **17**, 800-10.

Brimble, S. N., Sherrer, E. S., Uhl, E. W., Wang, E., Kelly, S., Merrill, A. H., Jr., Robins, A. J. and Schulz, T. C. (2007). The cell surface glycosphingolipids SSEA-3 and SSEA-4 are not essential for human ESC pluripotency. *Stem Cells* **25**, 54-62.

Brokken, L. J., Adamsson, A., Paranko, J. and Toppari, J. (2009). Antiandrogen exposure in utero disrupts expression of desert hedgehog and insulin-like factor 3 in the developing fetal rat testis. *Endocrinology* **150**, 445-51.

Buehr, M., Gu, S. and McLaren, A. (1993a). Mesonephric contribution to testis differentiation in the fetal mouse. *Development* **117**, 273-81.

Buehr, M., McLaren, A., Bartley, A. and Darling, S. (1993b). Proliferation and migration of primordial germ cells in We/We mouse embryos. *Dev Dyn* **198**, 182-9.

Bullejos, M. and Koopman, P. (2004). Germ cells enter meiosis in a rostro-caudal wave during development of the mouse ovary. *Mol Reprod Dev* **68**, 422-8.

Burgoyne, P. S. (1987). The role of the mammalian Y chromosome in spermatogenesis. *Development* **101 Suppl**, 133-41.

Capel, B. (2000). The battle of the sexes. *Mech Dev* **92**, 89-103.

Capel, B., Albrecht, K. H., Washburn, L. L. and Eicher, E. M. (1999). Migration of mesonephric cells into the mammalian gonad depends on Sry. *Mech Dev* **84**, 127-31.

Cha, Y., Sung, M. K., Jung, K. W., Kim, H. H., Lee, S. M. and Park, K. S. (2008). Epigenetic deregulation of the human Oct4 promoter in mouse cells. *Dev Genes Evol* **218**, 561-6.

Chambers, I., Silva, J., Colby, D., Nichols, J., Nijmeijer, B., Robertson, M., Vrana, J., Jones, K., Grotewold, L. and Smith, A. (2007). Nanog safeguards pluripotency and mediates germline development. *Nature* **450**, 1230-4.

Chambon, P. (1996). A decade of molecular biology of retinoic acid receptors. *FASEB J* **10**, 940-54.

Chang, C., Saltzman, A., Yeh, S., Young, W., Keller, E., Lee, H. J., Wang, C. and Mizokami, A. (1995). Androgen receptor: an overview. *Crit Rev Eukaryot Gene Expr* **5**, 97-125.

Chang, H. and Matzuk, M. M. (2001). Smad5 is required for mouse primordial germ cell development. *Mech Dev* **104**, 61-7.

Chauvigne, F., Menuet, A., Lesne, L., Chagnon, M. C., Chevrier, C., Regnier, J. F., Angerer, J. and Jegou, B. (2009). Time- and dose-related effects of di-(2-ethylhexyl) phthalate and its main metabolites on the function of the rat fetal testis in vitro. *Environ Health Perspect* **117**, 515-21.

Chedin, F., Lieber, M. R. and Hsieh, C. L. (2002). The DNA methyltransferase-like protein DNMT3L stimulates de novo methylation by Dnmt3a. *Proc Natl Acad Sci U S A* **99**, 16916-21.

Christman, J. K. (2002). 5-Azacytidine and 5-aza-2'-deoxycytidine as inhibitors of DNA methylation: mechanistic studies and their implications for cancer therapy. *Oncogene* **21**, 5483-95.

Cirio, M. C., Martel, J., Mann, M., Toppings, M., Bartolomei, M., Trasler, J. and Chaillet, J. R. (2008). DNA methyltransferase 1o functions during preimplantation development to preclude a profound level of epigenetic variation. *Dev Biol* **324**, 139-50.

Clark, A. M., Garland, K. K. and Russell, L. D. (2000). Desert hedgehog (Dhh) gene is required in the mouse testis for formation of adult-type Leydig cells and normal development of peritubular cells and seminiferous tubules. *Biol Reprod* **63**, 1825-38.

Clark, J. M. and Eddy, E. M. (1975). Fine structural observations on the origin and associations of primordial germ cells of the mouse. *Dev Biol* **47**, 136-55.

Colbert, N. K., Pelletier, N. C., Cote, J. M., Concannon, J. B., Jurdak, N. A., Minott, S. B. and Markowski, V. P. (2005). Perinatal exposure to low levels of the environmental antiandrogen vinclozolin alters sex-differentiated social play and sexual behaviors in the rat. *Environ Health Perspect* **113**, 700-7.

Colvin, J. S., Green, R. P., Schmahl, J., Capel, B. and Ornitz, D. M. (2001). Male-to-female sex reversal in mice lacking fibroblast growth factor 9. *Cell* **104**, 875-89.

Cool, J. and Capel, B. (2009). Mixed signals: development of the testis. *Semin Reprod Med* **27**, 5-13.

Cool, J., Carmona, F. D., Szucsik, J. C. and Capel, B. (2008). Peritubular myoid cells are not the migrating population required for testis cord formation in the XY gonad. *Sex Dev* **2**, 128-33.

Cooney, C. A., Dave, A. A. and Wolff, G. L. (2002). Maternal methyl supplements in mice affect epigenetic variation and DNA methylation of offspring. *J Nutr* **132**, 2393S-2400S.

Costello, J. F., Hong, C., Plass, C. and Smiraglia, D. J. (2009). Restriction landmark genomic scanning: analysis of CpG islands in genomes by 2D gel electrophoresis. *Methods Mol Biol* **507**, 131-48.

Culty, M. (2009). Gonocytes, the forgotten cells of the germ cell lineage. *Birth Defects Res C Embryo Today* **87**, 1-26.

Cupp, A. S., and Skinner, M.K. (2005). Embryonic Sertoli Cell Differentiation. In *Sertoli Cell Biology*, (ed. M. K. Skinner, and Griswold, M.D.): Elsevier Academic Press.

De Felici, M., Di Carlo, A. and Pesce, M. (1996). Role of stem cell factor in somatic-germ cell interactions during prenatal oogenesis. *Zygote* **4**, 349-51.

de Jong, J., Stoop, H., Gillis, A. J., van Gurp, R. J., van de Geijn, G. J., Boer, M., Hersmus, R., Saunders, P. T., Anderson, R. A., Oosterhuis, J. W. et al. (2008). Differential expression of SOX17 and SOX2 in germ cells and stem cells has biological and clinical implications. *J Pathol* **215**, 21-30.

De Jong, J., Weeda, S., Gillis, A. J., Oosterhuis, J. W. and Looijenga, L. H. (2007). Differential methylation of the OCT3/4 upstream region in primary human testicular germ cell tumors. *Oncol Rep* **18**, 127-32.

de Rooij, D. G. (2001). Proliferation and differentiation of spermatogonial stem cells. *Reproduction* **121**, 347-54.

de Sousa Lopes, S. M., Hayashi, K. and Surani, M. A. (2007). Proximal visceral endoderm and extraembryonic ectoderm regulate the formation of primordial germ cell precursors. *BMC Dev Biol* **7**, 140.

Deb-Rinker, P., Ly, D., Jezierski, A., Sikorska, M. and Walker, P. R. (2005). Sequential DNA methylation of the Nanog and Oct-4 upstream regions in human NT2 cells during neuronal differentiation. *J Biol Chem* **280**, 6257-60.

Di Carlo, A. D., Travia, G. and De Felici, M. (2000). The meiotic specific synaptonemal complex protein SCP3 is expressed by female and male primordial germ cells of the mouse embryo. *Int J Dev Biol* **44**, 241-4.

Dieckmann, K. P. and Skakkebaek, N. E. (1999). Carcinoma in situ of the testis: review of biological and clinical features. *Int J Cancer* **83**, 815-22.

Doerksen, T., Benoit, G. and Trasler, J. M. (2000). Deoxyribonucleic acid hypomethylation of male germ cells by mitotic and meiotic exposure to 5-azacytidine is associated with altered testicular histology. *Endocrinology* **141**, 3235-44.

Doerksen, T. and Trasler, J. M. (1996). Developmental exposure of male germ cells to 5-azacytidine results in abnormal preimplantation development in rats. *Biol Reprod* **55**, 1155-62.

Dolci, S., Pesce, M. and De Felici, M. (1993). Combined action of stem cell factor, leukemia inhibitory factor, and cAMP on in vitro proliferation of mouse primordial germ cells. *Mol Reprod Dev* **35**, 134-9.

Donovan, P. J., Stott, D., Cairns, L. A., Heasman, J. and Wylie, C. C. (1986). Migratory and postmigratory mouse primordial germ cells behave differently in culture. *Cell* **44**, 831-8.

Dudley, B. M., Runyan, C., Takeuchi, Y., Schaible, K. and Molyneaux, K. (2007). BMP signaling regulates PGC numbers and motility in organ culture. *Mech Dev* **124**, 68-77.

Egger, G., Liang, G., Aparicio, A. and Jones, P. A. (2004). Epigenetics in human disease and prospects for epigenetic therapy. *Nature* **429**, 457-63.

El-Gehani, F., Zhang, F. P., Pakarinen, P., Rannikko, A. and Huhtaniemi, I. (1998). Gonadotropin-independent regulation of steroidogenesis in the fetal rat testis. *Biol Reprod* **58**, 116-23.

Ema, M., Miyawaki, E. and Kawashima, K. (1998). Further evaluation of developmental toxicity of di-n-butyl phthalate following administration during late pregnancy in rats. *Toxicol Lett* **98**, 87-93.

Ema, M., Miyawaki, E. and Kawashima, K. (2000). Effects of dibutyl phthalate on reproductive function in pregnant and pseudopregnant rats. *Reprod Toxicol* **14**, 13-9.

Emanuel, P. O., Unger, P. D. and Burstein, D. E. (2006). Immunohistochemical detection of p63 in testicular germ cell neoplasia. *Ann Diagn Pathol* **10**, 269-73.

Enders, G. C. and May, J. J., 2nd. (1994). Developmentally regulated expression of a mouse germ cell nuclear antigen examined from embryonic day 11 to adult in male and female mice. *Dev Biol* **163**, 331-40.

Esteller, M. (2007). Cancer epigenomics: DNA methylomes and histone-modification maps. *Nat Rev Genet* **8**, 286-98.

Fan, J., Akabane, H., Zheng, X., Zhou, X., Zhang, L., Liu, Q., Zhang, Y. L., Yang, J. and Zhu, G. Z. (2007). Male germ cell-specific expression of a novel Patched-domain containing gene Ptchd3. *Biochem Biophys Res Commun* **363**, 757-61.

Farini, D., La Sala, G., Tedesco, M. and De Felici, M. (2007). Chemoattractant action and molecular signaling pathways of Kit ligand on mouse primordial germ cells. *Dev Biol* **306**, 572-83.

Ferrara, D., Hallmark, N., Scott, H., Brown, R., McKinnell, C., Mahood, I. K. and Sharpe, R. M. (2006). Acute and long-term effects of in utero exposure of rats to di(n-butyl) phthalate on testicular germ cell development and proliferation. *Endocrinology* **147**, 5352-62.

Fisher, J. S., Macpherson, S., Marchetti, N. and Sharpe, R. M. (2003). Human 'testicular dysgenesis syndrome': a possible model using in-utero exposure of the rat to dibutyl phthalate. *Hum Reprod* **18**, 1383-94.

Fitzpatrick, S. L., Sindoni, D. M., Shughrue, P. J., Lane, M. V., Merchenthaler, I. J. and Frail, D. E. (1998). Expression of growth differentiation factor-9 messenger ribonucleic acid in ovarian and nonovarian rodent and human tissues. *Endocrinology* **139**, 2571-8.

Fouse, S. D., Shen, Y., Pellegrini, M., Cole, S., Meissner, A., Van Neste, L., Jaenisch, R. and Fan, G. (2008). Promoter CpG methylation contributes to ES cell gene regulation in parallel with Oct4/Nanog, PcG complex, and histone H3 K4/K27 trimethylation. *Cell Stem Cell* **2**, 160-9.

Freberg, C. T., Dahl, J. A., Timoskainen, S. and Collas, P. (2007). Epigenetic reprogramming of OCT4 and NANOG regulatory regions by embryonal carcinoma cell extract. *Mol Biol Cell* **18**, 1543-53.

Fukuda, T., Hedinger, C. and Groscurth, P. (1975). Ultrastructure of developing germ cells in the fetal human testis. *Cell Tissue Res* **161**, 55-70.

Gaskell, T. L., Esnal, A., Robinson, L. L., Anderson, R. A. and Saunders, P. T. (2004). Immunohistochemical profiling of germ cells within the human fetal testis: identification of three subpopulations. *Biol Reprod* **71**, 2012-21.

Gazzerro, E. and Canalis, E. (2006). Bone morphogenetic proteins and their antagonists. *Rev Endocr Metab Disord* **7**, 51-65.

Gilbert, D. C., Chandler, I., McIntyre, A., Goddard, N. C., Gabe, R., Huddart, R. A. and Shipley, J. (2009). Clinical and biological significance of CXCL12 and CXCR4 expression in adult testes and germ cell tumours of adults and adolescents. *J Pathol* **217**, 94-102.

Ginsburg, M., Snow, M. H. and McLaren, A. (1990). Primordial germ cells in the mouse embryo during gastrulation. *Development* **110**, 521-8.

Giwercman, A., Berthelsen, J. G., Muller, J., von der Maase, H. and Skakkebaek, N. E. (1987). Screening for carcinoma-in-situ of the testis. *Int J Androl* **10**, 173-80.

Giwercman, A., Cantell, L. and Marks, A. (1991). Placental-like alkaline phosphatase as a marker of carcinoma-in-situ of the testis. Comparison with monoclonal antibodies M2A and 43-9F. *APMIS* **99**, 586-94.

Godin, I., Deed, R., Cooke, J., Zsebo, K., Dexter, M. and Wylie, C. C. (1991). Effects of the steel gene product on mouse primordial germ cells in culture. *Nature* **352**, 807-9.

Godin, I. and Wylie, C. C. (1991). TGF beta 1 inhibits proliferation and has a chemotropic effect on mouse primordial germ cells in culture. *Development* **113**, 1451-7.

Godmann, M., Gashaw, I., Eildermann, K., Schweyer, S., Bergmann, M., Skotheim, R. I. and Behr, R. (2009). The pluripotency transcription factor Kruppel-like factor 4 is strongly expressed in intratubular germ cell neoplasia unclassified and seminoma. *Mol Hum Reprod* **15**, 479-88.

Gonzalez-Herrera, I. G., Prado-Lourenco, L., Pileur, F., Conte, C., Morin, A., Cabon, F., Prats, H., Vagner, S., Bayard, F., Audigier, S. et al. (2006). Testosterone regulates FGF-2 expression during testis maturation by an IRES-dependent translational mechanism. *FASEB J* **20**, 476-8.

Greenbaum, M. P., Iwamori, N., Agno, J. E. and Matzuk, M. M. (2009). Mouse TEX14 is required for embryonic germ cell intercellular bridges but not female fertility. *Biol Reprod* **80**, 449-57.

Greenbaum, M. P., Yan, W., Wu, M. H., Lin, Y. N., Agno, J. E., Sharma, M., Braun, R. E., Rajkovic, A. and Matzuk, M. M. (2006). TEX14 is essential for intercellular bridges and fertility in male mice. *Proc Natl Acad Sci U S A* **103**, 4982-7.

Griswold, M. D. (1995). Interactions between germ cells and Sertoli cells in the testis. *Biol Reprod* **52**, 211-6.

Griswold, S. L. and Behringer, R. R. (2009). Fetal Leydig cell origin and development. *Sex Dev* **3**, 1-15.

Habert, R., Lejeune, H. and Saez, J. M. (2001). Origin, differentiation and regulation of fetal and adult Leydig cells. *Mol Cell Endocrinol* **179**, 47-74.

Hacker, A., Capel, B., Goodfellow, P. and Lovell-Badge, R. (1995). Expression of Sry, the mouse sex determining gene. *Development* **121**, 1603-14.

Haider, S. G. (2004). Cell biology of Leydig cells in the testis. *Int Rev Cytol* **233**, 181-241.

Hajkova, P., Erhardt, S., Lane, N., Haaf, T., El-Maarri, O., Reik, W., Walter, J. and Surani, M. A. (2002). Epigenetic reprogramming in mouse primordial germ cells. *Mech Dev* **117**, 15-23.

Hallmark, N., Walker, M., McKinnell, C., Mahood, I. K., Scott, H., Bayne, R., Coutts, S., Anderson, R. A., Greig, I., Morris, K. et al. (2007). Effects of monobutyl and di(n-butyl) phthalate in vitro on steroidogenesis and Leydig cell aggregation in fetal testis explants from the rat: comparison with effects in vivo in the fetal rat and neonatal marmoset and in vitro in the human. *Environ Health Perspect* **115**, 390-6.

Hammoud, S. S., Purwar, J., Pflueger, C., Cairns, B. R. and Carrell, D. T. (2009). Alterations in sperm DNA methylation patterns at imprinted loci in two classes of infertility. *Fertil Steril*.

Hart, A. H., Hartley, L., Parker, K., Ibrahim, M., Looijenga, L. H., Pauchnik, M., Chow, C. W. and Robb, L. (2005). The pluripotency homeobox gene NANOG is expressed in human germ cell tumors. *Cancer* **104**, 2092-8.

Hattori, N., Nishino, K., Ko, Y. G., Ohgane, J., Tanaka, S. and Shiota, K. (2004). Epigenetic control of mouse Oct-4 gene expression in embryonic stem cells and trophoblast stem cells. *J Biol Chem* **279**, 17063-9.

Hayashi, K., de Sousa Lopes, S. M. and Surani, M. A. (2007). Germ cell specification in mice. *Science* **316**, 394-6.

Hellwig, J., van Ravenzwaay, B., Mayer, M. and Gembardt, C. (2000). Pre- and postnatal oral toxicity of vinclozolin in Wistar and Long-Evans rats. *Regul Toxicol Pharmacol* **32**, 42-50.

Hess, R. A., Cooke, P. S., Hofmann, M. C. and Murphy, K. M. (2006). Mechanistic insights into the regulation of the spermatogonial stem cell niche. *Cell Cycle* **5**, 1164-70.

Heudorf, U., Mersch-Sundermann, V. and Angerer, J. (2007). Phthalates: toxicology and exposure. *Int J Hyg Environ Health* **210**, 623-34.

Hirshfield, A. N. (1992). Heterogeneity of cell populations that contribute to the formation of primordial follicles in rats. *Biol Reprod* **47**, 466-72.

Hoei-Hansen, C. E., Holm, M., Rajpert-De Meyts, E. and Skakkebaek, N. E. (2003). Histological evidence of testicular dysgenesis in contralateral biopsies from 218 patients with testicular germ cell cancer. *J Pathol* **200**, 370-4.

Holm, M., Hoei-Hansen, C. E., Rajpert-De Meyts, E. and Skakkebaek, N. E. (2003). Increased risk of carcinoma in situ in patients with testicular germ cell cancer with ultrasonic microlithiasis in the contralateral testicle. *J Urol* **170**, 1163-7.

Honecker, F., Stoop, H., de Krijger, R. R., Chris Lau, Y. F., Bokemeyer, C. and Looijenga, L. H. (2004). Pathobiological implications of the expression of markers of testicular carcinoma in situ by fetal germ cells. *J Pathol* **203**, 849-57.

Honecker, F., Stoop, H., Mayer, F., Bokemeyer, C., Castrillon, D. H., Lau, Y. F., Looijenga, L. H. and Oosterhuis, J. W. (2006). Germ cell lineage differentiation in non-seminomatous germ cell tumours. *J Pathol* **208**, 395-400.

Howell, C. Y., Bestor, T. H., Ding, F., Latham, K. E., Mertineit, C., Trasler, J. M. and Chaillet, J. R. (2001). Genomic imprinting disrupted by a maternal effect mutation in the Dnmt1 gene. *Cell* **104**, 829-38.

Hughes, I. A. and Acerini, C. L. (2008). Factors controlling testis descent. *Eur J Endocrinol* **159 Suppl 1**, S75-82.

Huhtaniemi, I. and Pelliniemi, L. J. (1992). Fetal Leydig cells: cellular origin, morphology, life span, and special functional features. *Proc Soc Exp Biol Med* **201**, 125-40.

Hutchison, G. R., Scott, H. M., Walker, M., McKinnell, C., Ferrara, D., Mahood, I. K. and Sharpe, R. M. (2008a). Sertoli cell development and function in an animal model of testicular dysgenesis syndrome. *Biol Reprod* **78**, 352-60.

Hutchison, G. R., Sharpe, R. M., Mahood, I. K., Jobling, M., Walker, M., McKinnell, C., Mason, J. I. and Scott, H. M. (2008b). The origins and time of appearance of focal testicular dysgenesis in an animal model of testicular dysgenesis syndrome: evidence for delayed testis development? *Int J Androl* **31**, 103-11.

Hutson, J. M., Hasthorpe, S. and Heyns, C. F. (1997). Anatomical and functional aspects of testicular descent and cryptorchidism. *Endocr Rev* **18**, 259-80.

Imperato-McGinley, J. (2002). 5alpha-reductase-2 deficiency and complete androgen insensitivity: lessons from nature. *Adv Exp Med Biol* **511**, 121-31; discussion 131-4.

Inawaka, K., Kawabe, M., Takahashi, S., Doi, Y., Tomigahara, Y., Tarui, H., Abe, J., Kawamura, S. and Shirai, T. (2009). Maternal exposure to anti-androgenic compounds, vinclozolin, flutamide and procymidone, has no effects on spermatogenesis and DNA methylation in male rats of subsequent generations. *Toxicol Appl Pharmacol* **237**, 178-87.

Jacobsen, G. K., Henriksen, O. B. and von der Maase, H. (1981). Carcinoma in situ of testicular tissue adjacent to malignant germ-cell tumors: a study of 105 cases. *Cancer* **47**, 2660-2.

Jeays-Ward, K., Hoyle, C., Brennan, J., Dandonneau, M., Alldus, G., Capel, B. and Swain, A. (2003). Endothelial and steroidogenic cell migration are regulated by WNT4 in the developing mammalian gonad. *Development* **130**, 3663-70.

Jelinic, P., Stehle, J. C. and Shaw, P. (2006). The testis-specific factor CTCFL cooperates with the protein methyltransferase PRMT7 in H19 imprinting control region methylation. *PLoS Biol* **4**, e355.

Jia, D., Jurkowska, R. Z., Zhang, X., Jeltsch, A. and Cheng, X. (2007). Structure of Dnmt3a bound to Dnmt3L suggests a model for de novo DNA methylation. *Nature* **449**, 248-51.

Jirtle, R. L. and Skinner, M. K. (2007). Environmental epigenomics and disease susceptibility. *Nat Rev Genet* **8**, 253-62.

Johnston, H., King, P. J. and O'Shaughnessy, P. J. (2007). Effects of ACTH and expression of the melanocortin-2 receptor in the neonatal mouse testis. *Reproduction* **133**, 1181-7.

Jost, A. (1947). The age factor in the castration of male rabbit fetuses. *Proc Soc Exp Biol Med* **66**, 302.

Jost, A. (1972). A new look at the mechanisms controlling sex differentiation in mammals. *Johns Hopkins Med J* **130**, 38-53.

Jost, A., Magre, S. and Agelopoulou, R. (1981). Early stages of testicular differentiation in the rat. *Hum Genet* **58**, 59-63.

Jue, K., Bestor, T. H. and Trasler, J. M. (1995). Regulated synthesis and localization of DNA methyltransferase during spermatogenesis. *Biol Reprod* **53**, 561-9.

Kanatsu-Shinohara, M., Toyokuni, S. and Shinohara, T. (2004). CD9 is a surface marker on mouse and rat male germline stem cells. *Biol Reprod* **70**, 70-5.

Kaneda, M., Okano, M., Hata, K., Sado, T., Tsujimoto, N., Li, E. and Sasaki, H. (2004). Essential role for de novo DNA methyltransferase Dnmt3a in paternal and maternal imprinting. *Nature* **429**, 900-3.

Kantarjian, H. M., O'Brien, S., Cortes, J., Giles, F. J., Faderl, S., Issa, J. P., Garcia-Manero, G., Rios, M. B., Shan, J., Andreeff, M. et al. (2003). Results of decitabine (5-aza-2'deoxycytidine) therapy in 130 patients with chronic myelogenous leukemia. *Cancer* **98**, 522-8.

Karl, J. and Capel, B. (1998). Sertoli cells of the mouse testis originate from the coelomic epithelium. *Dev Biol* **203**, 323-33.

Kato, Y., Kaneda, M., Hata, K., Kumaki, K., Hisano, M., Kohara, Y., Okano, M., Li, E., Nozaki, M. and Sasaki, H. (2007). Role of the Dnmt3 family in de novo methylation of imprinted and repetitive sequences during male germ cell development in the mouse. *Hum Mol Genet* **16**, 2272-80.

Kawakami, T., Zhang, C., Okada, Y. and Okamoto, K. (2006). Erasure of methylation imprint at the promoter and CTCF-binding site upstream of H19 in human testicular germ cell tumors of adolescents indicate their fetal germ cell origin. *Oncogene* **25**, 3225-36.

Kehler, J., Tolkunova, E., Koschorz, B., Pesce, M., Gentile, L., Boiani, M., Lomeli, H., Nagy, A., McLaughlin, K. J., Scholer, H. R. et al. (2004). Oct4 is required for primordial germ cell survival. *EMBO Rep* **5**, 1078-83.

Kelly, T. L., Li, E. and Trasler, J. M. (2003). 5-aza-2'-deoxycytidine induces alterations in murine spermatogenesis and pregnancy outcome. *J Androl* **24**, 822-30.

Kent, J., Wheatley, S. C., Andrews, J. E., Sinclair, A. H. and Koopman, P. (1996). A male-specific role for SOX9 in vertebrate sex determination. *Development* **122**, 2813-22.

Kerr, C. L., Hill, C. M., Blumenthal, P. D. and Gearhart, J. D. (2008). Expression of pluripotent stem cell markers in the human fetal testis. *Stem Cells* **26**, 412-21.

Kerr, J. B. and Knell, C. M. (1988). The fate of fetal Leydig cells during the development of the fetal and postnatal rat testis. *Development* **103**, 535-44.

Keshet, E., Lyman, S. D., Williams, D. E., Anderson, D. M., Jenkins, N. A., Copeland, N. G. and Parada, L. F. (1991). Embryonic RNA expression patterns of the c-kit receptor and its cognate ligand suggest multiple functional roles in mouse development. *EMBO J* **10**, 2425-35.

Kettlewell, J. R., Raymond, C. S. and Zarkower, D. (2000). Temperature-dependent expression of turtle Dmrt1 prior to sexual differentiation. *Genesis* **26**, 174-8.

Kim, S., Bardwell, V. J. and Zarkower, D. (2007a). Cell type-autonomous and non-autonomous requirements for Dmrt1 in postnatal testis differentiation. *Dev Biol* **307**, 314-27.

Kim, Y., Bingham, N., Sekido, R., Parker, K. L., Lovell-Badge, R. and Capel, B. (2007b). Fibroblast growth factor receptor 2 regulates proliferation and Sertoli differentiation during male sex determination. *Proc Natl Acad Sci U S A* **104**, 16558-63.

Klenova, E. M., Morse, H. C., 3rd, Ohlsson, R. and Lobanenkov, V. V. (2002). The novel BORIS + CTCF gene family is uniquely involved in the epigenetics of normal biology and cancer. *Semin Cancer Biol* **12**, 399-414.

Klose, R. J. and Bird, A. P. (2006). Genomic DNA methylation: the mark and its mediators. *Trends Biochem Sci* **31**, 89-97.

Knickmeyer, R. C. and Baron-Cohen, S. (2006). Fetal testosterone and sex differences in typical social development and in autism. *J Child Neurol* **21**, 825-45.

Kocer, A., Reichmann, J., Best, D. and Adams, I. R. (2009). Germ cell sex determination in mammals. *Mol Hum Reprod* **15**, 205-13.

Koopman, P., Gubbay, J., Vivian, N., Goodfellow, P. and Lovell-Badge, R. (1991). Male development of chromosomally female mice transgenic for Sry. *Nature* **351**, 117-21.

Koopman, P., Munsterberg, A., Capel, B., Vivian, N. and Lovell-Badge, R. (1990). Expression of a candidate sex-determining gene during mouse testis differentiation. *Nature* **348**, 450-2.

Koshida, K., Uchibayashi, T., Yamamoto, H. and Hirano, K. (1996). Significance of placental alkaline phosphatase (PLAP) in the monitoring of patients with seminoma. *Br J Urol* **77**, 138-42.

Kraggerud, S. M., Lee, M. P., Skotheim, R. I., Stenwig, A. E., Fossa, S. D., Feinberg, A. P. and Lothe, R. A. (2003). Lack of parental origin specificity of altered alleles at 11p15 in testicular germ cell tumors. *Cancer Genet Cytogenet* **147**, 1-8.

Kurimoto, K., Yabuta, Y., Ohinata, Y., Shigeta, M., Yamanaka, K. and Saitou, M. (2008). Complex genome-wide transcription dynamics orchestrated by Blimp1 for the specification of the germ cell lineage in mice. *Genes Dev* **22**, 1617-35.

La Salle, S., Mertineit, C., Taketo, T., Moens, P. B., Bestor, T. H. and Trasler, J. M. (2004). Windows for sex-specific methylation marked by DNA methyltransferase expression profiles in mouse germ cells. *Dev Biol* **268**, 403-15.

La Salle, S. and Trasler, J. M. (2006). Dynamic expression of DNMT3a and DNMT3b isoforms during male germ cell development in the mouse. *Dev Biol* **296**, 71-82.

Lambrot, R., Muczynski, V., Lecureuil, C., Angenard, G., Coffigny, H., Pairault, C., Moison, D., Frydman, R., Habert, R. and Rouiller-Fabre, V. (2009). Phthalates impair germ cell development in the human fetal testis in vitro without change in testosterone production. *Environ Health Perspect* **117**, 32-7.

Lawson, K. A., Dunn, N. R., Roelen, B. A., Zeinstra, L. M., Davis, A. M., Wright, C. V., Korving, J. P. and Hogan, B. L. (1999). Bmp4 is required for the generation of primordial germ cells in the mouse embryo. *Genes Dev* **13**, 424-36.

Lawson, K. A. and Hage, W. J. (1994). Clonal analysis of the origin of primordial germ cells in the mouse. *Ciba Found Symp* **182**, 68-84; discussion 84-91.

Lees-Murdock, D. J., De Felici, M. and Walsh, C. P. (2003). Methylation dynamics of repetitive DNA elements in the mouse germ cell lineage. *Genomics* **82**, 230-7.

Lei, N., Hornbaker, K. I., Rice, D. A., Karpova, T., Agbor, V. A. and Heckert, L. L. (2007). Sex-specific differences in mouse DMRT1 expression are both cell type- and stage-dependent during gonad development. *Biol Reprod* **77**, 466-75.

Lei, N., Karpova, T., Hornbaker, K. I., Rice, D. A. and Heckert, L. L. (2009). Distinct transcriptional mechanisms direct expression of the rat Dmrt1 promoter in sertoli cells and germ cells of transgenic mice. *Biol Reprod* **81**, 118-25.

Li, E., Bestor, T. H. and Jaenisch, R. (1992). Targeted mutation of the DNA methyltransferase gene results in embryonic lethality. *Cell* **69**, 915-26.

Li, H. and Kim, K. H. (2003). Effects of mono-(2-ethylhexyl) phthalate on fetal and neonatal rat testis organ cultures. *Biol Reprod* **69**, 1964-72.

Li, J. Y., Pu, M. T., Hirasawa, R., Li, B. Z., Huang, Y. N., Zeng, R., Jing, N. H., Chen, T., Li, E., Sasaki, H. et al. (2007). Synergistic function of DNA methyltransferases Dnmt3a and Dnmt3b in the methylation of Oct4 and Nanog. *Mol Cell Biol* **27**, 8748-59.

Lin, Y., Gill, M. E., Koubova, J. and Page, D. C. (2008). Germ cell-intrinsic and -extrinsic factors govern meiotic initiation in mouse embryos. *Science* **322**, 1685-7.

Lind, G. E., Skotheim, R. I. and Lothe, R. A. (2007). The epigenome of testicular germ cell tumors. *APMIS* **115**, 1147-60.

Livera, G., Delbes, G., Pairault, C., Rouiller-Fabre, V. and Habert, R. (2006). Organotypic culture, a powerful model for studying rat and mouse fetal testis development. *Cell Tissue Res* **324**, 507-21.

Loh, Y. H., Wu, Q., Chew, J. L., Vega, V. B., Zhang, W., Chen, X., Bourque, G., George, J., Leong, B., Liu, J. et al. (2006). The Oct4 and Nanog transcription

network regulates pluripotency in mouse embryonic stem cells. *Nat Genet* **38**, 431-40.

Looijenga, L. H., Hersmus, R., Gillis, A. J., Pfundt, R., Stoop, H. J., van Gurp, R. J., Veltman, J., Beverloo, H. B., van Drunen, E., van Kessel, A. G. et al. (2006). Genomic and expression profiling of human spermatocytic seminomas: primary spermatocyte as tumorigenic precursor and DMRT1 as candidate chromosome 9 gene. *Cancer Res* **66**, 290-302.

Looijenga, L. H., Stoop, H., de Leeuw, H. P., de Gouveia Brazao, C. A., Gillis, A. J., van Roozendaal, K. E., van Zoelen, E. J., Weber, R. F., Wolffenbuttel, K. P., van Dekken, H. et al. (2003). POU5F1 (OCT3/4) identifies cells with pluripotent potential in human germ cell tumors. *Cancer Res* **63**, 2244-50.

Looijenga, L. H., Verkerk, A. J., Dekker, M. C., van Gurp, R. J., Gillis, A. J. and Oosterhuis, J. W. (1998). Genomic imprinting in testicular germ cell tumours. *APMIS* **106**, 187-95; discussion 196-7.

Loukinov, D. I., Pugacheva, E., Vatolin, S., Pack, S. D., Moon, H., Chernukhin, I., Mannan, P., Larsson, E., Kanduri, C., Vostrov, A. A. et al. (2002). BORIS, a novel male germ-line-specific protein associated with epigenetic reprogramming events, shares the same 11-zinc-finger domain with CTCF, the insulator protein involved in reading imprinting marks in the soma. *Proc Natl Acad Sci U S A* **99**, 6806-11.

Loveland, K. L., Hogarth, C., Mendis, S., Efthymiadis, A., Ly, J., Itman, C., Meachem, S., Brown, C. W. and Jans, D. A. (2005). Drivers of germ cell maturation. *Ann N Y Acad Sci* **1061**, 173-82.

Lovell-Badge, R. and Robertson, E. (1990). XY female mice resulting from a heritable mutation in the primary testis-determining gene, Tdy. *Development* **109**, 635-46.

Lu, D. P., Hiroyuki Nakayama, Junko Shinozuka, Koji Uetsuka, Ryuichi Taki and Kunio Doi. (1998). 5-Azacytidine-induced Apoptosis in the Central Nervous System of Developing Rat Fetuses. *Journal of Toxicologic Pathology* **11**, 4.

Lucifero, D., Mann, M. R., Bartolomei, M. S. and Trasler, J. M. (2004). Gene-specific timing and epigenetic memory in oocyte imprinting. *Hum Mol Genet* **13**, 839-49.

Maatouk, D. M., Kellam, L. D., Mann, M. R., Lei, H., Li, E., Bartolomei, M. S. and Resnick, J. L. (2006). DNA methylation is a primary mechanism for silencing postmigratory primordial germ cell genes in both germ cell and somatic cell lineages. *Development* **133**, 3411-8.

MacLean, G., Li, H., Metzger, D., Chambon, P. and Petkovich, M. (2007). Apoptotic extinction of germ cells in testes of Cyp26b1 knockout mice. *Endocrinology* **148**, 4560-7.

Mahakali Zama, A., Hudson, F. P., 3rd and Bedell, M. A. (2005). Analysis of hypomorphic KitlSl mutants suggests different requirements for KITL in proliferation and migration of mouse primordial germ cells. *Biol Reprod* **73**, 639-47.

Mahood, I. K., Hallmark, N., McKinnell, C., Walker, M., Fisher, J. S. and Sharpe, R. M. (2005). Abnormal Leydig Cell aggregation in the fetal testis of rats exposed to di (n-butyl) phthalate and its possible role in testicular dysgenesis. *Endocrinology* **146**, 613-23.

Maldonado-Saldivia, J., van den Bergen, J., Krouskos, M., Gilchrist, M., Lee, C., Li, R., Sinclair, A. H., Surani, M. A. and Western, P. S. (2007). Dppa2 and Dppa4 are closely linked SAP motif genes restricted to pluripotent cells and the germ line. *Stem Cells* **25**, 19-28.

Marchand, O., Govoroun, M., D'Cotta, H., McMeel, O., Lareyre, J., Bernot, A., Laudet, V. and Guiguen, Y. (2000). DMRT1 expression during gonadal differentiation and spermatogenesis in the rainbow trout, Oncorhynchus mykiss. *Biochim Biophys Acta* **1493**, 180-7.

Mark, M., Ghyselinck, N. B. and Chambon, P. (2006). Function of retinoid nuclear receptors: lessons from genetic and pharmacological dissections of the retinoic acid signaling pathway during mouse embryogenesis. *Annu Rev Pharmacol Toxicol* **46**, 451-80.

Matsui, Y., Zsebo, K. M. and Hogan, B. L. (1990). Embryonic expression of a haematopoietic growth factor encoded by the Sl locus and the ligand for c-kit. *Nature* **347**, 667-9.

McCoshen, J. A. and McCallion, D. J. (1975). A study of the primordial germ cells during their migratory phase in Steel mutant mice. *Experientia* **31**, 589-90.

McKiernan, J. M., Goluboff, E. T., Liberson, G. L., Golden, R. and Fisch, H. (1999). Rising risk of testicular cancer by birth cohort in the United States from 1973 to 1995. *J Urol* **162**, 361-3.

McKinnell, C., Mitchell, R. T., Walker, M., Morris, K., Kelnar, C. J., Wallace, W. H. and Sharpe, R. M. (2009). Effect of fetal or neonatal exposure to monobutyl phthalate (MBP) on testicular development and function in the marmoset. *Hum Reprod* **24**, 2244-54.

McKinnell, C., Saunders, P. T., Fraser, H. M., Kelnar, C. J., Kivlin, C., Morris, K. D. and Sharpe, R. M. (2001). Comparison of androgen receptor and oestrogen receptor beta immunoexpression in the testes of the common marmoset (Callithrix jacchus) from birth to adulthood: low androgen receptor immunoexpression in Sertoli cells during the neonatal increase in testosterone concentrations. *Reproduction* **122**, 419-29.

McLaren, A. (1983). Studies on mouse germ cells inside and outside the gonad. *J Exp Zool* **228**, 167-71.

McLaren, A. (1991). Sex determination. The making of male mice. *Nature* **351**, 96.

McLaren, A. (1995). Germ cells and germ cell sex. *Philos Trans R Soc Lond B Biol Sci* **350**, 229-33.

McLaren, A. (2003). Primordial germ cells in the mouse. *Dev Biol* **262**, 1-15.

McLaren, A. and Lawson, K. A. (2005). How is the mouse germ-cell lineage established? *Differentiation* **73**, 435-7.

McLaren, A. and Southee, D. (1997). Entry of mouse embryonic germ cells into meiosis. *Dev Biol* **187**, 107-13.

McNatty, K. P., Fidler, A. E., Juengel, J. L., Quirke, L. D., Smith, P. R., Heath, D. A., Lundy, T., O'Connell, A. and Tisdall, D. J. (2000). Growth and paracrine factors regulating follicular formation and cellular function. *Mol Cell Endocrinol* **163**, 11-20.

Meeks, J. J., Weiss, J. and Jameson, J. L. (2003). Dax1 is required for testis determination. *Nat Genet* **34**, 32-3.

Menke, D. B., Koubova, J. and Page, D. C. (2003). Sexual differentiation of germ cells in XX mouse gonads occurs in an anterior-to-posterior wave. *Dev Biol* **262**, 303-12.

Merchant-Larios, H. and Centeno, B. (1981). Morphogenesis of the ovary from the sterile W/Wv mouse. *Prog Clin Biol Res* **59B**, 383-92.

Merchant, H. (1975). Rat gonadal and ovarioan organogenesis with and without germ cells. An ultrastructural study. *Dev Biol* **44**, 1-21.

Migrenne, S., Pairault, C., Racine, C., Livera, G., Geloso, A. and Habert, R. (2001). Luteinizing hormone-dependent activity and luteinizing hormone-independent differentiation of rat fetal Leydig cells. *Mol Cell Endocrinol* **172**, 193-202.

Mishina, Y., Rey, R., Finegold, M. J., Matzuk, M. M., Josso, N., Cate, R. L. and Behringer, R. R. (1996). Genetic analysis of the Mullerian-inhibiting substance signal transduction pathway in mammalian sexual differentiation. *Genes Dev* **10**, 2577-87.

Mitchell, R. T., Cowan, G., Morris, K. D., Anderson, R. A., Fraser, H. M., McKenzie, K. J., Wallace, W. H., Kelnar, C. J., Saunders, P. T. and Sharpe, R. M. (2008). Germ cell differentiation in the marmoset (Callithrix jacchus) during fetal and neonatal life closely parallels that in the human. *Hum Reprod* **23**, 2755-65.

Molyneaux, K. A., Stallock, J., Schaible, K. and Wylie, C. (2001). Time-lapse analysis of living mouse germ cell migration. *Dev Biol* **240**, 488-98.

Molyneaux, K. A., Zinszner, H., Kunwar, P. S., Schaible, K., Stebler, J., Sunshine, M. J., O'Brien, W., Raz, E., Littman, D., Wylie, C. et al. (2003). The chemokine SDF1/CXCL12 and its receptor CXCR4 regulate mouse germ cell migration and survival. *Development* **130**, 4279-86.

Monk, M. and McLaren, A. (1981). X-chromosome activity in foetal germ cells of the mouse. *J Embryol Exp Morphol* **63**, 75-84.

Morales, C. R., Fox, A., El-Alfy, M., Ni, X. and Argraves, W. S. (2009). Expression of Patched-1 and Smoothened in testicular meiotic and post-meiotic cells. *Microsc Res Tech* **72**, 809-15.

Munsterberg, A. and Lovell-Badge, R. (1991). Expression of the mouse anti-mullerian hormone gene suggests a role in both male and female sexual differentiation. *Development* **113**, 613-24.

Mylchreest, E., Cattley, R. C. and Foster, P. M. (1998). Male reproductive tract malformations in rats following gestational and lactational exposure to Di(n-butyl) phthalate: an antiandrogenic mechanism? *Toxicol Sci* **43**, 47-60.

Mylchreest, E., Sar, M., Cattley, R. C. and Foster, P. M. (1999). Disruption of androgen-regulated male reproductive development by di(n-butyl) phthalate during late gestation in rats is different from flutamide. *Toxicol Appl Pharmacol* **156**, 81-95.

Nakamura, A. and Seydoux, G. (2008). Less is more: specification of the germline by transcriptional repression. *Development* **135**, 3817-27.

Nef, S. and Parada, L. F. (1999). Cryptorchidism in mice mutant for Insl3. *Nat Genet* **22**, 295-9.

Negoescu, A., Guillermet, C., Lorimier, P., Brambilla, E. and Labat-Moleur, F. (1998). Importance of DNA fragmentation in apoptosis with regard to TUNEL specificity. *Biomed Pharmacother* **52**, 252-8.

Netto, G. J., Nakai, Y., Nakayama, M., Jadallah, S., Toubaji, A., Nonomura, N., Albadine, R., Hicks, J. L., Epstein, J. I., Yegnasubramanian, S. et al. (2008). Global DNA hypomethylation in intratubular germ cell neoplasia and seminoma, but not in nonseminomatous male germ cell tumors. *Mod Pathol* **21**, 1337-44.

Nichols, J., Zevnik, B., Anastassiadis, K., Niwa, H., Klewe-Nebenius, D., Chambers, I., Scholer, H. and Smith, A. (1998). Formation of pluripotent stem cells in the mammalian embryo depends on the POU transcription factor Oct4. *Cell* **95**, 379-91.

Noguchi, T. and Noguchi, M. (1985). A recessive mutation (ter) causing germ cell deficiency and a high incidence of congenital testicular teratomas in 129/Sv-ter mice. *J Natl Cancer Inst* **75**, 385-92.

O'Shaughnessy, P. J., Baker, P., Sohnius, U., Haavisto, A. M., Charlton, H. M. and Huhtaniemi, I. (1998). Fetal development of Leydig cell activity in the mouse is independent of pituitary gonadotroph function. *Endocrinology* **139**, 1141-6.

O'Shaughnessy, P. J., Fleming, L., Baker, P. J., Jackson, G. and Johnston, H. (2003). Identification of developmentally regulated genes in the somatic cells of the mouse testis using serial analysis of gene expression. *Biol Reprod* **69**, 797-808.

Oakes, C. C., Kelly, T. L., Robaire, B. and Trasler, J. M. (2007a). Adverse effects of 5-aza-2'-deoxycytidine on spermatogenesis include reduced sperm function and

selective inhibition of de novo DNA methylation. *J Pharmacol Exp Ther* **322**, 1171-80.

Oakes, C. C., La Salle, S., Smiraglia, D. J., Robaire, B. and Trasler, J. M. (2007b). Developmental acquisition of genome-wide DNA methylation occurs prior to meiosis in male germ cells. *Dev Biol* **307**, 368-79.

Obata, Y. and Kono, T. (2002). Maternal primary imprinting is established at a specific time for each gene throughout oocyte growth. *J Biol Chem* **277**, 5285-9.

Ohinata, Y., Payer, B., O'Carroll, D., Ancelin, K., Ono, Y., Sano, M., Barton, S. C., Obukhanych, T., Nussenzweig, M., Tarakhovsky, A. et al. (2005). Blimp1 is a critical determinant of the germ cell lineage in mice. *Nature* **436**, 207-13.

Okano, M., Bell, D. W., Haber, D. A. and Li, E. (1999). DNA methyltransferases Dnmt3a and Dnmt3b are essential for de novo methylation and mammalian development. *Cell* **99**, 247-57.

Okano, M., Xie, S. and Li, E. (1998). Dnmt2 is not required for de novo and maintenance methylation of viral DNA in embryonic stem cells. *Nucleic Acids Res* **26**, 2536-40.

Oosterhuis, J. W., Stoop, H., Honecker, F. and Looijenga, L. H. (2007). Why human extragonadal germ cell tumours occur in the midline of the body: old concepts, new perspectives. *Int J Androl* **30**, 256-63; discussion 263-4.

Orth, J. M., Gunsalus, G. L. and Lamperti, A. A. (1988). Evidence from Sertoli cell-depleted rats indicates that spermatid number in adults depends on numbers of Sertoli cells produced during perinatal development. *Endocrinology* **122**, 787-94.

Ottesen, A. M., Skakkebaek, N. E., Lundsteen, C., Leffers, H., Larsen, J. and Rajpert-De Meyts, E. (2003). High-resolution comparative genomic hybridization detects extra chromosome arm 12p material in most cases of carcinoma in situ adjacent to overt germ cell tumors, but not before the invasive tumor development. *Genes Chromosomes Cancer* **38**, 117-25.

Oulad-Abdelghani, M., Bouillet, P., Decimo, D., Gansmuller, A., Heyberger, S., Dolle, P., Bronner, S., Lutz, Y. and Chambon, P. (1996). Characterization of a premeiotic germ cell-specific cytoplasmic protein encoded by Stra8, a novel retinoic acid-responsive gene. *J Cell Biol* **135**, 469-77.

Palmer, S. J. and Burgoyne, P. S. (1991). In situ analysis of fetal, prepuberal and adult XX----XY chimaeric mouse testes: Sertoli cells are predominantly, but not exclusively, XY. *Development* **112**, 265-8.

Perakis, A. and Stylianopoulou, F. (1986). Effects of a prenatal androgen peak on rat brain sexual differentiation. *J Endocrinol* **108**, 281-5.

Perrett, R. M., Turnpenny, L., Eckert, J. J., O'Shea, M., Sonne, S. B., Cameron, I. T., Wilson, D. I., Meyts, E. R. and Hanley, N. A. (2008). The early human germ cell lineage does not express SOX2 during in vivo development or upon in vitro culture. *Biol Reprod* **78**, 852-8.

Pesce, M., Di Carlo, A. and De Felici, M. (1997). The c-kit receptor is involved in the adhesion of mouse primordial germ cells to somatic cells in culture. *Mech Dev* **68**, 37-44.

Pesce, M., Gioia Klinger, F. and De Felici, M. (2002). Derivation in culture of primordial germ cells from cells of the mouse epiblast: phenotypic induction and growth control by Bmp4 signalling. *Mech Dev* **112**, 15-24.

Pesce, M. and Scholer, H. R. (2000). Oct-4: control of totipotency and germline determination. *Mol Reprod Dev* **55**, 452-7.

Pikarsky, E., Sharir, H., Ben-Shushan, E. and Bergman, Y. (1994). Retinoic acid represses Oct-3/4 gene expression through several retinoic acid-responsive elements located in the promoter-enhancer region. *Mol Cell Biol* **14**, 1026-38.

Rajpert-De Meyts, E. (2006). Developmental model for the pathogenesis of testicular carcinoma in situ: genetic and environmental aspects. *Hum Reprod Update* **12**, 303-23.

Rajpert-De Meyts, E., Bartkova, J., Samson, M., Hoei-Hansen, C. E., Frydelund-Larsen, L., Bartek, J. and Skakkebaek, N. E. (2003). The emerging phenotype of the testicular carcinoma in situ germ cell. *APMIS* **111**, 267-78; discussion 278-9.

Rapley EA, Turnbull C, Al Olama AA, Dermitzakis ET, Linger R, Huddart RA, Renwick A, Hughes D, Hines S, Seal S, Morrison J, Nsengimana J, Deloukas P; UK Testicular Cancer Collaboration, Rahman N, Bishop DT, Easton DF and Stratton MR. (2009). A genome-wide association study of testicular germ cell tumor. *Nat Genet.* **41**, 807-10.

Ratnam, S., Mertineit, C., Ding, F., Howell, C. Y., Clarke, H. J., Bestor, T. H., Chaillet, J. R. and Trasler, J. M. (2002). Dynamics of Dnmt1 methyltransferase expression and intracellular localization during oogenesis and preimplantation development. *Dev Biol* **245**, 304-14.

Raymond, C. S., Kettlewell, J. R., Hirsch, B., Bardwell, V. J. and Zarkower, D. (1999a). Expression of Dmrt1 in the genital ridge of mouse and chicken embryos suggests a role in vertebrate sexual development. *Dev Biol* **215**, 208-20.

Raymond, C. S., Murphy, M. W., O'Sullivan, M. G., Bardwell, V. J. and Zarkower, D. (2000). Dmrt1, a gene related to worm and fly sexual regulators, is required for mammalian testis differentiation. *Genes Dev* **14**, 2587-95.

Raymond, C. S., Parker, E. D., Kettlewell, J. R., Brown, L. G., Page, D. C., Kusz, K., Jaruzelska, J., Reinberg, Y., Flejter, W. L., Bardwell, V. J. et al. (1999b). A region of human chromosome 9p required for testis development contains two genes related to known sexual regulators. *Hum Mol Genet* **8**, 989-96.

Renaud, S., Pugacheva, E. M., Delgado, M. D., Braunschweig, R., Abdullaev, Z., Loukinov, D., Benhattar, J. and Lobanenkov, V. (2007). Expression of the CTCF-paralogous cancer-testis gene, brother of the regulator of imprinted sites (BORIS), is regulated by three alternative promoters modulated by CpG methylation and by CTCF and p53 transcription factors. *Nucleic Acids Res* **35**, 7372-88.

Roberts, L. M., Visser, J. A. and Ingraham, H. A. (2002). Involvement of a matrix metalloproteinase in MIS-induced cell death during urogenital development. *Development* **129**, 1487-96.

Rodda, D. J., Chew, J. L., Lim, L. H., Loh, Y. H., Wang, B., Ng, H. H. and Robson, P. (2005). Transcriptional regulation of nanog by OCT4 and SOX2. *J Biol Chem* **280**, 24731-7.

Roosen-Runge, E. C. and Anderson, D. (1959). The development of the interstitial cells in the testis of the albino rat. *Acta Anat (Basel)* **37**, 125-37.

Rosenberg, C., Van Gurp, R. J., Geelen, E., Oosterhuis, J. W. and Looijenga, L. H. (2000). Overrepresentation of the short arm of chromosome 12 is related to invasive growth of human testicular seminomas and nonseminomas. *Oncogene* **19**, 5858-62.

Rudel, H., Schroder, W., von der Trenck, K. T. and Wiesmuller, G. A. (2009). Substance-related environmental monitoring: Work group 'Environmental Monitoring'-Position paper. *Environ Sci Pollut Res Int* **16**, 486-98.

Ruggiu, M., Speed, R., Taggart, M., McKay, S. J., Kilanowski, F., Saunders, P., Dorin, J. and Cooke, H. J. (1997). The mouse Dazla gene encodes a cytoplasmic protein essential for gametogenesis. *Nature* **389**, 73-7.

Runyan, C., Schaible, K., Molyneaux, K., Wang, Z., Levin, L. and Wylie, C. (2006). Steel factor controls midline cell death of primordial germ cells and is essential for their normal proliferation and migration. *Development* **133**, 4861-9.

Saitou, M., Barton, S. C. and Surani, M. A. (2002). A molecular programme for the specification of germ cell fate in mice. *Nature* **418**, 293-300.

Saitou, M., Payer, B., Lange, U. C., Erhardt, S., Barton, S. C. and Surani, M. A. (2003). Specification of germ cell fate in mice. *Philos Trans R Soc Lond B Biol Sci* **358**, 1363-70.

Sakai, Y., Suetake, I., Itoh, K., Mizugaki, M., Tajima, S. and Yamashina, S. (2001). Expression of DNA methyltransferase (Dnmt1) in testicular germ cells during development of mouse embryo. *Cell Struct Funct* **26**, 685-91.

Sakurai, T., Katoh, H., Moriwaki, K., Noguchi, T. and Noguchi, M. (1994). The ter primordial germ cell deficiency mutation maps near Grl-1 on mouse chromosome 18. *Mamm Genome* **5**, 333-6.

Sasaki, H., Ishihara, K. and Kato, R. (2000). Mechanisms of Igf2/H19 imprinting: DNA methylation, chromatin and long-distance gene regulation. *J Biochem* **127**, 711-5.

Schmahl, J., Eicher, E. M., Washburn, L. L. and Capel, B. (2000). Sry induces cell proliferation in the mouse gonad. *Development* **127**, 65-73.

Schmahl, J., Kim, Y., Colvin, J. S., Ornitz, D. M. and Capel, B. (2004). Fgf9 induces proliferation and nuclear localization of FGFR2 in Sertoli precursors during male sex determination. *Development* **131**, 3627-36.

Schneider, S., Kaufmann, W., Buesen, R. and van Ravenzwaay, B. (2008). Vinclozolin--the lack of a transgenerational effect after oral maternal exposure during organogenesis. *Reprod Toxicol* **25**, 352-60.

Schrans-Stassen, B. H., Saunders, P. T., Cooke, H. J. and de Rooij, D. G. (2001). Nature of the spermatogenic arrest in Dazl -/- mice. *Biol Reprod* **65**, 771-6.

Scott, D. J., Fu, P., Shen, P. J., Gundlach, A., Layfield, S., Riesewijk, A., Tomiyama, H., Hutson, J. M., Tregear, G. W. and Bathgate, R. A. (2005). Characterization of the rat INSL3 receptor. *Ann N Y Acad Sci* **1041**, 13-6.

Scott, H. M. (2007). The Role of Androgens in Testicular Development and Dysgenesis. In *MRC Human Reproductive Sciences Unit*, vol. PhD (ed.: University of Edinburgh.

Scott, H. M., Hutchison, G. R., Jobling, M. S., McKinnell, C., Drake, A. J. and Sharpe, R. M. (2008). Relationship between androgen action in the "male programming window," fetal sertoli cell number, and adult testis size in the rat. *Endocrinology* **149**, 5280-7.

Seki, Y., Hayashi, K., Itoh, K., Mizugaki, M., Saitou, M. and Matsui, Y. (2005). Extensive and orderly reprogramming of genome-wide chromatin modifications associated with specification and early development of germ cells in mice. *Dev Biol* **278**, 440-58.

Seki, Y., Yamaji, M., Yabuta, Y., Sano, M., Shigeta, M., Matsui, Y., Saga, Y., Tachibana, M., Shinkai, Y. and Saitou, M. (2007). Cellular dynamics associated with the genome-wide epigenetic reprogramming in migrating primordial germ cells in mice. *Development* **134**, 2627-38.

Seligman, J. and Page, D. C. (1998). The Dazh gene is expressed in male and female embryonic gonads before germ cell sex differentiation. *Biochem Biophys Res Commun* **245**, 878-82.

Sharpe, R. M., and Skakkebaek, N. E. (2003). Male reproductive disorders and the role of endocrine disruption: Advances in understanding and identification of areas for future research. *Pure and Applied Chemistry* **75**, 2023-2038.

Shi, S. R., Chaiwun, B., Young, L., Cote, R. J. and Taylor, C. R. (1993). Antigen retrieval technique utilizing citrate buffer or urea solution for immunohistochemical demonstration of androgen receptor in formalin-fixed paraffin sections. *J Histochem Cytochem* **41**, 1599-604.

Sinclair, A. H., Berta, P., Palmer, M. S., Hawkins, J. R., Griffiths, B. L., Smith, M. J., Foster, J. W., Frischauf, A. M., Lovell-Badge, R. and Goodfellow, P. N.

(1990). A gene from the human sex-determining region encodes a protein with homology to a conserved DNA-binding motif. *Nature* **346**, 240-4.

Skakkebaek, N. E. (1972). Possible carcinoma-in-situ of the testis. *Lancet* **2**, 516-7.

Skakkebaek, N. E. (1978). Carcinoma in situ of the testis: frequency and relationship to invasive germ cell tumours in infertile men. *Histopathology* **2**, 157-70.

Skakkebaek, N. E., Berthelsen, J. G. and Muller, J. (1982). Carcinoma-in-situ of the undescended testis. *Urol Clin North Am* **9**, 377-85.

Skakkebaek, N. E., Holm, M., Hoei-Hansen, C., Jorgensen, N. and Rajpert-De Meyts, E. (2003). Association between testicular dysgenesis syndrome (TDS) and testicular neoplasia: evidence from 20 adult patients with signs of maldevelopment of the testis. *APMIS* **111**, 1-9; discussion 9-11.

Skakkebaek, N. E., Rajpert-De Meyts, E. and Main, K. M. (2001). Testicular dysgenesis syndrome: an increasingly common developmental disorder with environmental aspects. *Hum Reprod* **16**, 972-8.

Skinner, M. K. and Fritz, I. B. (1985). Structural characterization of proteoglycans produced by testicular peritubular cells and Sertoli cells. *J Biol Chem* **260**, 11874-83.

Smiraglia, D. J., Szymanska, J., Kraggerud, S. M., Lothe, R. A., Peltomaki, P. and Plass, C. (2002). Distinct epigenetic phenotypes in seminomatous and nonseminomatous testicular germ cell tumors. *Oncogene* **21**, 3909-16.

Sonne, S. B., Almstrup, K., Dalgaard, M., Juncker, A. S., Edsgard, D., Ruban, L., Harrison, N. J., Schwager, C., Abdollahi, A., Huber, P. E. et al. (2009). Analysis of gene expression profiles of microdissected cell populations indicates that testicular carcinoma in situ is an arrested gonocyte. *Cancer Res* **69**, 5241-50.

Speed, R. M. (1982). Meiosis in the foetal mouse ovary. I. An analysis at the light microscope level using surface-spreading. *Chromosoma* **85**, 427-37.

Spivakov, M. and Fisher, A. G. (2007). Epigenetic signatures of stem-cell identity. *Nat Rev Genet* **8**, 263-71.

Strachan, T., Read, A. P. (2004). Human Molecular Genetics 3: Garland Publishing.

Stroheker, T., Regnier, J. F., Lassurguere, J. and Chagnon, M. C. (2006). Effect of in utero exposure to di-(2-ethylhexyl)phthalate: distribution in the rat fetus and testosterone production by rat fetal testis in culture. *Food Chem Toxicol* **44**, 2064-9.

Suetake, I., Shinozaki, F., Miyagawa, J., Takeshima, H. and Tajima, S. (2004). DNMT3L stimulates the DNA methylation activity of Dnmt3a and Dnmt3b through a direct interaction. *J Biol Chem* **279**, 27816-23.

Suh, E. K., Yang, A., Kettenbach, A., Bamberger, C., Michaelis, A. H., Zhu, Z., Elvin, J. A., Bronson, R. T., Crum, C. P. and McKeon, F. (2006). p63 protects the female germ line during meiotic arrest. *Nature* **444**, 624-8.

Suzuki, A. and Saga, Y. (2008). Nanos2 suppresses meiosis and promotes male germ cell differentiation. *Genes Dev* **22**, 430-5.

Suzuki, H., Tsuda, M., Kiso, M. and Saga, Y. (2008). Nanos3 maintains the germ cell lineage in the mouse by suppressing both Bax-dependent and -independent apoptotic pathways. *Dev Biol* **318**, 133-42.

Takahashi, K., Tanabe, K., Ohnuki, M., Narita, M., Ichisaka, T., Tomoda, K. and Yamanaka, S. (2007). Induction of pluripotent stem cells from adult human fibroblasts by defined factors. *Cell* **131**, 861-72.

Takahashi, K. and Yamanaka, S. (2006). Induction of pluripotent stem cells from mouse embryonic and adult fibroblast cultures by defined factors. *Cell* **126**, 663-76.

Tam, P. P. and Snow, M. H. (1981). Proliferation and migration of primordial germ cells during compensatory growth in mouse embryos. *J Embryol Exp Morphol* **64**, 133-47.

Tam, P. P. and Zhou, S. X. (1996). The allocation of epiblast cells to ectodermal and germ-line lineages is influenced by the position of the cells in the gastrulating mouse embryo. *Dev Biol* **178**, 124-32.

Tanaka, S. S., Toyooka, Y., Akasu, R., Katoh-Fukui, Y., Nakahara, Y., Suzuki, R., Yokoyama, M. and Noce, T. (2000). The mouse homolog of Drosophila Vasa is required for the development of male germ cells. *Genes Dev* **14**, 841-53.

Tilmann, C. and Capel, B. (1999). Mesonephric cell migration induces testis cord formation and Sertoli cell differentiation in the mammalian gonad. *Development* **126**, 2883-90.

Tomioka, M., Nishimoto, M., Miyagi, S., Katayanagi, T., Fukui, N., Niwa, H., Muramatsu, M. and Okuda, A. (2002). Identification of Sox-2 regulatory region which is under the control of Oct-3/4-Sox-2 complex. *Nucleic Acids Res* **30**, 3202-13.

Tomizuka, K., Horikoshi, K., Kitada, R., Sugawara, Y., Iba, Y., Kojima, A., Yoshitome, A., Yamawaki, K., Amagai, M., Inoue, A. et al. (2008). R-spondin1 plays an essential role in ovarian development through positively regulating Wnt-4 signaling. *Hum Mol Genet* **17**, 1278-91.

Toyooka, Y., Tsunekawa, N., Takahashi, Y., Matsui, Y., Satoh, M. and Noce, T. (2000). Expression and intracellular localization of mouse Vasa-homologue protein during germ cell development. *Mech Dev* **93**, 139-49.

Trasler, J. M. (2009). Epigenetics in spermatogenesis. *Mol Cell Endocrinol* **306**, 33-6.

Tremblay, K. D., Dunn, N. R. and Robertson, E. J. (2001). Mouse embryos lacking Smad1 signals display defects in extra-embryonic tissues and germ cell formation. *Development* **128**, 3609-21.

Tsuda, M., Sasaoka, Y., Kiso, M., Abe, K., Haraguchi, S., Kobayashi, S. and Saga, Y. (2003). Conserved role of nanos proteins in germ cell development. *Science* **301**, 1239-41.

Tung, P. S. and Fritz, I. B. (1986). Extracellular matrix components and testicular peritubular cells influence the rate and pattern of Sertoli cell migration in vitro. *Dev Biol* **113**, 119-34.

Tung, P. S. and Fritz, I. B. (1987). Morphogenetic restructuring and formation of basement membranes by Sertoli cells and testis peritubular cells in co-culture: inhibition of the morphogenetic cascade by cyclic AMP derivatives and by blocking direct cell contact. *Dev Biol* **120**, 139-53.

van de Geijn, G. J., Hersmus, R. and Looijenga, L. H. (2009). Recent developments in testicular germ cell tumor research. *Birth Defects Res C Embryo Today* **87**, 96-113.

von Schonfeldt, V., Krishnamurthy, H., Foppiani, L. and Schlatt, S. (1999). Magnetic cell sorting is a fast and effective method of enriching viable

spermatogonia from Djungarian hamster, mouse, and marmoset monkey testes. *Biol Reprod* **61**, 582-9.

Waddington, C. H. (1952). Selection of the genetic basis for an acquired character. *Nature* **169**, 278.

Wang, Y., Wysocka, J., Perlin, J. R., Leonelli, L., Allis, C. D. and Coonrod, S. A. (2004). Linking covalent histone modifications to epigenetics: the rigidity and plasticity of the marks. *Cold Spring Harb Symp Quant Biol* **69**, 161-9.

Weenen, C., Laven, J. S., Von Bergh, A. R., Cranfield, M., Groome, N. P., Visser, J. A., Kramer, P., Fauser, B. C. and Themmen, A. P. (2004). Anti-Mullerian hormone expression pattern in the human ovary: potential implications for initial and cyclic follicle recruitment. *Mol Hum Reprod* **10**, 77-83.

Welsh, M., Saunders, P. T., Fisken, M., Scott, H. M., Hutchison, G. R., Smith, L. B. and Sharpe, R. M. (2008). Identification in rats of a programming window for reproductive tract masculinization, disruption of which leads to hypospadias and cryptorchidism. *J Clin Invest* **118**, 1479-90.

Wernig, M., Meissner, A., Foreman, R., Brambrink, T., Ku, M., Hochedlinger, K., Bernstein, B. E. and Jaenisch, R. (2007). In vitro reprogramming of fibroblasts into a pluripotent ES-cell-like state. *Nature* **448**, 318-24.

Western, P., Maldonado-Saldivia, J., van den Bergen, J., Hajkova, P., Saitou, M., Barton, S. and Surani, M. A. (2005). Analysis of Esg1 expression in pluripotent cells and the germline reveals similarities with Oct4 and Sox2 and differences between human pluripotent cell lines. *Stem Cells* **23**, 1436-42.

Wilhelm, D., Washburn, L. L., Truong, V., Fellous, M., Eicher, E. M. and Koopman, P. (2009). Antagonism of the testis- and ovary-determining pathways during ovotestis development in mice. *Mech Dev* **126**, 324-36.

Wittassek, M., Wiesmuller, G. A., Koch, H. M., Eckard, R., Dobler, L., Muller, J., Angerer, J. and Schluter, C. (2007). Internal phthalate exposure over the last two decades--a retrospective human biomonitoring study. *Int J Hyg Environ Health* **210**, 319-33.

Yabuta, Y., Kurimoto, K., Ohinata, Y., Seki, Y. and Saitou, M. (2006). Gene expression dynamics during germline specification in mice identified by quantitative single-cell gene expression profiling. *Biol Reprod* **75**, 705-16.

Yamaguchi, S., Kimura, H., Tada, M., Nakatsuji, N. and Tada, T. (2005). Nanog expression in mouse germ cell development. *Gene Expr Patterns* **5**, 639-46.

Yamaji, M., Seki, Y., Kurimoto, K., Yabuta, Y., Yuasa, M., Shigeta, M., Yamanaka, K., Ohinata, Y. and Saitou, M. (2008). Critical function of Prdm14 for the establishment of the germ cell lineage in mice. *Nat Genet* **40**, 1016-22.

Yamasaki, K., Takahashi, M. and Yasuda, M. (2005). Two-generation reproductive toxicity studies in rats with extra parameters for detecting endocrine disrupting activity: introductory overview of results for nine chemicals. *J Toxicol Sci* **30 Spec No.**, 1-4.

Yao, H. H., Whoriskey, W. and Capel, B. (2002). Desert Hedgehog/Patched 1 signaling specifies fetal Leydig cell fate in testis organogenesis. *Genes Dev* **16**, 1433-40.

Yeo, S., Jeong, S., Kim, J., Han, J. S., Han, Y. M. and Kang, Y. K. (2007). Characterization of DNA methylation change in stem cell marker genes during differentiation of human embryonic stem cells. *Biochem Biophys Res Commun* **359**, 536-42.

Ying, Y., Liu, X. M., Marble, A., Lawson, K. A. and Zhao, G. Q. (2000). Requirement of Bmp8b for the generation of primordial germ cells in the mouse. *Mol Endocrinol* **14**, 1053-63.

Ying, Y., Qi, X. and Zhao, G. Q. (2001). Induction of primordial germ cells from murine epiblasts by synergistic action of BMP4 and BMP8B signaling pathways. *Proc Natl Acad Sci U S A* **98**, 7858-62.

Ying, Y. and Zhao, G. Q. (2001). Cooperation of endoderm-derived BMP2 and extraembryonic ectoderm-derived BMP4 in primordial germ cell generation in the mouse. *Dev Biol* **232**, 484-92.

Yoder, J. A., Soman, N. S., Verdine, G. L. and Bestor, T. H. (1997). DNA (cytosine-5)-methyltransferases in mouse cells and tissues. Studies with a mechanism-based probe. *J Mol Biol* **270**, 385-95.

Youngren, K. K., Coveney, D., Peng, X., Bhattacharya, C., Schmidt, L. S., Nickerson, M. L., Lamb, B. T., Deng, J. M., Behringer, R. R., Capel, B. et al. (2005). The Ter mutation in the dead end gene causes germ cell loss and testicular germ cell tumours. *Nature* **435**, 360-4.

Zamboni, L. and Upadhyay, S. (1983). Germ cell differentiation in mouse adrenal glands. *J Exp Zool* **228**, 173-93.

Zarkower, D. (2001). Establishing sexual dimorphism: conservation amidst diversity? *Nat Rev Genet* **2**, 175-85.

Zhang, F. P., Pakarainen, T., Zhu, F., Poutanen, M. and Huhtaniemi, I. (2004). Molecular characterization of postnatal development of testicular steroidogenesis in luteinizing hormone receptor knockout mice. *Endocrinology* **145**, 1453-63.